RECOVERY OF PLATINUM GROUP ELEMENTS FROM WASTE MATERIAL

by

Ayanda Maria Ngcephe

A thesis submitted to meet the requirements for the degree of

Master of Science

In the faculty of Natural and Agricultural Sciences

Department of Chemistry
University of the Free State
Bloemfontein

Supervisor: Prof. W. Purcell

June 2019

Declaration by Candidate

I hereby declare that this dissertation submitted for Master's degree in Chemistry at the University of the Free State is my own original work and has not been previously submitter to another university or faculty. I further declare that all sources cited and quoted are acknowledged by a list of comprehensive references.

Signature ……..… **Date**……

Ayanda Maria Ngcephe

Acknowledgements

I would like to express my sincere appreciation to those who contributed in making this challenging journey a success.

To my advisor, Prof. Purcell: Thank you for your outstanding guidance and for training me to become a better researcher. I learned substantially from you and I am truly blessed and proud to be one of your students.

To the analytical chemistry group (Dr. Nete, Dr. Sinha, Dr. Chiweshe, Sibongile Xaba, Lijo Mona, Qinisile Vilakazi and Roy Nkwankwazi): I thank you for your constant motivation, support and kindness. Your spirit of *ubuntu* is unexplainable. You are the most amazing lab buddies anyone could ever ask for!

To my mother (Rose Ngcephe) and sister (Ntombenhle Ngcephe): No amount of words can describe how blessed and grateful I am to have you in my life. Thank you for your continued support and words of encouragement. I will forever treasure the sacrifices you always make to see me succeed. Your love for me is beyond doubt.

Special thanks to the Chemistry Department and the National Research Foundation (NRF) for funding this project.

Ayanda Maria Ngcephe

Abstract

The aim of this study was to recover the platinum group elements (PGE) from recycled or waste material using hydrometallurgical techniques. The waste material that was investigated for the possible isolation of PGE is a spent automotive catalytic converter sample, ERM®-EBS504 which is a certified reference material for Pt, Pd and Rh. Surface analysis on the catalyst sample was performed using the scanning electron microscope coupled with energy dispersive X-ray spectroscopy (SEM-EDS) in order to identify the main components of the sample. However, the identification and quantification of the PGE using this technique was ineffective due to the concentrations of PGE in the catalyst sample which were below the detection limits of the SEM-EDS.

Two types of dissolution processes, namely *aqua-regia* open-beaker dissolution and sodium peroxide (Na_2O_2) fusion were employed to try and achieve the total dissolution of the automotive catalytic converter sample for the complete and accurate characterisation of PGE using the inductively coupled plasma optical emission spectroscopy (ICP-OES). *Aqua-regia* dissolution offered partial digestion of the sample and percentage recoveries of 66.9(4) %, 63.9(8) % and 41(1) % were obtained for Pt, Pd and Rh respectively at 80 °C and after a reaction time of 180 minutes. On the other hand, sodium peroxide was able to oxidise all the metals in the catalyst sample to easily soluble oxidation states which allowed for the further dissolution of the sample in *aqua-regia*. However, challenges in PGE quantification with the ICP-OES were experienced due to unacceptable and unsatisfactory PGE recoveries which were attributed to spectral interferences caused by the excess Na ions introduced from the Na_2O_2 flux. The introduction of Sc (361.363 nm) as an internal standard compensated effectively for the spectral interference and excellent PGE recoveries were obtained, namely 100(1) % for Pt, 100(3) % for Pd and 103(2) % for Rh. These results were successfully validated in accordance with the criteria of the Internal Standards Organisation (ISO 17025). This method was found suitable and reliable for the quantification of PGE in the automotive catalyst sample at different separation stages. The complete digestion and characterisation of the automotive catalyst sample enabled separation studies of PGE in various aqueous solutions.

Abstract

The separation methods were firstly studied on artificial samples which emulated to a degree of the original composition of the dissolved automotive catalyst sample. Both solvent extraction and selective precipitation methods were investigated for the possible separation and purification of PGE. Trioctylphisphine oxide (TOPO) and 2-mercaptopyridide *N*-oxide sodium salt (NaPT) were employed as extractants while NH_4OH and 8-hydroxyquinoline (oxine) were used as precipitants. Oxine was found to be highly selective towards the Pd in the solution precipitation in acidic solutions, resulting in the isolation of this element as a highly stable compound which was characterised using XRD, FT-IR, NMR and CHNS micro-elemental analysis. The selective precipitation of the non-precious elements in the presence of PGE using NH_4OH was found time-consuming and inconclusive results were obtained for the PGE.

Solvent extraction of PGE using TOPO was found very suitable for the extraction of PGE from chloride solutions. Various parameters which included HCl concentration, ligand concentration, type of diluent and type of stripping reagent were investigated in order to optimise the extraction and selectivity for PGE. An increase in HCl concentration suppressed the extraction of PGE by TOPO, while the degree of Pt extraction was unaffected by this variation. Maximum extraction of all the PGE was observed at 4 M HCl and at high TOPO concentrations. These results improved remarkably when kerosene and hexane were used as diluents. The presence of the non-precious elements interfered to some extent with the extraction of PGE with TOPO. However, various stripping reagents such as NH_4SCN proved to be highly selective in the stripping of Pt from Pd, Rh and the non-precious elements, while 2 M HCl proved to be selective towards Rh. Solvent extraction with NaPT proved to be more selective and effective towards Pd. This allowed for the selective isolation of Pd from the PGE and from the non-precious elements. The Pd-mercaptopyridine complex was isolated and successfully characterised with XRD, FT-IR, NMR and CHNS micro-elemental analysis.

These isolation methods were successfully applied to a dissolved and pre-concentrated catalyst sample, and Pt and Pd were successfully recovered with percentage recoveries of 87(4) % and 99(3) % respectively. However, the recovery of Rh using TOPO was unsuccessful, and this was attributed to the formation of the

highly stable $[RhCl_6]^{3-}$ in the presence of high chloride concentrations. The high chloride content in the solution were as a result of the formation and isolation of NaCl during the dissolution process which complicated the sample matrix, and thus the extraction process of PGE using TOPO. This method was also evaluated on a highly-concentrated rhodium waste solution which had been accumulated in the department, but proved to be ineffective. The recovery of Rh from this waste solution was achieved by the co-precipitation of the non-precious elements using oxine, resulting in Rh recovery of 80(4) % in the filtrate.

Key Words

Platinum group elements

Spent automotive catalytic converter

Recycling

Recovery

Dissolution

Separation

Precipitation

Solvent extraction

Quantification

Characterisation

Table of Contents

List of Figures

List of Figures

List of Figures

List of Tables

List of Tables

List of Abbreviations

Analytical Instruments

ICP-OES	Inductive coupled plasma optical emission spectroscopy
SEM-EDS	Scanning electron microscopy-energy dispersive spectroscopy
XRD	X-ray diffraction
FT-IR	Fourier transforms infrared spectroscopy
NMR	Nuclear magnetic resonance
AAS	Atomic absorption spectroscopy
INAA	Instrumental neutron activation analysis
GFAAS	High-resolution continuum source graphite furnace atomic absorption spectroscopy
CHNS	Carbon, hydrogen, nitrogen, sulphur

Ligands

TOPO	Trioctylphosphine oxide
NaPT	Mercaptopyridine *N*-oxide sodium salt
Oxine	8-Hydroxyquinoline

Miscellaneous Terms

PGE	Platinum group elements
PGM	Platinum group metals

EIEs	Easily ionisable elements
CRM	Certified reference material
DMSO	Dimethylsulfoxide
DMF	Dimethylformamide

Statistical Terms

LOD	Limit of detection
LOQ	Limit of quantification
RSD	Relative standard deviation
R^2	Linear regression coefficient
m	Slope

SI Units

^{o}C	Degree Celsius
ppm	Parts per million
Å	Angstrom
Psig	Pound-force per square inch gauge
cm^{-1}	Reciprocal centimetre
MHz	Mega hertz
nm	Nanometer

1 Motivation For This Study

1.1 BACKGROUND

The platinum group metals (PGM), also referred to as platinum group elements (PGE), are a group of six elements which include platinum (Pt), rhodium (Rh), palladium (Pd), ruthenium (Ru), iridium (Ir) and osmium (Os). Along with gold and silver, this group is also referred to as precious metals. The PGE are all elements in the second and third transition series and form part of groups eight to ten in the periodic table (**Figure 1.1)**.

Figure 1.1: The six platinum group metals[1]

Platinum was discovered in 1735 by Antonio de Ulloa y de la Torre-Giral. The name 'platinum' emerged from the Spanish word *platina*, meaning little silver. In the beginning, interest in this element was slow to progress since there were no renowned uses for it. A few years after its discovery, research by the Spanish government led to the discovery of the five additional PGE which were found as

[1] Lenson, B. (2015). What are the platinum group metals? Available at: http://www.specialtymetals.com/blog/2015/3/25/.what-are-the-platinum-group-metals. [Accessed: 08 March 2017].

impurities in the crude platinum.[2] Palladium was discovered by the British chemist, William Hyde Wollaston, while investigating the refining process of platinum, in 1803. Shortly after the discovery of palladium, Wollaston discovered rhodium in a platinum ore sample that was obtained from South America. Osmium and iridium were both discovered by Smithson Tennant in England, in 1803. Ruthenium was the last of the PGE to be isolated and identified. It was discovered by the Russian chemist and naturalist, Karl Karlovich Klaus, in 1844. Klaus discovered ruthenium in platinum ore samples obtained from the Ural Mountains in Russia, and gave it the name *ruthenia,* the Latin word for his home country, Russia.[3]

The PGE normally occur as mixed native or platinoid metals and are usually found in nickel, copper, iron and cobalt-bearing sulphide mineral deposits (**Figure 1.2**). Only palladium and platinum are found in their pure form in nature, while the other elements in this group occur as natural alloys of platinum. The PGE consist of less than 2 % of the weight of the earth's crust with relative abundances of approximately 0.0004 to 0.05 ppm.[4] Their low concentrations in mineral deposits make them difficult to mine and are therefore very expensive.

[2] Brooks, R.R. (1992). *Noble Metals and Biological Systems: Their Role in Medicine, Mineral Exploration, and the Environment*, CRC Press, p. 129.

[3] Precious metals. Available at: http://proelevate.info/precious metals/precious_metals_discoverers_and_name_etymologies.php. [Accessed: 18 May 2016].

[4] Hartley, F.R. (2013). *Chemistry of the Platinum Group Metals: Recent Developments*, Elsevier, p. 10.

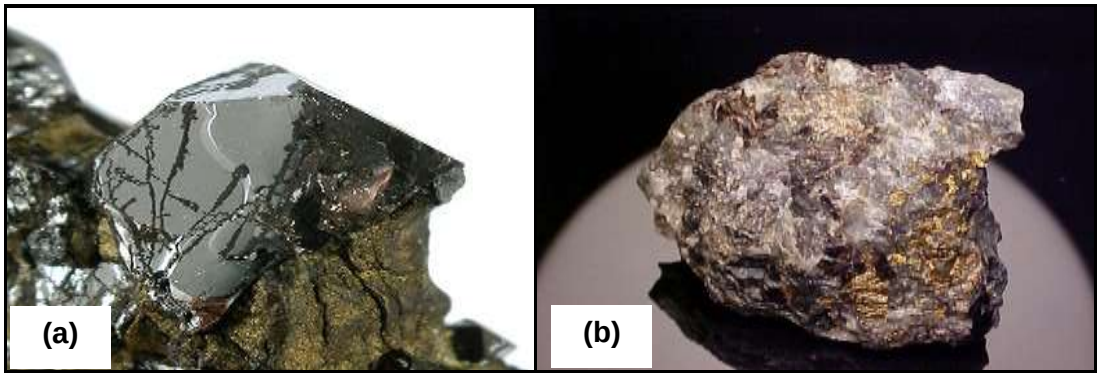

Figure 1.2: The PGE-bearing minerals, (a) sperrylite ($PtAs_2$), (b) braggite ((Pt,Pd,Ni)S) and cooperate ((Pt, Pd) S) with chalcopyrite ($CuFeS_2$)[5,6]

The primary producers of platinum group metals are Russia, Zimbabwe, South Africa and North America. The largest PGE deposits are located in the Bushveld Igneous Complex (BIC), located north of Johannesburg, South Africa. Estimates indicate that these contain roughly eighty percent of the world's known PGE resources and account for over eighty percent of the global annual PGE output.[7]

The platinum group metals possess exceptional catalytic properties. They are extremely corrosion-resistant, making them suitable to the manufacturing of fine jewellery. Other distinct properties include their inertness to chemical attack, excellent electrical properties and high resistance to heat due to their high melting points (from 1 769 to 3 050 °C). These properties make them highly demanded in a wide variety of industries.

Awareness of the important applications of PGE first began with the discovery of the anti-tumour properties of platinum followed by its introduction to automotive catalytic

[5] Sperrylite. Available at: https://commons.wikimedia.org/wiki/File:Sperrylite-mrz288c.jpg. [Accessed: 08 March 2017].

[6] Cooperite & braggite with chalcopyrite, Rustenburg Mine, Western Bushveld Complex, Northwest Province, South Africa.
Available at: http://www.mineralman.com/cooperite.111411.html. [Accessed: 08 March 2017].

[7] The process of mining REEs and other strategic elements. Available at: http://web.mit.edu/12.000/www/m2016/finalwebsite/solutions/newmines.html. [Accessed: 23 February 2017].

converters in motorised vehicles in the United States, Japan and Europe.[8] From **Figure 1.3**, it can be seen that the most important user of PGE is the automotive catalyst industry, followed by the jewellery industry. The automotive industry uses precious metals as catalysts in car exhaust systems to convert harmful exhaust gases, such as hydrocarbons (HC's), nitrous oxides (NO_x) and carbon monoxide (CO) to harmless gases, such as water vapour (H_2O), nitrogen gas (N_2) and carbon dioxide (CO_2).[9]

Figure 1.3: The global uses of platinum group elements[10]

1.2 PROBLEM STATEMENT

The risk of a steady supply of PGE in the near future is very high due to both economic and social issues. The extraction of PGE from mineral deposits is one of the most capital and labour-intensive operations in the world. It takes a period of approximately six months and up to 12 000 kg of ore to produce only 31.135 g of

[8] Townshend, A. (1994). Handbook on metals in clinical and analytical chemistry. *Analytica Chimica Acta*, 294(3), p. 338.

[9] Cooper, J. & Beecham, J. (2013). A study of platinum group metals in three-way autocatalysts. *Platinum Metals Rev*., 57(4), pp. 281-288.

[10] Lomini. (2015). Sustainable development report. Available at: http://sd-report.lonmin.com/2015/corporate-profile/. [Accessed: 23 May 2016].

pure PGE.[11] Furthermore, PGE are mainly obtained from underground mines because of their low concentrations in the earth's crust, thus making them expensive and dangerous to mine. Moreover, mine tailing causes a pollution problem in the environment. The instability of the world and the South African economy, high labour costs, as well as frequent and lengthy labour unrest all contribute to uncertainty regarding the future supply of PGE from ores alone. Another problem is the increase in the number of vehicles on the roads, which gives rise to an overall increase in pollution caused by exhaust emissions. This requires steps to continue improving air quality and reducing pollution, which inevitably create a greater demand for automotive catalysts in the future. Therefore, alternative sources of PGE are needed, one of which is recycled material.

1.3 RECOVERY OF PGE FROM RECYCLED MATERIAL

The recovery of PGE from scrap material has received considerable attention during the last few years. The high cost of mining, increasing demand, and the worldwide scarcity of PGE have led to the increased recovery of these elements from recycled material, such as spent automotive catalysts and other PGE waste concentrates to try and create new or alternative supplies of these elements for their increased global demand.

The PGE, mostly from spent automotive catalysts, are usually combined with ceria (CeO_2), alumina (Al_2O_3) and other oxides. For this reason, it is important that the individual PGE be isolated from other elements and from one another to ensure a high degree of purity as well as a high percentage of recoveries of the original amounts of PGE present in the catalysts.

In order to completely extract the PGE from these waste materials and successfully separate them from one another, it is important to understand their fundamental chemical behaviour in terms of separation and reactivity. In this regard, it is important to note that the PGE are less reactive than the base elements in aqueous solutions

[11] Bell, T. (2016). How is platinum metal produced?
Available at: https://www.thebalance.com/platinum-production-2340167

which enable the separation of PGE from the base elements. The separation of PGE from one another is also possible due to their different chemical behaviours in various aqueous solutions.

The basic separation process begins with the total dissolution of the PGE sample. Digestion methods, such as acid digestion, microwave digestion and flux fusion have been employed in previous studies to attempt a complete dissolution of PGE samples.[12,13] However, the dissolution of PGE with ordinary acids is challenging due to their chemical inertness. Major problems are often also associated with acid and microwave digestion methods which include incomplete sample dissolution and the use of highly corrosive and potentially explosive chemicals, such as $HClO_4$ and HF.

The separation and purification of the individual PGE is the final step in the recovering of precious metals from their solutions.[14] Hydrometallurgical separation methods, such as ion exchange, precipitation and solvent extraction have been applied in the separation of PGE from non-precious elements as well as from one another. The challenges related to the separation of PGE include poor recoveries, especially of rhodium and the contamination of platinum with palladium during the selective separation of these metals from each other, which is due to their chemical similarities.[15,16]

[12] Balaram, V., Anjaiah, K.V. & Kumar, A. (1999). Microwave digestion for the determination of platinum group elements, silver, and gold in chromite ore by ICP-MS. *Asian Journal of Chemistry*, 11(3), pp. 949-956.

[13] Pitre, J. & Bedard, M. (2013). Peroxide fusion dissolution for the determination of platinum, palladium and rhodium in automotive catalytic converters by ICP analysis, pp. 1-5.

[14] Mhmoud, M. H. H. & Barakarat, M. A. (2014). Extraction of rhodium from platinum solutions in presence of aluminium chloride with tri-octylphosphine oxide in toluene. *Adv.Appl.Sci.Res*., 5(4), pp. 100-106.

[15] Raper R., Clements F. S. & Fothergill, S.J. (1962). Separation of platinum from other metals, pp. 1-3.

[16] Nikoloski, A.N., Ang, K. & Li, D. (2015). The recovery of platinum, palladium and rhodium from acidic chloride leach solutions using ion exchange resins. *Hydrometallurgy,* 152, pp. 20-32.

High molecular weight amines, organophosphorus and sulfoxide compounds have been used in the separation of PGE by ion-exchange and solvent extraction from acidic mediums. Solvent extraction has proven to be the most promising method for recovering PGE from their chloride solutions due to a number of reasons: (i) the stability of newly-formed complexes are suitable for their extraction at low metal concentrations; and (ii) it often affords high-metal complex selectivity and purity.[17,18,19]

Bearing this in mind, the purpose of this research is to investigate the chemistry of platinum group elements recovery from the recycled material. Moreover, this study aims to determine the most suitable conditions in which PGE can be recovered and separated to ensure a state of high purity and high percentage of recoveries by hydrometallurgy.

1.4 AIMS AND OBJECTIVES

The aim of this study is therefore to develop a procedure for the recovery of PGE from automobile exhaust system waste, using separation techniques that are both robust and cost-effective. This research will focus mainly on the following objectives:

- To chemically characterise the supplied PGE-containing waste material, using ICP-OES and SEM-EDS in order to identify the chemical constituents of the material and their relative concentrations;

[17] Paiva, A.P., Carvalho, G.I. & Schneider, A.L. (2012). New extractants for the separation of platinum-group metals from chloride solutions and their application to recycling process. *4th International Conference on Engineering for Waste and Biomass Valorisation,* 251, pp. 1-6.

[18] Assuncao, A., Matos, A. & Rosa da Costa, A.M. (2016). A bridge between liquid-liquid extraction and the use of bacterial communities for palladium and platinum recovery as nanosized metal sulphides. *Hydrometallurgy,* 163, pp. 40-48.

[19] Gaikwad, A. P. & Kamble, G. S. (2013). Liquid anion exchange chromatographic extraction and separation of platinum (IV) with n-octylaniline as a metallurgical reagent: Analyses of real samples. *Journal of Chemistry,* 2013, Article ID 103192, pp.1-9.

- To develop an effective method for the dissolution of the provided PGE waste material that does not require the use of dangerous chemicals;
- To accurately and precisely quantify the PGE from waste material by ICP-OES;
- To develop methods that can isolate the platinum group elements from the non-precious elements in solution;
- To separate and purify the individual PGE from one another to ensure a state of high purity and a high percentage of recovery; and
- To validate the methods in accordance with the criteria of the Internal Standards Organisation (ISO 17025).

2 Overview of PGE

2.1 INTRODUCTION

The platinum industry has grown significantly since 1880, mainly due to its increasing demands in modern-day applications, such as in the automotive, jewellery and medical industries. South Africa is the world's leading primary producer of platinum group metals and accounts for approximately 80 % of worldwide platinum production. The first South African platinum deposit was discovered in 1924 by the geologist, Hans Merensky, at the Bushveld Igneous Complex (BIC), and mining and production from these deposits allowed South Africa to become the world's leading platinum producer.[20,21] Other PGE producers include Russia, Zimbabwe and North America while smaller quantities of PGE are also produced in countries, such as Columbia, China and Western Australia.

The exceptional physical and chemical properties of PGE make them suitable for numerous applications in our modern-day technology and industry. Platinum group metals are precious metals which are similar to gold and silver and are therefore scarce and expensive. In order to maintain their future supply to meet the increasing demand, it is crucial to recycle and recover them from waste material which will also have a positive outcome on the global economy.[22] This chapter provides a general overview of the platinum group elements.

---

[20] Renner, H., Schlamp, G. & Drost. E. (2012). Ullman's encyclopedia of industrial chemistry. *Platinum Group Metals*, 28, p. 321.

[21] Cawthorn, R.G. (2006). Centenary of the discovery of platinum in the Bushveld Complex. *Platinum Metals Rev.*, 50(3), pp. 130-133.

[22] Johnson Matthey. (2016). Why recycle? Available at: http://www.jmrefining.com/why-recycle. [Accessed: 23 May 2016].

2.2 NATURAL OCCURRENCE AND CRUSTAL ABUNDANCE LEVELS OF PGE

Most PGE deposits were formed in magmatic ore deposits which were formed during the cooling and crystallisation of magma and are found in mafic and ultramafic igneous rocks. Mafic and ultramafic magmas were saturated in sulphur in the form of immiscible sulphides which separated from the silicate magma and formed metal sulphide particles that turned into concentrated metals, such as copper, nickel and the entire PGE family. As the magma cooled, the PGE-enriched sulphide particles became concentrated and crystallised to form the PGE mineral deposits. **Figure 2.1** shows an example of a magmatic deposit in the Bushveld Igneous Complex (BIC) of South Africa.

Figure 2.1: Chromite- and anorthosite-layered igneous rocks in Critical Zone UG1 of the BIC at the Mononono River outcrop near Steelpoort, South Africa[23]

As indicated previously, platinum group metals co-exist with certain base metals, particularly nickel, copper or chromium. Usually one of these metals is predominant. As a result, the ore will be mined for one specific metal while others are isolate as by-products.[24] Palladium and platinum are the only PGE found in a pure form in nature while others occur as natural alloys of gold and platinum. There are few, scarce and

[23] Layered intrusion. Available at: https://en.wikipedia.org/wiki/Layered_intrusion. [Accessed: 20 March 2017].

[24] Elsevier. (2014). *The Platinum Group Metals Industry*. Available at: http://store.elsevier.com/The-Platinum-Group-Metals-Industry/William-Black/isbn-9781845699215. [Accessed: 12 September 2016].

distinct mineral species containing PGE. These include braggite ((Pt,Pd,Ni)S), cooperate ((Pt,Pd)S), sperrylite ($PtAs_2$), potarite(PdHg) or Pd_3Hg_2, stibia palladinite (Pd_3Sb) and laurite((Ru, Os)S_2)(**Figure 1.2, Chapter 1**).

The platinum group elements account for less than 2 % of the weight of the earth's crust with relative abundances of approximately 0.0004 to 0.05 ppm. **Figure 2.2** shows the relative abundance of different elements, of which PGE are clearly among the rarest, in the earth's crust.

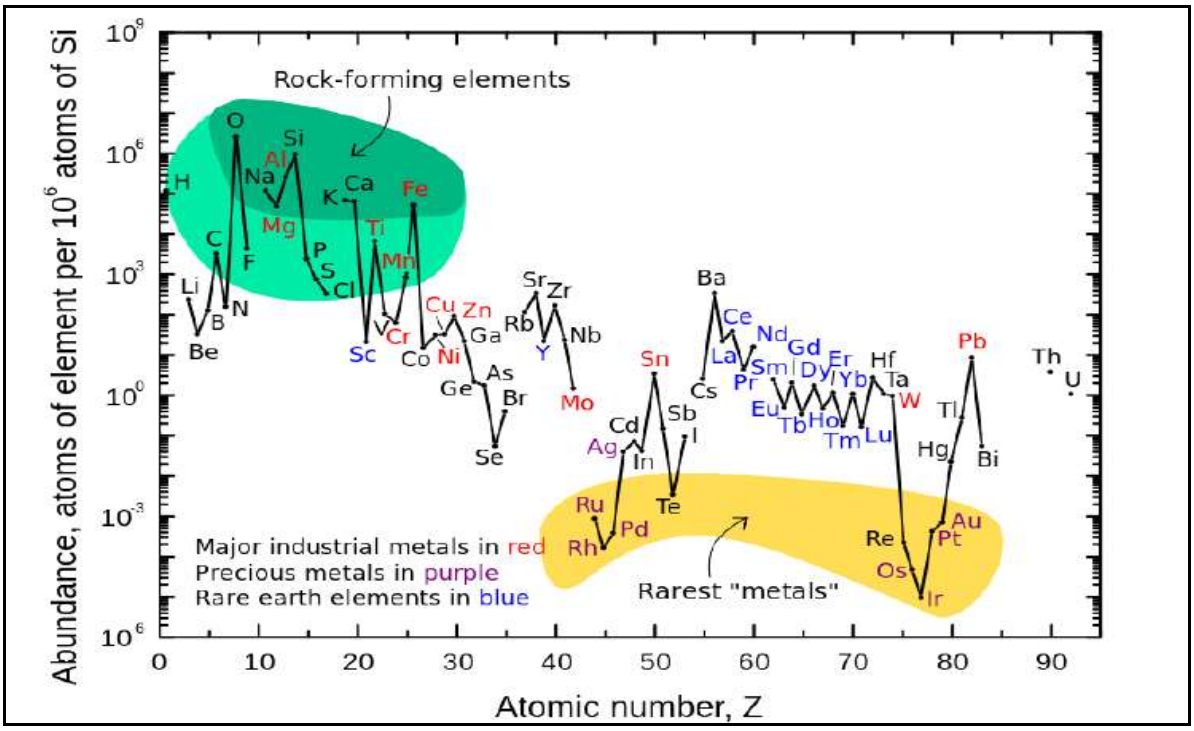

Figure 2.2: Abundance of elements in the earth's crust[25]

2.3 THE SOURCES OF PLATINUM GROUP ELEMENTS

2.3.1 Primary Production

The primary production of PGE represents the transfer of the metals from underground sources to above-ground mineral stock. PGE are usually produced as by-products during the isolation and purification of other elements, such as copper

[25] Douglas, F., Masciangioli, T. & Olson, S. (2012). *The Role of Chemical Sciences in Finding Alternatives to Critical Resources*, p. 8.

and nickel. Moreover, the extraction process of platinum group metals from ores is extremely energy-intensive and has negative environmental consequences.

Major deposits and producing countries

South Africa is the world's primary rhodium and platinum producer and is the second-largest producer of palladium following Russia (**Figure 2.3**).

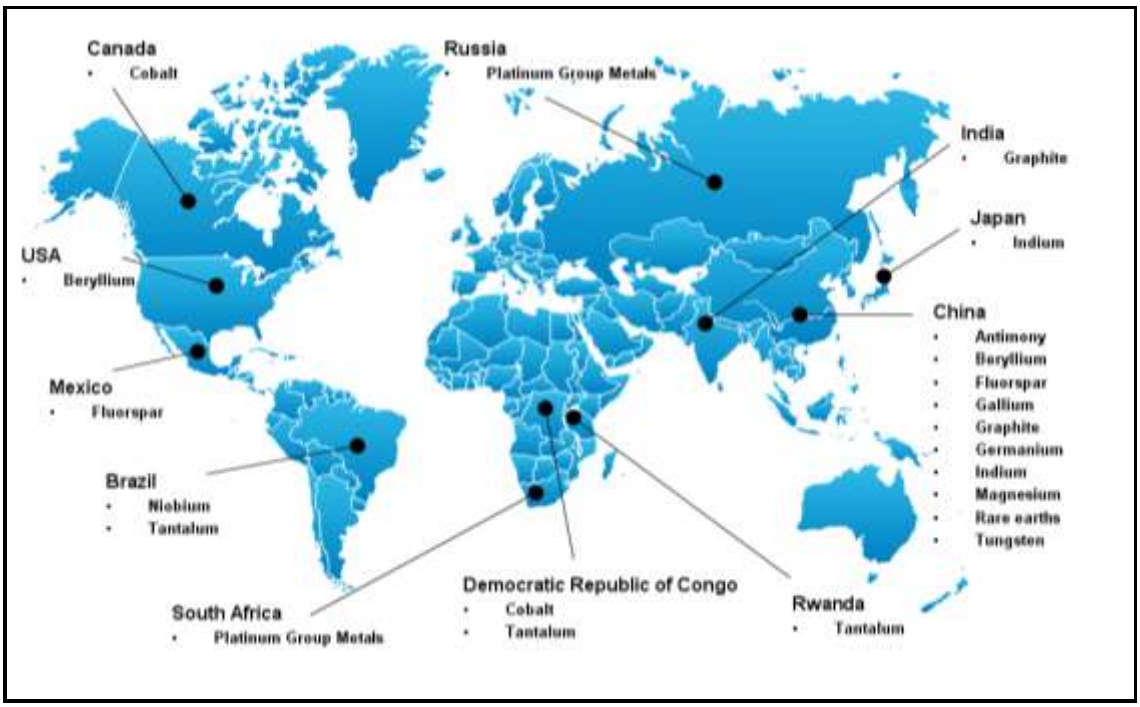

Figure 2.3: Primary PGE producers worldwide[26]

The world's largest known PGE deposit is situated at the BIC in South Africa (**Figure 2.4**). The BIC is a large, layered intrusion into the earth's crust and is located at the edge of the Transvaal Basin in SA.[27] It was formed about 2 000 million years ago and diagonally, it is 370 km long with its centre hidden deep underground while its edges are exposed above the ground. The Bushveld Igneous Complex contains three different mineral-bearing reefs, namely the UG2 Reef, the Merensky Reef and the

[26] Alonso, E. (2008). A case study of the availability of platinum group metals for electronics manufacturers. *2008 IEEE International Symposium on Electronics and the Environment.* Available at: http://dx.doi.org/10.1109/isee.2008.4562902. [Accessed: 29 March 2017].

[27] Bushveld Igneous Complex, South Africa. *NASA Jet Propulsion Laboratory*. Available at: https://www.jpl.nasa.gov/spaceimages/details.php?id=PIA16788 [Accessed 2016 February 2017].

Plat Reef. Whereas the Merensky Reef was the first to be mined for its PGE and is rich in gold, nickel and copper; the UG2 Reef is rich in chromite and has more reliable PGE content, but has a shortage of gold, copper and nickel; and the Plat Reef is broader and has smaller concentrations of PGE but a higher concentration of base metals.[28]

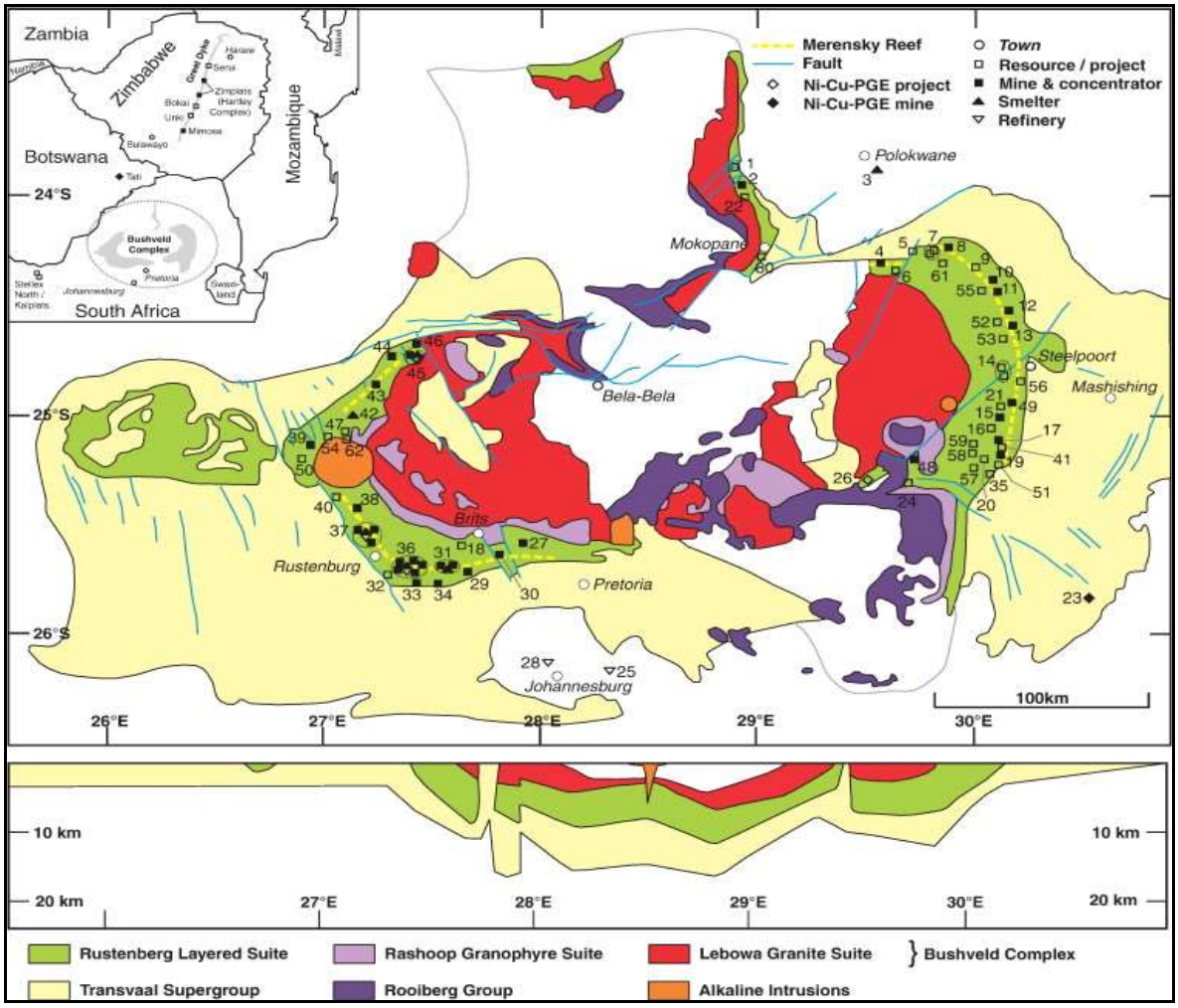

Figure 2.4: Geology of the BIC, South Africa[29]

The world's largest supplier of PGE is the Anglo-American Platinum mine (Amplants) in South Africa which supplies a range of mined, recycled and traded metals. It operates at the Mogalakwena open-pit mine and is based inside the Northern limb of

[28] Anglo American Platinum. (2014). Mogalakwena Mine and Polokwane smelters site visit, pp. 1-27.

[29] Mudd, G. M. (2012). Key trends in the resource sustainability of platinum group elements. *Ore Geology Reviews,* 46, pp. 106-117.

the BIC. The Mogalakwana mine (**Figure 2.5**) was founded in 1993 and is one of the largest open-pit platinum mines in the world.[30]

Figure 2.5: The open pit of the Mogalakwena mine[31]

Other noteworthy PGE deposits in the world include the Munni Munni Complex in Western Australia, the Stillwater Complex in the USA, the Great Dyke in Zimbabwe and Lac des Iles in Canada.

Mining companies in South Africa not only battle with geological conditions but also with threats of industrial actions, poor energy supply and a weak local currency.[32] Extended industrial actions and weak public management in South Africa could have a huge negative effect on global PGE supply, which could lead to an unstable PGE market.

[30] Anglo American Platinum. (2016). Available at: http://www.angloamericanplatinum.com/~/media/Files/A/Anglo-American-Platinum/annual-reports/investors-day-ver29.pdf. [Accessed: 01 August. 2016].

[31] Mine profile: Mogalakwena. Available at: http://www.angloamerican.com/media/our-stories/mine-profile-mogalakwena. [Accessed: 12 September 2016].

[32] Bafokeng Platinum. Available at: http://www.bafokengplatinum.co.za/reports/integrated-report-2015/our-global-PGE.php. [Accessed: 12 September 2016].

Extraction and Refinement

The mining of PGE ores is done by means of underground or open-mine techniques. The mineral deposits obtained from these mining processes are then grinded to very fine particle sizes and the different metal-rich particles separated, using gravity separation, followed by a flotation step to produce a concentrate that is rich in platinum group metals. The PGE-rich concentrate is then smelted to produce a PGE and Cu-Ni matte. The PGE are then extracted and purified at a precious metal refinery, with Cu and Ni produced as by-products.[33] The purification process is summarised in **Figure 2.6**.

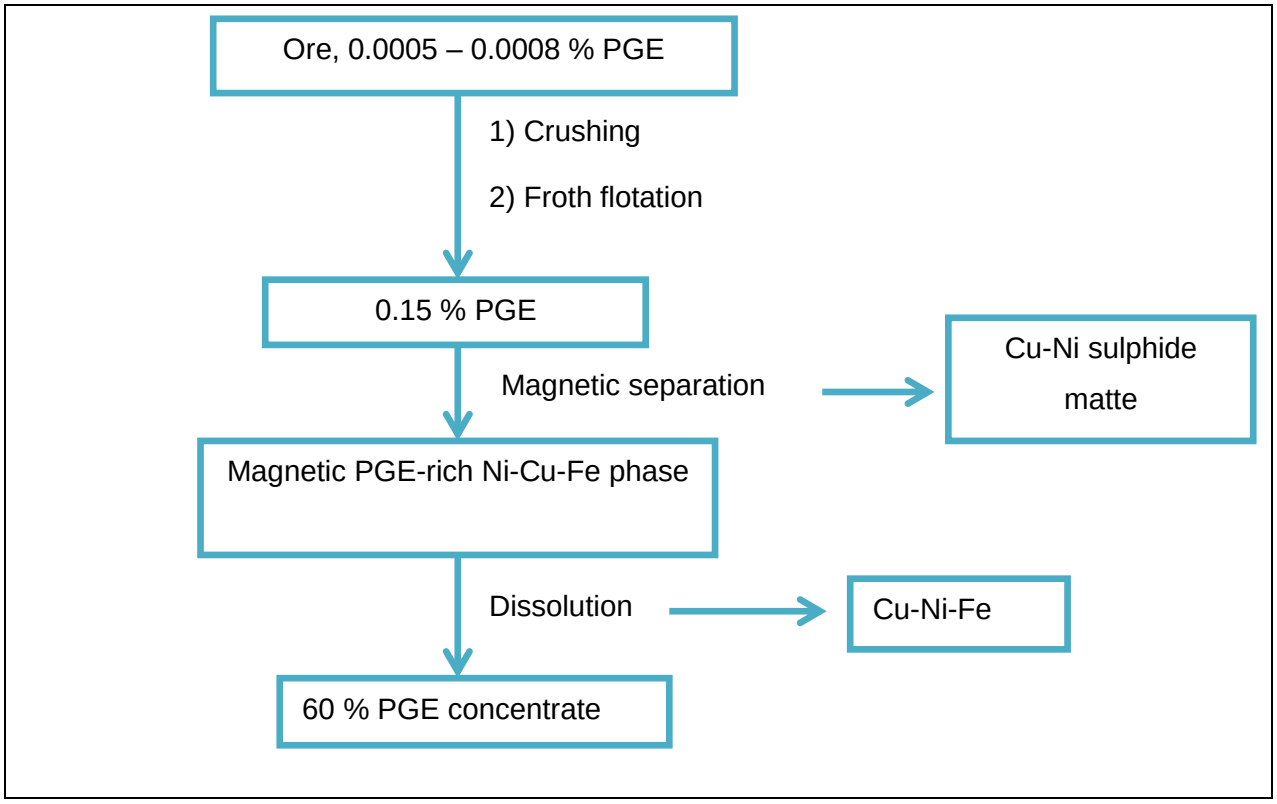

Figure 2.6: Purification flow diagram of platinum group metals from its ores[34]

[33] Othmer, K. (1998). *Encyclopedia of Chemical Technology*, Wiley, p.367.

2.3.2 Secondary Production

A secondary manufacturing process in the production of PGE involves the recycling of these metals from industrial products and scrap material as well as their recovery from waste or tailings generated during primary production. The leading source of waste material used in the recycling of PGE comes from the automotive industry in the form of spent automotive catalytic converters. The recycling of PGE is also important since it provides an additional source of PGE to mining, thereby protecting the environment and saving on resources.[35]

The recycled PGE material is divided into two groups, namely (i) high and medium-grade scrap, and (ii) low-grade scrap. The high- and medium-grade scrap contains more than 10 % of the PGE and includes gauze catalysts and fabricated ware. By contrast, the content of PGE in low-grade scrap is very small. Examples of low-grade material include that from the electronic industry, low-grade automotive catalysts and alumina-supported catalysts. **Figure 2.7** shows scrap automotive catalysts. The general procedure for the recovery of PGE from automotive catalyst scrap is shown in **Figure 2.8**.

Figure 2.7: Recycled automotive catalysts[36]

[35] Fornalczyk, A. & Mariola, S. (2009). Removal of platinum group metals from the used auto catalytic converter. *Metalurgia,* 48(2), p. 133.

[36] Available at: http://www.gclcevre.com/en-EN/Auto-Catalyst-Recycling,PGE_27.html. [Accessed: 20 March 2017].

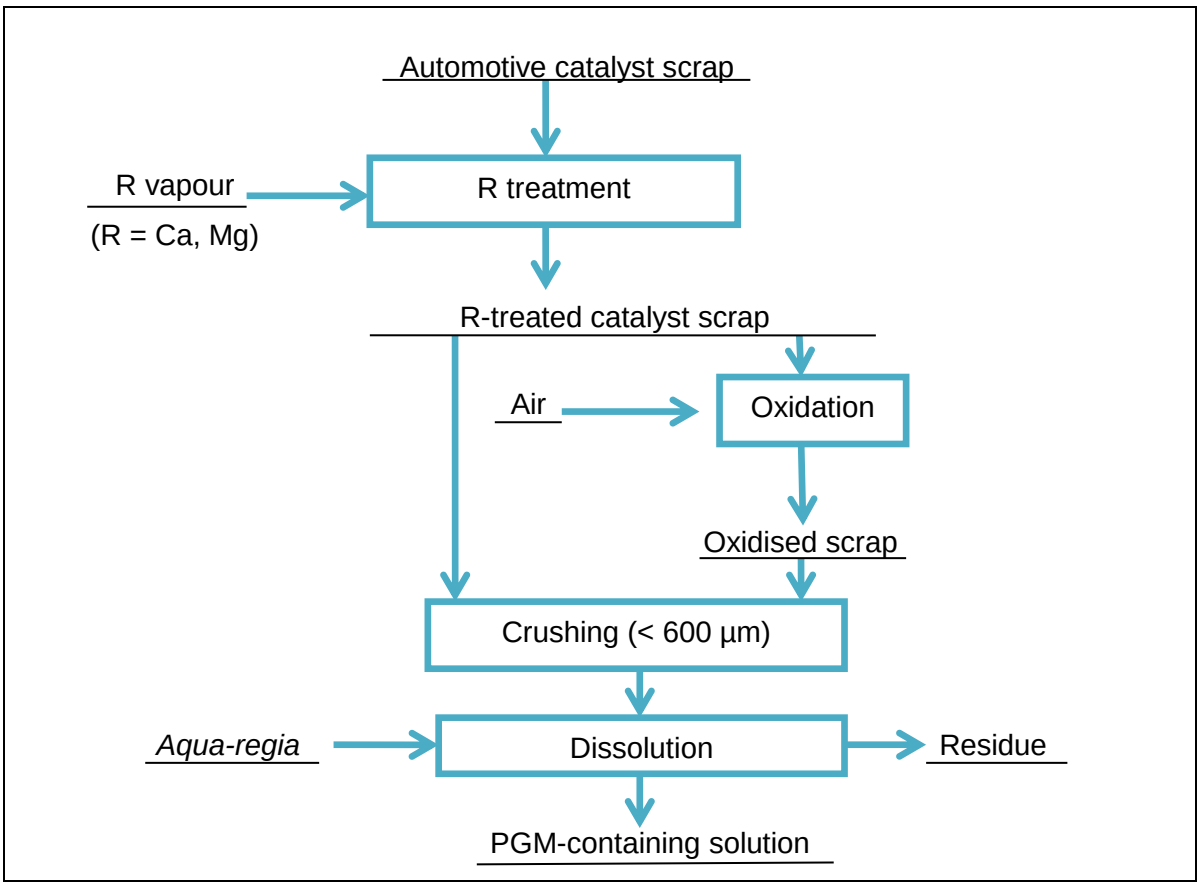

Figure 2.8: Flow chart for the recovery and beneficiation of PGE from spent automotive catalysts[37]

The Innovative Research and Products Inc. (iRap) group estimates that the value of the global PGE recycling market could possibly grow to US $9 bn by 2018 with an increasing supply of waste products from Asia. Growth in PGE recovery from recycling in Asia will beat the average of 9.2 % per annum, while the US market is expected to grow by 7.5 % and Europe by 7.7 %.[38]

A comparison of the estimated production of PGE by 2030, both from primary and secondary sources, is shown in **Figure 2.9**.

[37] Kayanuma, Y. (2004). Metal vapour treatment for enhancing the dissolution of platinum group elements. Available at: http://link.springer.com/content/pdf/10.1007/s11663-004-0075-8.pdf. [Accessed: 21 March 2017].

[38] Big value in recycling platinum. (2014). Available at: http://www.financialmail.co.za/fmfox/2014/05/02/big-value-in-recycling-platinum. [Accessed: 12 September 2016].

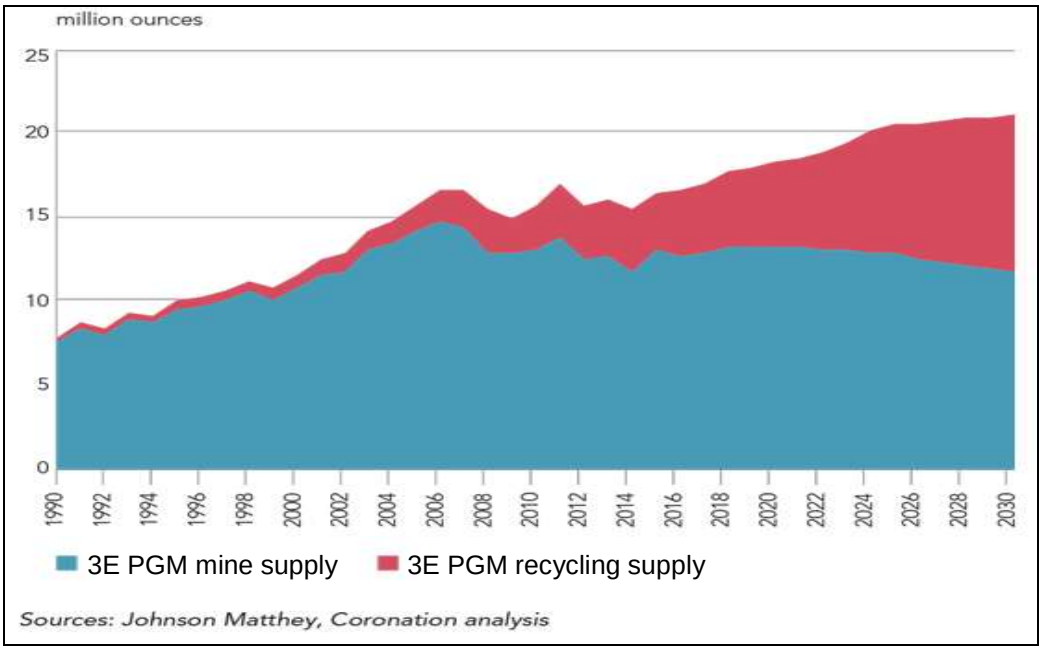

Figure 2.9: The expected PGE supply by the year 2030[39]

From **Figure 2.9** one can see that the supply of PGE from recycling is expected to be about the same as from primary mining activities by the year 2030, indicating that recycling will be vital in securing instant PGE supply.

The report given by the *U.S Geological Survey MSC* predicted that an estimated 125 000 kg of palladium, rhodium and platinum were globally recovered from old and new scrap in 2015 and includes approximately 55 000 kg recovered from recycled automotive catalytic converters alone.[40]

2.4 THE PROPERTIES OF PGE

PGE are transition elements, meaning that they have incomplete *d* or *f* shells in their neutral or cationic state. They are found in rows five and six and in groups eight to ten in the periodic table (**Figure 2.10**). All the platinum group elements are silvery

[39] Hops, N. (2013). Disruption in the automotive industry. Available at: http://www.coronation.com/za/personal/disruption-in-the-automotive-industry-april-2016. [Accessed: 15 February 2017].

[40] US Geological Survey, Mineral commodity summary 2016. Available at: http://minerals.usgs.gov/minerals/pubs/mcs/2016/mcs2016.pdf. [Accessed: 22 March 2017].

white, shiny metals although osmium has a slight blue tint. These elements have similar physical and chemical properties, but every metal behaves in a unique way. They are generally known for their ability to conduct electricity, high density, outstanding catalytic properties, and resistance to high temperatures and oxidation. Pt, Ir and Os are known as the heaviest metals, with platinum being 11 % heavier than gold. Pd, Rh and Ru are less dense while palladium has about the same density as silver.

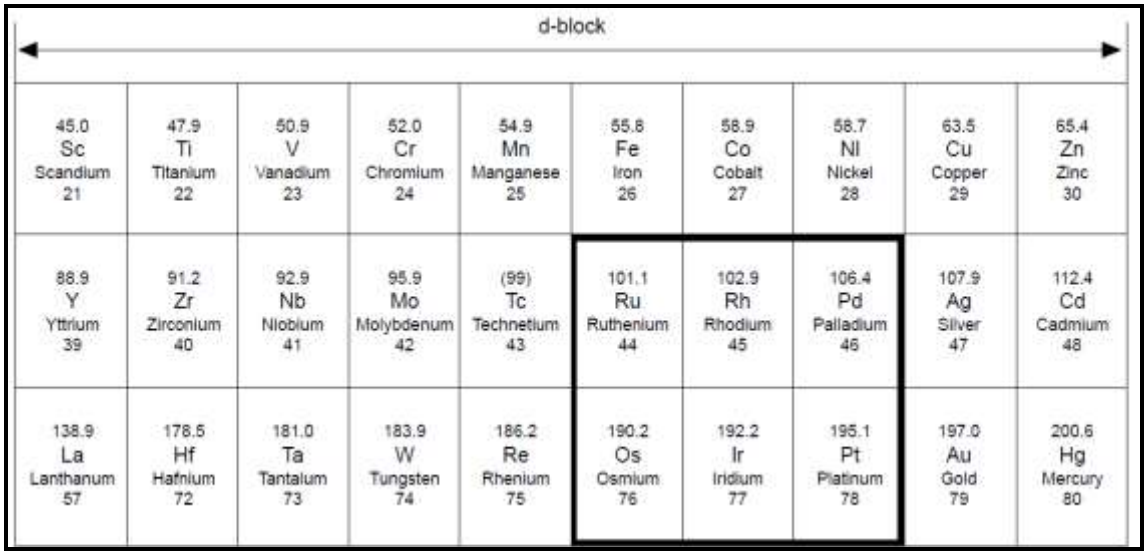

Figure 2.10: PGE and other transition elements in the periodic table[41]

Palladium and platinum are exceptionally corrosion and heat-resistant but are also soft and flexible; iridium and rhodium are difficult to work, whereas osmium and ruthenium are very hard and brittle, and almost unusable in the metallic state. Currently, osmium metal has little known applications in industry because it usually produces a very toxic tetroxide of osmium (OsO_4) when exposed to air. As other PGE are not likely to react with oxygen at room temperature, such reactions can only take place at elevated temperatures (**Table 2.2**).

Ruthenium and osmium crystallise into a hexagonal close-packed system (HCP) in their metallic form, which is reflected in their greater hardness, while others have face-cantered cubic structures (FCC). The physical and chemical properties of PGE

[41] Aspects of the platinum group metals. Available at: http://www.rsc.org/learn-chemistry/resource/download/res00002206/cmp00007484/pdf. [Accessed: 10 March 2017].

make them non-consumable and non-perishable which means restorability to their pure form. Thus, they can be re-used and recycled.

Table 2.1: Properties of the platinum group elements

Element	Pt	Pd	Rh	Ir	Ru	Os
Atomic weight	195.08	106.42	102.91	192.22	101.07	190.23
Atomic number	78	46	45	77	44	76
Density (g/cm^3)	21.45	12.02	12.41	22.65	12.45	22.61
Melting point (°C)	1769	1554	1960	2443	2310	3050
Vickers hardness no.	40	40	101	220	240	350
Electrical resistivity (μΩ.cm at °C)	9.85	9.93	4.33	4.71	6.80	8.12
Thermal conductivity (W/m/ °C)	73	76	150	148	105	87
Tensile strength (kg/mm^2)	14	17	71	112	165	-
Natural Isotopes	^{190}Pt, ^{192}Pt, ^{194}Pt,^{195}Pt ^{196}Pt,^{198}Pt	^{102}Pd, ^{104}Pd, ^{105}Pd, $^{106}Pd$$^{108}Pd$, ^{110}Pd	^{103}Rh	^{191}Ir, ^{193}Ir	^{96}Ru, ^{98}Ru, ^{99}Ru, ^{100}Ru, ^{101}Ru, ^{102}Ru, ^{104}Ru	^{184}Os, ^{186}Os, ^{187}Os, ^{188}Os,^{189}Os, ^{190}Os, ^{192}Os
Crystal Structure	FCC	FCC	FCC	FCC	HCP	HCP

Table 2.2: Reaction of platinum group elements with pure or atmospheric oxygen[42]

Element	Extent of oxide formation	Oxide formed	Formation temperature/°C
Pt	Negligible	PtO_2	< 1000
Pd	Superficial	PdO	> 750
Rh	Superficial	Rh_2O_3	~700
Ir	Superficial	IrO_2	~700
Os	Considerable	OsO_4	200
Ru	Superficial	RuO_2	700

2.5 THE CHEMISTRY OF PGE

PGE are transition elements and, like any other transition element, they tend to show variable oxidation states. The transition elements are the only group of elements whose valence electrons are found in more than one shell or energy level, which allows for many oxidation states. Another important property of transition elements is that they have a tendency to form a variety of complexes with anionic and neutral ligands, and the type of complex formed is determined by the oxidation state thereof. These elements form binary complexes, as well as coordination and organometallic compounds.

PGE differ from most transition elements and are soft Lewis acids, meaning that they are likely to form π-bonded complexes with ligands, such as thiourea, phosphine, S^{2-}, and SCN^-. On the other hand, most other transition elements are regarded as hard Lewis acids, which imply that they tend to form σ-bonded complexes with hard Lewis bases, such as NH_3, O^{2-} and F^-.[43]

Another important aspect of PGE in their pure state is their ability to resist chemical attack by different mineral acids and bases, which renders them crucial in the

[42] National Research Council (US). (1980). *Supply and Use Patterns for the Platinum-group Metals: National Academies*, p. 30.

[43] Edwards, R.I. & Bernfeld, G.I. (1986). *Gmelin Handbook of Inorganic Chemistry*, *8th edition*. Springer, p. 9.

jewellery industry. Their ability to resist corrosion and oxidation often makes these metals chemically inactive, hence the name ‘noble metals’, with the result that they also do not easily react with ligands to form different inorganic compounds. However, for the base metal group of elements, new complexes are easily formed with the substitution of one ligand by another. While these reactions are rapid, for PGE the rates of similar reactions are slow and almost incomplete. This is attributed to their high electronegativity and the electron configuration in the elements.[44]

PGE compounds find many applications in today’s technology and industry. For example, platinum organic compounds have significant anti-tumour activity (**Section 2.6**), while some PGE inorganic compounds, such as chloroplatinic acid ($H_2PtCl_6.xH_2O$), palladium chloride ($PdCl_2$) and rhodium tribromide ($RhBr_3.xH_2O$) are used as raw materials for catalytic processes.[45]

2.5.1 PGE Chloride Complexes

Chloride complexes are the most important compounds of PGE. The chloro complex anions are also the most studied compounds since the separation chemistry of PGE is greatly dependent on the properties of the stable PGE chloro complex anions. Aqueous chloride solutions are also the only economically viable mediums in which the PGE are dissolved and concentrated. The different PGE species found in chloride media are shown in **Table 2.3**.

[44] Reza, G. (2014). *Rare and Precious metals: Platinum*, *1st edition.* Juvenile Literature, p. 6.

[45] National Academy of Sciences. (1980). *Supply and Use Patterns for Platinum Group Metals*, Washington DC, p. 63.

Table 2.3: PGE chlorides in aqueous media[46]

Ruthenium		Rhodium		Palladium	
Ru(III)	$[RuCl_6]^{3-}$ $[RuCl_5(H_2O)]^{2-}$ $[RuCl_4(H_2O)_2]^{-}$ $[RuCl_3(H_2O)_3]$	**Rh(III)**	$[RhCl_6]^{3-}$ $[RhCl_5(H_2O)]^{2-}$ $[RhCl_4(H_2O)_2]^{-}$	**Pd(II)**	$[PdCl_4]^{2-}$
Ru(IV)	$[RuCl_6]^{2-}$ $[Ru_2OCl_{10}]^{4-}$ $[Ru_2OCl_8(H_2O)_2]^{2}$	**Rh(IV)**	$[RhCl_6]^{2-}$	**Pd(IV)**	$[PdCl_6]^{2-}$
Osmium		**Platinum**		**Iridium**	
Os(IV)	$[OsCl_6]^{2-}$	**Pt(II)**	$[PtCl_4]^{2-}$	**Ir(III)**	$[IrCl_6]^{3-}$ $[IrCl_5(H_2O)]^{2-}$ $[IrCl_4(H_2O)_2]^{-}$
		Pt(IV)	$[PtCl_6]^{2-}$	**Ir(IV)**	$[IrCl_6]^{2-}$

From **Table 2.3** it is clear that (i) PGE form a series of aqua chloro-complexes in oxidation states of +III; (ii) PGE in their tetravalent oxidation states form hexachloro complex ions, which occurs in high-chloride concentrations; (iii) platinum and palladium are the only PGE-forming tetrachloro complexes in aqueous chloride media, which occurs at relatively low-chloride concentrations; and (iv) unlike other PGE, ruthenium forms a series of oxo-bridged dimers in oxidation states of +IV.

46 Francesco, L., Grant, R. A. & Sherrington, D.C. (2005). A review of methods of separation of the platinum-group metals through their chloro-complexes. *Reactive and Functional Polymers,* 65(3), pp. 205-217.

The role of chloride concentration on the separation chemistry of PGE

The type of PGE metal chloride species which are formed in an aqueous solution is dependent on the concentration of the chloride solution. For example, in strong chloride solutions, the hexachloro palatinate (IV) complex, $[PtCl_6]^{2-}$ predominates in solutions whereas tetrachloro pallidate (II), $[PdCl_4]^{2-}$ is the dominant metal species at low HCl concentrations. However, hexachloro rhodate (III) complex $[RhCl_6]^{3-}$ is the dominating species when the HCl concentration is greater or equal to 6 M.[47] At low-chloride concentrations, a variety of PGE aqua-species are formed and, unlike other PGE, the Pt and Pd complexes are stable at low-chloride concentrations to produce complete anionic species, such as $[PtCl_4]^{2-}$ and $[PdCl_4]^{2-}$ respectively. Other PGE form mixed aqua-chloro complexes in the same conditions. For example, rhodium forms $[RhCl_4(H_2O)_2]^{-}$ or $[RhCl_5(H_2O)]^{2-}$ as different aqua-chloro species (see **Table 2.3**).

The reactivity of the PGE-chloride complexes with other ligands occurs in the following order:

$PdCl_4^{2-} > PtCl_4^{2-} > RhCl_6^{3-} > OsCl_6^{3-} > (Ru,Ir)Cl_6^{3-} >> (Pt,Ir,Ru,Os)Cl_6^{2-}$

The literature also indicates that the PGE tetrachlorides are more reactive than the hexachlorides and the type of chloride complex formed depends significantly on the oxidation state of the metal and the concentration of the acid. These differences in reactivity, as well as the type of complex formed in the reaction process, allows for the separation of PGE from one another. In their divalent oxidation states and low-HCl concentrations, palladium and platinum will form tetrachloro complexes, $[PdCl_4]^{2-}$ and $[PtCl_4]^{2-}$, respectively, which are very reactive to substitution by soft donor ligands. The rates of substitution reactions for these complexes are also rapid as compared to those of other PGE in higher-oxidation states, which allows for the possible isolation of Pd and Pt from other PGE.

[47] Nokoloski, N.A. & Ang, K. (2014). Review of the application of ion exchange resins for the recovery of platinum group elements in hydrochloric acid solutions. *Mineral Processing & Extractive Metal. Rev*., 35, pp. 369-389.

2.5.2 Reactions of PGE with Other Halides[48]

Platinum group elements also react with other halogens to form a variety of new metal halide complexes according to the equation:

$$2M + nX_2 \rightarrow 2MX_n \quad \textbf{(2.1)}$$

where M is a metal, X is a halogen and MX_n is a metal halide and include fluorine, chlorine, iodine and bromine as halogens.

Platinum

Different platinum halides are synthesised according to the following equations:

$$Pt \xrightarrow[500°C]{Cl_2} PtCl_2 \quad \textbf{(2.2)}$$

$$Pt \xrightarrow{Br_2} PtBr_3 + PtBr_4 \xrightarrow{250°C} PtBr_3 \quad \textbf{(2.3)}$$

$$Pt \xrightarrow[\text{Sealed tube, 60°C}]{KI/I_2/H_2O} PtI_3 \quad \textbf{(2.4)}$$

Palladium

The synthesis of palladium halides often involves the direct reaction of the element with a halogen gas.

$$Pd \xrightarrow[>260°C]{Cl_2} PdCl_2 \quad \textbf{(2.5)}$$

$$Pd \xrightarrow{HBr\ /Br_2} PdBr_2 \quad \textbf{(2.6)}$$

[48] Cotton, S.A. (1997). Chemistry of precious metals. *Uppingham School, Rutland, UK*, pp. 1-185.

$$Pd \xrightarrow[\text{Sealed tube/140°C}]{\text{5\% HI}} PdI_2 \qquad \textbf{(2.7)}$$

Rhodium

Rhodium halides normally form complexes with the metal in the +3-oxidation state.

$$Rh \xrightarrow[800°C]{Cl_2} RhCl_3 \qquad \textbf{(2.8)}$$

$$Rh \xrightarrow[Br_2,\ 400°C]{45\%/HBr,\ Br_2,\ \Delta} RhBr_3\ (red) \qquad \textbf{(2.9)}$$

$$Rh \xrightarrow[400°C]{I_2} RhI_3\ (black) \qquad \textbf{(2.10)}$$

$$RhCl_3 \xrightarrow[500°C]{F_2} RhF_3\ (red) \qquad \textbf{(2.11)}$$

Iridium

Iridium closely resembles rhodium as metal and produces halide complexes with the metal in higher-oxidation states.

$$IrF_4 \xrightarrow{400°C} IrF_3\ (black) \qquad \textbf{(2.12)}$$

$$Ir \xrightarrow[600°C]{Cl_2} \alpha\text{-}IrCl_3\ (brown) \xrightarrow[vacuum]{750°C} \beta\text{-}IrCl_3\ (deep\ red) \qquad \textbf{(2.13)}$$

Ruthenium

The type of halide complexes isolated for Ru normally contain the metal in its higher-oxidation state.

$$Ru \xrightarrow[450°C,\ 20\ atm]{Br_3} RuBr_3\ (brown\text{-}black) \qquad \textbf{(2.14)}$$

$$Ru \xrightarrow{F_2} RuF_5\ (green) \qquad \textbf{(2.15)}$$

Osmium

Osmium, unlike other platinum group elements, forms chlorides and bromides in a range of oxidation states. Osmium halides can be prepared as follows:

$$Os \xrightarrow[700°C]{Cl_2} OsCl_4 \qquad \textbf{(2.16)}$$

$$Os \xrightarrow[10atm,\ 470°C]{Br_2} OsBr_4 \qquad \textbf{(2.17)}$$

$$Os \xrightarrow[600°C/450\ atm]{F_2} OsF_7 \qquad \textbf{(2.18)}$$

2.5.3 Organometallic Compounds

The first PGE organometallic compound to be synthesised and isolated is the potassium tri-chloro (ethylene) palatinate (II), also commonly known as the Zeise's salt.[49] This compound is one of the first examples of a transition metal alkene complex with the platinum atom situated within a square planar geometry. It was synthesised by a reaction between K_2PtCl_4 and ethylene, with $SnCl_2$ as a catalyst. The in-depth study of this compound played an important role in the evolution of the bonding theory in both organic and inorganic chemistry.[50]

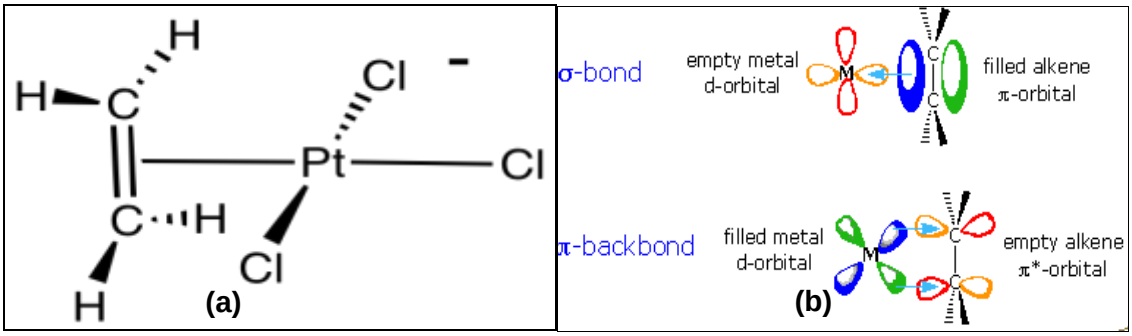

Figure 2.11: (a) Potassium tri-chloro (ethylene) palatinate (II), (b) orbital interaction between platinum metal (M) and ethylene[51]

The bonding between the platinum metal and the ethylene occurs as a result of the π-bond electron donation of the ethylene molecule to the vacant Pt^{2+} d-orbitals, while the filled d-orbital on the Pt^{2+} ions donates the electron density to the empty π-antibonding (LUMO) of the ethylene, resulting in the formation of this rather unexpected stable molecule.[52] Other common PGE organometallic compounds, their properties and their formation are summarised in **Table 2.4**.

[49] Miessler, G.L. & Tarr, D.A. (2004). *Inorganic Chemistry*, *3rd edition*, p. 457.

[50] Shoemaker, A.K. & Leadbeater, N.E. (2009). A fast and easy approach to the synthesis of Zeise's salt using microwave heating. *Inorganic chemistry communications*, 12(5), pp. 341-342.

[51] Organometallic chemistry.
Available at: https://en.wikipedia.org/wiki/Organometallic_chemistry . [Accessed: 06 February 2017].

[52] Kots, J.C., Treichel, P.M. & Townsend, J.R. (2010). *Chemistry and chemical reactivity*, *7th edition*, p. 430.

Table 2.4: Organometallic complexes of platinum group elements[53]

Complex	Form	Structure type	Comment
π-$C_5H_5Ru(CO)_2C_2H_5$	Colourless oil m.p. -5 °C	π-cyclopentadienyl alkyl	Volatile. Stable in air Petroleum soluble
$(Et_3P)_2PdCl(COCH_3)$	Yellow crystals m.p. 50 °C	Alkyl	Formed by CO insertion into $PdClCH_3(PEt_3)_2$
$K[C_2H_4PtCl_3]$	Pale yellow crystals	Olefin	Water-soluble
$[C_7H_8RhCl]_2$	Yellow crystals m.p. ~240 °C	Olefin (norbornadiene)	Soluble in organic solvents. Air-stable. Halogen bridged
$Pt(PPh_3)_2(C_4Fe)$	White crystals m.p. 215 °C	Acetylene	Stable. Soluble in organic solvents
π-$C_5H_5Rh(C_5F_6O)$	Orange crystals m.p. 150 °C	Acetylene-derived cyclopentadienone	Extremely chemically inert
$(\pi$-$C_5H_5)_2Ru$	White crystals	Sandwich	Undergoes aromatic substitution reactions. Oxidisable $(\pi$-$C_5H_5)_2Ru^+$
$C_6H_9OPdCl(C_6H_7N)$	Yellow needles	Allylic	Has mesityl oxide bound as allyl group with free ketone group

[53] Wilkinson, G. (1964). Organometallic compounds of the platinum metals. *Platinum Metals Rev.,* 8(1), pp. 16-22.

2.6 THE IMPORTANCE OF PGE

The unique chemical and physical characteristics of PGE make these elements extremely important to modern-day technology and industry. The need for platinum group metals is mostly driven by the ecological or environmental constrains put on the automotive industry. Commercially, platinum and palladium are most important while other PGE are mostly used as alloying agents with platinum and palladium. Markets reveal that the demand for PGE, especially for automotive catalysts, has steadily increased over the past years and surpassed the global supply of these metals (**Figure 2.12**). This is mainly attributed to the rapid growth of the automotive industry, especially in India and China. However, this is also due to legislative demands to improve air quality and reduce the emission of toxic and smog materials.

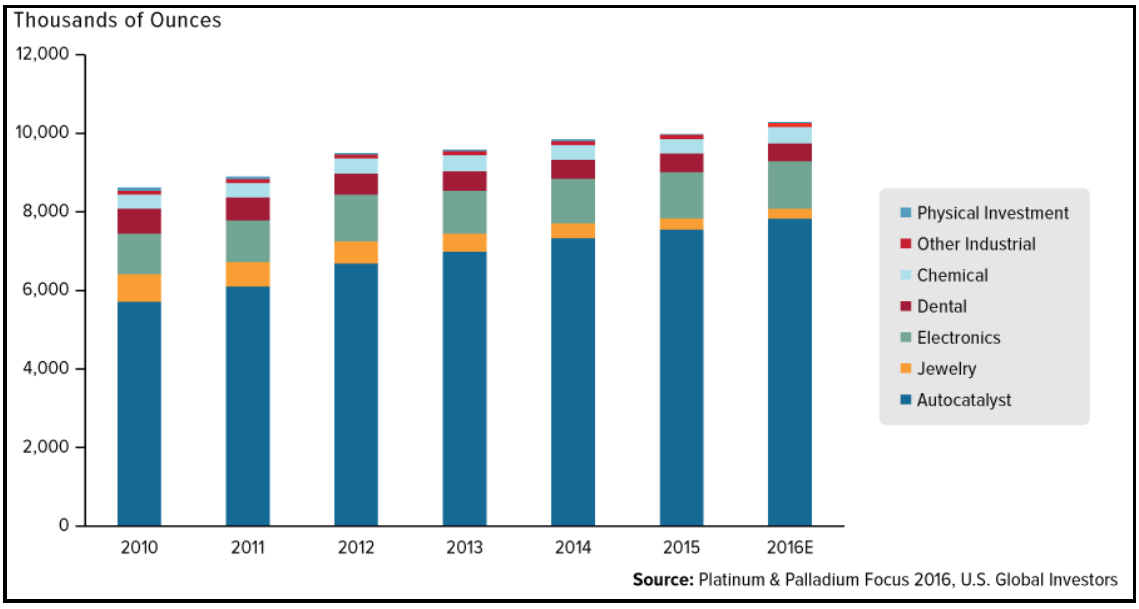

Figure 2.12: The increasing demand for PGE in the automotive industry over the years[54]

[54] Holmes, F. (2016). US Global Investors. Available at: http://www.usfunds.com/investor-library/frank-talk/category/topics/gold/. [Accessed: 02 May 2017].

2.6.1 The Automotive Industry

The automotive industry is the leading consumer of PGE and utilises about 60 % of the produced PGE, mainly as catalysts (**Figure 2.13**). These catalysts are said to be the leading technology used to control the emissions from petrol engines. The catalysts use a metallic or ceramic substrate with an active coating and include Al_2O_3, CeO_2 and other oxides in combination with the PGE (Pd, Pt and Rh). The following conversion reactions of the toxic smog gases to less harmful gases occur in the automotive catalyst:

The reduction of nitrogen oxides to nitrogen and oxygen:

$$2NO_x \longrightarrow xO_2 + N_2 \qquad \textbf{(2.19)}$$

Oxidation of carbon monoxide to carbon dioxide:

$$2CO + O_2 \longrightarrow 2CO_2 \qquad \textbf{(2.20)}$$

Oxidation of unburned hydrocarbons to carbon dioxide and water:

$$C_xH_{2x+2} + [(3x+1)/2]O_2 \longrightarrow xCO_2 + (x+1)H_2O \qquad \textbf{(2.21)}$$

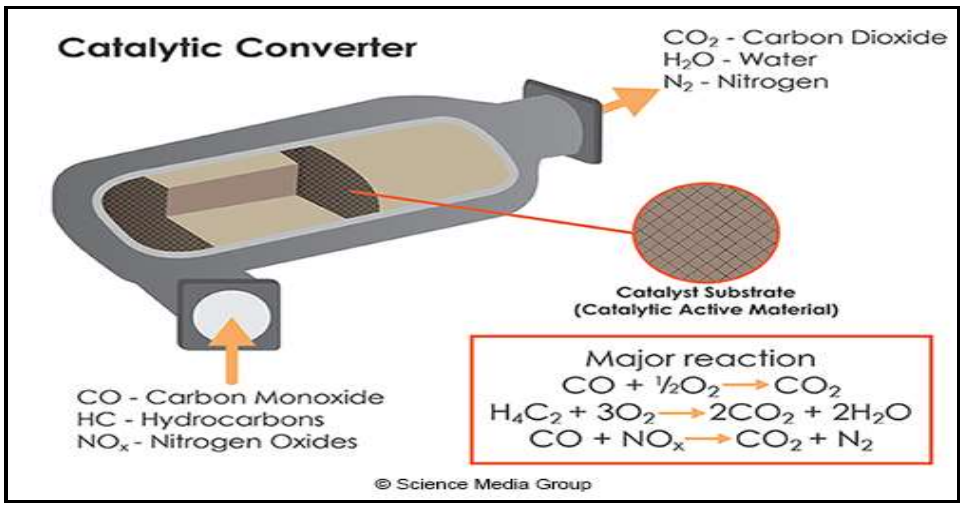

Figure 2.13: The three-way catalytic converter[55]

[55] Catalytic Converters: Chemistry of Air Pollution. Available at: http://www.uen.org/Lessonplan/preview.cgi?LPid=37774. [Accessed: 20 May 2016].

2.6.2 The Jewellery Industry

Platinum group elements are also popularly used in conjunction with coloured stone and diamond jewellery due to their strength and durability (**Figure 2.14**). Platinum jewellery is usually combined with other PGE or base metals, such as copper or cobalt to make it more malleable. Normally, the value of platinum jewellery is determined by its purity. The most common platinum alloys include 95 % platinum and 5 % ruthenium or 90 % platinum and 10 % iridium.

Figure 2.14: Platinum combined with diamond jewellery[56]

2.6.3 The Medical Industry

Another application of PGE is the use of some metal complexes as anti-tumour agents in chemotherapy since they react well with biological materials, thus making them suitable for use in the medical industry. The first drug that was manufactured for use as an anti-cancer agent was *cis*-platin. Other drugs include carboplatin and oxaliplatin (**Figure 2.15**).[57] These drugs have been employed in the treatment of various types of cancers including breast, testicular, lung and ovarian cancer.

[56] Goldsmiths-fine diamond and platinum jewellery. Available at: http://www.sa-online-shopping.co.za/portal/business/4222/goldsmiths-fine-diamond-and-platinum-jewellery. [Accessed: 30 March 2017].

[57] Johnson Matthey. (2017). Platinum group metal compounds in cancer chemotherapy, *Technol. Rev*., 61(1), pp. 52-59.

Furthermore, platinum and palladium metals are used in conjunction with silver and gold to make alloys suitable for dental bridges, inlays and crowns.

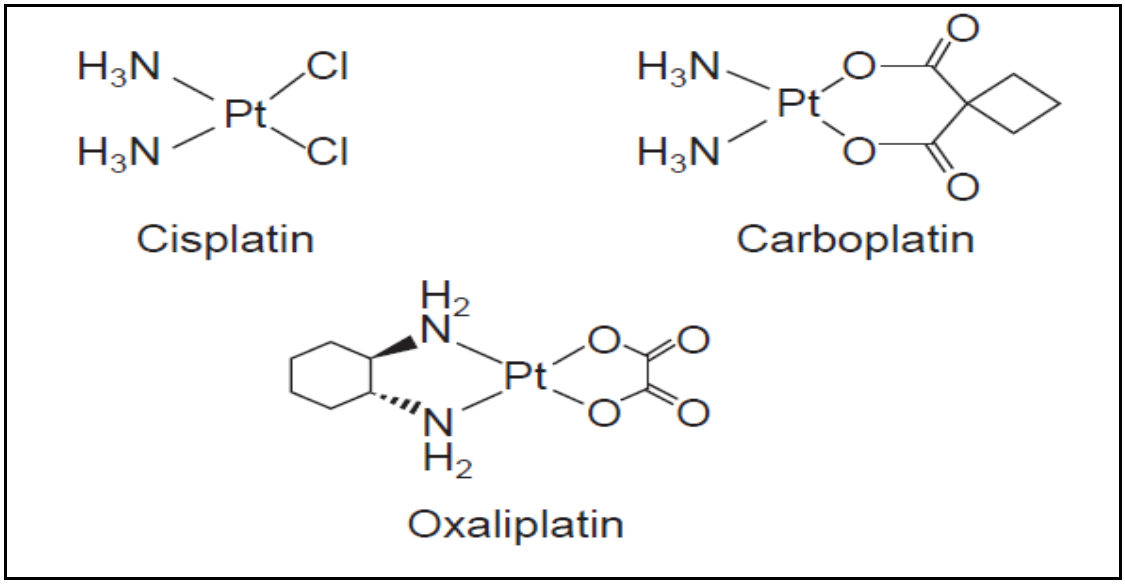

Figure 2.15: Globally marketed platinum-containing drugs[57]

2.6.4 Other Uses

The electronics industry uses palladium in the coatings of ceramic capacitors found in mobile phones and laptops. PGE are also employed in the petroleum industry to upgrade the acetone content of gasoline. They also serve as excellent catalysts in the commercial production of nitrogen fertilisers and nitric acid.

2.7 CONCLUSIONS

PGE possess unique physical and chemical properties which make them crucial to modern-day technology and industry. Markets predict that the demand for PGE is expected to grow in the near future and the supply of PGE is at a higher risk due to geological, social and political issues. Therefore, the recycling of PGE is regarded as one of the most strategic and quickest ways to escape the dependency on PGE mining alone.

Although PGE are extremely inert as compared to other transition elements, they are able to form a variety of stable compounds with different ligands. This property is very

important in their recovery from the recycled material. The separation chemistry of PGE is mostly dependent on the chemistry of their chloride anions, and the study of these chloride anions assists in developing a better understanding of the separation of platinum group elements from one another and from other elements.

3 Literature Review

3.1 INTRODUCTION

Complete sample digestion is critical to the recovery of PGE from waste material such as automotive catalysts since most of the extraction and hydrometallurgical separation techniques are performed in aqueous solutions. Properties that make these metals very resistant to chemical attack include high resistance to tarnish and wear (**Chapter 2, Section 2.4**). The dissolution and liberation of PGE from the waste material is mostly achieved using *aqua-regia* or HCl, which yields a variety of PGE chlorido species in solution. The separation and purification of PGE in these solutions are mainly achieved by utilising the differences in the chemistry of their anionic chloride complexes (**Chapter 2, Section 2.5**). The separation of PGE from base metals is possible since their chlorido complexes are generally more stable than those of base metals. However, the similarity in the chemical behaviour of chloride-PGE complexes complicates the separation of these elements from each other. The characterisation, quantification and possible isolation of the PGE from these types of samples are also very challenging as a result of their extremely low concentrations and the presence of interfering matrices when ICP-MS and ICP-OES are used.

Several studies have focused on the recovery of PGE from automotive catalysts; environmental samples, for example; road dust and chromite ores. However, most of these studies focused on the PGE alone, with the result that there are no clear indications as to how the presence of numerous interfering elements affect the recovery of PGE. In addition, little information is available on the recovery of PGE from mineral ores. This chapter will focus on the literature available on PGE recovery methods from various materials.

3.2 DIGESTION METHODS

The complete conversion of solid samples into solution is considered critical in wet chemistry as it determines the success of the chemical analysis as well as possible beneficiation. Methods, such as microwave-assisted acid digestion, open-vessel digestion, cyanide leaching, chlorination, fire assay and peroxide fusion have been reported in the digestion of PGE in the analysis of different organometallic, inorganic and recycled materials, as well as environmental and geological samples. Amongst these techniques, microwave-assisted acid digestion and peroxide-fusion methods have received enormous attention due numerous reasons, including their ability to achieve reasonable dissolution of the above-mentioned samples, requiring small amounts of reagents and limiting sample loss.

3.2.1 Microwave-Assisted Acid Digestion

Microwave-assisted acid digestion has been employed for the dissolution of PGE samples due to advantages, such as the ability to control reaction temperature and pressure. The method also minimises the possible introduction of contaminants and is considered a fast and energy-efficient way of dissolving the PGE. It is often preferred over open or heated closed systems. The most commonly-used acids associated with microwave digestion of PGE are *aqua-regia*, HCl, HNO_3, $HClO_4$ and HF.

Microwave digestion with HCl, HNO_3 and aqua-regia

The dissolution of platinum group metals and compounds is mainly achieved using a strong oxidising agent such as *aqua-regia. Aqua-regia* usually brings about partial digestion and utilises a combination of nitric and hydrochloric acid to dissolve oxides, sulphides and silicates. The combination of HCl and HNO_3 produces nitrosyl chloride as a powerful oxidising agent as well as Cl^- as a coordinating ligand which reacts with the PGE samples.

The following reactions take place when the PGE are dissolved in *aqua-regia* [58]:

$$3Pt(s) + 18HCl(aq) + 4HNO_3(aq) \longleftrightarrow 3[PtCl_6]^{2-}(aq) + 6H^+(aq) + 4NO(g) + 8H_2O \quad \textbf{(3.1)}$$

$$3Pd(s) + 12HCl(aq) + 2HNO_3(aq) \longleftrightarrow 3[PdCl_4]^{2-}(aq) + 6H^+(aq) + 2NO(g) + 4H_2O \quad \textbf{(3.2)}$$

$$2Rh(s) + 12HCl(aq) + 2HNO_3(aq) \longleftrightarrow 2[RhCl_6]^{3-}(aq) + 6H^+(aq) + 2NO(g) + 4H_2O \quad \textbf{(3.3)}$$

Aqua-regia usually affords complete dissolution for palladium and platinum in some samples, and the reactions occur even faster as a result of microwave digestion, while rhodium partially dissolves in this acid mixture. Osmium, ruthenium and iridium, on the other hand, do not react with *aqua-regia*.

The dissolution of Pd, Pt and Rh from a used autocatalyst material, using microwave-assisted dissolution was studied by Suoranta et al.[59] Different acids, which included HCl, HNO_3 and *aqua-regia*, were used in this study to try and achieve complete dissolution of the solid samples. The samples were reacted with these acids at five different temperatures, ranging between 90 °C and 210 °C. HCl and *aqua-regia* were successful in leaching over 90 % of the PGE in these samples at temperatures higher than 150 °C. The recoveries decreased slightly (78 % to 93 %) at a temperature of 120 °C and decreased further at 90 °C. The recoveries ranged from 31 % to 90 %, when HCl was used. The study indicated that on its own, HNO_3 was an extremely poor solvent to dissolve PGE from the used catalyst samples.

58 De Aberasturi, J. (2011). Recovery by hydrometallurgical extraction of the platinum-group metals from car catalytic converters. *Minerals engineering*, 24(6), pp. 505-513.

59 Suoranta, T., Zugazua, O. & Niemela, M. (2015). Recovery of palladium, platinum, rhodium and ruthenium from catalyst materials using microwave-assisted leaching and cloud point extraction. *Hydrometallurgy*, 154, pp. 56-62.

Okori et al.[60] investigated the quantification of PGE in urban road dust. The samples were dissolved, using microwave-assisted acid digestion with *aqua-regia*. The digested samples were evaporated until dry and the residues re-dissolved, using HCl (2 ml, 0.5 M). After re-dissolving, the solutions were added to a cation exchange column (AG 50W-X8). The low affinities of PGE anion complexes for the resin were confirmed as they were instantly eluted from the column. Additional HCl was added, and the eluents collected. Analysis of the eluent samples proved that the method was effective in removing all the PGE from the column while major impurities (Mg, Fe, Na, Ti and K) were retained in the column. The PGE-containing eluents were evaporated until dry and re-dissolved in 3 % HNO_3 solution and quantified with ICP-MS. Validation of the method was performed by analysing dust reference material, BCR 723. The results showed good agreement between the certified and the measured values (**Table 3.1**). From the study, it was concluded that the global quantity of PGE in the environment is increasing due to the introduction of catalytic converters to vehicles in the process of reducing dangerous emission from the exhaust systems.

Table 3.1: The concentrations of PGE in BCR 723 obtained by ICP-MS[60]

Element	Measured value (ng/g)	Certified value (ng/g)
^{105}Pd	4.8 ± 0.16	6.10 ± 1.9
^{195}Pt	75.5 ± 1.16	81.3 ± 2.5
^{103}Rh	8.6 ± 0.02	12.8 ± 1.3

Microwave digestion with HF and $HClO_4$

HF and $HClO_4$ are highly corrosive mineral acids and are often used for the digestion of many refractory samples. Dissolution of PGE samples, using microwave digestion in the presence of these acids is usually incomplete, regardless of their aggressive nature. The two acids are more effective when used in combination with *aqua-*

[60] Okorie, I.A., Entwistle, J. & Dean, J.R. (2015). Platinum group elements in urban road dust. *Current Science*, 109(5), pp. 938-942.

regia.[61] Successful dissolution by these acids also depends on the mineralogy of the sample.

Balaram et al.[62] quantified the PGE, Ag and Au content in different CRM samples (PTM-1, CHR-Pt+, and CHR-Bkg) and some chromite ore samples, using microwave digestion. Cesium was employed as an internal standard. These samples (0.5 g) were transferred to PFA-microwave digestion vessels, and HF (3 ml), $HClO_4$ (2 ml), *aqua-regia* (5 ml) and cesium (1 ml) were added to the vessel and digested in the microwave. The PTM-1 and CHR-Bkg samples produced clear solutions, while a black residue remained in the vessel for the CHR-Pt+. This residue was digested again, using the same experimental conditions. However, no further dissolution was observed. The experimental results obtained for the elements in different samples, agreed with the certified reference materials for PTM-1 and CHR-Bkg (see **Table 3.2**). As for CHR-Pt+, low recoveries for Ir, Ru and Rh were obtained while the results for Au, Pt and Pd were in good agreement with the certified values. The developed method was also employed for the dissolution of various chromite ore samples, the results of which are reported in **Table 3.3**. From the study, it was concluded that microwave digestion, using their method, was effective for the dissolution of chromite ore samples.

[61] Totland, M.M., Jarvis, I. & Jarvis, K.E. (1995). Microwave digestion and alkali fusion procedures for the determination of the platinum group elements and gold in geological material by ICP-MS. *Chemical Geology*, 124, pp. 21-36.

[62] Balaram, V., Anjaiah, K.V. & Kumar, A. (1999). Microwave digestion for the determination of platinum group elements, silver, and gold in chromite ore by ICP-MS. *Asian Journal of Chemistry*, 11(3), pp. 949-956.

Table 3.2: The concentrations (ug/g) of precious metals in different reference materials[62]

Element	PTM-1		CHR-Pt+		CHR-Bkg	
	ICP-MS value (n=6)	Certified value	ICP-MS value (n=6)	Certified value	ICP-MS value (n=6)	Certified value
Ru	0.34 ± 0.03	0.35	0.80 ± 0.01	9.2	0.07 ± 0.01	0.067
Rh	0.94 ± 0.01	0.9	1.00 ± 0.05	4.7	0.03 ± 0.01	0.009
Pd	7.89 ± 0.47	8.1	83.13 ± 4.15	90.9	0.11 ± 0.01	0.07
Ag	65.80 ± 4.6	66	23.24 ± 1.39	--	20.06 ± 0.65	--
Os	0.11 ± 0.01	0.14	0.89 ± 0.09	1.9	0.03 ± 0.01	0.027
Ir	0.4 ± 0.03	0.3	1.25 ± 0.11	6.2	0.71 ± 0.06	1.028
Pt	5.75 ± 0.41	5.8	58.01 ± 2.32	58	0.10 ± 0.01	0.05
Au	1.70 ± 0.15	1.8	4.51 ± 0.24	4.3	0.04 ± 0.01	0.028

Table 3.3: The concentrations (ug/g) of precious metals in different chromite ore samples[62]

Element	Su-1	Ti-1	Ka-1	KI-1	Kt-1
Ru	0.12 ± 0.01	0.10 ± 0.01	0.08 ± 0.01	0.05 ± 0.01	0.03 ± 0.01
Rh	0.06 ± 0.01	0.05 ± 0.01	0.05 ± 0.01	0.04 ± 0.01	0.03 ± 0.01
Pd	0.24 ± 0.02	0.19 ± 0.02	0.17 ± 0.01	0.21 ± 0.01	0.21 ± 0.02
Ag	570.83 ± 17.11	36.65 ± 1.75	19.78 ± 1.20	64.37 ± 1.95	1452.68 ± 43.56
Os	0.03 ± 0.01	0.04 ± 0.01	0.08 ± 0.01	0.05 ± 0.01	0.07 ± 0.01
Ir	0.08 ± 0.01	0.11 ± 0.01	0.12 ± 0.01	0.11 ± 0.01	0.03 ± 0.01
Pt	0.12 ± 0.01	0.08 ± 0.01	0.07 ± 0.01	0.09 ± 0.01	0.14 ± 0.01
Au	0.07 ± 0.01	0.08 ± 0.01	0.05 ± 0.01	0.09 ± 0.01	0.13 ± 0.01

3.2.2 Cyanide Leaching

Cyanide leaching is commonly employed in the extraction of gold from low-grade ores and is considered highly efficient and profitable. This method has also been used for the recovery of PGE, both from ores and recycled material, and offers high selectivity for PGE.[63] The process is based on the reaction of PGE with sodium cyanide (NaCN) at elevated pressures and at temperatures ranging from 120 °C to 180 °C. However, the main drawback of this method is the toxic nature of NaCN, and poisoning can occur through inhalation, ingestion and eye contact.[64]

Desmond et al.[65] investigated PGE recovery from different automobile catalyst samples, using cyanide leaching. Three different types of automobile catalysts were investigated, namely a spent monolith, virgin monolith and a spent pellet catalyst sample. The experiments were conducted in an autoclave lined with a Teflon fluorocarbon polymer. The reactions were carried out in the presence of 5 % NaCN solution for one hour at a temperature of 160 °C and a pressure of 250 psig. These conditions proved to be successful in terms of dissolving in excess of 97 % of the PGE from the virgin monolith. More than 85 % of the PGE in the used monolith and about 90 % of those in the used pellet catalyst sample were leached. About 99.8 % of the leached PGE were recovered as a precipitate by heating the solution to 250 °C at a reaction pressure of 600 psig for one hour in an autoclave to decompose the cyanide complexes.

3.2.3 Chlorination

Chlorination is a process of calcination and reduction by CO in the presence of NaCl. During the process, air is blown into the solution and chlorinated successively at a

[63] Sibrell, P.L., Atkinson, G.B. & Walters, L.A. (1994). Cyanide leaching chemistry of platinum group metatals. *Berau of Mines*, pp. 1-18.

[64] Mineral Policy Centre. (2000). Cyanide leach mining packet, pp. 1-20.

[65] Desmond, D.P., Atkinson, G.B. & Kuckzynski, R.J. (1991). High temperature cyanide leaching of platinum group metals from automobile catalysts. *Report of Investigation 9384, U.S Bereau of Mines*, pp. 1-14.

temperature of 1 200 °C. Kim et al.[66] investigated carbochlorination (**Figure 3.1**), using a carbon monoxide (CO) and chlorine (Cl_2) gas combination to extract Rh and Pt from a spent automotive catalyst. CO was employed as a reducing agent to produce a thermodynamically favourable reaction. They investigated the effect of time, partial pressures and flow rate of CO and Cl_2 on the efficiency of PGE extraction. After optimising the conditions, about 95.9 % of Pt and 92.5 % of Rh were recovered from the catalyst sample. The base metal chlorides were also recovered in the condensate containing the PGE. The influence of the overall gas flow on the PGE and base elements recoveries were investigated, and it was concluded that the chlorides produced from base elements could be minimised by decreasing the flow rate of the gas mixture without deterioration of the PGE recoveries.

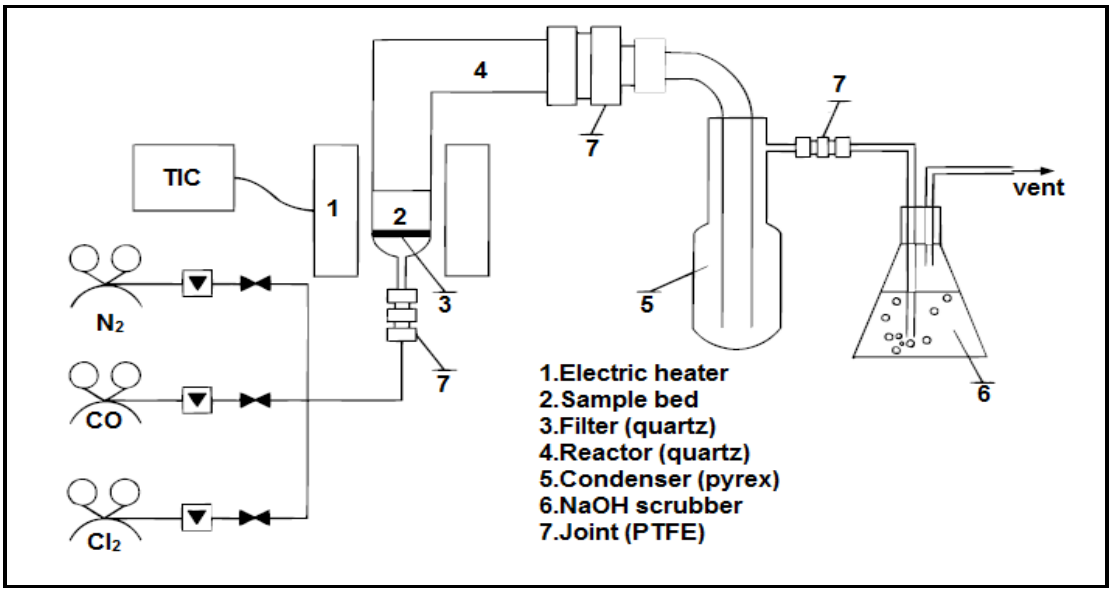

Figure 3.1: Schematic diagram of the experimental apparatus of carbochlorination[66]

3.2.4 Flux Fusion Methods

Nickel sulphide (NiS) fire assay

Fire assay is very popular in industrial processes for the separation and concentration of gold and the PGE from high-grade ores. The method involves the fusion of a PGE sample with a mixture of SiO_2, Ni and S in the presence of alkaline

[66] Kim, C., Woo, S.I. & Jeon, S.H. (2000). Recovery of platinum group metals from recycled automotive catalytic converters by carbochlorination. *Ind. Eng. Chem. Res.*, 39, pp. 1185-1192.

fluxes, such as $Na_2B_4O_7$ and Na_2CO_3 in a clay crucible at a temperature of 1 000 °C for about an hour. The resulting NiS button is isolated from the slag, pulverised and then digested in concentrated HCl. The undissolved PGE sulphides are then separated and digested in HCl and HNO_3.[67] The method was adopted in the 1970s at the National Institute for Metallurgy in South Africa for the determination of PGE from ores and concentrates from the Merensky Reef.[68] The process is considered to be fast, flexible, simple and inexpensive. Many studies also focused on the dissolution of PGE from chromite ore samples by NiS fire assay methods.[69,70,71] The results of these studies indicate that this method is more successful in the dissolution of chromite ores than most other dissolution methods. The results, however, indicate that this method does not completely dissolve all the chromite grains in the glassy slag and that only partial attack was observed.[72] In addition, the method is highly suitable for mineral ores with high PGE concentrations. Nevertheless, major problems, such as sample loss and inaccuracy of PGE concentrations may arise.

The method was improved by Bedard et al.,[73] who investigated the extraction of the PGE present in the UG2 chromite layer in the BIC by NiS fire assay but used sodium metaphosphate as flux. This method achieved complete dissolution of the refractory

[67] Frimpong, A., Fryer, B.J. & Longerich, H.G. (1995). Recovery of precious metals using nickel sulphide fire assay collection. *Analyst*, 120, pp. 1675-1680.

[68] Alfassi, Z. B. & Chien, M.W. (1992). *Preconcentration techniques for trace elements*, CRC Press, p. 407.

[69] Li, C., Chai, C. & Mao, X. (1998). Determination of platinum group elements and gold in two Russian candidate reference materials SCHS-1 and SLg-1 by ICP-MS after nickel sulphide fire essay preconcentration. *Geostandards and Geoanalytical Research*, 22(2), pp. 195-197.

[70] Sun, Y., Chu, Z. & Xia, X. (2009). An improved Fe-Ni sulphide essay for determination of Re, PGE and Os isotopic ratios by ICP and negative thermal ionization mass spectrometers. *Applied Spectroscopy*, 63(11), pp. 1232-1239.

[71] Asif, M. & Parry, S.J. (1990). Nickel sulphide fire essay for collecting platinum group elements and gold from chromite ores using reduced bead size. *Mineralogy and Petrology*, 42(1), pp. 321-326.

[72] Ruthenium Recovery in Chromitites by NiS-fire Assay. Available at: https://nicholas.duke.edu/people/faculty/boudreau/9thPtSymposium/Bedard_Abstract.pdf. [Accessed: 07 July 2017].

chromite grains, which is extremely important in terms of promoting full recovery of the PGE. Optimum dissolution of the chromite grains was achieved by fusing the sample (10 g) with a mixture of $Na_6P_6O_{14}$ (10 g), SiO_2 (9 g), Na_2CO_3 (15 g), $Li_2B_4O_7$ (30 g), Ni (7.5 g) and S (4.5 g). It was concluded from this study that the added sodium metaphosphate flux plays a crucial role in improving the recovery of PGE due to its ability to increase the dissolution of the chromite ore.

Sodium peroxide (Na_2O_2) fusion

Peroxide fusion is considered as an alternative to acid digestion since it is a safe, fast and efficient method for the complete digestion of PGE samples.[74,75] The fusion is performed at lower temperatures (500 °C to 600 °C), thus avoiding the possible loss of volatile elements. Sodium peroxide fusion is frequently used for refractory ores and recycled PGE materials, where total dissolution is required. It is a strong oxidising agent and is used to oxidise the metal compounds from low metallic oxidation states to higher water-soluble and stable oxidation states. It can be performed in automated systems to improve productivity and safety, maintain repeatable sample preparations, and avoid spattering and cross-contamination.

The disadvantage of using sodium peroxide fusion is the introduction of EIEs which may interfere with the ICP-OES analysis, potentially leading to poor accuracy and precision of the results. However, accuracy can be improved by using a suitable internal standardisation in order to compensate for the interference caused by the EIEs.[51]

[73] Bedard, L.P. & Barnes, S. (2004). Improved platinum-group element extraction by NiS fire assay from chromitite ore samples using a flux containing sodium metaphosphate. *Geostandards and Analytical Research*, 28(2), pp. 311-316.

[74] Enzweiler, J. & Potts, T.J. (1995).The separation of platinum, palladium and gold from silicate rocks by the anion exchange separation of chloro complexes after a sodium peroxide fusion. *Talanta*, 42(10), pp. 1411-1418.

[75] Nogueria, C.A. & Figueredo, A.M.G. (1995). Determination of platinum, palladium, iridium and gold in selected geological reference materials by radiochemical neutron activation analysis: Comparison of procedures based on *aqua-regia* leaching and sodium peroxide sintering. *Analyst*, 20, pp. 1443-1441.

Pitre and Bedard[76] developed a sodium peroxide (Na_2O_2) digestion method for the dissolution of automotive catalytic converter samples with the aid of *aqua-regia* dissolution of the resultant melt. Two spent automotive catalyst reference materials (ERM®-EB504 and NIST SRM 2556) were investigated. The elemental content was determined, using ICP-OES. This method produced results with good accuracy and precision for Pd, Pt and Rh. The elemental recoveries are reported in **Tables 3.4** and **3.5**. Matrix matching and the use of Cd (226.502 nm) as an internal standard, combined with a strict interference management scheme, improved the recoveries of the metals to 100 ± 11 %.

Table 3.4: Accuracy and precision measurements on ERM®-EB504[76]

Element	Wavelength (nm)	Average experimental values (%) n=10	Certified values (%)	Accuracy (%)	RSD (%)
Pd	248.892	0.026	0.0279	93	4
Pt	193.700	0.17	0.1777	94	3
Rh	343.489	0.034	0.0338	100	2

Table 3.5: Accuracy and precision measurements on NIST SRM 2556[76]

Element	Wavelength (nm)	Average experimental values (%) n=10	Certified values (%)	Accuracy (%)	RSD (%)
Pd	248.892	0.030	0.03326	92	2
Pt	193.700	0.068	0.06974	98	3
Rh	343.489	0.003	0.00512	(62)	3

[76] Pitre, J. & Bedard, M. (2013). Peroxide fusion dissolution for the determination of platinum, palladium and rhodium in automotive catalytic converters by ICP analysis, pp. 1-5.

In another study, Choi et al.[77] investigated the separation of Au, Pd, Pt, Rh, Ru and Ir in chromite samples by anion exchange chromatography and then quantified the elements with ICP-OES. The chromite mineral samples were dissolved by sodium peroxide (Na_2O_2) fusion in a zirconium crucible. Chromium interference on Au quantification was also investigated. Au and the trace PGE quantities were pre-concentrated and separated with anion exchange chromatography after the Cr(VI) was reduced to Cr(III) using hydrogen peroxide. Au was selectively eluted, using an acetone-HNO_3-H_2O solution. The PGE remaining in the resin (except Pt) were eluted as a group, using hydrochloric acid, while Pt was eluted, using nitric acid. The recoveries obtained for Au, Pt and Pd were 100.7 ± 2.0 %, 96.6 ± 1.3 %, and 96.1 ± 1.8 % respectively. The dissolution procedure is summarised in **Figure 3.2**.

[77] Choi, K., Lee, C. & Park, Y. (2001). Separation of gold, palladium and platinum in chromite by anion exchange chromatography for inductively coupled plasma atomic emission spectrometric analysis. *Bull. Korean Chem. Soc.*, 22(8), pp. 801-806.

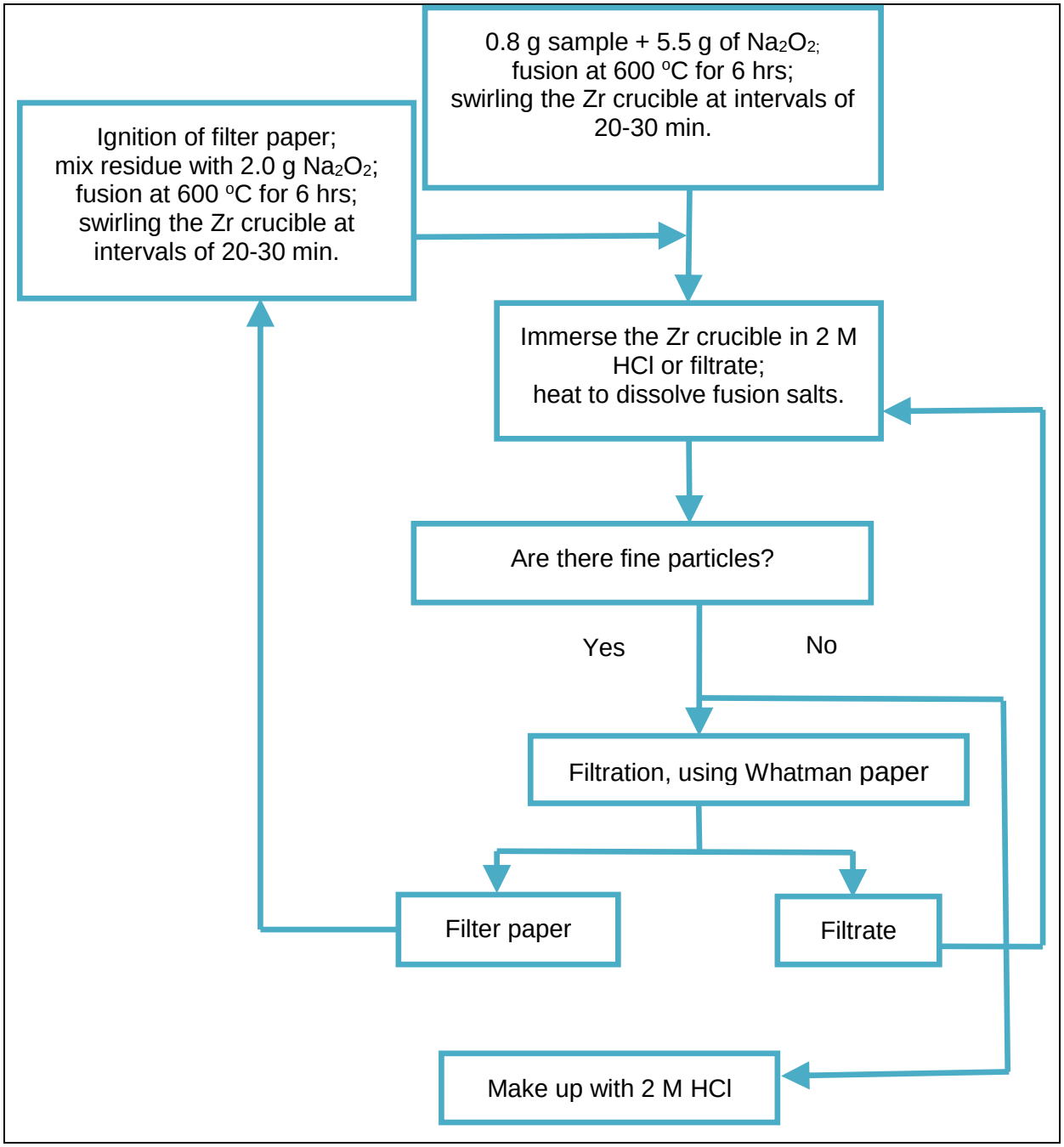

Figure 3.2: Fusion dissolution procedure for the chromite sample[77]

3.3 SEPARATION METHODS

3.3.1 Ion Exchange

Ion exchange chromatography has been employed in the separation of platinum group metals produced from primary mineral ore samples, as well as secondary sources, ranging from the used automotive catalytic converters to electronic scrap

material. This method has also become an increasingly acceptable alternative for the recovery of PGE from uncontaminated aqueous solutions due to their affordability and selectivity.

Gaita et al.[78] developed an ion exchange method for the recovery of PGE from highly acidic solutions containing Fe, Al, Pb and Ce which was obtained from the dissolution of a used automotive catalytic converter sample. The metals from the used catalyst sample were reacted with hydrochloric acid (5 M) and sodium chlorate (0.4 M) at 70 °C for optimum dissolution. Three different anion exchange resins, Amberlite IRA-93, Amberlite IRA-400 and Amberlite IRA-68 were used to investigate the recovery of the metals, using HCl (4 M) solutions containing 25 ppm of each metal. Quantitative recovery of Pt and Pd was achieved with the two resins; Amberlite IRA-93 and Amberlite IRA-400. However, Amberlite IRA-68 was found to be best suited to recovering all the PGE. The PGE were eluted selectively by firstly stripping Rh with HCl (6 M), then Pd and Pt with 1 and 5 % of NH_4OH solutions respectively. The results are shown in **Table 3.6**.

[78] Gaita, R. & Al-Bazi, S.J. (1995). An ion-exchange method for selective separation of palladium, platinum and rhodium from solutions obtained by leaching automotive catalytic converters. *Talanta*, 42(2), pp. 249-255.

Table 3.6: Recovery and stripping efficiencies of palladium, platinum and rhodium, using Amberlite IRA-400, IRA-93 and IRA-68 resins[78]

	% Recovery			% Stripping efficiency		
Resin	**Pt**	**Pd**	**Rh**	**Pt**	**Pd**	**Rh**
IRA-400	99	95	25	69	100	92
IRA-93	99	95	30	75	100	100
IRA-68	83	74	45	63	68	60

Nikoloski et al.[79] also studied the recovery of PGE in a used automotive catalyst sample dissolved in acidic chloride solutions, using ion exchange resins for separation. The ion exchangers that were evaluated included a resin with a thiouronium functional group, a resin with polyamine functional group and a resin with a quaternary ammonium functional group. The former exhibited the best separation performance for Pd(II) and Pt(IV) chloride complexes whereas all three resins showed poor affinities towards the Rh(III) chloride complex. The eluents that were used included HCl, thiourea and NaSCN. The researchers concluded that a complete elution of Pd and Pt can be accomplished for all ion exchangers, using acidic thiourea solutions as eluent.

3.3.2 Solvent Extraction

Solvent extraction is also an accepted technique for the isolation of PGE from low concentrated samples. This method provides several advantages, such as high metal purity and selectivity.[80] Organophosphorus compounds, amines and sulfoxides have been studied for the possible extraction of PGE from aqueous solutions, and have

[79] Nikoloski, A.N., Ang, K. & Li, D. (2015). The recovery of platinum, palladium and rhodium from acidic chloride leach solutions using ion exchange resins. *Hydrometallurgy* ,152, pp. 20-32.

[80] Ghandi, M.R., Yamada, M. & Kondo, Y. (2015). Selective extraction of Pd (II) ions from automotive catalyst residue in Cl^- media by O-thiocarbamoyl-functionalized thiacalix[*n*]arenes. *Hydrometallurgy*, 151, pp. 133-140.

been mentioned in numerous reports on the application of this method in the extraction of the PGE from aqueous chloride solutions.[81]

Amines

Amines proved to be effective reagents in the extraction of PGE from mineral and weak organic acid medium. Studies on the extraction and separation of PGE, using four *N,N′* tetrasubstituted malonamide derivatives were reported by Paiva et al.[82] The extractants were specially synthesised in order to evaluate their efficiency in the extraction of a specific material or a group of metals from aqueous chloride matrices. Different reactions were observed between the amines for Pt(IV) and Pd(II). The four malonamide derivatives, namely *N,N′*-dimethyl-*N,N′*-dihexyltetradecylmalonamide (DMDHTDMA), *N,N′*-dimethyl-*N,N′*-dihexylmalonamide (DMDHMA), *N,N′*-dimethyl-*N,N′*-dicyclohexyltetradecylmalonamide (DMDCHTDMA) and *N,N′*-dimethyl-*N,N′*-dicycloexylmalonamide (DMDCHMA), are shown in **Figure 3.3**. All the *N,N′*-tetrasubstituted malonamide derivatives extracted both metal ions, and the degree of extraction depended upon the HCl concentration. From the results, it was concluded that HCl concentrations and the structure of the malonamide derivative played a crucial role in the efficiency of Pd(II) and Pt(IV) extraction. The overall results suggested that these extractants may be good candidates for further evaluation in the separation of PGE, resulting from recycled material.

[81] Sun, P. & Lee, M.S. (2013). Recovery of platinum from chloride leaching solution of spent catalysts by solvent extraction. *Materials Transactions*, 54(1), pp. 74-80.

[82] Paiva, A.P., Carvalho, G.I. & Schneider, A.L. (2012). New extractants for the separation of platinum-group metals from chloride solutions and their application to recycling process. *4th International Conference on Engineering for Waste and Biomass Valorisation*, 251, pp. 1-6.

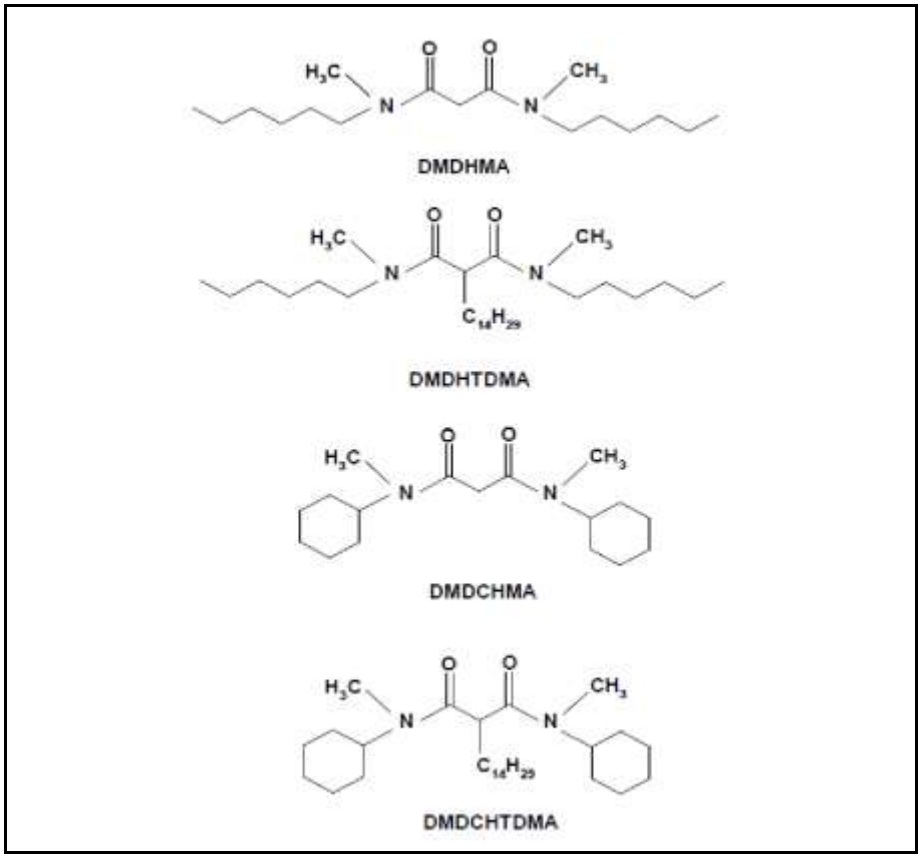

Figure 3.3: The structures of the *N,N′*-tetrasubstituted malonamide derivatives synthesised and used as extractants[82]

Similar malonamide derivatives were investigated in another solvent extraction study done by Assuncao et al.[83] The purpose of their study was to investigate the recovery of PGE, employing both solvent extraction and biological methods, using anaerobic bacterial group. The Pt(IV) and Pd(II) present in aqueous phase were extracted into the organic phases containing the malonamide derivatives *N,N′*-dimethyl-*N,N′*-dicyclohexyl tetradecylmalonamide (DMDCHTDMA) and *N,N′*-dicyclohexylsuccinamide (DMDCHSA) dissolved in 1,2- dichloroethane respectively. Extraction efficiencies of 99 % and 79 % were obtained for Pt(IV) and Pd(II) respectively. Seawater was used to strip the metals in the organic phase, with efficiencies of 86 % for Pt(IV) and 100 % for Pd(II). The metals were finally recovered by precipitation, using metabolic products produced from sulphate-reducing bacteria. The structures of the extractants are shown in **Figure 3.4**.

[83] Assuncao, A., Matos, A. & Rosa da Costa, A.M. (2016). A bridge between liquid-liquid extraction and the use of bacterial communities for palladium and platinum recovery as nanosized metal sulphides. *Hydrometallurgy*, 163, pp. 40-48.

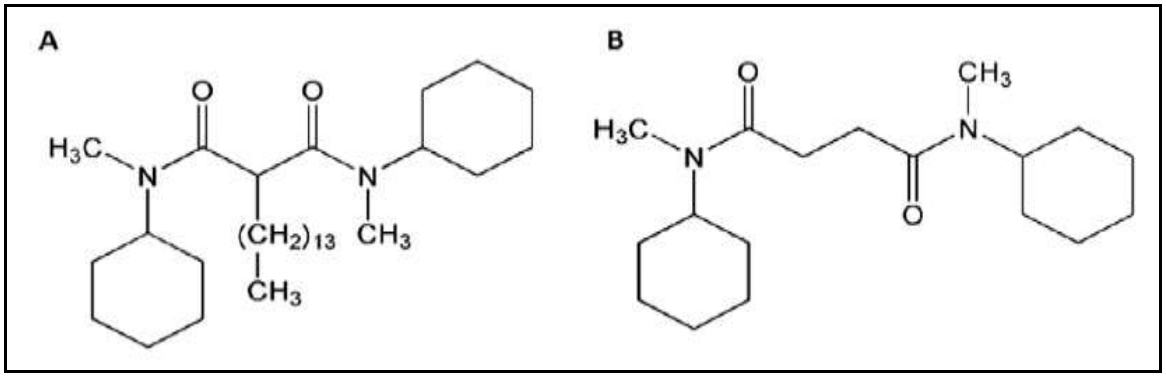

Figure 3.4: Molecular structures of (A) DMDCHSA and (B) DMDCHTDMA[83]

Gaikwad et al.[84] developed a method for the extraction of Pt(IV) from an ascorbate media, employing n-octylaniline. They investigated the influence of different experimental parameters, such as pH, equilibrium time, organic solvent and extractant concentration on the extraction efficiency of Pt(IV). The interference of various anions and cations in the extraction efficiency was also investigated. Various masking agents were employed to enhance the selectivity of the method for Pt(IV). The developed method was successfully applied in the determination of Pt(IV) in synthetic and binary mixtures.

The recovery of Pd and Pt from chloride solutions by solvent extraction using Alamine 300 as an extractant was researched by Swain et al.[85] They evaluated the effect of different parameters, such as the extractant concentration, HCl concentration, NaCl concentration and the concentrations of the metals in the feed solution. From their results, it was observed that the percentage of the extracted Pd decreased from 97.8 % to 76.5 % while that of Pt decreased from 99.9 % to 87.1 %, with an increase in the concentration of HCl from 0.5 to 7.5 M. They concluded that both metals showed similar extraction behaviour in this HCl concentration range due to the similarity of their chloro complexes ($PdCl_4^{2-}$ and $PtCl_6^{2-}$) when Alamine 300 is used. The quantitative results also indicated an improvement in the extraction

[84] Gaikwad, A.P. & Kamble, G.S. (2013). Liquid Anion Exchange Chromatographic Extraction and separation of Platinum (IV) with n-Octylaniline as a metallurgical Reagent: Analyses of Real samples. *Journal of Chemistry*, 2013, Article ID 103192, pp. 1-9.

[85] Swain, B., Joeng, J. & Kim, S. (2010). Separation of platinum and palladium from chloride solution by solvent extraction using Alamine 300. *Hydrometallurgy*, 104(1), pp. 1-7.

percentage and separation factor, with an increase in extractant concentration. At higher NaCl concentrations and lower HCl concentrations, the Pt extraction increased while that of Pd was relatively poor. The extraction was explained by the following equations:

$$PtCl_6^{2-}{}_{aq} + 2R_3NH^+Cl_{org} \rightleftharpoons (R_3NH)_2(PtCl_6)_{org} + 2Cl^-{}_{aq} \quad \textbf{(3.4)}$$

$$PdCl_4^{2-} + 2R_3NH^+Cl^-{}_{org} \rightleftharpoons (R_3NH)_2(PdCl_4)_{org} + 2Cl^-{}_{aq} \quad \textbf{(3.5)}$$

The Pd and Pt in the organic phases were selectively stripped, using HCl and NaSCN respectively. The researchers concluded that the method can be applied successfully to these kinds of solutions, with the isolation of about 98 % of pure Pd and 99.99 % of pure Pt from HCl solutions.

Chen-Yu Peng et al.[86] employed Alamine 336 dissolved in kerosene for the extraction of palladium from HCl solutions. The effect of various stripping reagents, such as thiourea, NaCl, HCl, $AlCl_3$, KCl and $BaCl_2$ were investigated. The concentration of Pd in the acidic solutions was analysed by atomic absorption spectrophotometry (AAS). The results indicated that that the concentrations of the extractant and that of HCl played an important role in the extraction behaviour of Pd. An increase in the concentration of the extractant increased the Pd recovery while an increase in the HCl concentration suppressed the extraction of the metal. Their results established that a mixture of thiourea (0.5 M) and HCl (0.5 M) was best for Pd stripping. With regard to metal recovery, the extraction efficiency of Pd (0.001 M) reached 99.9 % when Alamine 336 (0.5 M) and HCl (1 M) were used.

[86] Peng, C. & Tsai, T. (2012). Recovery of palladium (II) from acidic chloride solution using kerosene containing tri-n-octyl/decyl amine (Alamine 336). *Desalination and Water Treatment* , 47(1-3), pp. 105-111.

Organophosphorus compounds

Cyanex compounds containing P=O or P=S as a functional group are widely used in the extraction of metal ions. These extractants are organophosphorus compounds that act both as chelating and solvating extractants and have been applied in the extraction of PGE. Gupta and Singh[87] investigated the extraction behaviour of Pd(II), Pt(IV) and Rh(III) from HNO_3, HCl and H_2SO_4 media, using cyanex 923 dissolved in toluene. The experiments were performed by varying the temperature, equilibrium time, concentration of the extractant and diluent. The stability of the extractant, loading capacity, regeneration extraction and the influence of associated metals were also investigated in this study. A summary of the method is shown in **Figure 3.5**. The recoveries of 97.73 %, 98.9 %, 99.7 % and 99.6 % were obtained for Pd(II), Pt(IV), Rh(III) and Au(III) respectively.

[87] Gupta, B. & Singh, I. (2013). Extraction and separation of platinum, palladium and rhodium using Cyanex 923 and their recovery from real samples. *Hydrometallurgy*, 134-135, pp. 11-18.

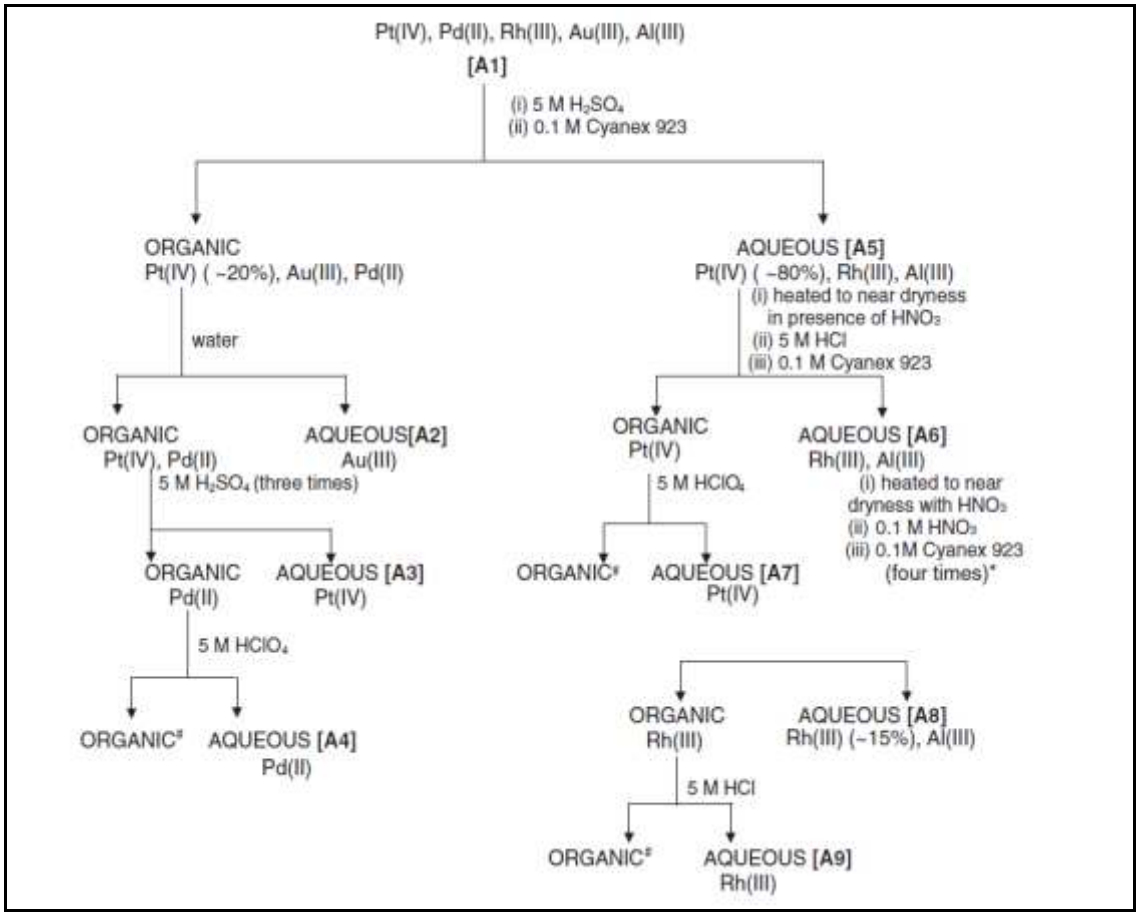

Figure 3.5: Flow chart for the recovery of Pd(II), Pt(IV), Rh(III) and Au(III) from synthetic mixture, using Cyanex 923[87]

Cieszynska et al.[88] studied the extraction of Pd(II) from HCl solutions using trihexyl (tetradecyl) phosphonium bis-(2, 4, 4-trimethylpentyl) phosphinate (Cyphos®IL 104) in the presence of toluene. Toluene was used to overcome a number of limitations caused by the high viscosity of the Cyphos®IL 104. The results showed that Pd(II) extraction was affected by both the temperature of the solution and the concentration of HCl. An increase in the concentration of HCl resulted in a decrease in Pd(II) extraction while an increase in temperature resulted in a slight decrease in the extraction of Pd(II). It was concluded that a combination of toluene and Cyphos®IL 104 can be successfully used to extract Pd(II) in a chloride medium. The Pd(II) extraction from chloride media appeared to be fast, effective and mainly dependent on the HCl concentration.

[88] Cieszynska, A. & Winsniewski, M. (2012). Extractive recovery of palladium (II) from hydrochloric acid solutions with Cyphos®IL104. *Hydrometallurgy*, 113-114, pp. 79-85.

Sulfoxides

Furthermore, research indicates that sulfoxides can also be applied in the solvent extraction processes of the PGE. Sulfoxides are chemical compounds containing a sulfinyl functional group attached to two carbon atoms and are generally represented by the structural formula R-S(=O)-R', where R and R' are organic groups.

Preston and Du Preez[89] studied the extraction of Pt(II), Pt(IV), Pd(II), Ir(III), Ir(IV) and Rh(III) in HCl solutions using different dialkyl sulfoxides of the type RR'SO, R_2'SO and R_2SO, where R and R' represent alkyl and cycloalkyl functional groups respectively. The order of extraction of the metals in di-*n*-hexyl sulfoxide (0.5 M) dissolved in xylene from solutions containing HCl (1-6 M) was found to be Pd(II) > Pt(II) > Ir(IV) > Pt(IV) > Rh(III) > Ir(III). Metal distribution studies indicated that Pt(IV) and Ir(IV) were extracted in the form of ion-pairs, such as $(L_2.H_3O^+)(L_3.H_3O^+)PtCl_6^{2-}$ and $(L_3.H_3O^+)_2IrCl_6^{2-}$, where L is the dialkyl sulfoxide. For Pt(II) and Pd(II), one or two of the chloride ligands from the chlorometallate anion (MCl_4^{2-}) was replaced by the sulfoxide. The distribution data corresponded with the extraction of $PdCl_2L_2$ at low HCl concentrations (1-2 M) and $(L_2.H_3O^+)$ $PdCl_3L^-$ at higher acid concentrations (4-6 M).

3.3.3 Precipitation of Platinum Group Elements

Another and more traditional method of PGE isolation is that of precipitation with the ammonium chloride procedure and is typically applied in the separation and purification of platinum.[90] The hexachloro complexes of the PGE precipitate readily from aqueous chloride solution as their ammonium salts, which allows for their recovery from solution. This method is considered difficult, tedious and, during the purification of platinum, the metal is usually contaminated with substantial amounts of

[89] Preston, J.S. & du Preez, A.C. (2002). Solvent extraction of platinum-group metals from hydrochloric acid solutions by dialkyl sulfoxides. *Solvent extraction and ions exchange*, 20(3), pp. 359-374.

[90] Duclos, L., Svecova, L. & Laforest, V. (2016). Process development and optimization for platinum recovery from PEM fuel cell catalyst. *Hydrometallurgy*, 160, pp. 79-89.

other PGE. The method is best applied if one of the PGE has to be separated from the non-precious elements in the absence of the other PGE.

Platinum, palladium and rhodium are precipitated as hexachloro complexes, namely $Pt/Pd(IV)Cl_6^{2-}$ and $Rh(III)Cl_6^{-}$ by the saturation of the decomposed chloride solution with ammonium chloride:

$$2NH_4Cl + [MCl_6]^{2-} \rightleftharpoons [NH_4]_2[MCl_6]\ (s) + 2Cl^- \qquad \textbf{(3.6)}$$

where M is the metal.

The PGE which have stable trivalent oxidation states form a variety of aqua-complexes which are in equilibrium with one another and will remain in solution:

$$[MCl_6]^{3-} + mH_2O \rightleftharpoons [MCl_{6-m}\ (H_2O)_m]^{(3-m)-} + mCl^- \qquad \textbf{(3.7)}$$

In a study conducted by Raper et al.,[91] it was observed that any water-soluble amide that can readily hydrolyse in acidic solutions to produce ammonium ions that can be used for the precipitation of PGE. The ignition of these products produced a platinum metal sponge. The aim of their study was to separate uncontaminated platinum from palladium, using ammonium chloride, urea and acetamide. The results for the three amides were compared, and it was found that the use of urea and acetamide yielded better results than the ammonium chloride precipitation. This was attributed to the isolation of a less contaminated platinum precipitate compared to ammonium chloride. The results are shown in **Tables 3.7, 3.8** and **3.9**.

[91] Raper R., Clements F.S. & Fothergill, S.J. (1962). Separation of platinum from other metals, pp. 1-3.

Table 3.7: The precipitation of platinum with urea[91]

Experiment number	Pt solution (ml)	HCl (ml)	Urea (g)	Pt yield (%)	Amount of Pd in Pt (%)
1	50	25	6	94.4	0.0007
2	50	20	6	90.0	0.0006
3	200	200	30	96.6	0.0006

Table 3.8: The precipitation of platinum with acetamide[91]

Grams in 50 millilitres of solution		Grams of Pt recovered	Percentage of Pd in Pt recovered
Pt	Pd	Pt	Pd
5.0	0.25	4.993	0.018
5.0	0.5	4.996	0.027

Table 3.9: The precipitation of platinum with ammonium chloride[91]

Grams in 50 millilitres of solution		Grams of Pt recovered	Percentage of Pd in Pt recovered
Pt	Pd	Pt	Pd
5.0	0.25	5.001	0.69
5.0	0.5	5.028	1.04

3.4 ANALYTICAL TECHNIQUES FOR DETERMINING PGE

3.4.1 ICP-MS Methods

The inductively coupled plasma mass spectrometry (ICP-MS) is a sensitive detection method with multi-elemental capability, which is often used for the determination of low-concentration PGE in environmental samples. The method separates ions or atoms based on their mass-to-charge ratios, and thus also provides valuable isotopic information. However, spectral interferences can strongly affect the accuracy of PGE measurement.

Balaram et al.[92] developed a method for determining PGE and Au with ICP-MS in crust and polymetallic ocean ferromanganese nodule reference samples. These analyses were performed after the isolation and pre-concentration of the PGE, using the nickel sulphide fire essay. Various parameters, such as matrix matching calibration and flux composition were optimised and the best experimental conditions which were appropriate for the analysis of PGE and Au were selected. Calibration standards were prepared and quantified using PGE reference materials, WMS-1 and WMG-1. Exceptionally low detection limits in the range of 0.004 to 0.016 ng/g were obtained for PGE and Au, and it was concluded that the developed method can be used to accurately and precisely quantify PGE and Au in these crust and manganese nodules samples in marine geological studies.

Muller and Heumann[93] developed a method for the simultaneous determination of Pd, Pt, Ir and Ru using isotope dilution inductively plasma mass spectroscopy (ID-ICP-MS). The ^{108}Pd, ^{194}Pt, ^{191}Ir and ^{99}Ru isotopes were selected for the analysis of the elements. Interfering elements were eliminated by means of chromatographic separation, using anion exchange chromatography. The method was found time-effective, accurate and suitable for the determination of platinum group metals in environmental samples.

A rapid and reliable method for the determination of PGE in gold and geological samples, using ICP-MS, was developed by Zhu and Jin[94]. Lu was employed as an internal standard after the sodium peroxide fusion and tellurium co-precipitation steps. The PGE were pre-concentrated and isolated from interfering elements using

[92] Balaram, V., Mathur, R. & Banakar, V.K. (2006). Determination of the platinum group elements and gold in manganese nodule reference samples by nickel-sulphide fire essay and Te co-precipitation with ICP-MS. *Indian Journal of Marine Science*, 35(1), pp. 7-16.

[93] Muller, V. & Heumann, K.G. (2000). Isotope dilution inductively coupled plasma quadrupole mass spectrometry in connection with a chromatographic separation for ultra-trace determinations of platinum group elements (Pt, Pd, Ru and Ir) in environmental samples. *Fresenius J. Anal. Chem*., 368(1), pp. 109-115.

[94] Jin, X & Zhu, H. (2000). Determination of platinum group elements and gold in geological samples with ICP-MS using a sodium peroxide fusion and tellurium co-precipitation. *J. Anal.At. Spectrom*., 15, pp. 747-751.

tellurium co-precipitation. Excellent detection limits in the range of 1 to 9 pg/g^{-1} were obtained for the metals. The experimental results for the reference materials were in good agreement with the certified values.

3.4.2 ICP-OES/AES Methods

The ICP-AES/OES is increasingly replacing the AAS instruments in laboratories worldwide as a reliable, accurate, precise and rapid technique which is able to perform multi-element PGE analysis detection in ppb order levels. The technique has been used as a method of choice in the quantification of many metals, including PGE.

Mokgalaka et al.[95] studied a method for the quantification of PGE and Au in a spent automotive catalyst sample, using ICP-OES, with Sc and Y as internal standards. The effect of sodium on the determination of PGE and gold, and the use of internal standards to compensate for the sodium ion matrix effect on the accuracy of PGE analysis were investigated. The results indicated that the emission intensities of the analytes decreased with an increase in sodium concentrations. It was discovered that Sc internal standard compensates effectively for any intensity decrease for PGE as compared to Y.

Chiweshe et al.[96] investigated a method for the quantification of Rh, employing the ICP-OES technique, with cobalt as an internal standard. Rh was quantified in various samples which included CRM (ERM®-EB504), pure Rh powder, $RhCl_3.3H_2O$, as well as different organometallic complexes. Outstanding Rh recoveries in these samples were obtained, the results of which are shown in **Table 3.10**. They found that the accuracy of Rh recovery was affected by the presence of EIEs and unmatched matrix acid, which resulted in a decrease in Rh recovery of up to 16 %. It was concluded

[95] Mokgalaka, N.S., Mc Crindle, R.I. & Botha, B.M. (2002). Internal standard method for the determination of Au and some platinum group metals using inductively coupled plasma optical emission spectrometry. *S. Afr. J. Chem.*, 55, pp. 72-86.

[96] Chiweshe, T.T., Purcell, W. & Venter, J. (2012). Quantification of rhodium in a series of organometallic compounds using cobalt as an internal standard. *S. Afr. J. Chem*., 66, pp. 7-16.

that matrix matching, together with cobalt internal standard, can be applied to overcome matrix problems caused by easily ionised elements (EIEs), foreign metal ions, background emission and other fluctuations occurring during analysis with ICP-OES, which resulted in poor accuracy of Rh recoveries.

Table 3.10: Rhodium recoveries in different samples[96]

Sample	Internal standard	Average Rh recovery (%)	RSD (%)
CRM	External calibration	89.2	0.3
CRM	Standard edition	98.0	0.7
CRM	Y	140	1
CRM	Co	100	1
Rhodium powder	External calibration	65.8	0.8
Rhodium powder	Co	100	1
$RhCl_3.3H_2O$	Co	99.8	0.3
$[Rh(acac)CO_2]$	Co	100	1
[Rh(acac)(DPP)(CO)]	Co	99.7	0.5
$[Rh(acac)(DPP)(CO)(CH_3)(I)]$	Co	100	1
$[Rh(cupf)(CO)_2]$	Co	100	2
$[Rh(cupf)(PPh_3)(CO)]$	Co	99.7	0.4
$[Rh(cupf)(PPh_3)(CO)(CH_3)(I)]$	Co	100.1	0.4

Wemyss and Scott[97] developed a technique for the simultaneous quantification of PGE and Au in ores and related plant materials by means of ICP-OES. The results obtained for the standard reference materials were compared to the certified values and those obtained by atomic mass spectroscopy (AAS). The ICP-OES results were found satisfactory and it was concluded that the method was appropriate for the rapid determination of PGE in these samples. However, the results for iridium were inconclusive as the values were close to the ICP-OES detection limits and were all below those of the AAS.

[97] Wemyss, Y.B. & Scott, R.H. (1978). Simultaneous determination of platinum group metals and gold, in ores and related plant materials by inductively coupled plasma-optical emission spectrometry. *Analytical Chemistry*, 50(12), pp. 1694-1697.

3.4.3 GFAAS Methods

GFAAS is also frequently used for the analysis of PGE and other elements since it offers a number of advantages, which include affordability, very good detection limits and has little spectral interference. However, temperature limitations, use of graphite cuvettes, and refractory element quantification are still rather limited and can only determine one to six elements at a time, thus making the method time consuming and limited in terms of dynamic range.

Eskina et al.[98] investigated the possible use of high-resolution continuum source graphite furnace atomic absorption spectroscopy (GFAAS) for the determination of PGE from spent ceramic-based auto catalysts. The elements were first isolated and concentrated using a heterochain-polymer S, N- containing adsorbent. Two methods for the dissolution of the samples were used, namely autoclave decomposition in *aqua-regia* and high temperature melting flux with $K_2S_2O_7$. It was discovered that both methods limited the direct determination of the metals in question. The first method resulted in the incomplete digestion of the spent auto catalyst of samples; the unreacted precipitate contained Si and rhodium metal which dissolved with difficulty. While the second method allowed for the complete dissolution of the metal, background interferences appeared due to the chemical composition of the flux, which negatively affected the analysis.

[98] Eskina, V.V., Dalnova, O.A. & Filatova, D.G. (2016). Separation and preconcentration of platinum-group metals from spent autocatalysts solutions using a hetero-polymeric S,N-containing sorbent and determination by high-resolution continuum source graphite furnace atomic absorption spectrometry. *Talanta,*159, pp. 103-110.

3.4.4 X-Ray Spectrometry

Aberasturi et al.[99] also quantified the PGE present in catalytic converters. The chemical composition of the catalysts was obtained by X-ray diffraction (XRD) and field scanning electron microscopy (SEM). The main parts of the catalytic converters were characterised by X-ray powder diffraction, while SEM was used to observe the distribution of the PGE (**Figures 3.6** and **Figure 3.7)**.

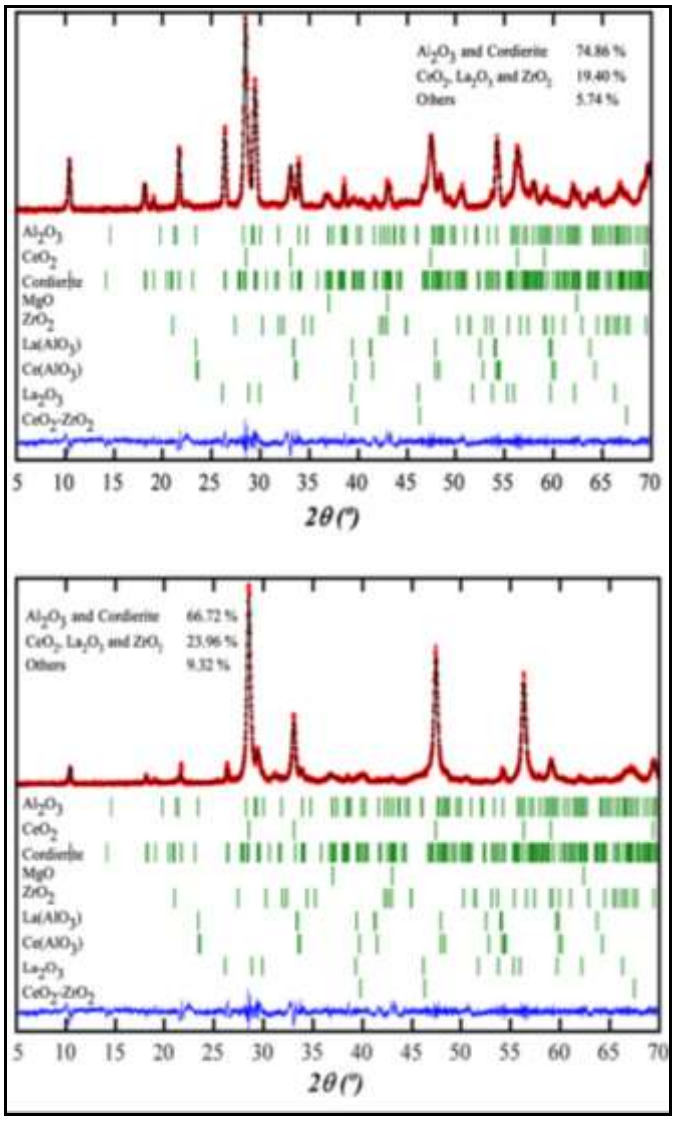

Figure 3.6: Diffractograms of the two catalytic converters[99]

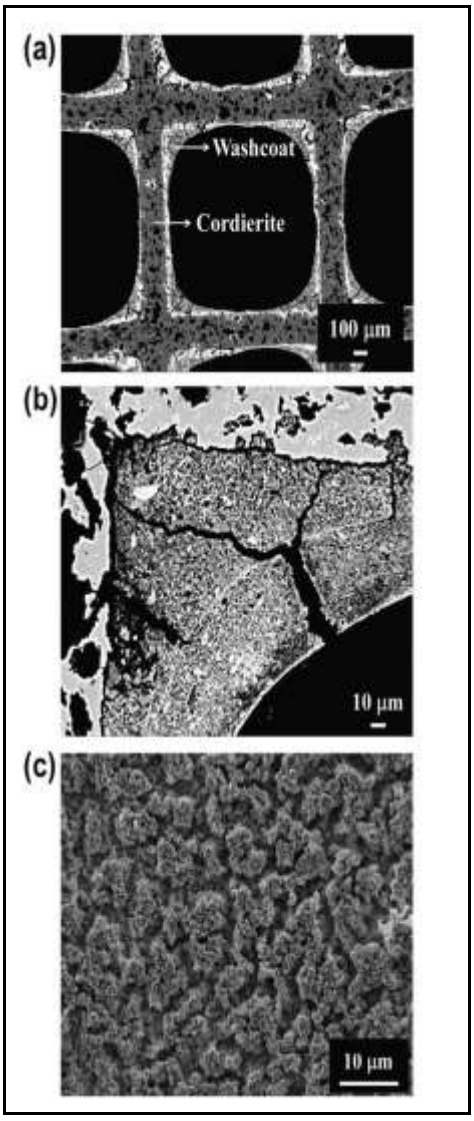

Figure 3.7: SEM images of the honeycomb structure[99]

[99] De Aberasturi, D.J Pinedo, R. & De Larramendi, I. (2011). Recovery by hydrometallurgical extraction of the platinum-group metals from car catalytic converters. *Minerals Engineering* 24, pp. 505-513.

According to the results obtained by XRD-SEM, it was concluded that the main components in both catalysts were alumina (Al_2O_3), cordierite ($2MgO.2Al_2O_3.5SiO_2$) and some secondary components, namely La_2O_3, CeO_2 and ZrO_2 (**Figure 3.6**). **Figures 3.7** (a) and (b) indicate the cross-section images of the catalysts, while (c) shows the surface of the catalytic converter. The SEM image indicates that a wash coat was developed in several porous and roughness coats (**Figure 3.7**).

3.4.5 INAA Methods

Instrumental neutron activation analysis (INAA) is considered one of the most useful analytical techniques for PGE and gold determination due to its exceptional sensitivity and accuracy. The method involves the irradiation of samples with neutrons and the resulting gamma ray spectrum of the elements is then analysed. It can be employed to determine the concentrations of ultra-trace and major elements in a variety of matrices. Alfassi et al.[100] developed a method of INAA for the determination of platinum in air samples. The samples were collected from filters, with the ^{199}Au daughter of ^{199}Pt in the presence of spectral interferences from the ^{47}Sc daughter of ^{47}Ca. This approach was adopted since the determination of platinum by ^{199}Pt is limited due to its short half-life of 30.8 min. Thus, the platinum was determined by means of ^{199}Au daughter of ^{199}Pt. It was found that the method was indeed suitable for trace analysis of Pt in filter samples.

3.5 CONCLUSIONS

This literature indicates that a substantial amount of work has been conducted on the recovery of PGE from various materials, especially from recycled automotive catalytic converters. The research reveals that there are numerous challenges in dissolving the PGE-containing samples. These challenges include incomplete PGE sample dissolution and aggressive methods, such as microwave-assisted acid digestion methods, the use of aggressive acids such as HF and $HClO_4$, and the use of highly toxic chemicals such as NaCN, which have been used for sample digestion. On the

[100] Alfassia, Z.B., Probst, T.U. & Rietz, B. (1998). Platinum determination by instrumental neutron activation analysis with special reference to the spectral interference of Sc-47 on the platinum indicator nuclide Au-199. *Analytica Chimica Acta,* 360, pp. 243-252.

other hand, NiS fire assay digestion methods proved to be more convenient in the recovery of PGE from refractory samples such as chromite mineral ore samples. However, this method requires a large number of reagents to achieve dissolution (**Section 3.2.4.1**) and is therefore potentially not economically viable. Furthermore, the introduction of EIEs during the NiS fire essay and peroxide fusion methods negatively affect the quantification of PGE, using the popular ICP-OES analytical quantification method. However, peroxide fusion is considered more effective than other dissolution methods since it is safer, faster and offers complete dissolution of PGE samples (**Section 3.2.4.2**).

The literature also shows that the separation of PGE is mostly carried out in aqueous chloride media. Organophosphorus, high molecular weight amines and sulfoxide compounds were found to be effective in solvent extraction and in ion exchange separation processes. The separation of PGE by precipitation methods proved to be ineffective due to poor selectivity. As a result, there is limited literature on research done using this approach for the separation of PGE.

The most common methods for PGE analysis include ICP-MS/OES, GFAAS and SEM-EDS. According to the literature, it appears as though ICP-OES and ICP-MS are the most popular and effective techniques due to their ability to perform multi-element analysis, as well as their high accuracy and precision, wide linear dynamic range and the fact that they allow for trace and ultra-trace metal analysis.

4 Selected Experimental Methods

4.1 INTRODUCTION

The literature review on the recovery of PGE from various materials was conducted in **Chapter 3**. The knowledge gained through this literature review assisted in bringing about understanding regarding the latest research on this topic and in the evaluation of the strengths and weaknesses of previous studies. As a result, this evaluation contributed to the process of method and technique selection used in this study.

The selection of the most suitable analytical techniques is important in method development and hydrometallurgical beneficiation. The successful development of an analytical method depends on many aspects, including proper sample preparation, as well as suitable characterisation and quantification, while beneficiation depends on effective and efficient separation and isolation techniques. In this study, the selection of analytical methods depended on a few factors, which included: (i) the elements of interest, (ii) the type of sample material, (iii) the concentration of the analytes of interest and, lastly, (iv) the availability of equipment and reagents.

The aim of this chapter is to review the analytical principles, equipment and analytical and separation techniques used throughout this study. Sample dissolution, separation, quantification and characterisation methods are introduced in this chapter.

4.2 SAMPLE DISSOLUTION

Complete sample dissolution is the first and most critical step in the hydrometallurgical beneficiation process. This step ensures the total liberation of all the elemental components for the solid samples and their effective separation in aqueous solutions. In order to completely dissolve a sample, all its components must be converted into a soluble form and be brought into solution. There are various types of sample digestion methods, including open-beaker acid digestion, microwave acid-assisted digestion and flux fusion methods. Open-beaker acid digestion and flux fusion methods, which were used in this study, will be discussed.

4.2.1 Open-Beaker Acid Digestion

Open-beaker acid digestion involves the use of different mineral acids for the decomposition of inorganic and organic samples. Typically, the dissolution is performed on a hot plate, and the success thereof is usually judged based on the presence or absence of any insoluble residue in the solution. Some of the commonly-used mineral acids are shown in **Table 4.1**.

Table 4.1: Common mineral acids for open-vessel dissolution[101]

Mineral acid	Boiling point (°C)	Comment
Hydrochloric acid (HCl)	108.6	Often used for the digestion of iron alloys, and forms soluble chlorides with all elements, except Ag, Hg and Ti.
Nitric acid (HNO_3)	83	An oxidising agent which forms soluble nitrates with all elements, except Au, Pt, Al, B, Cr, Ti and Zr.
Aqua-regia (3HCl: 1HNO_3)	108	Digestion of precious metals and sulphides
Sulphuric acid (H_2SO_4)	337	Usually employed with other acids for the digestion of plastics, minerals and ores
Perchloric acid ($HClO_4$)	203	Extremely strong oxidiser which reacts vigorously with organic compounds and attacks almost all metals
Hydrofluoric acid (HF)	19.5	Usually used in combination with other acids for the digestion of minerals, ores, soil, rocks and plants
Phosphoric acid (H_3PO_4)	200	Dissolves Al_2O_3, chromite ores, iron oxides and slag

[101] Theory of sample preparation using acid digestion, pressure digestion and microwave digestion. Available at: https://www.perkinelmer.com/lab-solutions/resources/docs/FLY_5-Tips-to-Improving-Your-Sample-Digestion_012640_01.pdf. [Accessed: 01 February 2018].

The drawbacks of open-vessel acid digestion include temperature limitations, risk of contaminants from the atmosphere and loss of volatile elements during digestion, which may lead to false results. In many cases, this method is also time consuming and often leads to unsatisfactory results.

4.2.2 Flux Fusion Method

Flux fusion is usually used for samples which withstand dissolution with common mineral acids. The method involves the fusion of a sample and a molten inorganic salt known as a flux. The flux dissolves a sample and, upon cooling, the resulting solid is then dissolved in acid or water. The increased dissolving strength of a flux is mainly due to the formation of high-concentration ionic liquids at elevated temperatures (200-1200 °C), which react with the solid compound to produce inorganic molten salts.[102] The reaction between the sample and the fluxes occurs via the normal dissolution processes which include acid/base reactions, complex formation and, finally, oxidation/reduction, depending on the nature of the solid sample.

The most common crucibles used for flux fusion dissolution are platinum, nickel, zirconium and porcelain. The fluxes usually employed for fusion are shown in **Table 4.2**.

[102] Kenkel, J. (2013). *Analytical Chemistry for Technicians, 4th edition*, CRC Press, p. 30.

Table 4.2: Common fluxes for fusion methods[103]

Flux	Fusion temperature (°C)	Type of crucible	Type of sample decomposed
$Na_2S_2O_7$ or $K_2S_2O_7$	Up to red heat	Pt, quartz, porcelain	For insoluble oxides and oxide-containing samples, particularly those of Al, Be, Ta, Ti, Zr, Pu and the rare earths
NaOH or KOH	450-600	Ni, Ag, glassy carbon	For silicates, phosphates and fluorides
Na_2CO_3 or K_2CO_3	900-1000	Ni, Pt for short periods (use lid)	For silicates and silica-containing samples (clays, minerals, rocks and glasses)
Na_2O_2 or	600	Ni, Ag, Zr,Au, Pt (<500)	For sulphides, acid-insoluble alloys of Fe, Ni, Cr, Mo, W and Li, Pt alloys, Cr, Zn and Sn minerals
H_3BO_3 or	250	Pt	For analysis of sand, aluminium silicates, titanite, corundum and enamels
$Na_2B_4O_7$ or	1 000-1 200	Pt	For Al_2O_3, ZrO_2 and zirconium ores, minerals of the rare earths, Ti, Nb and Ta, aluminium-containing minerals, iron ores and slags
$Li_2B_4O_7$ or $LiBO_2$	1 000-1 100	Pt, graphite	For almost anything, except sulphides and metals
NH_4HF_4, NaF, KF Or KFH_2	900	Pt	For the removal of silicon, the destruction of silicates and rare earth minerals, and the analysis of oxides of Nb, Ti, Ta and Zr

103 Marlap. (2004). Sample dissolution. Available at: https://www.epa.gov/sites/production/files/2015-05/documents/402-b-04-001b-13-final.pdf. [Accessed: 03 July 2017].

The disadvantages of flux fusion dissolution include the high sample: flux ratios needed for successful dissolution, the influence of high salt content (EIE effect of Na^+ or K^+) on the quantitative analysis, especially using spectroscopic methods such as ICP-OES. In addition, the possible dissolution of the crucible by the flux can lead to additional contamination problems which may result in the false or inaccurate quantification of target elements.

4.3 SEPARATION AND PURIFICATION METHODS

Most materials are not pure substances and usually exist as mixtures. This phenomenon requires effective separation methods to separate, isolate and purify the different elements. The success of separation depends on the conversion of the different elements in the sample into products which have distinctly different chemical and physical properties and which will allow for their separation and isolation. Separation methods are crucial in the chemical and petroleum refining industries, and in the materials processing industries.

4.3.1 Precipitation Methods

Selective precipitation is a separation technique in which an analyte in a sample is selectively converted into an insoluble product called a precipitate, in the presence of all the other analytes. This product is separated from all the other water-soluble components by means of a simple filtration or centrifugation process.

For optimal precipitation, a number of conditions must be considered. Firstly, the solubility of the required product should be very low (small K_{sp}). Secondly, the precipitation should preferably be carried out on diluted solutions in order to minimise contamination by co-precipitation. Thirdly, a slight excess of reagent may be required for successful precipitation. Finally, the slow mixing of the reagent and the slow stirring of the sample solution are important.

Unfortunately, most precipitants are not selective towards a specific analyte and there is always the possibility that the precipitant will react with both the target analyte and other unwanted elements. The direct precipitation on small amounts of the analyte is often a challenge and the separation of trace elements can be successfully achieved

by the initial precipitation of any high-concentrated interfering cations with a suitable reagent. Another limitation of precipitation methods is that foreign metal ions are adsorbed at the surface of the precipitate. This leads to an impure product which needs to be further purified by means of an additional precipitation step or other separation methods.[104]

4.3.2 Solvent Extraction Methods

Solvent extraction or liquid-liquid extraction is one of the most popular metal-refining techniques due to its speed, simplicity, wide range, high selectivity and metal purity. Solvent extraction has been employed in many chemical industries to produce pure chemical compounds, ranging from pharmaceuticals to biomedical heavy metal separation, environmental waste purification and analytical chemistry.[105] The extraction process requires two immiscible liquids or phases, such as aqueous and organic solution. The separation is accomplished by the difference in the solubility of the analyte between these two phases (**Figure 4.1**).[106]

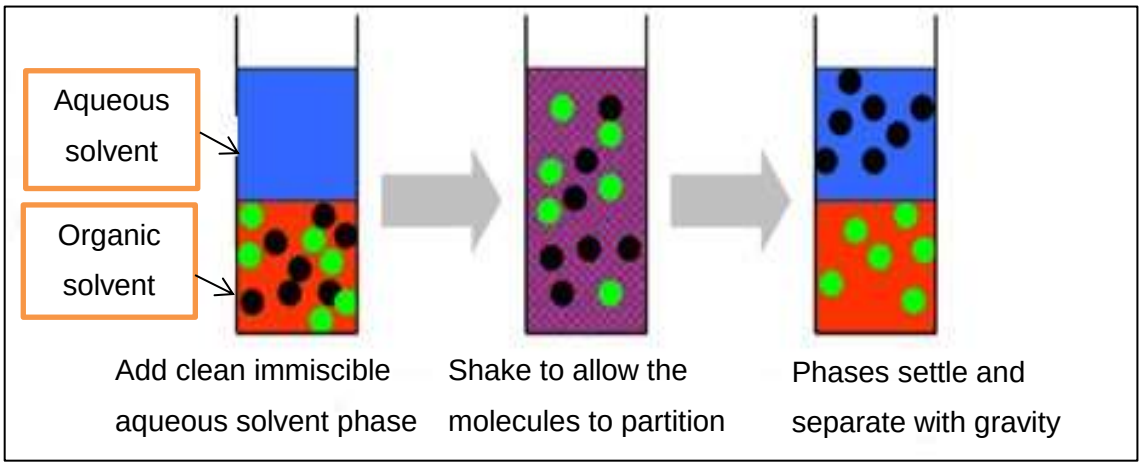

Figure 4.1: Principle of solvent extraction[107]

[104] Lajunen, L. (2004). *Spectrochemical Analysis by Atomic Absorption and Emission*, *2nd edition*, Royal Society of Chemistry, p. 313.

[105] Rydberg, J., Cox, M. & Musikas, C. (2004). *Solvent Extraction Principles, Revised and Expanded*, *2nd Edition*, CRC Press, p. 3.

[106] Kislik, V.S. (2012). *Solvent extraction: Classical and Novel Approaches*, *1st edition*, Elsevier, p. 6.

[107] Europian Rare Earth Recycling Network. Available at: http://erean.eu/wordpress/msx-technology-to-be-up-scaled/. [Accessed: 14 February 2018].

The distribution of an analyte between two immiscible solvents is determined by the distribution coefficient and the distribution ratio. The distribution coefficient, K_D, is an equilibrium constant, expressed as the ratio of the solute concentration in the two immiscible solvent phases (**Equations 4.1** and **4.2**). This is established by shaking the reaction mixture containing the solute which distributes between the two phases.

$$A_{(aq)} \rightleftharpoons^{K_D} A_{(org)} \qquad \textbf{(4.1)}$$

where (aq) represents the aqueous phase and (org) represent the organic phase.

The ratio of the activities of A between the two immiscible solvents is constant and is defined by the following equation:[108]

$$K_D = \frac{(a_A)_{org}}{(a_A)_{aq}} \approx \frac{[A]_{org}}{[A]_{aq}} = \frac{\text{Concentration of species A in organic phase}}{\text{Concentration of species A in aqueous phase}} \qquad \textbf{(4.2)}$$

$(a_A)_{org}$ and $(a_A)_{aq}$ are the activities of A in each of the two phases and are the molar concentrations of A in the two different solvents.

The concentration of the analyte remaining in the two different solvents after a certain number of extractions is calculated, using the distribution constant.[109] The distribution constant also provides guidance regarding the most efficient way of performing an extractive separation.

The amount of A remaining in the aqueous solution after i extractions, using an organic solvent is calculated by means of the following equation:

$$[A]_i = \left(\frac{V_{aq}}{V_{org}K_d + V_{aq}}\right)^i [A]_0 \qquad \textbf{(4.3)}$$

[108] Dean, J.R. (2003). *Methods for environmental trace analysis*. John Wiley and Sons, p. 100.

[109] Skoog, D.A., West, D.M. & Holler, F.J. (2014). *Fundamentals of analytical chemistry*, 9th edition, Cengage learning, p. 853.

where $[A]_i$ is the concentration of solute A remaining after extracting with i portions of the organic solvent, V_{aq} mL is the volume of the original aqueous solution, V_{org} is the volume of the organic solvent used for extraction, and $[A]_0$ represents the original concentration of A in the aqueous portion.

Solvent extraction of metal ions

In order for a metal ion to be transferred from an aqueous soluble species to an organic soluble species, it must be converted from an ionic form to a neutral compound. The types of extractions can be grouped based on the nature of the extracted species or the mechanism involved in the extraction process. There are three main types of possible extractions, namely ionic-pair extraction, chelating extraction and solvating extraction.

Ionic pair extraction

This type of solvent extraction involves the extraction of a negative metal ion as neutral species into the organic layer. In many cases, high molecular weight amines are used to form ionic-pair compounds. Some of the most common ionic pair extractants include trioctylamine (TOA), triisooctylamine and Aliquat 336. The extraction of a metal ion through this type of solvent extraction is said to be strongly influenced by the structure and branching of the amine.[110]

Solvating extraction

In this extraction mechanism, the extractant may be the organic phase itself or a ligand dissolved in a diluent (organic solvent or water). This type of extraction involves the extraction of neutral metal complexes from aqueous solutions into the organic phase.[111] The metal species is usually coordinated with two different types of ligands which include a water-soluble ligand or an electron-donating ligand. Solvating extraction is also known as neutral extraction. Examples of solvating extractants

[110] Khopkar, M.S. (1998). *Basic Concepts of Analytical Chemistry*, *2nd Edition*, New Age International, pp. 106-110.

[111] Zhang, J., Zhao, B. & Schreiner, B. (2016). *Separation Hydrometallurgy of Rare Earths.* Springer, p. 40.

include organophosphorus compounds, such as TBP (Tributyl phosphate) and TOPO (Trioctylphosphine oxide). MIBK (Methyl Isobutyl Ketones) and some alcohols are also used as solvating extractants. While these types of extractions are kinetically fast, they offer low selectivity.

Chelating extraction

Chelating extraction is when the extraction of a metal ion proceeds by means of the formation of a chelate or close-ring structure with the extraction ligand forming a neutral metal species which may be soluble in the organic solvent. Chelating extractants are ligands containing two or more coordination sites. Cupferron (**Figure 4.2**) is an example of a chelating agent and is often used for the extraction of iron.

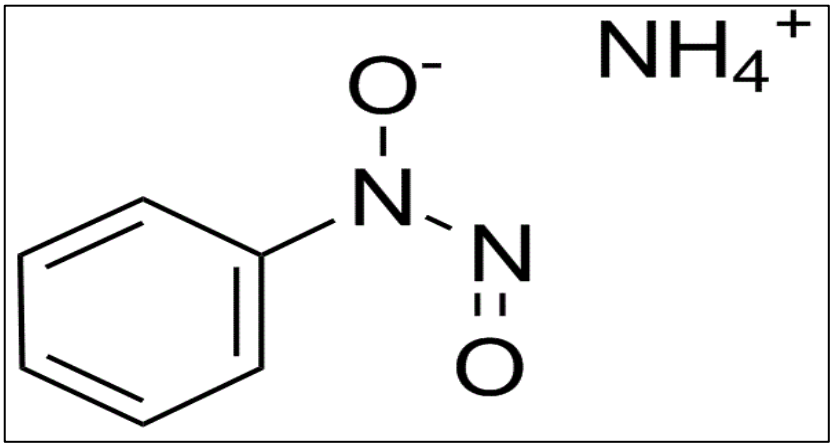

Figure 4.2: The structure of cupferron[112]

The extraction of a metal, M^{n+} by a chelating reagent, HL can be represented by the following reaction mechanism:

$$M_{aq}^{n+} + nHL_{org} \rightleftharpoons^{K_{ex}} ML_{n\,org} + H^{+}_{aq} \qquad \textbf{(4.4)}$$

The extraction constant, K_{ex} is expressed by:

[112] Cupferron. Available at: http://www.ebiochemicals.com/Wiki/Qceb000031853_IR.html. [Accessed: 28 February 2018].

$$K_{ex} = \frac{[ML_n]_{org}[H^+]^n_{aq}}{[M^{n+}]_{aq}[HL]^n_{org}} \quad \textbf{(4.5)}$$

The extraction coefficient, E which determines the amount of the metal that will move from an aqueous phase into the organic phase in a single contact, can be expressed by means of the following equation:

$$E = \frac{[M^{n+}]_{org}(V_{org})}{[M^{n+}]_{aq}(V_{aq})} \quad \textbf{(4.6)}$$

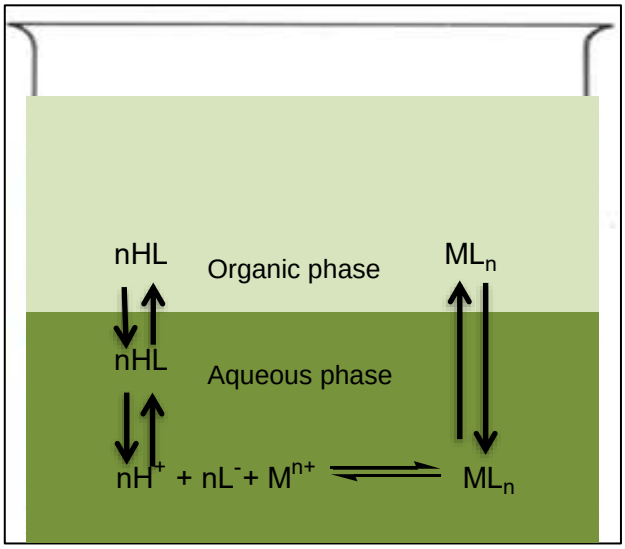

Figure 4.3: Solvent extraction of a metal ion by a chelating ligand

Stripping (back-extraction) of the analyte from the organic layer is not only important for beneficiation but also for quantification. Metal species in the aqueous solutions are usually easily reduced to their metallic form for further uses, while ICP-OES analyses do not tolerate organic solvents in the plasma flame due to carbon build-up. The analysis of metal species in the presence of an organic solvent leads to poor reproducibility, and the ICP-OES plasma tends to die during analysis. In addition, if a proper solvent has been used, selective back-extraction of the analyte under different experimental conditions can be achieved if the analyte of interest has also been extracted with interfering species into the organic layer.

4.4 QUANTIFICATION AND CHARACTERISATION TECHNIQUES

Quantification and characterisation techniques are essential for the successful determination of the chemical composition of the sample. These methods are also important in a hydrometallurgical process at different separation and purification stages as they determine the success of a separation procedure. Different identification methods, including SEM-EDS, ICP-OES IR, XRD, NMR and LECO CHNS micro-elemental analysis were employed in this study and will be discussed below.

4.4.1 SEM-EDS

Scanning electron microscopy (SEM), coupled with energy dispersive X-ray spectroscopy (EDS), is one of the most widely-used surface characterisation techniques. It is used in many fields, including metallurgy, geology, biology and medicine, for chemical characterisation or elemental analysis of solid samples. The method is considered relatively fast, cost-effective and suitable for surface analyses.

Principles of SEM-EDS

The SEM-EDS employs a focused beam of high-energy electrons to produce a variety of electromagnetic radiation at the surface of the sample (**Figure 4.4**). This radiation, which is obtained from the electron-sample interaction, reveals important information regarding the sample, including the chemical composition, sample texture, crystalline structure as well as the position of the materials making up the sample.

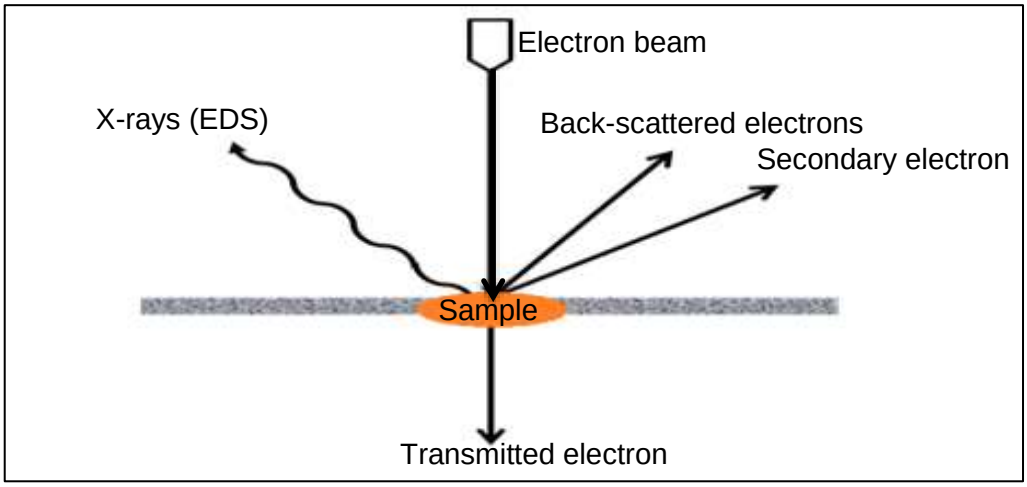

Figure 4.4: The electron-sample interaction in SEM-EDS[113]

During the bombardment of the sample with an electron beam, the inner core electrons of the different atoms in the sample are excited to produce unique X-rays, as well as secondary and back-scattered radiation (**Figure 4.4**). The SEM detects the emitted radiation from the back-scattered and secondary electrons to produce high-resolution images of three-dimensional samples (**Figure 4.6**). A high-resolution SEM can reveal details down to 25 Å. The EDS on the other hand, provides elemental identification and quantitative information by detecting the different X-rays emitted from the sample, which can be used to characterise the elemental composition of the analysed sample.

The X-rays in EDS are generated from the sample in two steps (**Figure 4.5**). During the initial step, the electron beam strikes the sample and transfers part of its energy to the electrons in the sample. The inner core electrons of the different atoms absorb this energy and are ejected from their shells, subsequently creating an electron hole within the atom's core electron structure, leaving behind positively charged holes. During the second step, these positively charged holes attract the negatively charged electrons from the higher-energy shells which cascade down the energy levels to fill the holes in the lower-energy shells. This process results in the release of X-rays, which are characteristic of the energy difference between the two energy shells and are unique to each element in the periodic table. These X-rays are then detected by an energy dispersive spectrometer and the data is used to produce an X-ray spectrum, showing

[113] Electron microscopy lab. Available at: http://www.odont.uio.no/iob/english/services/public-services/electron-microscopy/. [Accessed: 13 February 2018].

peaks corresponding to the elements in the sample. A typical EDS spectrum is shown in **Figure 4.6.**

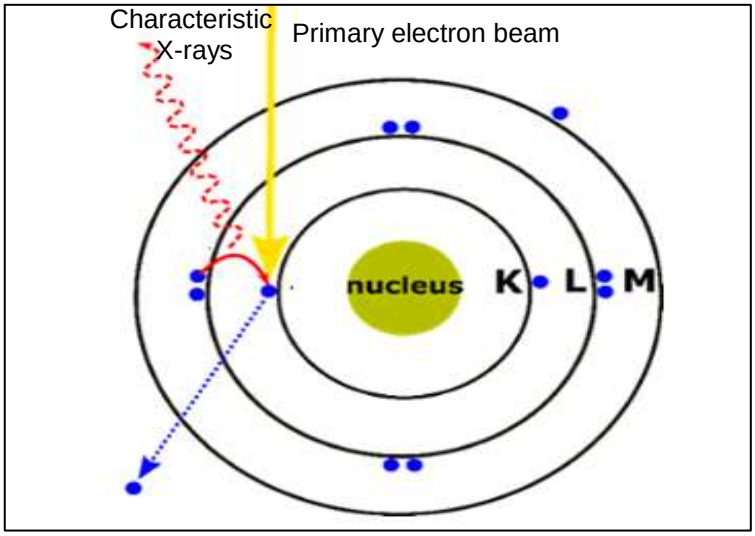

Figure 4.5: The X-ray generation process[114]

EDS are able to identify and quantify all elements in the periodic table, except light elements, such as H, He and Li.

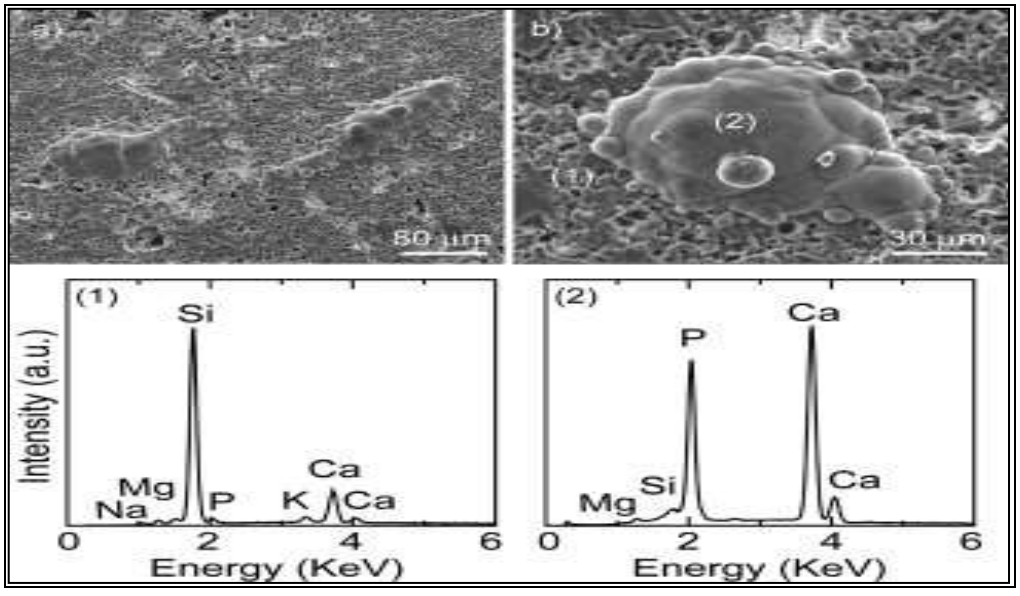

Figure 4.6: SEM images and corresponding EDS spectra[115]

[114] EDX analysis with a scanning electron microscope. Available at: http://blog.phenom-world.com/edx-analysis-scanning-electron-microscope-sem. [Accessed: 28 August 2018].

[115] Lopez-Esteban, S. & Gremillard, L. (2008). Interfaces in graded coatings on titanium-based implants. *Journal of Biomedical Materials Research,* pp. 1010-1021.

The accuracy and precision of the SEM-EDS may be influenced by several factors, which include the overlapping of energy peaks, for example the overlapping of TiK_β and VK_α peaks or MnK_β and FeK_α peaks. The quantitative analysis of heterogeneous materials, and thus the nature of the sample, often produces false results, affecting the accuracy of the analyses. Other drawbacks include its poor energy resolution and its inability to detect characteristic X-rays of components below 0.1 to 0.05 % level. Trace elements of oxides below 500 ppm can be determined by SEM-EDS, but quantification at these levels is often unreliable.[116]

4.4.2 Infrared Spectroscopy (IR)

Infrared spectroscopy, also known as vibrational spectroscopy, has been commercially available and used for material characterisation since 1940. The technique is employed for the analysis of a wide range of inorganic and organic samples as solids, liquids or gases.[117] It measures the absorption of the different infrared frequencies of a sample placed in the path of an IR beam and each molecule absorbs frequencies that are characteristic of its structure.

In order for a molecule to display infrared absorptions, its dipole moment must change during vibration. All molecular species absorb IR radiation, except for homonuclear molecules, such as Cl_2, O_2 and N_2. This is attributed to the fact that the dipole moments of these molecules are inactive. There are different types of IR instruments, but the most frequently used is the Fourier Transform Infrared Spectrometer (FT-IR), which was used in this study.

Principles of FT-IR

Infrared spectroscopy involves the interaction of radiation with matter and provides valuable information regarding the presence of certain functional groups or types of bonds. IR deals with the electromagnetic spectrum which lies between the visible and

[116] Advantages and disadvantages of the EDS technique. Available at: http://www.globalsino.com/EM/page4661.html. [Accessed: 30 October 2017].

[117] Staurt, B., H. (2004). Infrared spectroscopy: *Fundamentals and Applications.* John Wiley & Sons, p. 1.

microwave regions (**Figure 4.7**). Infrared radiation can excite vibrational and rotational transitions within the molecule, but is insufficient to excite the electrons within the molecule to undergo electronic transitions.[118]

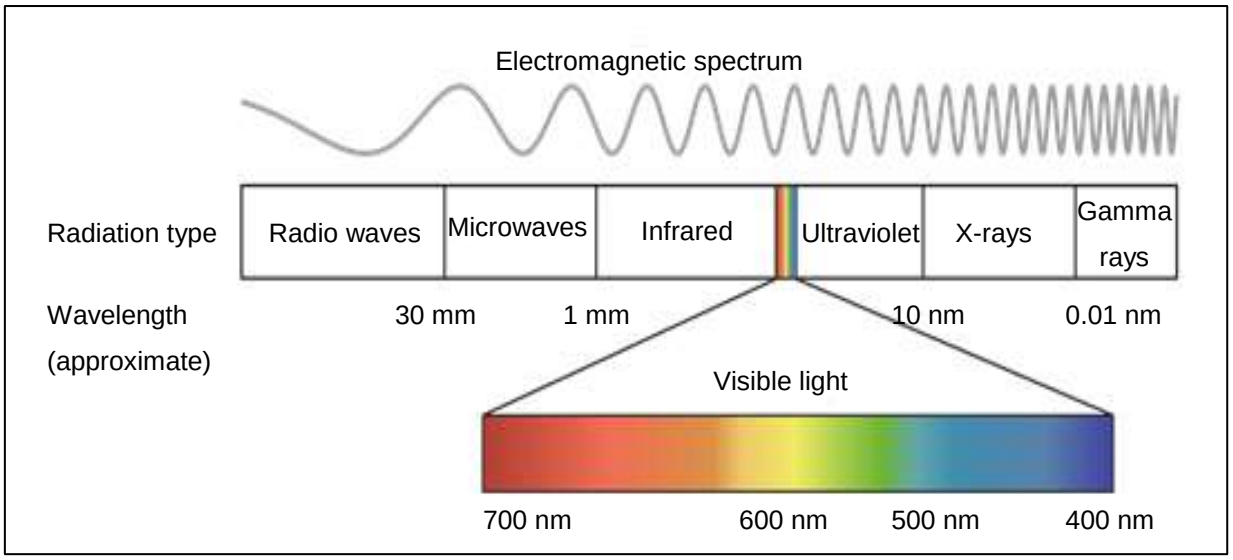

Figure 4.7: A typical electromagnetic spectrum[119]

FT-IR uses an optical device called an interferometer to record information about a sample positioned in the path of an infrared beam. Most interferometers use a beam splitter (**Figure 4.8**). The main purpose of a beam splitter is used to divide the incoming IR beam into two optical beams. One beam reflects from a fixed mirror while the other from a flat mirror in motion. When these beams reflect away from their respective mirrors, they recombine and meet at the beam splitter. The path of one beam travels at a fixed distance while the path of the other constantly changes due to its moving mirror. The signal produced at the interferometer is a result of the two beams interfering with each other.[120]

[118] Skoog, D.A., West, D.M. & Holler, F.J. (2014). *Fundamentals of analytical chemistry*, *9th edition.* Cengage learning, p. 812.

[119] Light and photosynthetic pigments. Available at: https://www.khanacademy.org/science/biology/photosynthesis-in-plants/the-light-dependent-reactions-of-photosynthesis/a/light-and-photosynthetic-pigments. [Accessed: 25 January 2018]

[120] *Introduction to Fourier Transform Infrared Spectrometry*, (2001) Thermo Nicolet Corporation, p. 4.

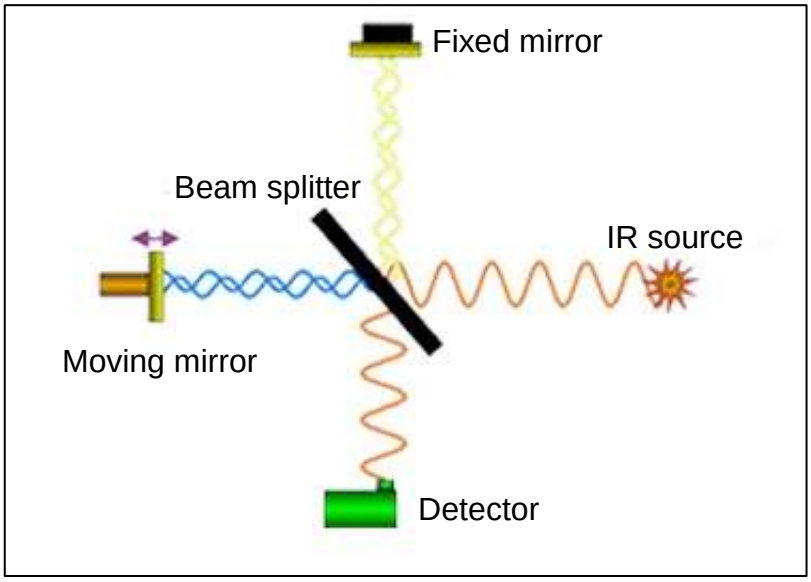

Figure 4.8: FT-IR interferometer[121]

FT-IR is considered more powerful than other, older versions of IR spectrometers, such as dispersive and filter methods. This is because it offers several advantages which include increased sensitivity, precise measurements, requiring no external calibration and being a relatively quick method.

When infrared radiation strikes the molecule, some radiation is absorbed by the bonds in the molecule while others are transmitted. The molecules absorb the energy of the infrared radiation and respond by changing its vibrating properties. The different types of vibration which are affected in the original molecule include stretching, rocking, scissoring, twisting and wagging (**Figure 4.9**). The resulting signal at the detector is a spectrum representing a molecular fingerprint of the sample. The spectrum shows absorption peaks which correspond with the frequencies of vibrations between the bonds of the atoms in the sample.

[121] Introduction to FTIR spectroscopy. Available at: https://www.thermofisher.com/za/en/home/industrial/spectroscopy-elemental-isotope-analysis/spectroscopy-elemental-isotope-analysis-learning-center/molecular-spectroscopy-information/ftir-information/ftir-basics.html. [Accessed: 15 February 2018].

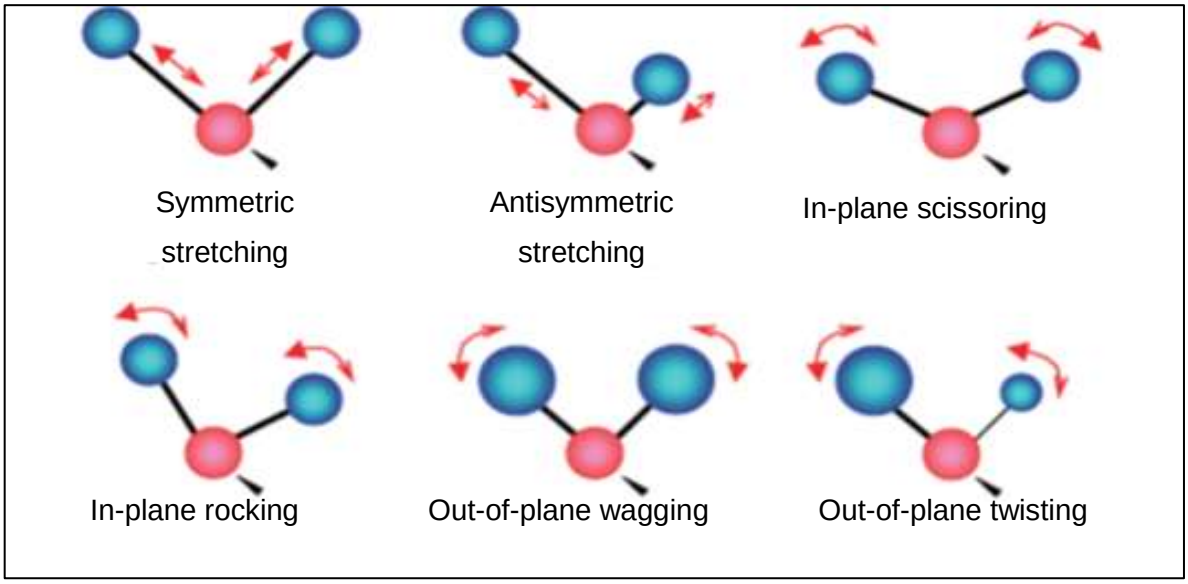

Figure 4.9: Molecular vibration and rotation modes[122]

A typical IR spectrum shows wave number (cm^{-1}) in the x-axis and the percentage (%) of absorption or transmission in the y-axis as shown in **Figure 4.10**. The absorption bands in the 4 000 to 1 500 cm^{-1} regions allow for the characterisation of functional groups within a molecule, while the lower energy portion (1 500 to 400 cm^{-1}) normally contains a very complex set of peaks caused by multiple vibrations involving several atoms and is known as the fingerprint area. This region is unique to each compound, except for chiral organic molecules in their crystalline state, and can assist in compound identification. Typical vibrational frequencies of functional groups are shown in **Table 4.3**.

[122] Tamura, K. Nanko, T. & Matsuo, J. (2010). TDLS200 tunable diode laser gas analyser and its application in industrial process, *Tokogawa Technical Report*, 53(2), pp. 113-116.

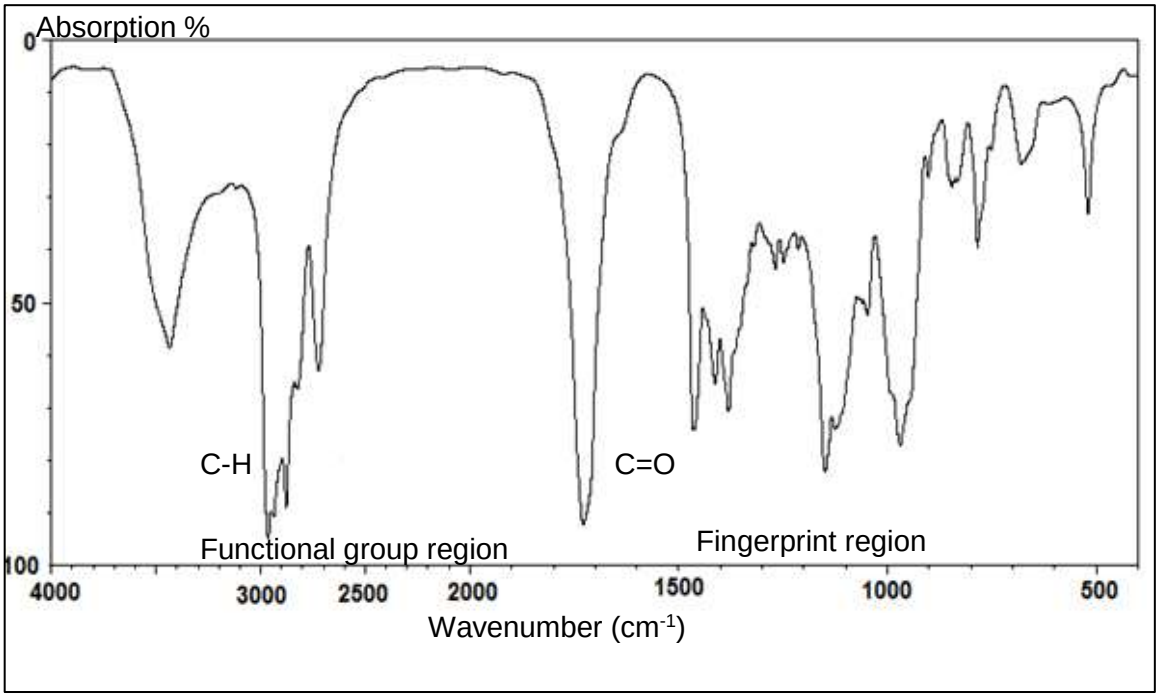

Figure 4.10: IR spectrum showing a functional group and a fingerprint region[123]

Table 4.3: Typical vibrational frequencies of functional groups[124]

Bond	Molecule	Wave number (cm^{-1})
C-O	Alcohols, ethers, esters, carboxylic acids	1 300-1 000
C=O	Aldehydes, ketones, esters, carboxylic acids	1 750-1 680
C=O	Amides	1 680-1 630
N-H (Stretching)	Amines and amides	3 500-3 100
-N-H (Bending)	Amines and amides	1 640-1 550
O-H	Alcohols	3 650-3 200
C-N	Amines	1 350-1 000
S-N	Mercaptans	2 550

[123] Spectroscopy. Available at: http://www.chem.ucalgary.ca/courses/351/Carey5th/Ch13/ch13-ir-1.html. [Accessed: 22 January 2018].

[124] Spectroscopic techniques. Available at: http://nptel.ac.in/courses/102103044/module2/lec10/6.html. [Accessed: 22 January 2018].

4.4.3 Inductively Coupled Plasma Optical Emission Spectroscopy (ICP-OES)

Currently, Inductively Coupled Plasma (ICP) is one of the most popular techniques for multi-element analysis. The strengths of ICP as an analytical technique include its speed of analyses, wide linear dynamic concentration range and low detection limits.[125] ICP techniques are also suitable for trace metal analyses and are applicable to a wide range of samples, such as metals, plastics, proteins, soils and ceramics.

There are two commonly-used kinds of ICP detection techniques for identification and quantification, namely optical emission spectroscopy (OES) and mass spectrometry (MS). Both techniques use high-temperature argon plasmas as an energy source. However, the plasma in ICP-OES is used to excite the electrons in outer energy levels within metal ions and atoms in the sample to higher vacant energy levels. These excited electrons return to their ground states after a very short time and release the absorbed energy as characteristic photons, which are then detected by the spectrometer. On the other hand, in ICP-MS, the plasma generates sample ions with different mass-to-charge ratios. These ions with different mass-to-charge ratios are transported through a region where a potential field, usually using a quadrupole, is used to separate the different species based on their mass-to-charge ratios. ICP-MS is mostly used for trace and ultra-trace analysis of elements.

ICP techniques are different from other quantification techniques such as atomic absorption spectroscopy (AAS) in that these techniques are able to measure a number of refractory elements, such as Ta, Zr, B, P and rare earths, which are difficult to analyse in AAS. This method can also be used to determine the elemental content in non-aqueous samples, including organic or slurry samples, which merely require different sample introduction systems. The success of ICP techniques for elemental quantification is attributed to the high temperatures that can be reached in an ICP argon plasma (10 000 K), while a typical maximum temperature of an AAS acetylene or air flame is only about 2 300 °C.

[125] Brundle, C.R., Evans C.A. & Wilson, S. (1992). *Encyclopedia of Materials Characterization*, p. 634.

It is important to note that in this study, quantitative analyses were mostly conducted using the ICP-OES technique due to its availability, simplicity and suitability. The advantages and disadvantages of which are shown in **Table 4.4**.

Table 4.4: The advantages and disadvantages of using ICP-OES[126]

Advantages	Disadvantages
Rapid, simultaneous, multi-element analyses	Spectral interferences
Low detection limits	Matrix effects from contaminant species
Wide linear dynamic range up to six orders of magnitude (10^6)	Matrix effects from solvent
Applicable for analyses of gases, liquids, or solids	Difficulty in analysing solids without dissolution
Can analyse more than 70 elements in one run	Inefficient sample introduction
Simpler method development does not need specialists with technical expertise.	Detection limits too high for some applications
Cheaper option if the elements do not need lower detection limits offered by ICP-MS	Drift and insufficient precision for some applications
Detection limits in parts per billion (ppb)	Only analytical grade reagents are sufficient.

Principles of ICP-OES

The ICP-OES is an emission technique based on the spontaneous emission of photons from atoms and ions that have been excited in a radio frequency (RF) discharge, using high-temperature plasma. This excitation results in the emission of electromagnetic radiation by the different atoms and ions at wavelengths characteristic of each element. There are three main parts of the ICP-OES, namely the sample introduction system, plasma and a spectrometer (**Figure 4.11**).

126 Olesik, J. W. (1991). Elemental analysis using ICP-OES and MS: An evaluation and assessment of remaining problems, *American Society*, 63(1), pp. 12-21.

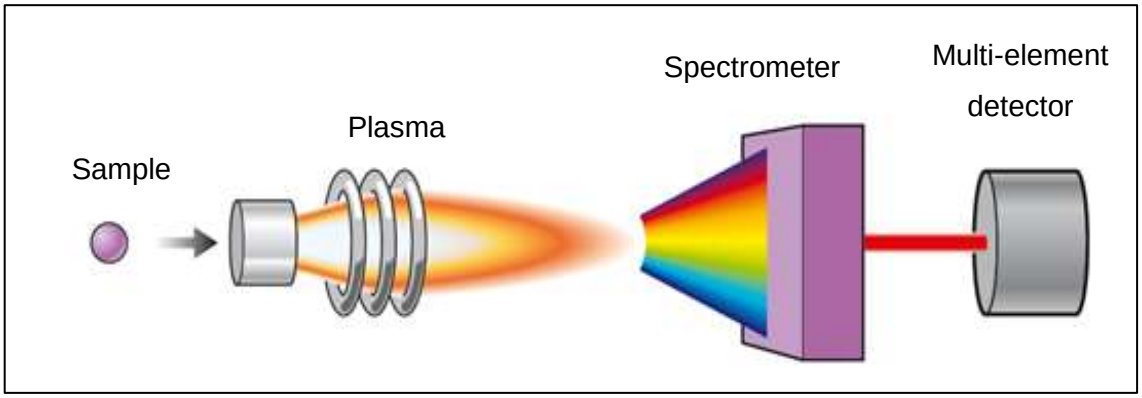

Figure 4.11: Basic components of the ICP-OES[131]

The sample introduction system

The ICP-OES sample introduction system includes a peristaltic pump, nebuliser, Teflon tubing, spray chamber and torch (**Figure 4.12**).

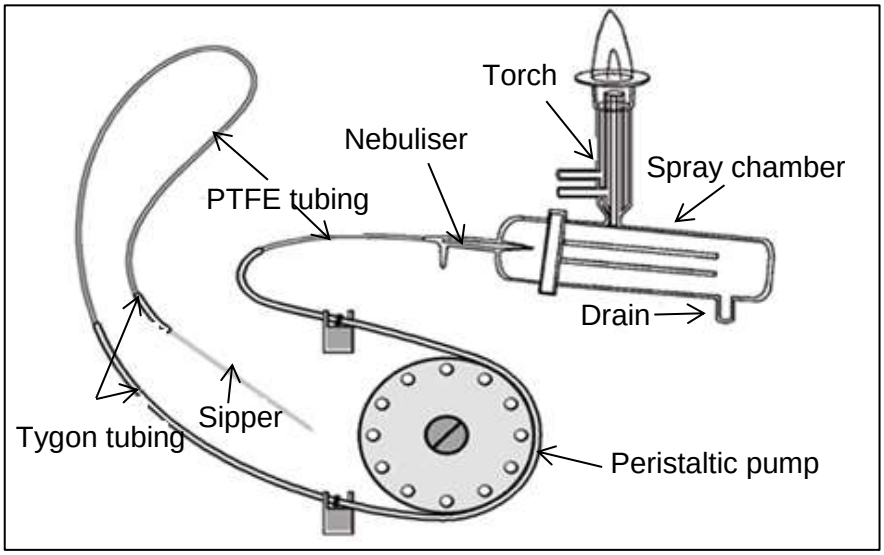

Figure 4.12: ICP-OES sample introduction system[127]

Peristaltic pump

The pump uses a process known as peristalsis to push the sample solution through the tubing with the aid of a series of rollers. This process carries the solution from the sample vessel to the nebuliser. The tubing is made of material that is not easily damaged by acidic solutions.

[127] Sample introduction system for ICP-OES and ICP-MS. Available at: http://www.spectroscopyonline.com/sample-introduction-icp-ms-and-icp-oes. [Accessed: 23 May 2017].

Nebuliser

When the liquid sample enters the nebuliser, it is converted into an aerosol that can be transported to the plasma, where it is dissolved, vaporised, atomised, ionised and excited. During nebulisation, the sample is pushed into the capillary tube by a high-pressure stream of argon gas flowing around the tip of the tube. This pressure breaks the liquid into droplets of various sizes in the spray chamber.

Spray chamber

The spray chamber is located between the torch and the nebuliser. The purpose of a spray chamber is to remove the large droplets from the aerosol before it enters the plasma. These droplets contain about 1 % to 5 % of the sample and the remaining 99 % or 95 % is drained into a waste container.[128]

The torch

The ICP-OES torch is composed of three concentric quartz tubes for argon gas flow and aerosol injection. The spacing between the outer tubes is extremely small so that the gas can flow between them in spiral movements at high speed, thus keeping the walls of the torch cool.

The plasma

The plasma in the ICP-OES is initiated at the end of the torch by means of a radio frequency (RF) induction coil through which a high-frequency, alternative current flows. This induces an alternate magnetic field which accelerates electrons into circular motions. Ionisation occurs as a result of collision between the electrons and the argon atom, producing a highly stable plasma, which has a temperature of 6 000 to 7 000 K and can reach 10 000 K in the induction zone (**Figure 4.13**). Ionisation and atomisation of the sample take place in the high-temperature flame at the torch tip. The high temperatures excite the outer valence electrons to higher energy levels. These excited electrons return to their ground states after a very short time, releasing the absorbed

[128] Csuros, M. & Csuros, C. (2002). *Environmental Sampling and analysis for Metals.* CRS Press, p. 167.

energy as characteristic photons of particular wavelengths.[129]

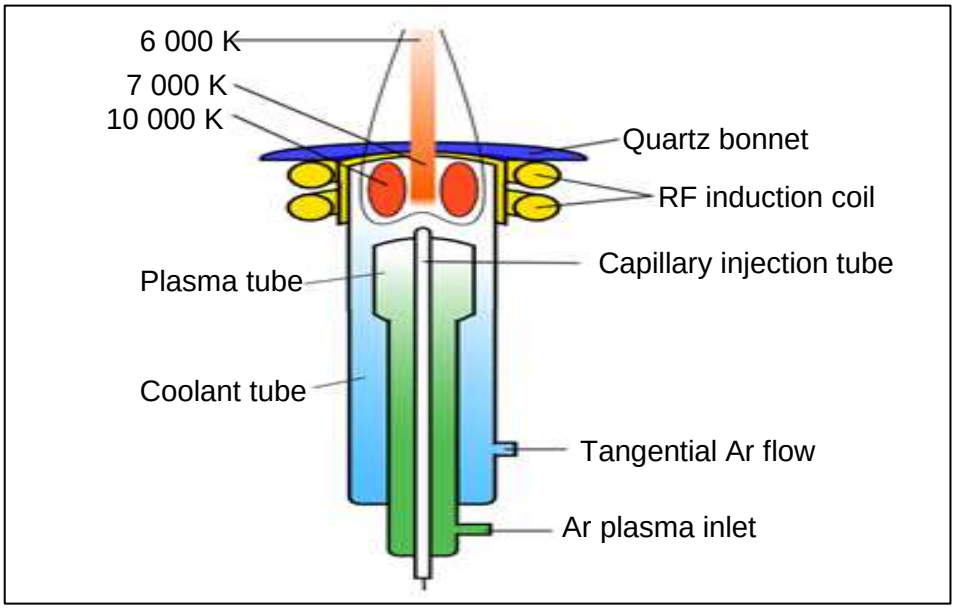

Figure 4.13: ICP-OES plasma source[130]

The spectrometer

The ICP-OES spectrometer uses an Echelle grating, a mirror and a prism to split the photons emitted from the high-temperature plasma source into separate wavelengths. The spectrometer then measures the intensities and the positions of these wavelengths which, in turn, are used to identify and quantify the elements within the sample (**Figure 4.14**).

[129] General instrumentation. Available at: http://www.ru.nl/science/gi/facilities-activities/elemental-analysis/icp-oes/. [Accessed: 03 July 2017].

[130] Available at: https://chem.libretexts.org/TextbookMaps/AnalyticalChemistryTextbookMaps/Map%3AAnalyticalChemistry2.0(Harvey)/10SpectroscopicMethods/10.7%3AAtomicEmissionSpectroscopy. [Accessed: 29 January 2018].

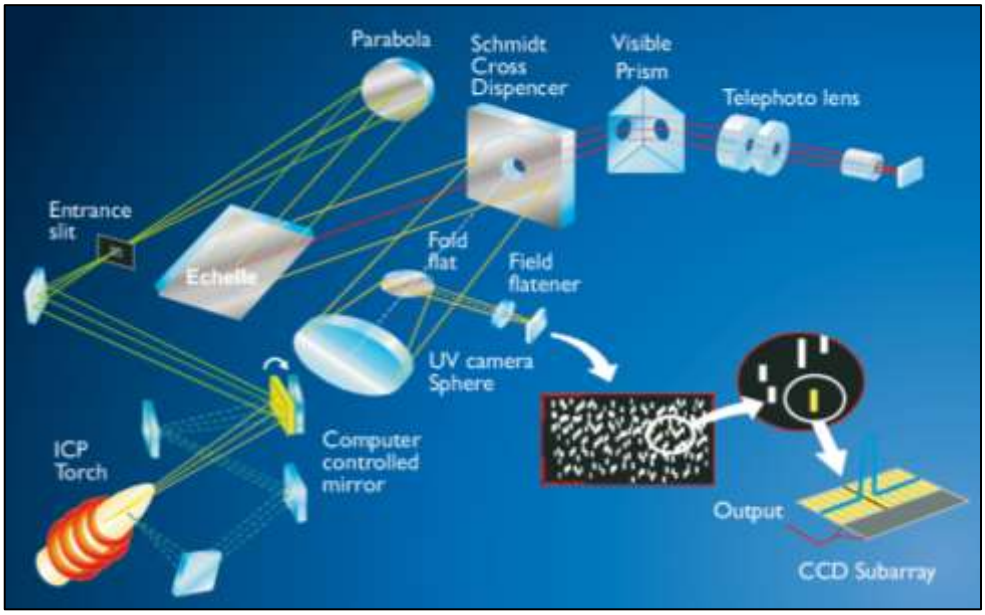

Figure 4.14: An Echelle ICP-OES spectrometer[131]

Spectral interferences in trace metal analysis by ICP-OES can be a serious problem in elemental quantification. However, these interferences can be minimised by employing matrix matching calibration, internal standardisation and wavelength correction. **Figure 4.15** shows an example of possible spectral interference that can occur during ICP-OES analysis of cadmium in the presence of iron. From this example, it is clear that the Cd line at 226.502 nm overlaps with the Fe emission line at 225.9 nm. However, this problem is easily solved by the selection of the Cd line at 228.802 nm with no interference from Fe.

[131] ICP-AE: Philips Innovation Services. (2012).

Available at: http://www.innovationservices.philips.com/sites/default/files/materials-analysis-icp-aes.pdf. [Accessed: 23 August 2016].

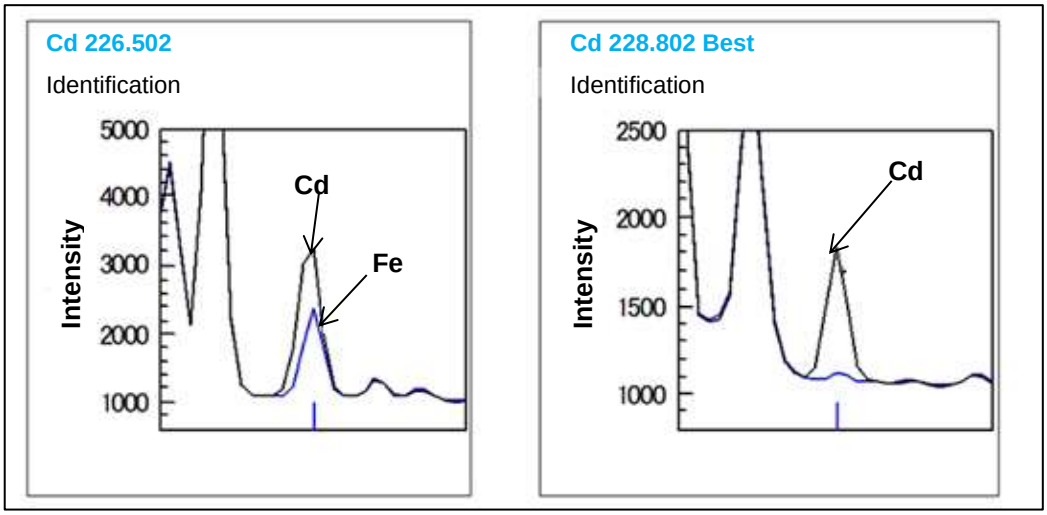

Figure 4.15: Spectral interference of iron on cadmium[132]

4.4.4 X-Ray Diffraction (XRD)

X-ray diffraction is considered one of the most powerful analytical techniques for investigating both the geometric nature of the three-dimensional array of molecules within a crystal as well as the exact nature of the product. The X-rays have much shorter wavelengths (0.01 to 10 nm) than visible light (**Figure 4.7**), which allow them to be used to investigate the elemental content and arrangement of atoms within the crystal. The two main types of XRD which are used for scientific purposes are X-ray crystallography and X-ray powder diffraction.

X-ray crystallography, also referred to as single X-ray diffraction, is a technique that is employed to study the array of atoms of a crystalline solid in three dimensional spaces in which the crystalline atoms cause a beam of incident X-rays to diffract in different directions (**Figure 4.16**). The directions of possible diffractions are determined by the shape and size of the unit cell of the material.[133] The resulting patterns assembled by the diffraction of the X-rays through the closely-packed lattice of atoms in a crystal can then be processed to reveal information about the crystal details, such as packing symmetry, bond lengths and angles, and the size of the repeating unit that forms a

[132] Environmental Solutions. Available at: https://www.ssi.shimadzu.com/industry/industry_environmental_icp_aes.cfm. [Accessed: 26 February 2018].

[133] X-ray diffraction. Available at: https://www.xos.com/XRD. [Accessed: 12 February 2018].

crystal. One major limitation of single X-ray crystallography is that it can only analyse crystals of a certain quality and size.

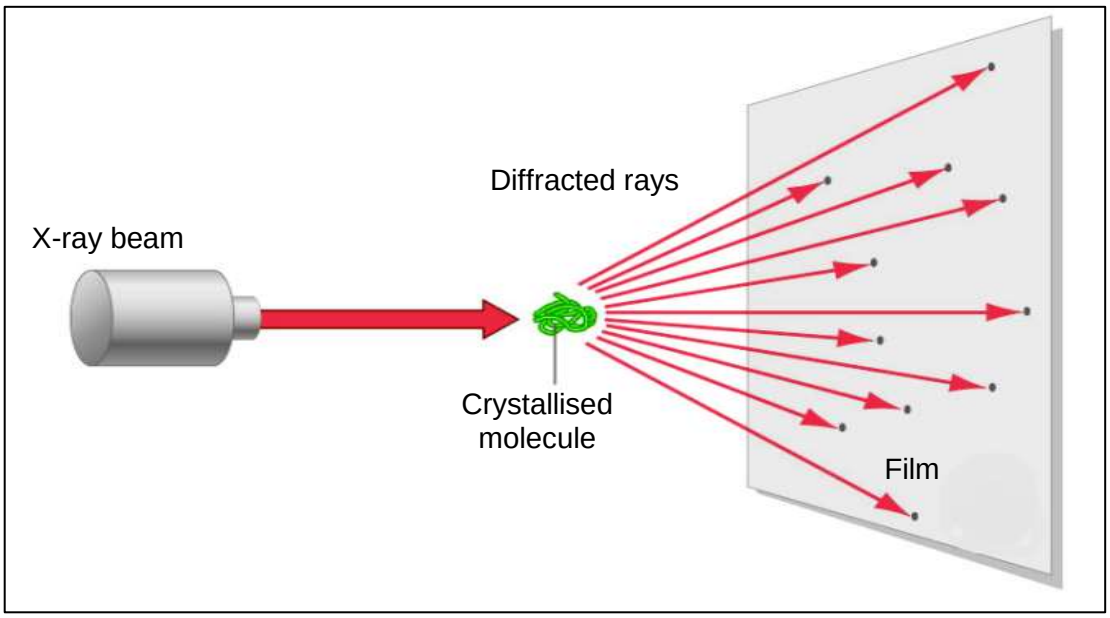

Figure 4.16: Schematic diagram of X-ray crystallography[134]

Bragg's Law (**Equation 4.7** and **Figure 4.17**) is used to describe the diffraction of X-rays by a crystal. The law states that the X-rays reflected from different parallel planes within a crystal interfere constructively when the path difference is an integral multiple of the wavelength of X-rays:

$$n\lambda = 2d \sin\theta \qquad \textbf{(4.7)}$$

where n is an integer order of reflection, λ is the wavelength of incident X-rays, *d* is the interplanar spacing of the crystal and θ is the angle of incidence.

A measuring instrument called a diffractometer is used to detect the diffraction of X-rays from the crystallised molecule and to record its diffraction intensity as a function of diffraction angle. The three main components of a diffractometer are an X-ray source, a goniometer and an X-ray detector. The molecule is mounted on a goniometer which positions the crystallised molecule at selected orientations. The molecule is then

[134] X-ray crystallography. Available at: http://260h.pbworks.com/w/page/30814223/X%20Ray%20Crystallography. [Accessed: 12 February 2018].

radiated with a monochromatic beam of X-rays, generating a diffracted pattern. The detector counts the number of X-rays diffracted by the molecule and the intensity of each diffracted X-ray is used in a number of different computer programmes, such as SAINT-Plus, XPREP, SADABS, SHELXTL and SHELXS[135,136,137,138,139] and using mathematical Fourier transform calculations to determine the position of every atom in a crystal, resulting in a three-dimensional image of the molecule.

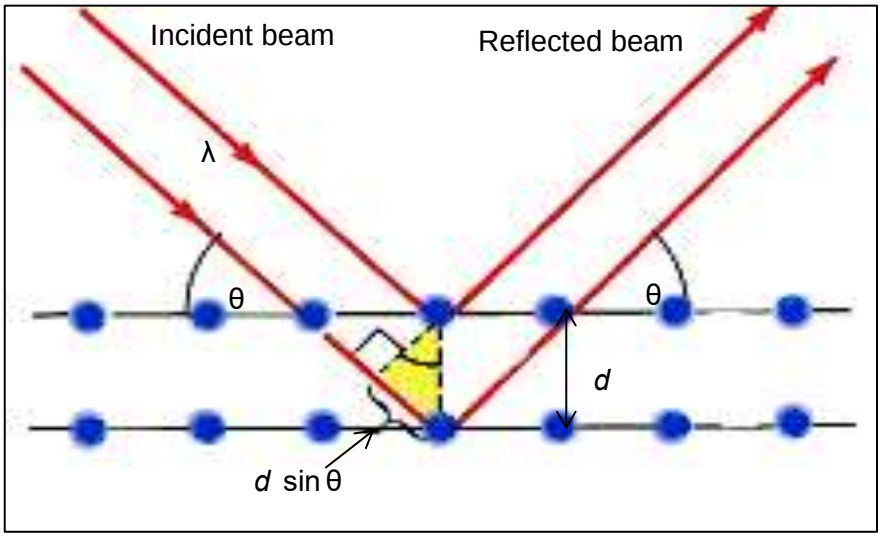

Figure 4.17: Bragg's Law[140]

Powder diffraction, on the other hand, allows for the rapid, non-destructive analysis of multi-component mixtures. This method enables for the rapid analyses and

[135] Muldoon, J. & Brown, S.N. (2003). Unsymmetrically bridging aryls of iridium, *Organometallics*, 22, pp. 4480-4489.

[136] Zhou,Z., Deng, Y. & Wan, H. (2004). Structural diversities of cobalt (II) coordination polymers with citric acid, *Crystal Growth & Design*, 5(3), pp. 1109-1117.

[137] Thim, R., Dietrich, H.M. & Borath, M. (2018). Pentamethylcyclopentadienyl-supported rare-earth-metal benzyl, amide and imide complexes, *Organometallics*, 37, pp. 2769-2777.

[138] Kraft, S.J., Fanwich, P.E. & Bart, S.C. (2010). Synthesis and characterization of a uranium(III) complex containing a redox-active 2,2-bipyridine ligand, *Inorg.Chem*, 49, pp. 1103-1110.

[139] Pan, S., Smit, J.P. & Watkins, B. (2006). Synthesis, crystal structure and nonlinear optical properties of $Li_6CuB_4O_{10}$, *J.Am.Chem.Soc*, 128(35), pp. 11631-11634.

[140] 100th anniversary of the discovery of crystallography. Available at: http://www.chemistryviews.org/details/ezine/2064331/100th_Anniversary_of_the_Discovery_of_X-ray_Diffraction.html. [Accessed: 12 February 2018].

identification of unknown materials, as well as for the characterisation of materials and products in disciplines, such as mineralogy and archaeology, without the need for extensive sample preparation. Databases, such as the Cambridge Structural Database, International Centre for Diffraction Data or Powder Diffraction File (PDF) are used to compare the diffraction patterns of the newly-isolated products with that of known standards to successfully identify and characterise the products. However, structural determination by X-ray powder diffraction may not be as accurate as that by single X-ray diffraction.

4.4.5 Nuclear Magnetic Resonance (NMR) Spectroscopy

The NMR is a spectroscopic technique that is most often used to identify the carbon-hydrogen framework of organic compounds and has been widely employed by scientists to obtain detailed chemical structures of synthesised products. NMR was first described and measured in molecular beams by Isador Rabi in 1938, and in 1946 its application was expanded by Felix Bloch and Edwards Mills Purcell to include solid and liquid samples. Since then, applications in the use of NMR for identifying and quantifying different kinds of chemical compounds have developed rapidly and are currently a very powerful tool used in academic research and in the medical and industrial fields.

The success of the NMR technique may be attributed to its ability to identify the structure of a molecule by observing the interaction of nuclei with an odd number of protons when placed in a powerful magnetic field. Radio waves, which have the longest wavelengths in the electromagnetic spectrum, are the source of NMR (**Figure 4.7**). These have low frequencies in the range of 60 to 900 MHz.

As an analytical technique, NMR is based on the principle that a nucleus has a natural spin orientation and that all nuclei are electrically charged. Almost all the elements have at least one isotope that has an uneven number of protons in its nucleus. This makes it NMR active since only nuclei with unequal quantum spin numbers, for example ***I*** = multiples of ½, are detectable by NMR and include ^{13}C, ^{1}H, ^{19}F, ^{31}P and ^{15}N. The most important NMR-active nuclei in organic chemistry are ^{1}H and ^{13}C.

Principles of NMR

Nuclei with unequal spin, for example ½, have two possible orientations, namely a parallel and anti-parallel, with two energy levels corresponding to magnetic quantum numbers, *m* of + ½ and - ½ (**Figure 4.19**). Without any applied external magnetic field, these nuclei will have random orientations of equal energy. When they are introduced to an external magnetic field, normally originating from a radiofrequency pulse, all the nuclei will align with or oppose the applied field (**Figure 4.18**). This will result in the flipping of some of the nuclei from parallel to anti-parallel (**Figure 4.20**), resulting in an increase in energy from low-energy spin (parallel) to higher-energy spin (anti-parallel), thus absorbing energy. The energy required to stimulate a magnetic dipole moment from parallel to anti-parallel is the difference between the two energy states. The excited nuclei will drop back to their low-energy states, emitting energy. The field strength at which the nuclei absorb energy while resonating is used to determine the structure of a molecule.

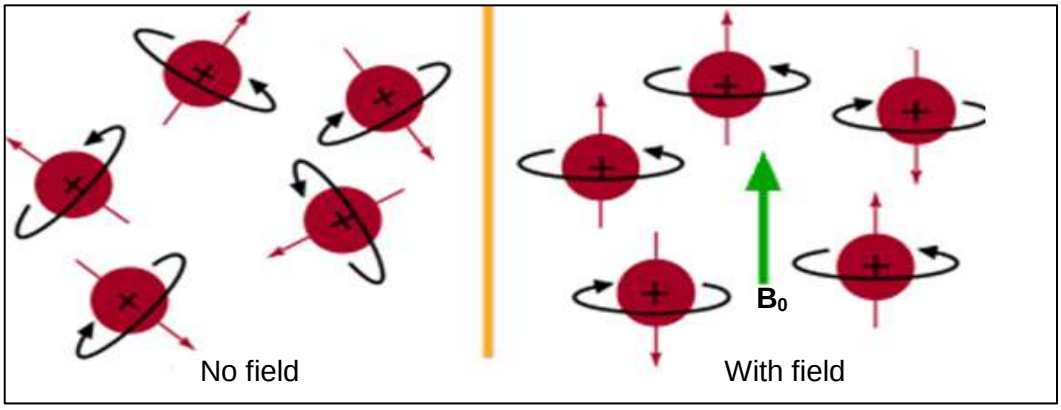

Figure 4.18: Nuclei in the absence and presence of an external magnetic field[141]

[141] Nuclear magnetic resonance spectroscopy. Available at: http://www.chem.ucalgary.ca/courses/350/Carey5th/Ch13/ch13-nmr-1.html. [Accessed: 23 January 2019].

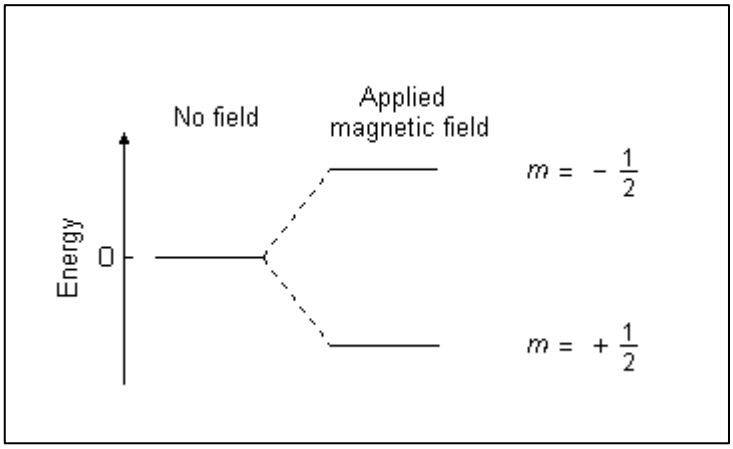

Figure 4.19: Energy levels of a nucleus with a spin quantum number of ½[142]

In addition, the electrons surrounding the nucleus generate a local magnetic field which shields the nucleus from the applied magnetic field. For example, when a proton nucleus is subjected to a powerful external magnetic field ($\mathbf{B_0}$), circulation in the electron cloud surrounding the nucleus is induced, which produces a secondary magnetic field (**B**) which shields the nucleus from the external magnetic field ($\mathbf{B_0}$) (**Figure 4.20**).[143] The nucleus responds by generating an electromagnetic signal with a frequency characteristic of the magnetic field in the nucleus. This magnetic field is affected by the electron shielding which strongly depends on the chemical environment and the orientation of the neighbouring nuclei, resulting in a phenomenon known as spin-spin coupling (*J* coupling). Splitting of the signal of each nucleus occurs, producing two or more lines, which is also used to extract useful information about the chemical environment of the nucleus.

[142] Nuclear magnetic resonance spectroscopy: Theoretical principles. Available at: https://teaching.shu.ac.uk/hwb/chemistry/tutorials/molspec/nmr1.htm. [Accessed: 23 January 2019].

[143] What is shielding and deshielding in NMR. Available at: https://socratic.org/questions/what-is-shielding-and-deshielding-in-nmr-can-you-give-me-an-example. [Accessed: 06 December 2018].

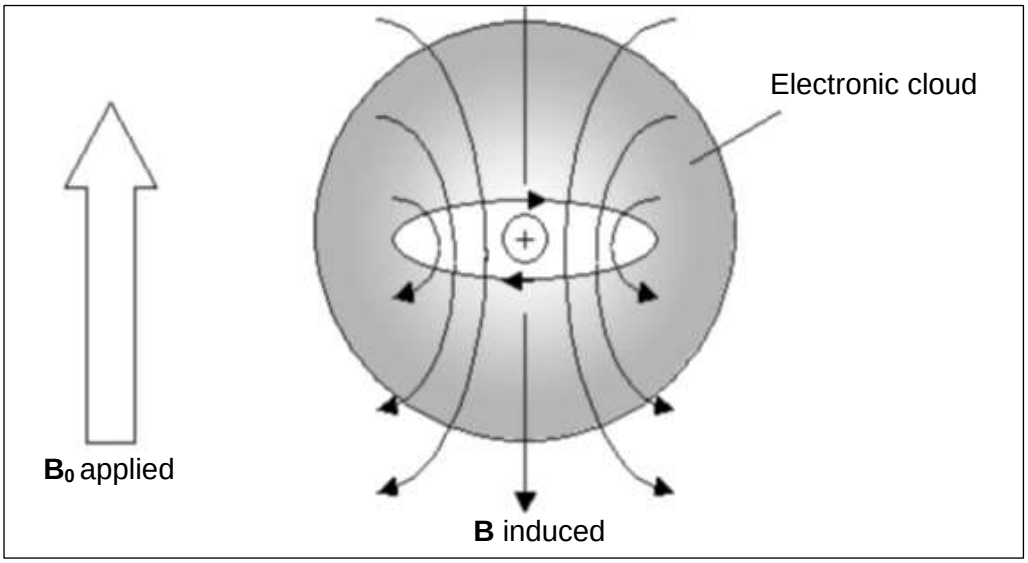

Figure 4.20: A nucleus introduced to a strong external magnetic field ($\mathbf{B_0}$) causes electrons around the nucleus to circulate, thus generating an opposing magnetic field (**B** to $\mathbf{B_0}$)[144]

The strength of an external magnetic field ($\mathbf{B_0}$) that is experienced by the nucleus is presented as chemical shift. The chemical shift allows for distinguishing magnetically-inequivalent nuclei within a molecule and is expressed in parts per million (ppm) relative to the resonance-observed proton frequency of tetramethylsilane (TMS) hydrogens, a reference compound for NMR, and has a chemical shift position of zero.

Since the electrons surrounding the nucleus shield the proton from the external magnetic field, this causes the nucleus to experience a lower magnetic field, resonating at a lower frequency. Any influence which increases this effect will result in a lower chemical shift and is referred to as shielding, while an opposite influence will lead to an increase in the resonant frequency or chemical shift and is referred to as deshielding. Typical proton chemical shift ranges for various functional groups are shown in **Figure 4.21**.

[144] Gerothanassis, I.P., Troganis, A. & Exarchou, V. (2002). Nuclear magnetic resonance spectroscopy: Basic principles and phenomena, 3(2), *Research and Practice in Europe*, pp. 229-252.

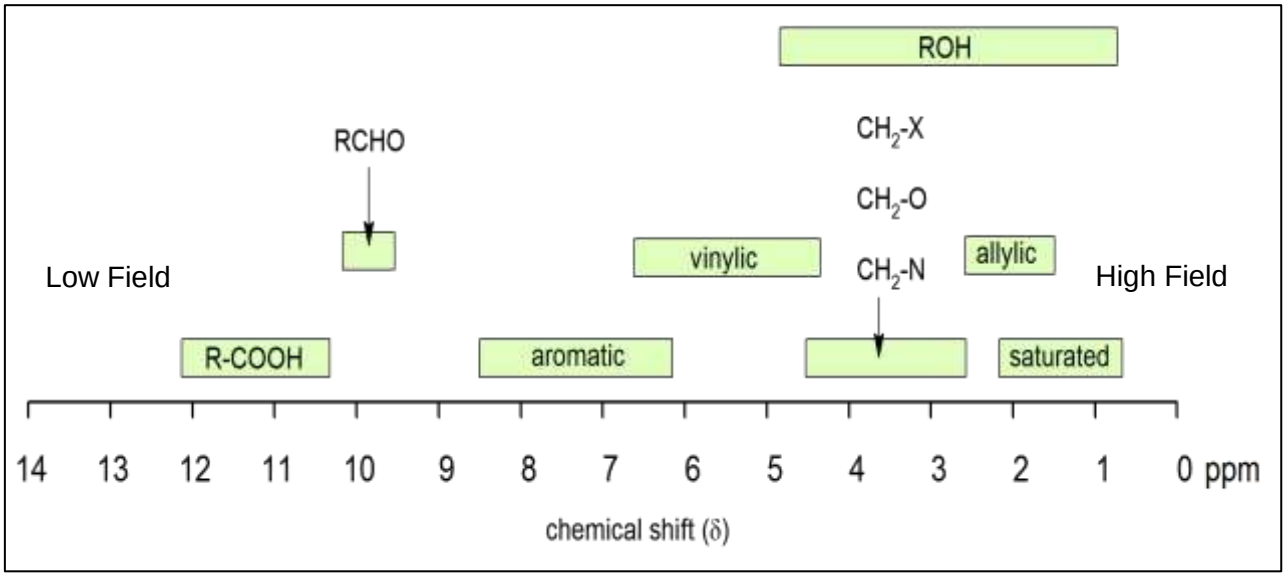

Figure 4.21: Proton chemical shift range[145]

Practically, the NMR experiment involves the introduction of a dissolved sample to a magnetic field generated by a superconducting magnet. The superconducting magnet produces a constant magnetic field which induces microscopic magnetisation in the sample. The linear oscillating electromagnetic field is then generated by a transmitter with desirable magnetic field strength to interact with the nuclei in the sample. The NMR signal (Free Induction Decay), initiated at the probe after irradiation by radio frequency (RF) pulses is first amplified and identified by a detector to produce spectra of peak intensity against chemical shift measured in ppm.[146] Whereas modern NMR spectrometers use Fourier Transform (FT) spectrometers to detect signal, Continuous Wave (CW) spectrometers were popular in the past. The main components of the NMR spectrometer are shown in **Figure 4.22** and the advantages and disadvantages of the NMR technique are included in **Table 4.5**.

[145] Chemical shifts in proton NMR spectroscopy. Available at: https://courses.lumenlearning.com/suny-mcc-organicchemistry/chapter/chemical-shifts-in-proton-nmr-spectroscopy/. [Accessed: 15 January 2019].

[146] Teng, Q. (2013). *Structural Biology: Practical NMR Applications*, *2nd Edition.* Springer, p. 65.

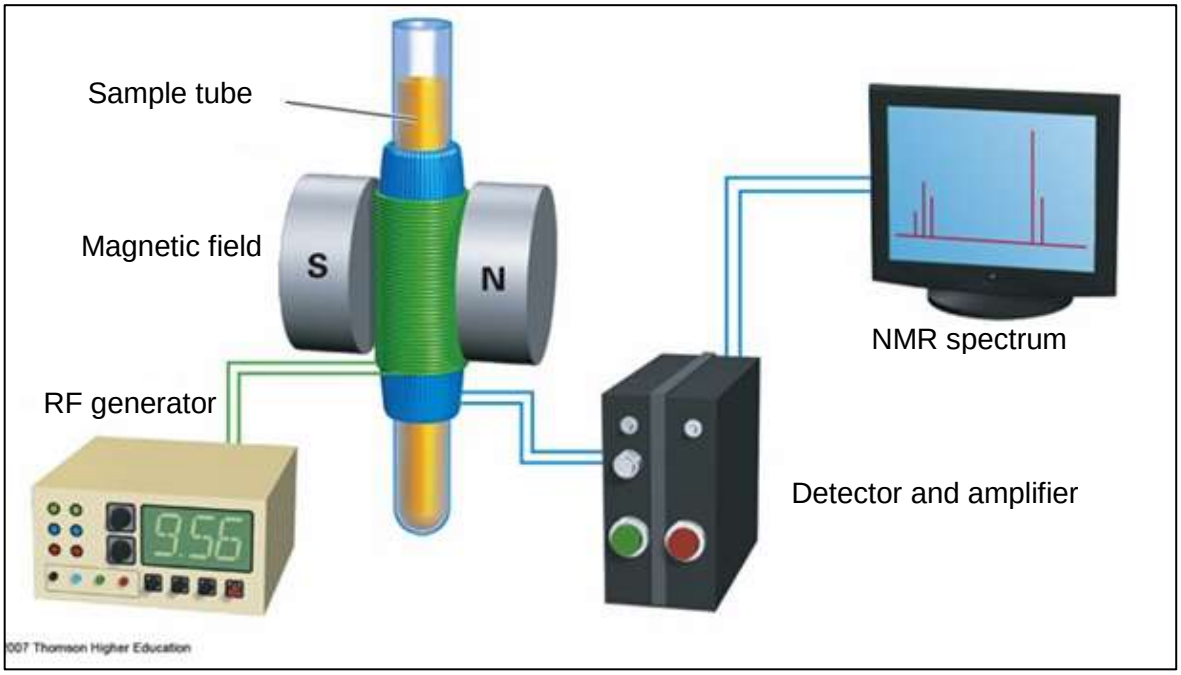

Figure 4.22: Schematic diagram of the NMR instrument[147]

Table 4.5: The advantages and disadvantages of using NMR as an analytical technique

Advantages	Disadvantages
Structural details obtained	Very expensive
Minimal sample preparation	Limited qualitative results
Small sample volumes required	Longer analysis time for ^{13}C
Non-destructive analysis	Poor sensitivity

147 Structure determination: Nuclear magnetic resonance. Available at: https://slideplayer.com/slide/8418782/. [Accessed: 14 December 2018].

4.4.6 LECO CHNS Combustion Micro-Elemental Analysis

The LECO CHNS instrument uses combustion to successfully determine the elemental composition of inorganic and organic compounds. The technique is capable of handling different types of samples, including solids, liquids, volatiles and viscous samples in a wide variety of industries, including pharmaceuticals, polymers, petrochemicals and chemicals.[148,149] It is often used as a confirmation tool to help identify the type and purity of compounds after synthesis or purification stages. Usually, the elements that are analysed by means of this technique include hydrogen, carbon, sulphur and nitrogen.

Principles of LECO CHNS Micro-Elemental Analysis

The LECO CHNS elemental analysis employs a unique combination of a flow-through carrier gas system and highly-selective Infrared (IR) and thermal conductivity detection (TCD) systems.[150] The combustion process involves the decomposition of the sample being analysed at high temperatures to convert the compounds in question to their elementary products as N_2, CO_2, SO_2, and H_2O.

During the analysis of solid materials, a sample (2 mg) is weighed in a high-purity tin crucible, after which it is sealed and placed in an autoloader where it is automatically dropped into the high-temperature combustion furnace (950 °C) in an oxygen-rich environment, allowing the sample to combust. The combustion converts hydrogen to H_2O, carbon to CO_2, sulphur to SO_2 and nitrogen to N_2. The combustion gases are swept away from the furnace by helium carrier gas through a tube containing high-purity copper turnings at 650 °C, which removes any oxygen not consumed in the initial combustion stage and converts some nitrogen oxides to nitrogen gas.[151] The gases are then progressed into the detection systems as they are released. Individual IR cells

[148] Sergio, C.M., Redigolo, M.M. & Amaral, P.O. (2015). Analysis of hydrogen, carbon, sulphur and volatile compounds in U_3Si_2-Al nuclear fuel. *International Nuclear Atlantic Conference*, pp. 1-7.

[149] Hassel, A.W., Merzlikin, S. & Mingers, A. (2013). Methodology of hydrogen measurements in coated steels, European Union, pp. 1-155.

[150] Guerra, C. (2004). Inert gas fusion analyser, *LECO Corporation,* pp. 1-5.

[151] Thompson, M. (2008). AMC technical briefs, *The Royal Society of Chemistry*, pp. 1-2.

are used for the simultaneous detection of C, H and S, while the nitrogen is measured, using the TCD system. Once the concentration of each combustion product has been determined, the empirical or molecular formula of the sample can be calculated (**Figure 4.23**).

Detection by the IR cells is based on the principle that H_2O, CO_2 and SO_2 absorb infrared energy at distinctive wavelengths in the infrared spectrum. The incident IR energies at these wavelengths are absorbed as the gases pass through the IR absorption cells. The detection by the TCD system is based on the principle that the heated filaments within a bridge circuit are maintained at a fixed voltage in a flowing stream of helium gas. Changes with regard to the composition of a gas stream cause a change in the resistance of the filaments; this change is usually caused by the nitrogen from the sample and is recorded as an analytical signal.[152]

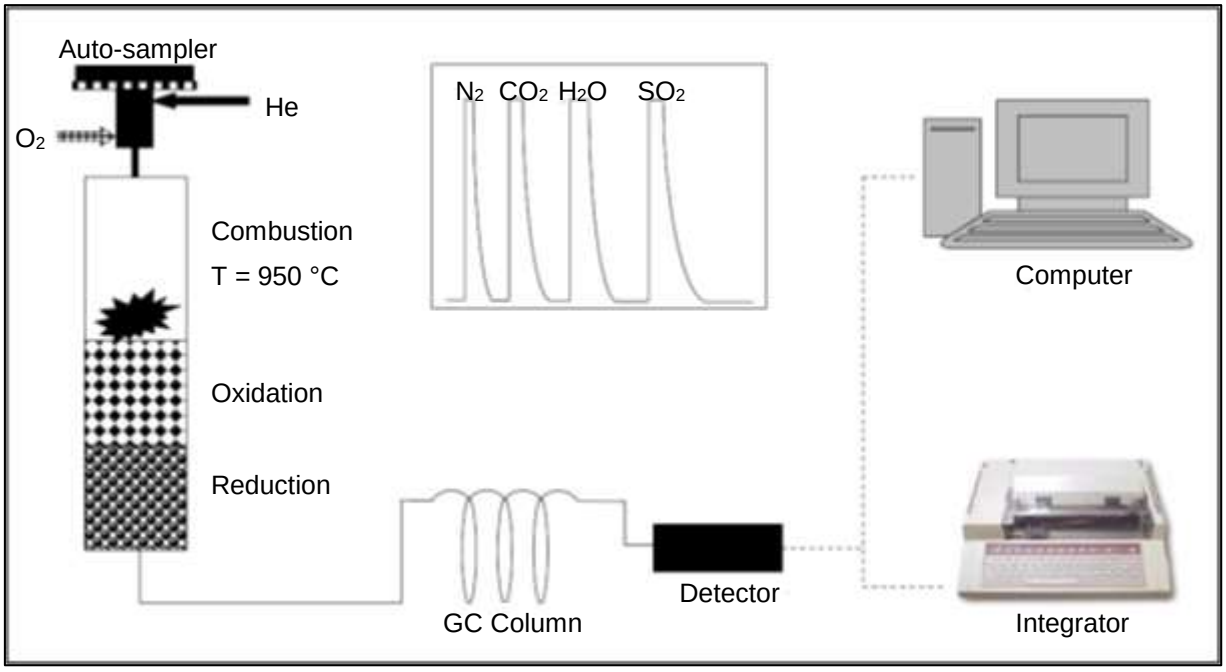

Figure 4.23: The basic setup for CHNS micro-analyser[153]

[152] LECO Corporation. (2017). Oxygen and nitrogen in solid iron, steel, nickel-base and cobalt alloys, pp. 1-3.

[153] Thompson, M. (2008). CHNS elemental analysers. Available at: http://www.rsc.org/images/chns-elemental-analysers-technical-brief-29_tcm18-214833.pdf. [Accessed: 21 January 2019].

As previously indicated, these micro-elemental CHNS instruments perform simultaneous analyses on non-metals, with good precision and efficiency, and can accurately detect low levels of these elements (0.002 % to 0.5 %). Only small amounts of a sample are required (~ 2 mg) and the analysis takes only about 5 minutes. Quantification with the micro-elemental CHNS instrument requires simple calibrations of each element, using high-purity micro-analytical standards, such as EDTA, cysteine or acetanilide. The instrument also enables drift corrections for better quality of results.

4.5 METHOD VALIDATION

Method validation is very crucial in analytical chemistry as it determines whether an analytical process used for a particular sample or system is appropriate for its use. The results obtained by means of this process are used to determine the reliability or quality of analytical results. The validation parameters are summarised in **Figure 4.24** and are explained below.

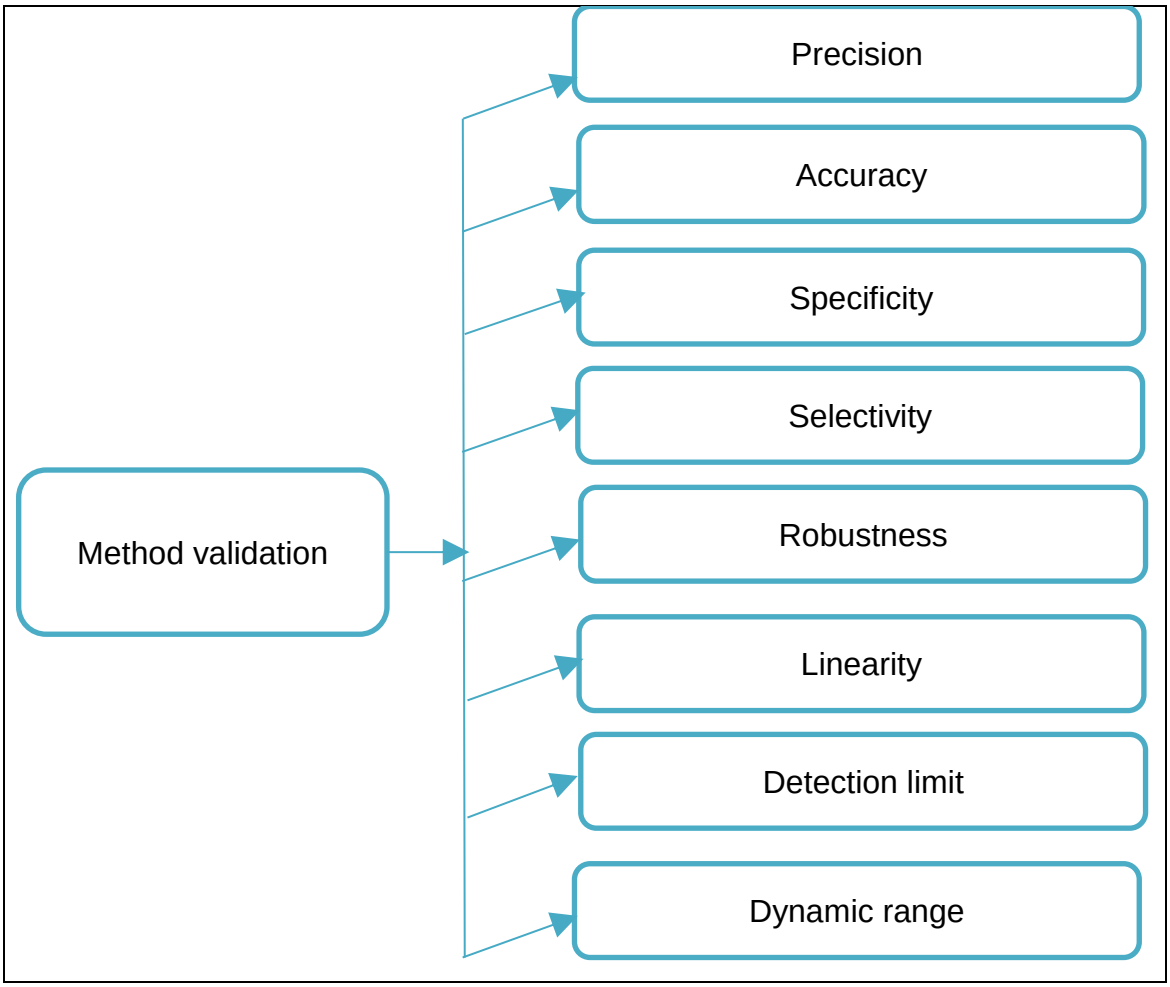

Figure 4.24: Summary of validation parameters

4.5.1 Precision

Precision is described as the agreement or closeness of results obtained from replicate measurements of the same sample under the same experimental conditions. The parameters used to describe precision include variance, standard deviation and coefficient of variation. Precision can be considered at three levels, namely intermediate precision, reproducibility and repeatability.[154]

Standard deviation(s)

The standard deviation is represented by the following equation:

$$s = \sqrt{\frac{\sum_{i=1}^{N}(x_i - \bar{x})^2}{N-1}} \qquad \textbf{(4.8)}$$

where $(x_i - \bar{x})^2$ represents the deviation of value x_i from the mean $\bar{x}$ and *N* represents the number of measurements. The quantity *N*-1 is known as the number of degrees of freedom.

Relative standard deviation (RSD) and coefficient of variation (CV)

The relative standard deviation (RSD) is the standard deviation divided by the mean value ($\bar{x}$) of the data set. RSD is sometimes given by the symbol s_r:

$$\text{RSD} = s_r = \frac{s}{\bar{x}} \qquad \textbf{(4.9)}$$

The coefficient of variation (CV) is the relative standard deviation multiplied by 100 %:

$$\text{CV} = \text{RSD in \%} = \frac{s}{\bar{x}} \times 100\% \qquad \textbf{(4.10)}$$

Repeatability

Repeatability represents precision under the same operating conditions over a short period of time.

Intermediate precision

[154] Huber, L. (2010). *Validation of analytical methods*, Agilent Technologies, p. 18.

Intermediate precision involves variations within laboratories, such as different days, equipment and analysts.

Reproducibility

This level of precision is determined by the collaboration between laboratories, and collaborative studies, and is normally employed to the standardisation method. This type of collaboration is also required in the certification of standard reference materials.

4.5.2 Accuracy

Accuracy is described as the agreement between an accepted or known reference value and an experimentally measured value. Accuracy can be expressed in terms of either absolute, relative error or by means of the comparison of results, using the Student's *t*-test.

Absolute Error

The absolute error, E in the measurement of a quantity, x is expressed by the equation:

$$E = x_i - x_t \qquad \textbf{(4.11)}$$

where x_t is the true or accepted value of the quantity.

Relative Error

The relative error, E_r is often a more convenient quantity as compared to the absolute error. The percentage of the relative error is given by the equation:

$$E_r = \frac{x_i - x_t}{x_t} \times 100\% \qquad \textbf{(4.12}$$

The t-Test

The *t*-test value is calculated according to **Equation 4.13** and is used to decide whether there is any statistical difference between the true or expected mean and the experimentally-obtained mean at known confidence level.

$$t = \frac{\bar{x} - \mu}{s/\sqrt{N}} \quad \textbf{(4.13)}$$

where t is the t-statistic value, μ is the true mean, s is the standard deviation, N is the sample size and $\bar{x}$ is the mean of experimental results.

4.5.3 Specificity

Specificity is defined as the ability to evaluate the analyte unequivocally in the presence of components which may be expected to be present. This might include impurities, degradants, and matrices. In the quantification of the analyte with ICP-OES, specificity involves the process of investigating the possible spectral interference on the analyte measurement and proper wavelength alignment. A comparison of the results obtained, using direct calibration curve, will provide information concerning matrix effects.

4.5.4 Selectivity

Selectivity refers to the level to which an analytical method is free from interference by different species present in the sample matrix. Since no analytical procedure is completely free from interference, this requires frequent steps to minimise the effects of these interferences. Both selectivity and specificity evaluate a method's ability to accurately quantify only the analyte of interest and the magnitude of intercept of the obtained calibration curve, which should go through the origin is usually used as an indicator of the selectivity of a method.

4.5.5 Robustness

Robustness is described as the ability of the method to withstand any change caused by small but deliberate variations in method parameters. In the case of quantitative analyses using the ICP-OES technique, instrumental parameters, such as injection volume, flow rate, RF power, resolution capability and detection wavelengths are usually varied within a realistic range and the quantitative influence of these variables determined.

4.5.6 Linearity

Linearity is described as the ability of an analytical process to obtain experimental results that are directly proportional to the concentration of the analyte within a given range. At least five standard solutions with different concentrations are used to obtain a plot of the signals as a function of the analyte concentrations. From this plot, one can determine the linear regression equation and linear regression coefficient, *R*.

If it is assumed that a linear correlation exist between the measured response (y) and the standard analyte concentration (x), a linear regression equation can be expressed by means of the equation:

$$y = mx + b \qquad \textbf{(4.14)}$$

where m is the slope or sensitivity of the line, and b is the y intercept.

The linear regression equation from the calibration curve is used to estimate the concentration of the unknown analyte (**Figure 4.19**). The regression coefficient (*R*) is calculated according to **Equation 4.15**:

$$R^2 = \frac{[n(\sum xy)-(\sum x \sum y)]^2}{[(n(\sum x^2)-(\sum x)^2)(n(\sum y^2)-(\sum y)^2]} \qquad \textbf{(4.15)}$$

The R^2 value must be greater than 0.997 to be considered as acceptable linearity. An example of good linearity is shown in **Figure 4.25**.

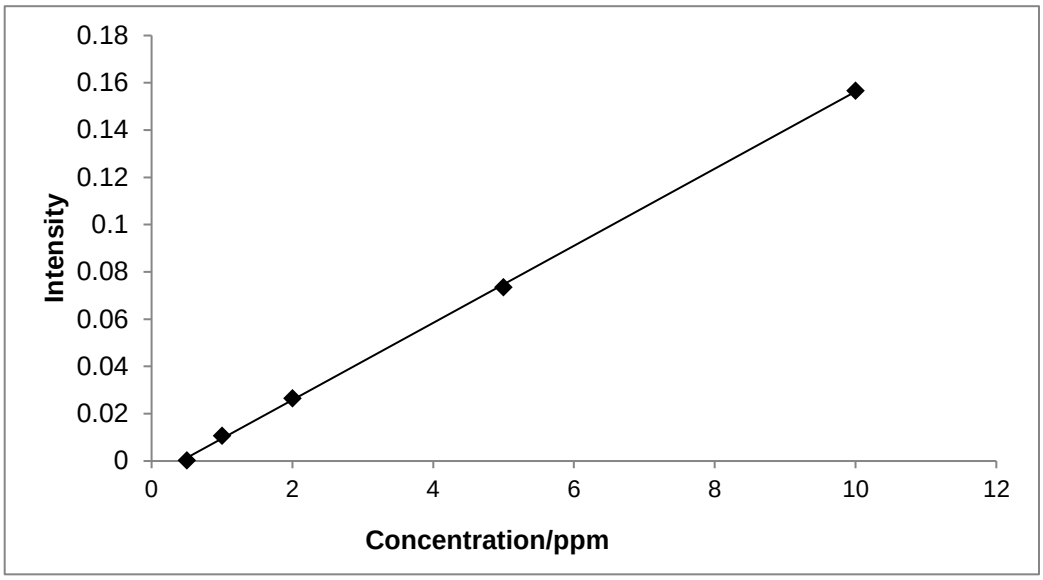

Figure 4.25: Linearity with regression coefficient ≥ 0.997

4.5.7 Detection Limit (LOD), Limit of Quantification (LOQ) and Dynamic Range (DR)

Detection limit (LOD)

The detection limit is described as the lowest quantity of the analyte within a sample that can be detected at a known confidence level. Detection limit is determined by the ratio of the size of the analytical signal to the magnitude of the statistical fluctuations in the blank signal, and is calculated according to **Equation 4.16**.

$$\mathrm{LOD} = \frac{3 \times s_b}{\mathrm{m}} \qquad \textbf{(4.16)}$$

where s_b is the standard deviation of the blank and m is the slope of the calibration curve.

Limit of quantification (LOQ)

The limit of quantification is the lowest amount of analyte in a sample which can be quantitatively measured with suitable accuracy and precision, and can be determined, using **Equation 4.17**.

$$\mathrm{LOQ} = 10 \times \mathrm{LOD} \qquad \textbf{(4.17)}$$

Dynamic range (DR)

The dynamic range (**Figure 4.26**) varies from the lowest concentration at which quantitative measurements can be made (limit of quantification (LOQ)) to the concentration at which the calibration curve deviates from linearity (limit of linearity (LOL)). Dynamic range can also be described as the range over which the detector still responds to the varying concentrations.[155]

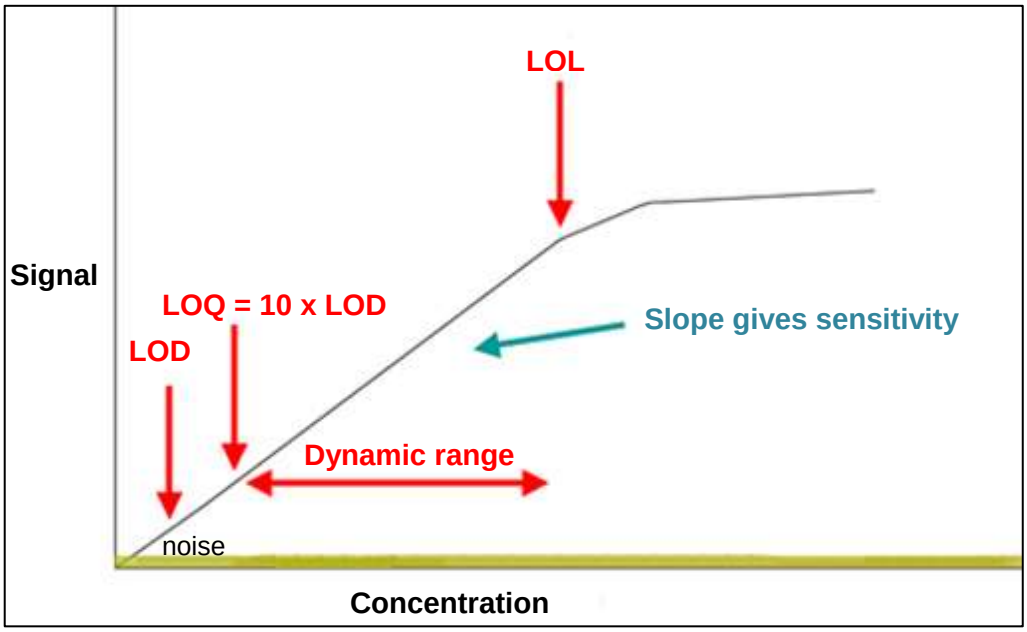

Figure 4.26: The determination of LOD, LOQ and LOL from the calibration curve (**Equations 4.16** and **4.17**)[156]

[155] Skoog, D.A., Holler, F.J. & Crouch, S.R. (2007).*Principles of Instrumental Analysis, 7th edition,* Cengage Learning, p. 19.

[156] Calibration curve: Available at: https://upload.wikimedia.org/wikipedia/commons/0/0c/Calibration_curve.png. [Accessed: 15 February 2018].

4.6 CONCLUSIONS

The accurate characterisation of complex chemical matrices involves three major experimental steps, namely the successful and complete dissolution of the samples, the accurate quantification of the chemical composition of the dissolved samples, and the identification or characterisation (solid and in solution) of the original or isolated compounds.

This study included all three of the above-mentioned steps, and the individual techniques used in the study were selected based on criteria, such as the availability of equipment and reagents, accuracy needed (concentration of the analytes of interest) and the types of samples investigated.

In this regard, the ability of the SEM-EDS to determine the nature of solid samples through surface analysis was found useful for the successful determination of the catalyst matrix. For the dissolution of the catalyst material, both acid digestion and flux fusion methods were investigated. The outstanding advantages of ICP-OES methods which include its low-detection limits, wide linear dynamic range and, most importantly, its ability to quantify trace metals with high accuracy and precision, allowed for the successful quantification of PGE and other elements that were present in the catalyst sample and in all liquid samples. Finally, precipitation and solvent extraction methods were applied to dissolved reaction mixtures to bring about the separation of the PGE from the non-precious metals and from one another. FT-IR, NMR, LECO and XRD were used to characterise some of the isolated products after they had gone through the separation and product-isolation steps. The validation parameters mentioned in this chapter proved to be useful in terms of ensuring the quality of the methods developed in this study.

5 Experimental Methods for the Recovery of PGE

5.1 INTRODUCTION

The accelerated demand for PGE has surpassed the global supply from primary sources due to geological, social and political issues (**Chapter 2**). The scarcity and significance of PGE have resulted in the renewed search of novel, fast and effective methods for recovering these metals from recycled materials. However, the recovery of these metals is not an easy task due to their high resistance to chemical reactions. Furthermore, the low concentrations of PGE in these materials and their chemical similarities make separation extremely challenging (**Chapter 3**). However, the recovery of PGE from these recycled materials is crucial for their continued use in modern-day applications. Moreover, elucidating the chemical behaviour of the PGE in the presence of complicated matrices is extremely relevant in their recovery from different sources.

This chapter deals with the experimental methods used in this study to arrive at an understanding of the chemistry and the possible recovery of PGE in the ERM®-EBS504 automotive catalytic converter. Firstly, the solid catalyst sample was analysed using the SEM-EDS in order to obtain information on the sample matrix. Secondly, the sample was digested using acid and flux fusion methods to facilitate the complete dissolution of the catalyst sample for total chemical analysis. Thirdly, a variety of parameters, such as reaction time and reaction temperatures, were investigated in order to optimise the dissolution processes. Fourthly, accurate quantification of the elements present in the sample was performed using the ICP-OES. Lastly, the validation parameters discussed in **Chapter 4** were evaluated to ensure the suitability of the developed methods.

The separation methods used in this study include selective precipitation and solvent extraction techniques. Synthetic mixtures were used in order to optimise the separation conditions before being applied to the automotive catalytic converter sample. Variations in experimental conditions, such as the acid concentrations, pH, ligand concentrations and the extraction solvent type, were investigated to effect proper separation of the PGE from the non-precious metals and from one another with a degree of high purity as well as with high-percentage recoveries. The PGE that were investigated during the development of separation methods include Pt, Pd, Rh, Ir and Ru.

5.2 EQUIPMENT AND REAGENTS

5.2.1 Inductively Coupled Plasma Optical Emission Spectroscopy (ICP-OES)

A computer-controlled TELEDYNE LEEMAN LABS dual-view spectrometer was used for the semi-quantitative and quantitative analyses of all the aqueous solutions in this study. The standard operating conditions of the ICP-OES are reported in **Table 5.1**.

Table 5.1: The operating conditions of the ICP-OES

Parameter	Condition
RF power	1.2 kW
Coolant gas flow	14.0 L/min
Auxiliary gas flow	0.2 L/min
Sample uptake rate	25 RPM
Nebuliser pressure	40 PSI

5.2.2 The Catalyst Sample

The spent automotive catalytic converter sample (ERM®-EBS504) investigated in this study is a European Reference Material and was certified by the Bundesanstalt für Materialforschung and Prüfung (BAM) in collaboration with the

Committee of Chemists of the GDMB, Gasellschaft für Bergbau, Metallurgie, Rohstoff and Umwelttechnik.

5.2.3 Weighing

A Shimadzu AW320 and a Sartorious CP Series, Model CPA26P electronic balances were used in this study to accurately weigh samples to four significant figures. The samples were weighed on a glass vial or tin crucible.

5.2.4 Bench-Top Magnetic Stirrer Equipment

A bench-top LASEC digital hotplate stirrer was used for open vessel digestion of the ERM-BS®504 automotive catalysts sample, as well as for other chemical reactions.

5.2.5 Preparation of Ultra-Pure Water

Ultra-pure water was used for all analytical preparations in this study. This water was prepared using an ultra-reverse osmosis system bought from AJD Traders, and its quality was determined as 0.00 µS/cm, using a Hanna DIST 3(HI98304S) conductivity meter.

5.2.6 Scanning Electron Microscopy Coupled with Energy Dispersive X-ray Spectroscopy (SEM-EDS)

An Oxford X-MaxN energy dispersive X-ray spectrometer (EDS), equipped with a Tescan VEGA3 scanning electron microscope (SEM), was used for the surface analysis of the ERM®-EBS504 automotive catalyst sample.

5.2.7 X-Ray Crystallography

A Bruker X8 Apex II 4K diffractometer, utilising SHELXS-97, was used to collect the intensity data for the structural determinations of some of the isolated products. Structural refinements were performed using SHELXL-97. Refinements were carried out using F^2 against all reflections, and the R-factor (wR) and goodness of fit (S) were based on the F^2, while standard R-factors were based on F, with F set at zero

for a negative F^2. Threshold expression of $F2>2\sigma(F^2)$ was used only for the calculation of R-factors. SAINT-Plus was employed for all cell refinements, while both XPREP and SAINT-Plus were used for data reduction. The absorption effects were corrected using the multi-scan technique and software package, SADABS. The direct method package, SIR-97, was used in combination with WinGX and SHELX-97 to solve and refine the crystal structures. The graphic representations of the crystal structures were obtained by means of the program, DIAMOND. All diagrams were generated using SHELXTL and PLATON (DIAMOND/Mercury).

5.2.8 Furnace

A Thermolyne furnace with heating temperatures ranging from 25 to 1 100 °C was used for the flux fusion studies of the ERM®-EBS504 automotive catalyst samples.

5.2.9 Micro-Pipettes

Adjustable Brand Transferpettes (1 ml to 10 ml) and Gilson Pipetman (100 µL to 1 000 µL) mico-pipettes were used for the accurate transfer solutions.

5.2.10 Glassware

The Schott Duran type (100, 250 and 600 ml) beakers were used for sample digestion and separation methods. The Blau brand A-grade glass type volumetric flasks (50.0, 100.0 and 200.0 ml) were used for sample dilutions.

5.2.11 pH Meter

CyberScan pH 1 500 Bench pH/mV Meter from EUTECH instruments, certified under ISO 9001 was used for measuring the pH of solutions. The pH meter was calibrated using sets of calibration buffer solutions with pH values of 2, 4, 7 and 10, which were bought from THERMO SCIENTIFIC. These buffer solutions were certified by NIST Standard Reference Materials. The pH meter was rinsed in ultra-pure water between measurements to avoid cross-contamination.

5.2.12 Fourier Transform Infrared Spectroscopy (FT-IR)

The infrared spectra in this study were recorded in the range of 4 000 to 400 cm^{-1} using a DIgilab Scimtar Series spectrometer.

5.2.13 CHNS Combustion Micro-Elemental Analysis

A TruSpec Micro LECO CHNS instrument was used for the determination of H, C, S and N in the isolated organometallic products.

5.2.14 Melting Point Determination

The melting points of some of the isolated products were determined using the GALLENKAMP melting point apparatus.

5.2.15 Acids and Reagents

All chemicals used in this research were commercially obtained and used as received without any further purification. **Table 5.2** shows all the chemicals used in this study, their purities and supplier.

Table 5.2: A list of chemicals used in this study

Chemical	Formula	Purity	Supplier
Reagents			
Sodium peroxide (granular)	Na_2O_2	95 %	Merck
8-Hydroxyquinoline	C_9H_7ON	99.9 %	Merck
Ammonium iron (II) sulphate hexahydrate	$H_8FeN_2O_8S_2.6H_2O$	99.0 %	Sigma-Aldrich
Copper chloride	$CuCl_2.2H_2O$	99.0 %	Merck
Zinc nitrate hexahydrate	$N_2O_6Zn.6H_2O$	98.0 %	Merck
Cerium (III) nitrate hexahydrate	$CeN_3O_9.6H_2O$	99.0 %	Sigma-Aldrich
Magnesium sulphate heptahydrate	$MgSO_4.7H_2O$	98.0 %	Merck
Aluminium sulphate octadecahydrate	$Al_2(SO_4)_3.18H_2O$	97 %	ACE
Ammonium hydroxide	NH_4OH	25 %	ACE
Mercaptopyridine *N*-oxide sodium salt	C_5H_4NNaOS	96 %	Sigma-Aldrich
Trioctylphosphine oxide (TOPO)	$C_{24}H_{51}OP$	97 %	Sigma-Aldrich
N'N-dimethylthiourea	$C_3H_8N_2S$	99 %	Sigma-Aldrich
Ammonium thiocyanate	NH_4SCN	99 %	Univar
Toluene	C_7H_8	99.8 %	Merck
Kerosene	--	--	Sigma-Aldrich
Chloroform	$CHCl_3$	99.5 %	Merck
Hexane	C_6H_{14}	99 5 %	Merck
Acids			
Nitric acid (TG)	HNO_3	55 %	ACE
Nitric acid (AR)	HNO_3	65 %	ACE
Hydrochloric acid (AG)	HCl	32 %	ACE
Glacial acetic acid (AG)	CH_3COOH	99.7 %	ACE

5.2.16 Cleaning of Apparatus

All the glassware was soaked in diluted 55 % HNO_3 for periods longer than 24 hours, rinsed and then dried in a dust-free environment before use.

5.2.17 ICP-OES Calibration Standards

Table 5.3: The ICP-OES calibration standards used this study

Element	Diluted in	Elemental concentration µg/ml	Supplier
Multi-element standard IV (Al, Ag, B, Ba, Bi, Ca, Cd, Co, Cr, Cu, Fe, Ga, In, K, Li, Mg, Mn, Na, Ni, Pb, Sr, TI and Zn	HNO_3 (7 %)	1 000	Merck
Si	HNO_3	1 002 ± 6	Inorganic Ventures
Ce, Eu, la, Pr, Sm	HNO_3 (7 %)	1 000	Inorganic Ventures
Pt	HCl (10 %)	998 ± 5	Inorganic Ventures
Pd	HNO_3 (0.5 mol/l)	1 000	Merck
Rh	HCl (15 %)	1 001 ± 6	Inorganic Ventures
Ir	HCl (10 %)	1 001 ± 3	Inorganic Ventures
Ru	HCl (10 %)	1 000 ± 4	Inorganic Ventures
Cd (Internal)	HNO_3 (2-3 %)	1 000	Merck
Sc (Internal)	HNO_3 (7 %)	1 002 ± 5	Inorganic Ventures

5.2.18 Preparation of ICP-OES Calibration Curves and Selection of Wavelengths

The selection of best lines that were free from interferences for all the non-precious elements (Al, Mg, Fe, Ce, Cu and Zn) and for the PGE (Pd, Pt, Rh, Ir and Ru) was performed using Echelle images. The selected wavelengths used throughout this study are shown in **Table 5.4**. All standards were prepared by appropriate dilutions of the 1 000 ppm ICP-OES standards which were purchased from Merck and Inorganic Ventures by pipetting appropriate volumes (**Table 5.3**). Sets of calibration standards containing 0, 0.5, 1, 2, 5, 10 and 30 ppm of the metal concentrations were made for non-precious elements in 2 % HNO_3, while the PGE calibration standards were prepared separately from the non-precious elements to reduce the effect of spectral

interferences. This was done by preparing sets of calibration standards containing 0, 0.25, 0.5, 1, 2 and 10 ppm of PGE in 2 % HCl. The ICP-OES operating conditions are shown in **Table 5.2**, and were kept constant in all analyses. The LODs and LOQs at these selected wavelengths were calculated (**Chapter 4, Equation 4.16** and **Equation 4.17**) from the calibration curves and are shown in **Table 5.3**.

Table 5.4: The selected wavelengths, viewing modes and detection limits of all the elements that were investigated in this study using the ICP-OES

Element	Selected wavelength/nm	Viewing mode	LOD	LOQ	R^2
Al	396.152	Axial	0.009785	0.09785	1.0000
Mg	279.55	Radial	0.003044	0.03044	0.9997
Fe	259.94	Axial	0.003609	0.03609	0.9997
Ce	418.66	Axial	0.02233	0.2233	0.9999
Cu	324.75	Axial	0.001295	0.01295	0.9996
Zn	206.20	Axial	0.01174	0.1174	0.9997
Si	243.515	Radial	0.1230	1.230	0.9988
Pd	340.458	Radial	0.0289	0.289	0.9999
Pt	265.945	Axial	0.0013	0.01260	0.9998
Rh	343.489	Radial	0.01526	0.1526	0.9999
Ir	224.268	Axial	0.0200	0.2000	0.9999
Ru	240.272	Axial	0.0065	0.0651	0.9999

5.3 SEM-EDS ANALYSIS OF THE ERM®-EBS504 AUTOMOTIVE CATALYST SAMPLE

Surface characterisation on the ERM®-EBS504 automotive catalyst sample (**Figure 5.1**), which is a certified reference material for Pd, Pd and Rh, was performed using SEM-EDS. This was done in order to investigate the major components of the catalyst material and texture. The SEM image is shown in **Figure 5.2a** and the corresponding EDS spectrum in **Figure 5.2b**.

Figure 5.1: The ERM®-EBS504 automotive catalyst sample

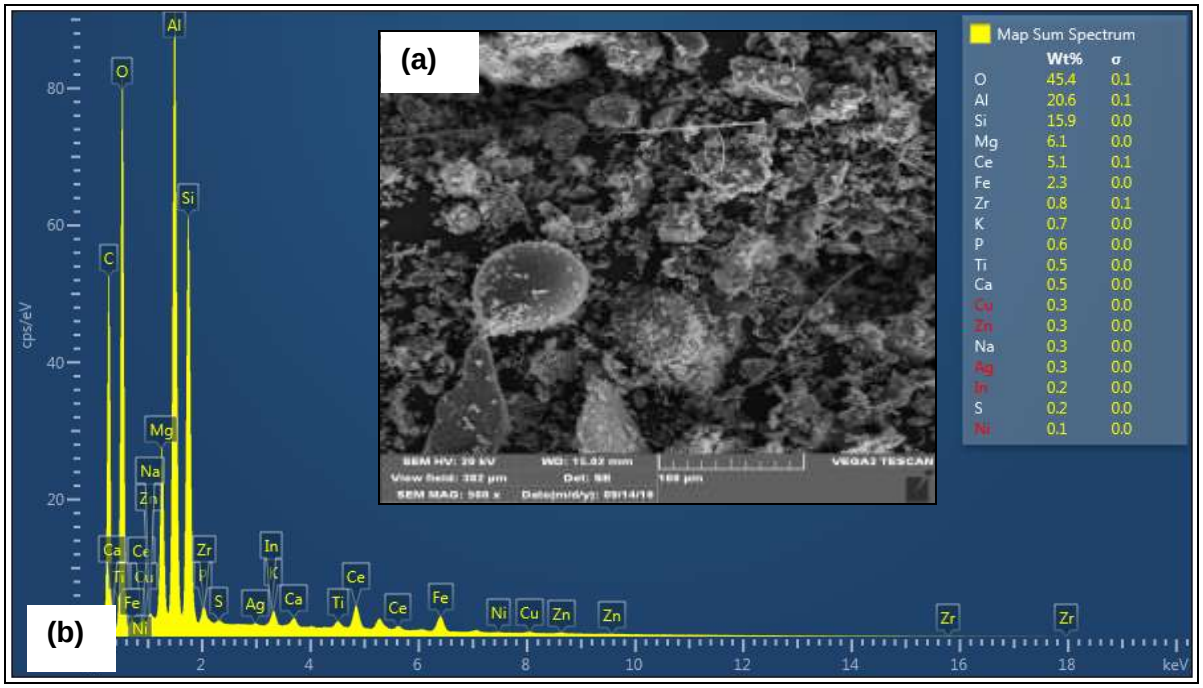

Figure 5.2: (a) The SEM image and (b) corresponding EDS spectrum of the ERM®-EBS504 catalyst material

The EDS spectrum in **Figure 5.2b** shows that the dominating elements in the catalyst material are O, Al, Si, Mg, Ce and Fe, with percentage weights of 45.4, 20.6, 15.9, 6.1, 5.1 and 2.3 % respectively. Since oxygen is the main element in the catalyst, these elements are mainly present as metal oxides. The EDS spectrum shows no indication of PGE in the catalyst material as their concentration is below the detection limits of the EDS, although they were detected when the sample was completely dissolved as discussed in **Section 5.4**.

SEM analysis in **Figure 5.2a**, showed that the catalyst powder is not very homogeneous, which might have led to the inaccurate quantification of the components present in the catalyst material. Therefore, these results are only used as estimates to describe the sample matrix.

5.4 DISSOLUTION OF THE PGE CATALYST SAMPLE AND QUANTIFICATION USING ICP-OES

In order to identify the total elemental content of the catalyst material and afford separation of the PGE from the sample, it was important to develop a dissolution technique which completely dissolves the catalyst sample.

5.4.1 Dissolution Using the Sodium Peroxide (Na_2O_2) Fusion Method

5.4.1.1 Experimental

The automobile catalyst sample (ERM®-EBS504) was dried in an oven for three hours prior to dissolution. Approximately 0.1 g of the sample was weighed accurately and mixed with sodium peroxide (~1 g). The mixture was allowed to fuse in a furnace for 40 minutes at 600 °C in a Zr crucible. The resulting chocolate-like melt was cooled, and water was added to it in the crucible. An exothermic reaction was observed during the addition of water and the melt turned into a milky solution. This solution was then transferred into a beaker where it was stirred using a magnetic stirrer, and *aqua-regia* (20 ml) was added slowly until a clear yellow solution with no remaining residue was observed. This yellow solution was slowly heated for another 10 minutes. The cooled, clear yellow solution was transferred into a volumetric flask (100.0 ml), filled to the mark with ultra-pure water and analysed using ICP-OES. The elemental percentages of the different elements in the dissolved sample were calculated, the results of which are shown in **Tables 5.5** to **5.7**. Internal standards, including Sc and Cd, were investigated to ensure accurate quantification of the PGE and to compensate for Na ions spectral interferences.

5.4.1.2 Results and discussion

The results in **Table 5.5** show the weight percentages of all the non-precious elements present in the used automobile catalyst.

Table 5.5: The weight percentages of non-precious elements found in the catalyst sample using the ICP-OES technique

		% Weight	
Element	**Wavelength/nm**	**SEM-EDS**	**ICP-OES**
Mg	277.51	6.1	5.3(3)
Al	167.079	20.7	20.5(7)
Si	243.515	15.9	13.2(8)
Fe	275.574	2.3	1.40(5)
Ce	401.239	5.1	3.4(3)
Cu	327.396	0.3	1.24(5)
Zn	213.856	0.3	2.1(1)

The comparative weight percentages of the non-precious metals in **Table 5.5** correlate well with one another. The slight difference between the values obtained by means of the SEM-EDS and those obtained using the ICP-OES can be attributed to the difference in the sample selection or homogeneity during the two processes as well as the difference in the relative accuracy which can be achieved using the two methods.

The percentage weights and recoveries of PGE obtained after a complete dissolution of the catalyst sample (CRM) using the Na_2O_2 fusion method are reported in **Tables 5.6** and **5.7**.

Quantification using external or direct calibration with accurate matrix matching resulted in unacceptable, inaccurate and high Pt, Pd and Rh recoveries of 115(1),

219(7) and 105(1) % respectively. These results corroborate previously reported results[157] which clearly indicated the sensitivity and inaccuracy of PGE quantification using unmatched matrix or direct calibration. Interferences were reported as a result of high alkali metal concentrations, and anion content. In the current study, the high Na content from the Na_2O_2 flux may be responsible for the high percentage recoveries of Pd in particular. In previous studies, the use of internal standard addition calibration proved to be extremely useful in the correction of analytical results which resulted in the attainment of more accurate and realistic PGE recoveries. Cadmium[158] and scandium[159] were used successfully as internal standards in previous studies. The current study was continued using both these elements as internal standards, Cd (226.502 nm) and Sc (361.353 nm), to try and improve the PGE quantification in the autocatalyst sample. The introduction of Cd as an internal standard resulted in weight percentages of 0.1366 for Pt, 0.0352 for Pd and 0.0440 for Rh, which equate to 76.8(6), 126.1(3) and 130.0(4) % recoveries respectively. This is clearly not an improvement in PGE recovery. Pitre and Bedard[76] were able to obtain excellent recoveries of 100 ± 11 % after dissolving the ERM®-EBS504 sample by means of the peroxide fusion method and using Cd as an internal standard. The unsatisfactory results obtained in this study might be due to the difference in instruments and in the selected wavelengths which used 193.700 and 248.892 nm as the wavelengths for Pt and Pd quantification and which unfortunately were not offered by the ICP-OES used in this study. However, the percentage recoveries of PGE improved significantly when Sc was employed as an internal standard, the results of which were 100(1), 100(3) and 103(2) % for Pt, Pd and Rh respectively. These results imply that Sc should be used to accurately quantify the PGE in the ERM®-EBS504 catalyst sample during various separation stages. These analytical results were validated in **Section 5.8**.

[157] Chiweshe, T.T., Purcel, W. & Venter, J.A. (2009). *Quantification of Rhodium in a Series of Inorganic and Organometallic Compounds,* University of the Free State, pp. 95-96.

[158] Pitre, J. & Bedard, M. (2013). Peroxide fusion dissolution for the determination of platinum, palladium and rhodium in automotive catalytic converters by ICP analysis, pp. 1-5.

[159] Mokgalaka, N.S., McCrindle, R.I. & Botha, B.M. (2002). Internal standard method for the determination of Au and some platinum group metals using inductively coupled plasma optical emission spectrometry. *S. Afr. J. Chem.*, 55, pp. 72-86.

Table 5.6: The certified and ICP-OES-determined weight percentages of the PGE in the ERM®-EBS504 catalyst sample after flux fusion with Na_2O_2

	% Weight			
Element	**CRM (Certified)**	**External calibration**	**Cd internal standard**	**Sc internal standard**
Pt	0.1777	0.2057	0.1366	0.1781
Pd	0.0279	0.0612	0.0352	0.0280
Rh	0.0338	0.0357	0.0440	0.0348

Table 5.7: The calculated percentage recoveries of the PGE from the ERM®-EBS504 catalyst sample after flux fusion with Na_2O_2 using different ICP-OES analysis techniques

	% Recovery		
Element	**External calibration**	**Cd internal standard**	**Sc internal standard**
Pt	115(1)	76.8(6)	100(1)
Pd	219(7)	126.1(3)	100(3)
Rh	105(1)	130.0(4)	103(2)

The successful use of sodium peroxide fusion to aid complete dissolution of the automotive catalyst sample can be attributed to its ability to oxidise all the elements in the sample to soluble oxidation states.

5.4.2 Dissolution Using *Aqua-Regia*

The results reported in the literature review in **Chapter 3**, **Section 3.2** indicated that *aqua-regia* is the most effective acid for dissolving the PGE-containing material. Therefore, it was decided that this acid combination would be used to try and dissolve the ERM®-EBS504 catalyst sample using more moderate experimental conditions.

5.4.2.1 Experimental

About 0.2 g aliquots of the catalyst sample were weighed and dissolved in *aqua-regia* solution at different experimental conditions. The dissolution of the sample using *aqua-regia* was performed on a hotplate and required constant stirring. Experimental conditions, such as the temperature of dissolution (18 to 80 °C) and time (30 to 180 minutes), were investigated and optimised in order to improve the dissolution process. To determine the success of each dissolution process, the dissolved sample solutions were cooled to room temperature, filtered, washed in ultra-pure water and transferred into volumetric flasks (100.0 ml), filled to the mark with ultra-pure water and analysed using ICP-OES. The elements that were quantified include all the main elements (base and other metals) and the PGE present in the catalyst as determined by semi-quantitative analysis using the SEM-EDS and the ICP-OES.

5.4.2.2 Results and discussion

The complete dissolution of the catalyst material was unsuccessful as visual inspection clearly indicated the presence of undissolved material remaining in the beakers after the dissolution periods at all experimental conditions under investigation. However, the quantification of the PGE in solution after filtration of samples, indicated an increase in the percentage thereof with an increase in reaction temperature and time. The results for PGE dissolution are shown in **Tables 5.8** and **5.9**.

The maximum percentage recoveries for Pt, Pd and Rh obtained at 80 °C and a reaction time of 180 minutes, were found to be 66.9(4), 63.9(8) and 41(1) % respectively.

Table 5.8: The weight percentages and recoveries of PGE into solution from the autocatalyst after dissolution using *aqua-regia* at different reaction temperatures, t = 90 minutes

	% Weight			% Recovery		
Temperature (°C)	**Pd**	**Pt**	**Rh**	**Pd**	**Pt**	**Rh**
18	0.00639	0.02821	0.00159	22.9(3)	16(1)	4.7(1)
60	0.00754	0.07908	0.00258	27.0(3)	44.5(2)	7.6(3)
80	0.01041	0.08932	0.00999	37(2)	50.3(7)	29.6(3)

Table 5.9: The weight percentages and recoveries of PGE in the autocatalyst at different reaction times after dissolution using *aqua-regia*, T = 80 °C

	% Weight			% Recovery		
Time (min)	**Pd**	**Pt**	**Rh**	**Pd**	**Pt**	**Rh**
30	0.00674	0.08292	0.00398	24.1(3)	46.7(5)	12.0(4)
60	0.00722	0.09096	0.00639	25.9(1)	51.2(1)	18.9(6)
120	0.00930	0.10305	0.01220	33.3(1)	58.00(8)	36.1(2)
180	0.01783	0.11885	0.01385	63.9(8)	66.9(4)	41(1)

The reactions between Pt, Pd and Rh with *aqua-regia* are said to occur as follows (**Chapter 3, Equations 3.1** to **3.3**):

$$3Pt(s) + 18HCl(aq) + 4HNO_3(aq) \longleftrightarrow 3[PtCl_6]^{2-}(aq) + 6H^+(aq) + 4NO(g) + 8H_2O$$

$$3Pd(s) + 12HCl(aq) + 2HNO_3(aq) \longleftrightarrow 3[PdCl_4]^{2-}(aq) + 6H^+(aq) + 2NO(g) + 4H_2O$$

$$2Rh(s) + 12HCl(aq) + 2HNO_3(aq) \longleftrightarrow 2[RhCl_6]^{3-}(aq) + 6H^+(aq) + 2NO(g) + 4H_2O$$

The analytical results also indicated the partial dissolution of the non-precious elements present in the catalytic converter by *aqua-regia* under these selected experimental conditions. The results are reported as percentage recoveries (compared to metal content determined in **Section 5.4.1**) of these elements as indicated in **Figures 5.3** and **5.4**. The results show a pronounced increase in Fe dissolution with an increase in temperature compared to that of other elements, and increased from 18.5(2) % at 18 °C to 70(1) % at 80 °C (**Figure 5.3**).

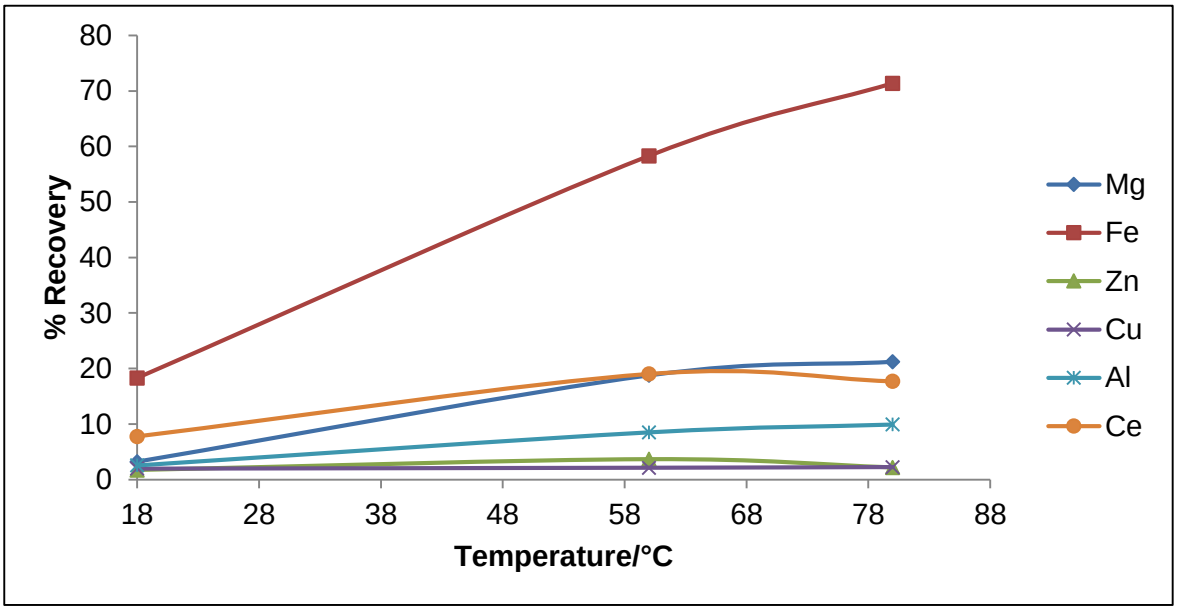

Figure 5.3: The influence of temperature on the dissolution of non-precious metals present in the catalyst using *aqua-regia*, t= 90 minutes

The results in **Figure 5.4** also indicate a slight increase in Fe dissolution with an increase in reaction time and Fe content in the aqueous solution, and increased Fe dissolution from 69(1) % after 30 minutes to 78.7(4) % after 180 minutes reaction time.

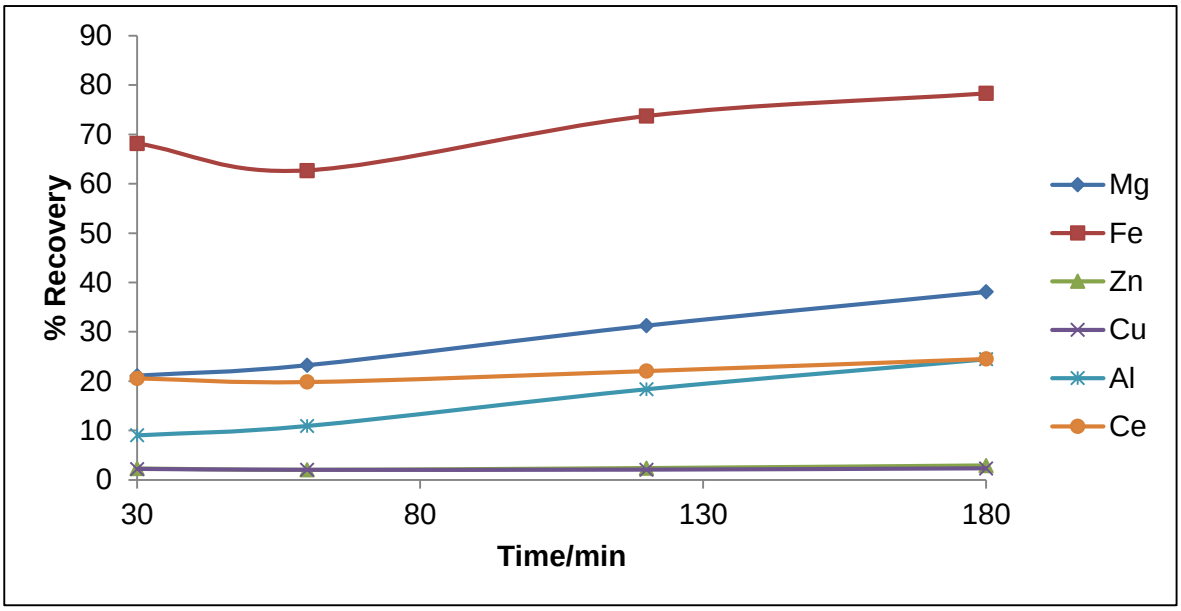

Figure 5.4: The effect of reaction time on the dissolution of non-precious elements using *aqua-regia*, T = 80 °C

A number of conclusions can be drawn from these results. The first is that *aqua-regia* is unable to completely dissolve the autocatalyst at temperatures below 80 °C. However, there is a clear indication that the *aqua-regia* is able to leach some of the PGE (up to 60 % of the Pt and Pd) from the catalyst sample at these conditions and the degree of PGE leaching is dependent on the reaction time and temperature. Finally, it is also clear that substantial Fe dissolution takes place with an increase in temperature and reaction time, resulting in PGE solution contamination. These results also suggest that dissolution/leaching can occur in closed reaction systems such as in microwave digestion where higher temperatures and pressures can be reached during the digestion stage. However, this technique was not investigated in this study.

5.5 SEPARATION OF THE NON-PRECIOUS ELEMENTS FROM THE PGE USING PRECIPITATION METHODS

The total chemical characterisation of the automotive catalyst sample in **Section 5.4** indicated a complicated elemental matrix containing at least six non-precious and three precious elements. It was therefore decided to investigate the possible removal of the non-precious elements from the matrix using selective precipitation methods.

In order to simplify the study, it was decided to first investigate the possible precipitation of the non-precious elements using artificial and pure matrices and to then try and apply the method to the automotive catalyst sample. In the first part of the study, NH_4OH was used to investigate the reaction of all the non-precious metals as well as the PGE with OH^- at elevated alkalinity levels and, in the second part, the reaction of both groups of elements with oxine (8-hydroxyquinoline).

5.5.1 Precipitation of Non-Precious Elements by Controlling the Acidity of the Solution Using NH_4OH

5.5.1.1 Experimental

Effect of reaction time

Stock solutions containing 1 000 ppm for each non-precious metal (Mg, Fe, Zn, Al, Cu and Ce) were prepared from the pure metal salts as indicated in **Table 5.2**, and a mixture containing 3 ml of these selected elements was prepared. This mixture was stirred at room temperature using a magnetic stirrer. The pH of the solution was raised and kept constant at about 7 by adding NH_4OH dropwise. The reaction time was increased from 10 to 120 minutes in order to investigate the effect of reaction time on the precipitation of these metals using NH_4OH. The resulting suspensions were centrifuged for 20 minutes. The supernates were isolated from the precipitates. HCl (10 ml, 10 M) was added to dissolve the precipitates and the resulting solutions were then transferred into volumetric flasks (100.0 ml) and filled to the mark with ultra-pure water. Additional HCl (10 ml, 10 M) was added to the dissolved elemental ions, which was necessary to maintain the pH of the solution below zero and to prevent any hydrolysis after filling the samples to 100 ml. The solutions were then analysed by means of ICP-OES. The percentage recoveries of elements in the precipitates at various reaction times were calculated, the results of which are illustrated in **Figure 5.5**.

Effect of pH

From the previously prepared stock solutions of non-precious metals, a mixture containing 3 ml of each metal solution was made. The elements dissolved in these solutions were precipitated as a function of pH by the stepwise addition of NH_4OH. The precipitant (NH_4OH) was added dropwise while stirring until the desired pH was reached. The experiments were performed at room temperature at different pH levels ranging from 4 (visible precipitation) to 11. The resulting suspensions were centrifuged for 20 minutes to separate the precipitates, which were then dissolved in HCl (10 ml, 10 M), transferred into volumetric flasks (100.0 ml) and analysed using ICP-OES. The percentage metal recoveries present in the precipitates at the various pH levels were calculated, the results of which are shown in **Figure 5.6**.

While the literature review did not indicate PGE hydroxide precipitation in the pH range investigated, the above-mentioned experimental procedure was repeated on a set of solutions containing only the PGE. However, the experiments were also conducted on the individual PGE-containing solutions. The results from this part of the study indicated no visual PGE precipitation at all pH levels investigated.

Precipitation of non-precious metals in the presence of PGE

A synthetic mixture containing the non-precious elements, each with a concentration of 30 ppm and PGE (1 ppm of each metal) was made. The solution was mixed thoroughly, and the pH of a solution was raised to about 7 in order to remove Cu, Fe, Ce and Al. The suspension was centrifuged to separate the precipitates from the supernate. The precipitate was dissolved in HCl (10 ml, 10 M) and transferred into a beaker (250 ml). To the supernate, more NH_4OH was added to raise the pH to about 8 in order to recover mostly Zn. This precipitate was also separated by centrifugation, dissolved in HCl (10 ml) and mixed with the other solution containing Al, Cu, Ce and Fe. The pH of the remaining filtrate was finally raised to a pH of 11 to precipitate Mg and any other remaining elements. The final portion of the remaining precipitate was dissolved in HCl (10 ml, 10 M), and mixed with the other precipitate solutions. To the remaining supernate, HCl (10 ml, 10 M) was added. Both the precipitate and final supernate solutions were transferred into volumetric flasks (100.0 ml), filled to the mark and analysed using ICP-OES. The percentage recoveries of elements in both

the supernate and precipitate were determined, the results of which are illustrated in **Figures 5.7** and **5.8**.

5.5.1.2 Results and discussion

From the results in **Figure 5.5**, it appears that Al, Fe, Cu and Ce were collectively precipitated at pH 7 with high percentage recoveries. The results also indicated that their recoveries remained constant as the reaction time was increased from 10 to 120 minutes, suggesting the complete precipitation immediately and completely at a pH of 7. The recovery of Zn improved with an increase in reaction time from 49.9(3) % at 10 minutes to 65.5(1) % at 120 minutes, while no precipitation of Mg was observed, even with an increase in reaction time. The results also show that Mg can be selectively separated from these elements at a pH of 7.

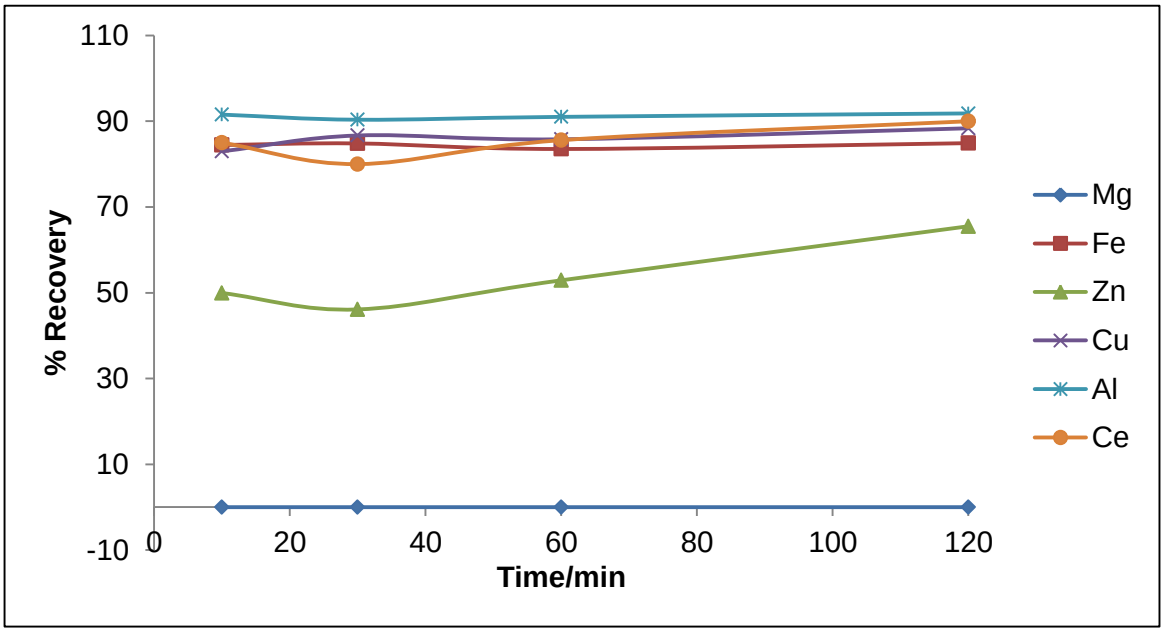

Figure 5.5: The effect of time on non-precious metal precipitation with NH_4OH, pH = 7

Figure 5.6 indicates an improvement in the percentage recoveries of Zn and Mg with an increase in pH. Mg started to precipitate at a pH just above 9, and increased, reaching a maximum percentage recovery of 96.9(3) % at a pH of 11. Zn reaches its maximum percentage recovery of 91.64(5) % at a pH of 8, after which it starts to decrease, dropping to 9.1(3) % at a pH of 11.The percentage Cu and Al recoveries also start to decrease dramatically after a maximum recovery of these elements is

reached. Fe is the only element whose percentage recovery remained constant from 6 to 11 and is completely precipitated throughout this pH range.

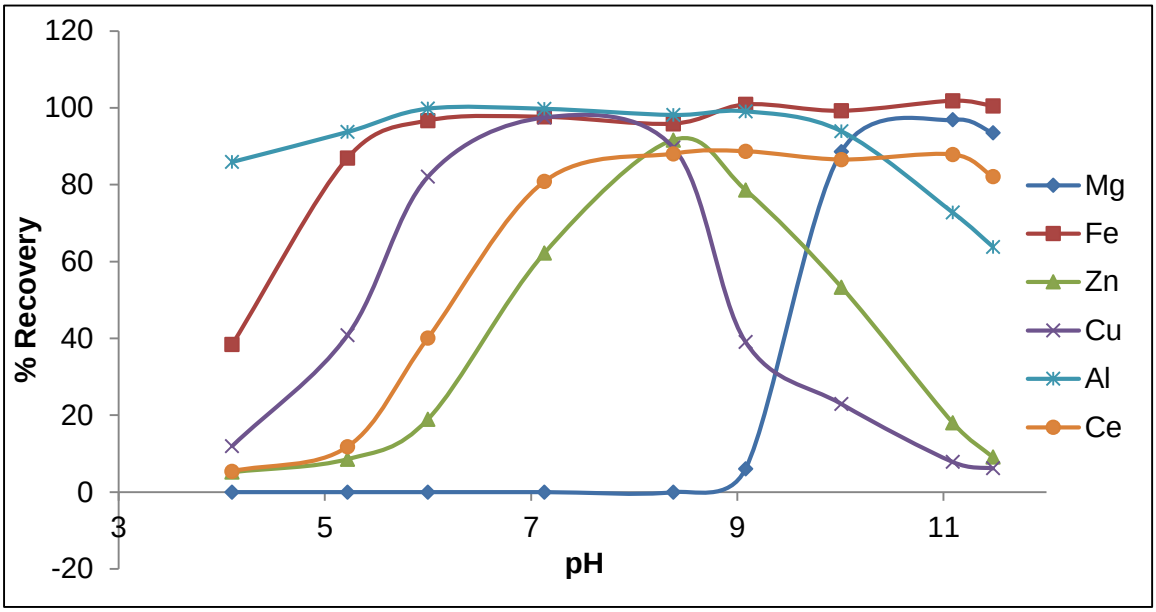

Figure 5.6: Precipitation of non-precious metals by pH changes using NH_4OH, t = 90 min

The resistance of $Mg(OH)_2$ precipitation at a pH below 9 is attributed to its high solubility product constant (K_{sp}). From **Table 5.11**, it can be seen that the solubility product constant for $Mg(OH)_2$ is 7.1×10^{-12}, and is significantly higher than that of the other elements that were studied. It can also be observed that the solubility product constant for $Al(OH)_3$ is 3.0×10^{-34}, which is the lowest compared to others, and is shown in its high percentage recovery of 85.92(3) % at a pH of only 4.

Table 5.10: The solubility product constants of non-precious elements at standard conditions

Element	K_{sp}
$Mg(OH)_2$	7.1×10^{-12}
$Fe(OH)_2$	4.1×10^{-15}
$Cu(OH)_2$	4.8×10^{-20}
$Zn(OH)_2$	3.0×10^{-16}
$Al(OH)_3$	3.0×10^{-34}
$Ce(OH)_3$	2.0×10^{-20}

The decrease in the percentage recoveries of Cu, Zn and Al after reaching a certain pH is due to the conversion of a metal hydroxide to the metal ammonia complex, which are soluble in solution. **Equations 5.1** and **5.2** illustrate these reactions for Cu: Formation of copper hydroxide complex at pH = 7:

$$Cu^{2+}\,(aq) + 2HO^{-}\,(aq) \rightleftharpoons Cu(OH)_2\,(s) \qquad (\mathbf{5.1})$$

Formation of copper ammonia complex at pH > 7:

$$Cu^{2+}\,(aq) + 4NH_3\,(aq) \rightleftharpoons Cu(NH_3)_4\,(aq) \qquad (\mathbf{5.2})$$

These results confirm that pH plays a very important role in the precipitation of metals with hydroxides, NH_4OH in this investigation. The results also indicate that a set of precipitation steps can be applied to recover or remove the non-precious metals as hydroxides, while leaving the PGE in solution.

The results, after the precipitation of non-precious metals in the presence of PGE, are shown in **Figures 5.7** and **5.8**. The graph in **Figure 5.7** indicates that the non-precious metals were mostly in the precipitate, while trace amounts were still present in the filtrate.

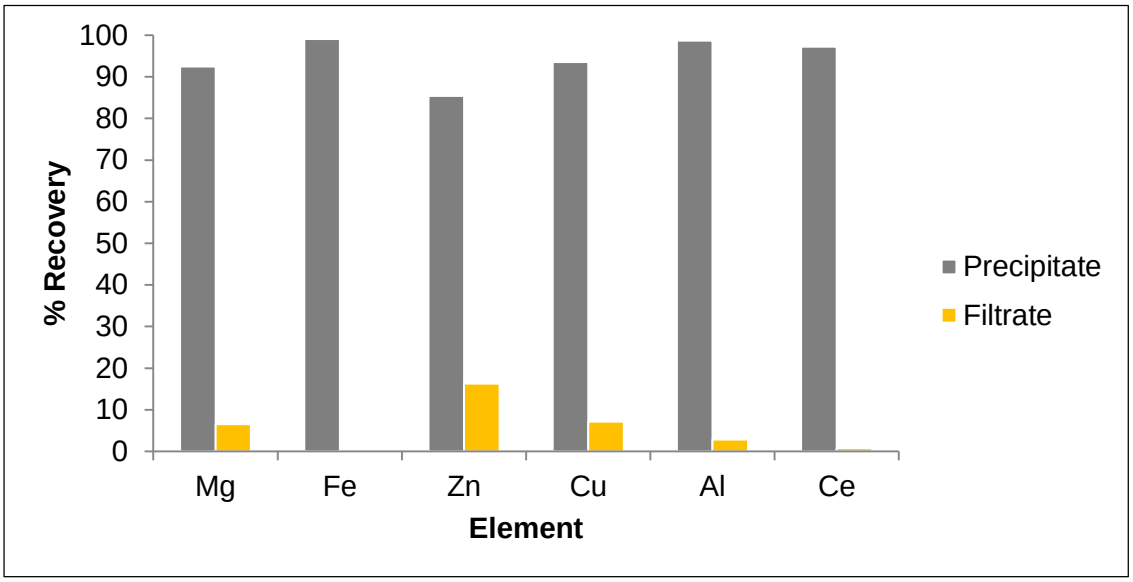

Figure 5.7: The percentage recoveries of non-precious metals in the filtrate and precipitate after precipitation with NH_4OH

The results for the PGE in **Figure 5.8** show that most of the PGE were adsorbed in the precipitates, except for Pd which was left in the filtrate. The loss of PGE might be due to the numerous steps required to precipitate the non-precious elements.

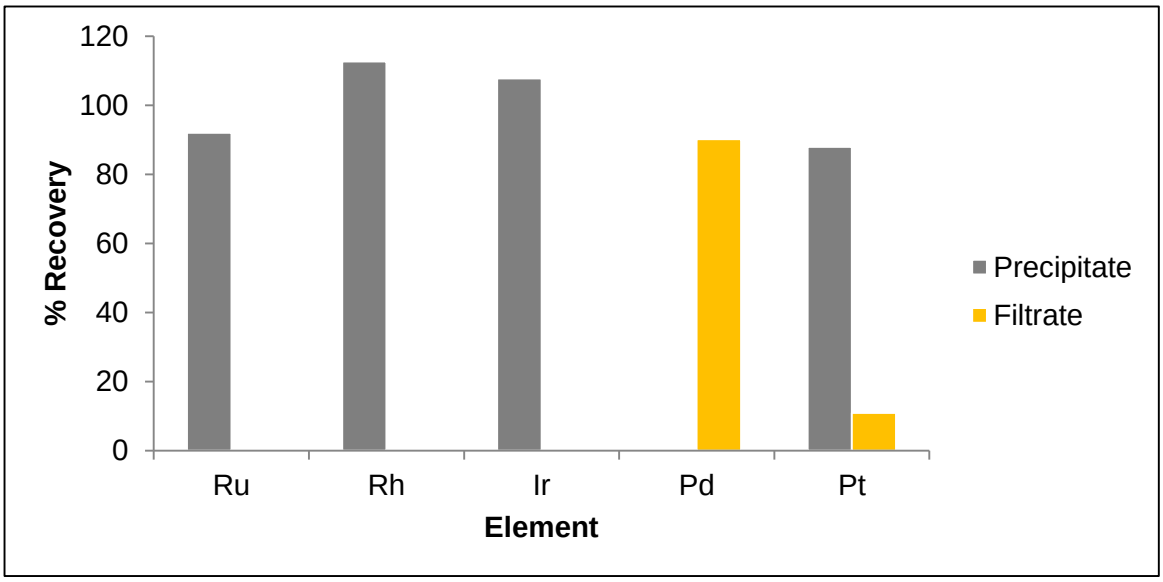

Figure 5.8: The percentage recoveries of PGE in the filtrate and precipitate after the precipitation of non-precious metals with NH_4OH

5.5.2 Precipitation with 8-Hydroxyquinoline (Oxine)

5.5.2.1 Experimental

Effect of oxine concentration

Stock solutions containing 1 000 ppm of non-precious elements were prepared. A solution containing 50 ppm of each non-precious element was prepared. Oxine (1 ml, 0.5 M), which was previously dissolved in glacial acetic acid, was added to the solution while stirring using a magnetic stirrer. The pH of a solution was kept constant at 2.8 and the experiments were performed at room temperature. The resulting precipitates were dissolved in HCl (10 ml, 10 M) and transferred into volumetric flasks (100.0 ml), filled to the mark and analysed using ICP-OES. The percentage recoveries of metals in the precipitates were calculated for each element at various oxine concentrations, the results of which are illustrated in **Figure 5.10**.

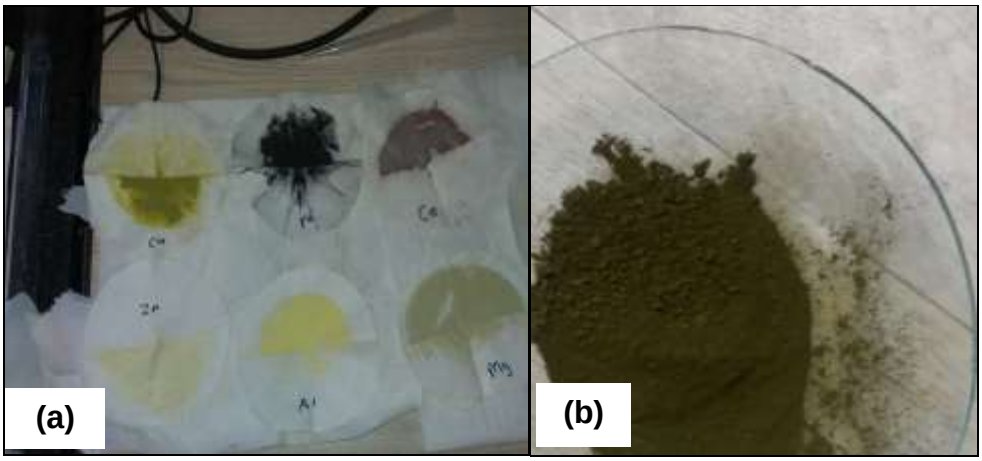

Figure 5.9: Precipitates of metal oxine compounds; (a) precipitation of metals separately; (b) co-precipitation of metals at pH = 10

Effect of reaction time

5 ml of each prepared stock solution containing the non-precious elements was transferred into a beaker (250 ml). The mixture was stirred at room temperature while adding oxine (1 ml, 0.5 M). The precipitation time allowed varied between 10 and 120 minutes, while the pH was kept constant at 2.8. The resulting precipitates were dissolved in HCl (10 ml, 10 M) and transferred into volumetric flasks (100.0 ml), filled to the mark with ultra-pure water and taken for ICP-OES analysis. The results on the effect of reaction time on the precipitation of non-precious elements with oxine are reported in **Figure 5.11**.

Effect of pH

From each non-precious metal stock solution, 50 ppm was transferred into a beaker (250 ml). This mixture was stirred at room temperature while adding the oxine (1 ml, 0.5 M). The experiment was repeated at various pH values in order to investigate the effect of pH on the precipitation of non-precious metals with oxine, while the concentration of oxine and reaction time were kept constant at 0.5 M and 30 minutes respectively. The resulting precipitates were dissolved in HCl (10 ml, 10 M), transferred into volumetric flasks (100.0 ml) and filled to the mark with ultra-pure water. The samples were taken for ICP-OES analysis to determine the amount of metals recovered at different pH levels, the results of which are shown in **Figure 5.12**.

Precipitation of PGE with oxine

The precipitation of PGE with oxine was also studied using the stock PGE standard solutions in order to determine whether they also form insoluble complexes with this ligand. The tests were conducted on individual PGE solutions containing elemental concentrations of 10 ppm of each metal. The solutions were evaporated till dry and dissolved in HCl (20 ml, 10 M) or HNO_3 (20 ml, 14 M). Oxine (1 ml, 0.5 M) in glacial acetic acid was added; the solutions were stirred at room temperature and the pH raised by adding NH_4OH. No precipitation was observed for any of the PGE when dissolved in HCl at all pH levels (from 0 to 9). However, yellow precipitation formation was observed after 10 minutes and at pH < 0 for Pd in the presence of HNO_3. The product was dried and characterised with FT-IR (see **Figure 5.15**).

The resistance of the Pd to forming a chelate with oxine in HCl may be due to the high stability of the Pd chloride complex as compared to Pd nitrate compound present in the nitric acid solutions. This observation was very encouraging since it pointed to the possible selective precipitation of Pd from the rest of the elements since it reacted with the oxine in highly acidic conditions as compared to the non-precious metals and the absence of other PGE precipitation in the presence of oxine. Initial conditions, however, predict that large amounts of Pd are required for precipitation, thus limiting this method to highly concentrated Pd solutions.

Precipitation of Pd in the presence of non-precious metals and other PGE

A synthetic mixture containing Pd, Pt, Rh, Ir and Ru (10 ppm) (from 1 000 ppm standards) and the non-precious metals (30 ppm) was prepared (from stock solutions). The mixture was evaporated till dry and dissolved in HNO_3 (20 ml, 14 M). Oxine (1 ml, 0.5 M) was added to the mixture while being stirred at room temperature. A yellow precipitate (**Figure 5.10**) started to form and the reaction was allowed to proceed for 30 minutes. The precipitate was filtered, washed in ultra-pure water and air-dried at room temperature. The precipitate was then recrystallised in DMSO, and orange needle-like crystals suitable for X-ray crystallography were isolated (**Section 5.5.2.3**). This product was also characterised with the FT-IR and was identical to product isolated after the reaction between the pure Pd and oxine

(**Figure 5.15**). The melting point of this product, presumely $Pd(oxine)_2$ crystals was determined to be between 338 and 340 °C.

The quantification of this product using ICP-OES was not possible. Whereas the isolated product was highly insoluble in acids, it was only soluble in solutions with a pH of ± 9 or in organic solvents such as chloroform. However, other characterisation techniques, including LECO, FT-IR, NMR and XRD, were used to further characterise this compound and to confirm the presence of Pd.

Figure 5.10: Precipitate formed when palladium reacts with oxine, pH < 0

5.5.2.2 Results and discussion

Effect of oxine concentration

The results in **Figure 5.11** clearly indicate the presence of large quantities of Cu in the isolated precipitate and insignificant amounts of the rest of the non-precious elements at a pH of 2.8. An increase in oxine concentration from 0.1 to 0.5 M only affords a small increase in the precipitation of all the non-precious elements to a maximum of 5 %. Cu on the other hand, reacted completely differently to the increase in oxine concentration and its presence in the precipitate increased from 42.43(5) % at 0.1 M to 94.18(1) % at 0.5 M. These results suggest that Cu can be easily isolated from elements, such as Al, Fe, Zn, Ce and Mg, in the presence of oxine.

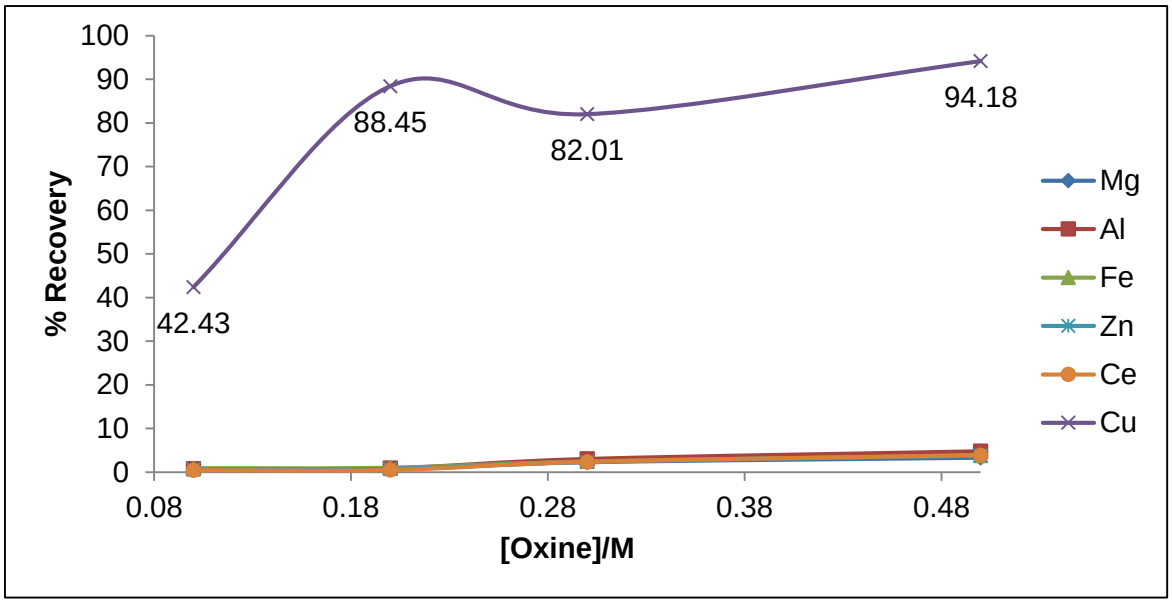

Figure 5.11: Effect of ligand concentration on elemental recovery in the precipitate phase at a pH of 2.8

Effect of reaction time

The results in **Figure 5.12** indicate that reaction time has a negligible influence on the elemental precipitation of most of the non-precious elements in the solution and their recovery remains constant for a period of 120 minutes. The results also confirm the selective precipitation of Cu at a pH of 2.8 during this period.

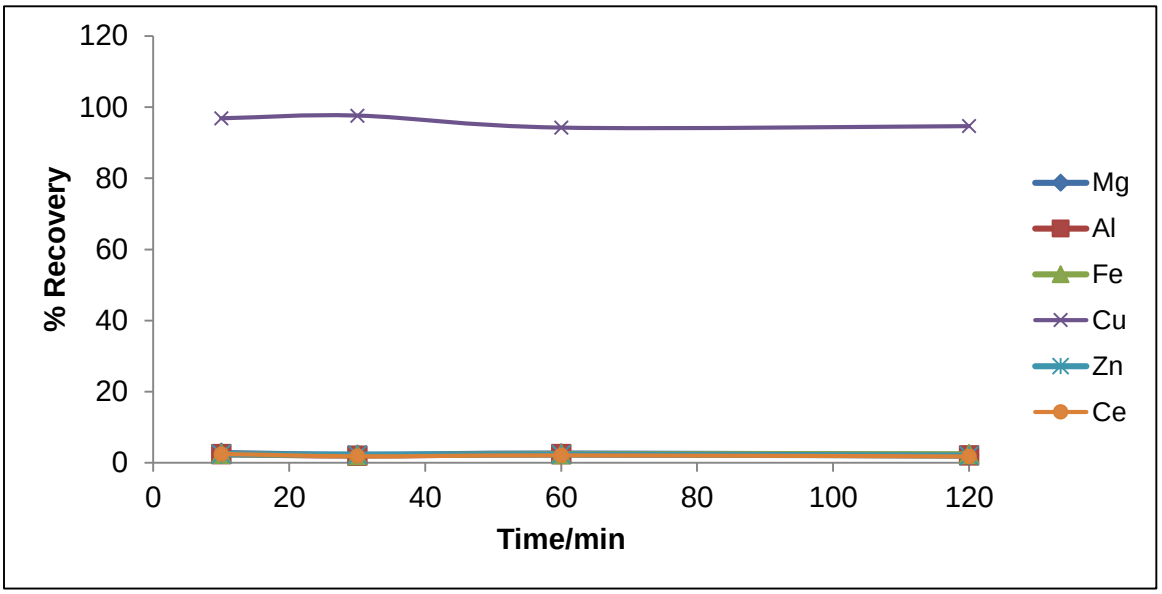

Figure 5.12: Effect of time on metal recovery by oxine precipitation at [oxine] = 0.5 M, pH = 2.8

Effect of pH

The percentage recoveries of these elements were also investigated at various pH levels. From the results in **Figure 5.13** it is clear that the percentage recoveries of other elements increase as the pH is raised. Fe reaches a maximum percentage recovery of 98(3) % at pH = 7.42, while both Al and Zn reach maximum percentage recoveries of 100(1) % and 101.7(2) % respectively at pH = 7.49. Ce reaches a maximum percentage precipitation at pH = 8.03 with 99.98(5) % recovered. The only other element, Mg, reaches maximum percentage recovery of only 71.6(2) % at pH = 9.62, but increases to 100 % at pH levels of 10 and higher.

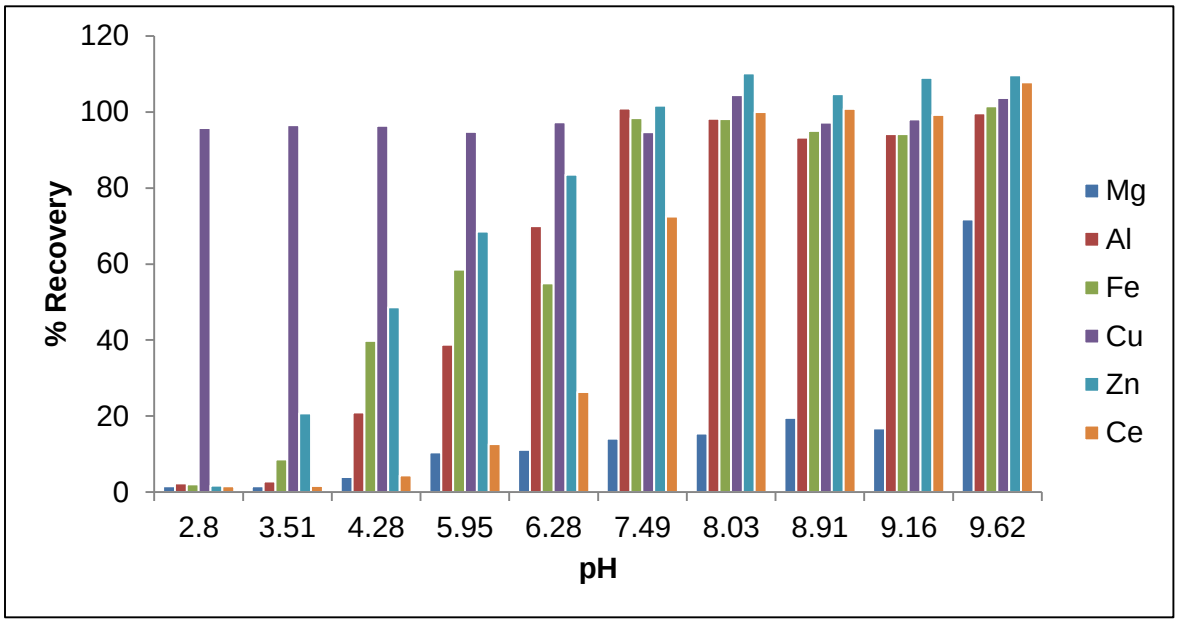

Figure 5.13: Effect of pH on the precipitation of non-precious elements at [oxine] = 0.5 M

The precipitation of these elements, using oxine as a reagent, differs from that of NH_4OH in **Section 5.5.1** in that two of the non-precious elements, Cu and Zn, return to solution (dissolve) at pH levels higher than 8.5 when NH_4OH is used (**Figure 5.6**). Moreover, maximum precipitation for all the elements occurs at different pH levels, while a one-step precipitation at a pH of 10 can remove all non-precious elements from the solution when oxine is used. This may be the result of the combination of product formation with both oxine and OH^-.

5.5.2.3 Characterisation of the precipitated Pd oxine compound

LECO CHNS micro-elemental analysis

About 0.2 mg of the uncrystallised yellow product isolated in **Section 5.5.2.1** was weighed in a tin crucible and analysed for N, C and H content, using the LECO micro-elemental analysis instrument. The results indicated that this compound contains 6.3(2) % of N, 58.6(4) % of C and 3.23(1) % of H. These results were compared with the theoretical values predicted for $Pd(oxine)_2$ and are shown in **Table 5.11**. The experimentally obtained elemental percentages and that of predicted $Pd(oxine)_2$ agree very well with each other and predicted the possible structure of the isolated Pd oxine compound as indicated in **Figure 5.14**.

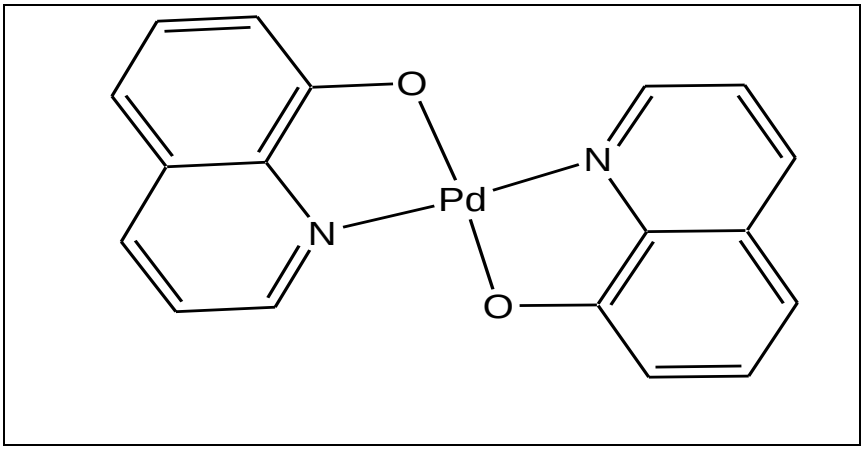

Figure 5.14: The predicted structure of Pd oxine compound

Table 5.11: Experimental and theoretical weight percentages of the elements in the $Pd(oxine)_2$ compound

Element	N	C	H	S	O
Experimental %	6.3(2)	58.6(4)	3.23(1)	0	--
Theoretical %	7.10	54.82	3.05	0	8.12

--Not analysed

Analysis of isolated Pd compound using the FT-IR

The FT-IR spectrum of the isolated $Pd(oxine)_2$ compound is reported in **Figure 5.15**. The peak at 1 581 cm^{-1} is indicative of C=C aromatic stretching while the peaks at 1 302 and 1 372 cm^{-1} are characteristic of aromatic C-N-C amine resonance peaks. The peak at 1 462 cm^{-1} is attributed to the C=N stretching, and aromatic C-O stretching is observed at 1 123 cm^{-1}. The spectrum also shows characteristic aromatic ring at 823 and 742 cm^{-1} which are attributed to the quinolone ring. The broad peak at 3 055 cm^{-1}, which is usually attributed to oxine O-H stretching, is absent in the $Pd(oxine)_2$ structure of the compound, indicating the loss of the acidic H^+ as a result of the binding of the oxine with Pd metal to form $Pd(oxine)_2$.

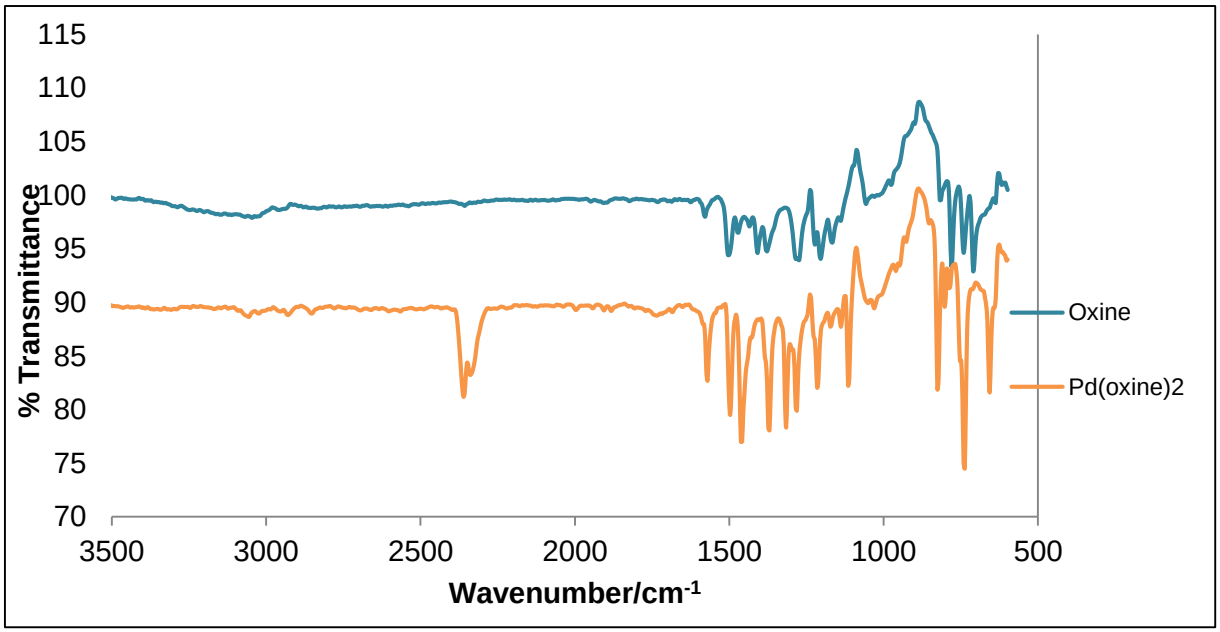

Figure 5.15: The IR spectra of the oxine ligand (8-hydroxyquinonline) and the isolated $Pd(oxine)_2$ compound

The IR spectrum of the $Pd(oxine)_2$ orange crystals is shown in **Figure 5.16**. The spectrum shows characteristic peaks which are very similar to those of the uncrystallised $Pd(oxine)_2$ complex, and shows an aromatic C=C stretching peak at 1 564 cm^{-1}, aromatic amine resonance stretching peaks for C-N-C at 1 311 and 1 369 cm^{-1}, C=N stretching at 1 458 cm^{-1} and aromatic C-O stretching at 1 120 cm^{-1}. The spectrum shows the characteristic peaks of an aromatic ring stretching at 821 and 736 cm^{-1} which are also attributed to the quinolone ring. However, new peaks in the crystal structure of $Pd(oxine)_2$ are observed at 2 923 and 2 858 cm^{-1} and are attributed to the DMSO which was used as a crystallisation solvent. The FT-IR results for $Pd(oxine)_2$ were compared to that of a $Cd(oxine)_2$ complex obtained by Khan[160](**Table 5.12**) which also showed similar stretching frequencies.

[160] Khan M.A. (2014). Solvothermal synthesis of luminescent bis-(8-hydroxyquinoline) cadmium complex nanaostructures. *Mater.Sci.Eng*, 60, pp. 1-9.

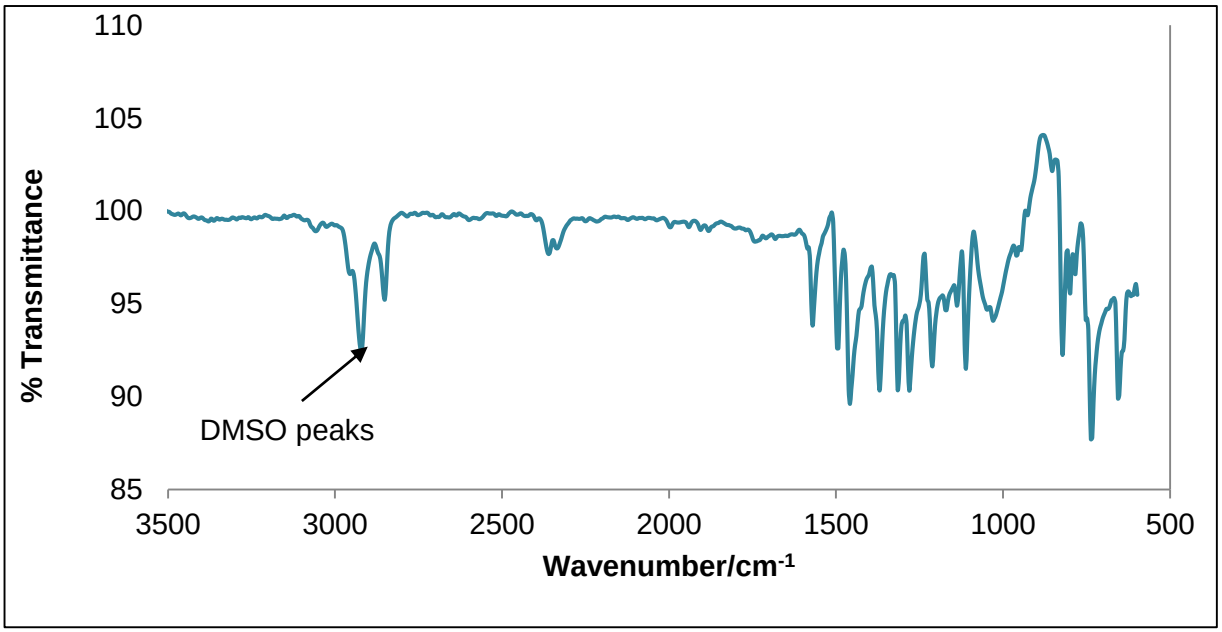

Figure 5.16: IR spectra of the crystallised Pd oxine compound

Table 5.12: Comparison of the FT-IR stretching frequencies

	Stretching Frequency/cm^{-1}					
Sample	**ν(C=C)**	**ν(C-N-C)**	**ν(C-O)**	**ν(C=N)**	**Aromatic**	**ν(H-O)**
Oxine	1 575	1 283, 1 378	1 156	1 469	810, 738	3 055
$Pd(oxine)_2$ powder	1 581	1 302, 1 372	1 123	1 462	823 ,742	--
$Pd(oxine)_2$ crystal	1 564	1 311,1 369	1 120	1 458	821 ,736	--
$Cd(oxine)_2$[160]	1 571	1 280,1 387	1 105	1 425	821 ,739	--

NMR analysis of the $Pd(oxine)_2$ crystal

The $Pd(oxine)_2$ crystals were dissolved in deuterated chloroform, and an NMR analysis was performed on the compound. The proton NMR was recorded at 25 °C on a Bruker 400 MHz Fourier spectrometer and the carbon on a Bruker 75 MHz. The ^{1}H NMR spectrum is shown in **Figure 5.17**, while the ^{13}C and HQSC NMR spectra are reported in **Figures 5.18** and **5.19** respectively.

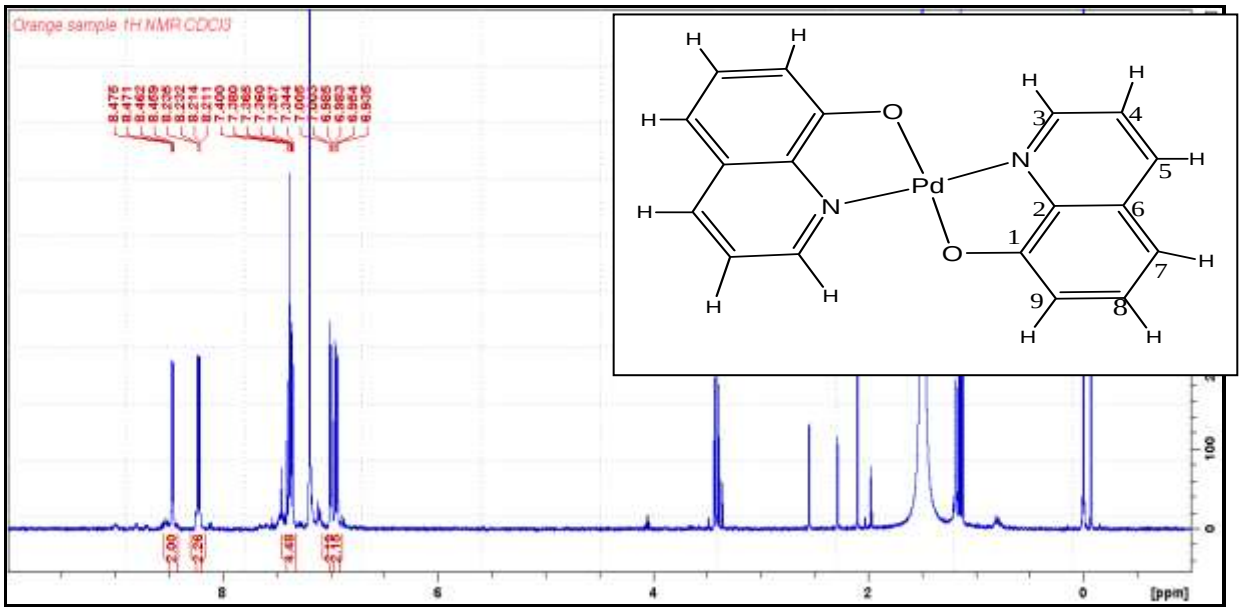

Figure 5.17: The full ^{1}H NMR indicating the oxine rings and the possibility of DMSO in the sample

The proton NMR spectrum of $Pd(oxine)_2$ crystals shows the six different proton environments as indicated in the predicted structure. The peaks at 3.5 and 2.5 ppm are due to DMSO which was used as a crystallisation solvent. According to the proton, carbon and the HQSC NMR spectra, the peaks can be assigned as follows: ^{1}H NMR (400 MHz, $CDCl_3$): δ = 8.47 (2H, dd, *J* = 4.91, 1.36 Hz, H3), 8.22 (2H, dd, *J* = 8.40, 1.33 Hz, H5), 7.38 (2H, t, *J* = 7.98, 7.90 Hz, H8), 7.35 (2H, t, *J* = 8.40, 4.94 Hz, H4), 6.99 (2H, dd, *J* = 7.9, 0.79 Hz, H7), 6.94 (2H, dd, 7.96, 0.56 Hz, H9). ^{13}C NMR (75 MHz, $CDCl_3$): δ = 167.88 (C1), 145.70 (C3), 138.98 (C5), 130.74 (C6), 130.54 (C8), 121.12 (C2), 120.69 (C4), 114.40 (C7), 112.35(C9).

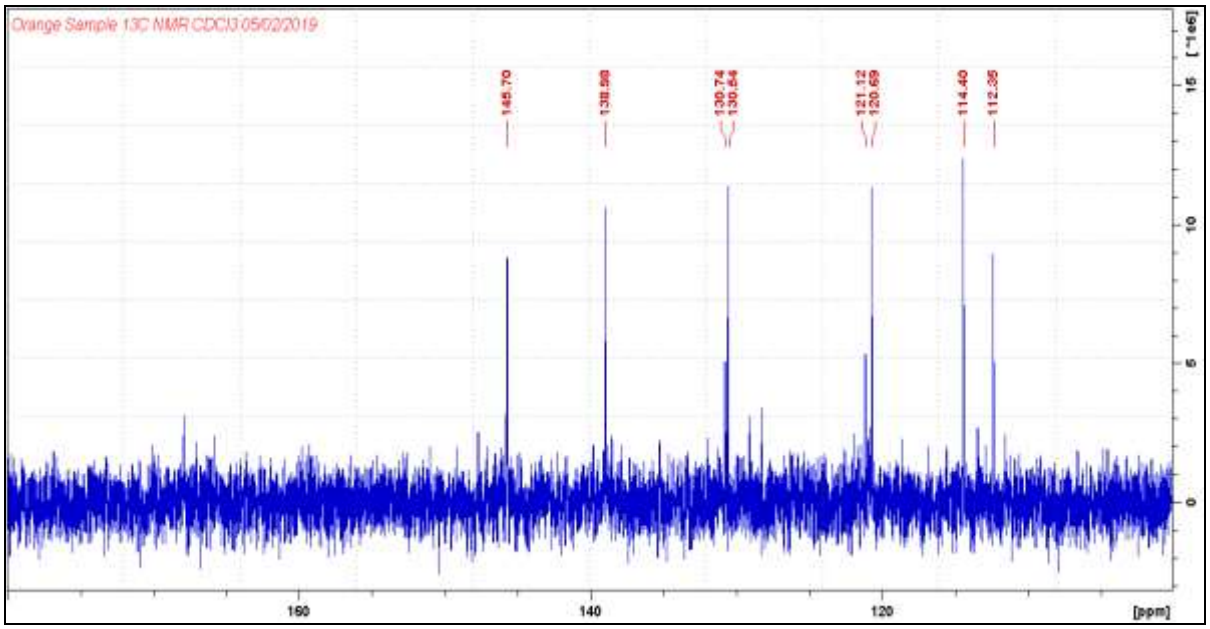

Figure 5.18: The ^{13}C NMR spectrum of the $Pd(oxine)_2$ crystals

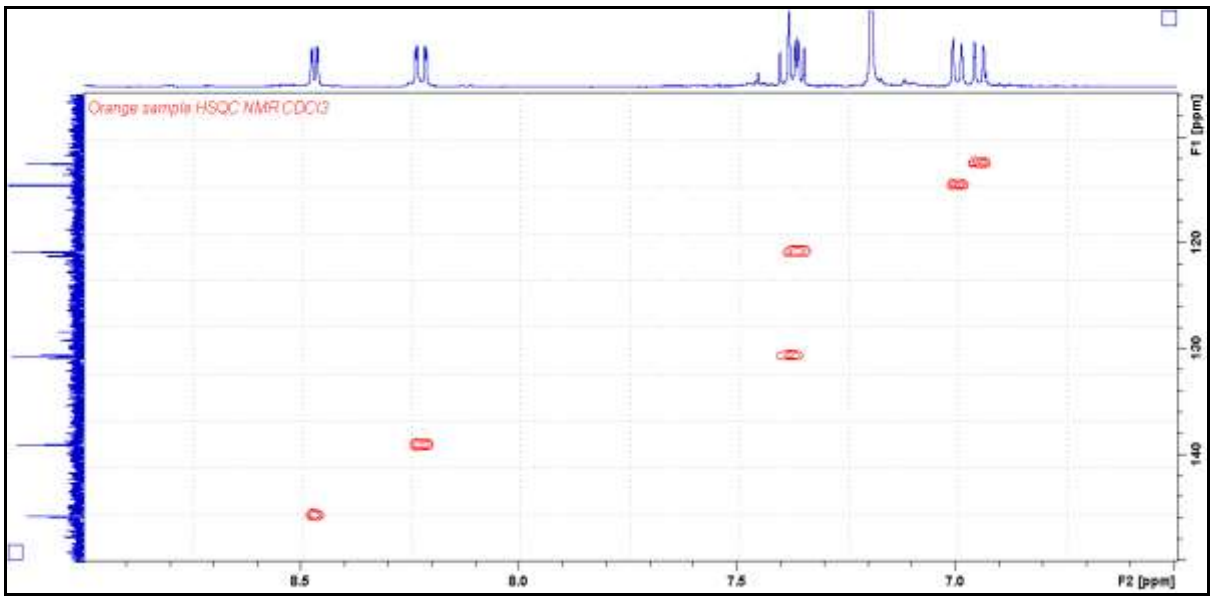

Figure 5.19: The ^{1}H -^{13}C HSQC NMR spectrum of $Pd(oxine)_2$ crystals

The NMR results clearly confirm the predicted structure of the isolated product as $Pd(oxine)_2$. However, the presence of the DMSO peaks are unexpected and may be due to a wet sample or the presence of DMSO in the isolated product.

X-ray crystallography: Crystal structure of Pd(oxine)$_2$

The Pd crystals obtained from DMSO in this study crystallised in a monoclinic system, space group $P2_1/n$, with *a* = 11.204(4), *b* = 4.7803(17), *c* = 13.545(5) Å, α = 90, β = 105.580(13), γ = 90°, V = 698.8(4) and *Z* = 2. Complete structural data is reported in **Table 5.13**, and the selected bond lengths and distances are summarised in **Table 5.14**. An ORTEP view of the crystal structure of Pd(oxine)$_2$ is shown in **Figure 5.20**, while its packed unit cell is illustrated in **Figure 5.21**. The crystal structure confirms that Pd metal was successfully precipitated with oxine in a highly acidic solution, at a pH below zero. The structure shows that Pd is coordinated to the oxine in a bidentate manner to form a square planar molecule, with N and O atoms in *cis* positions.

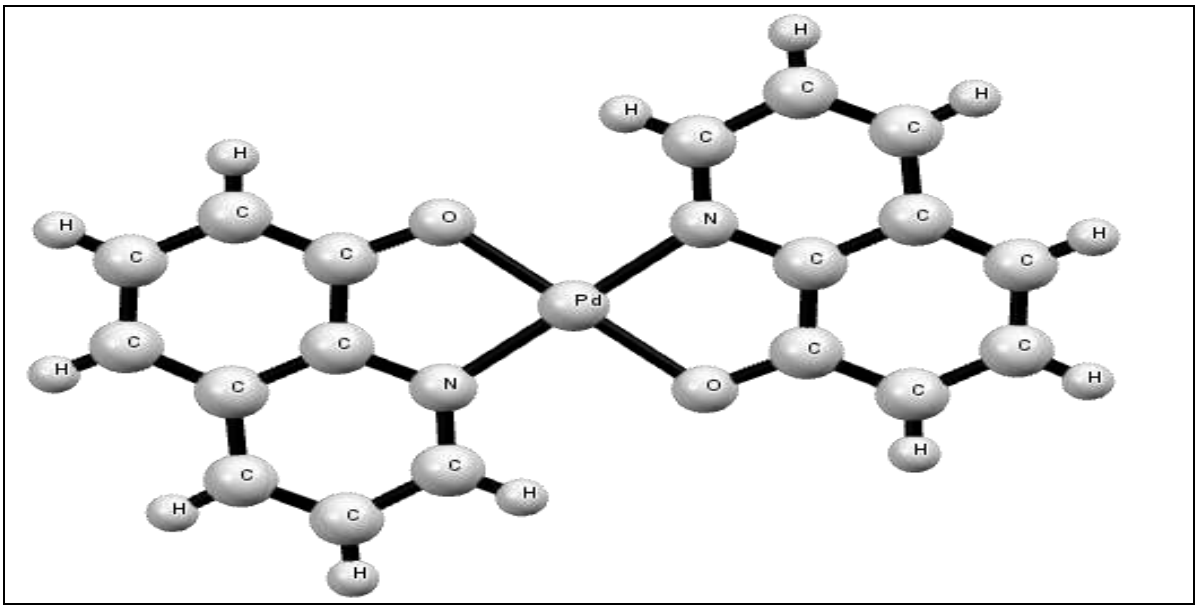

Figure 5.20: An ORTEP view of the Pd(oxine)$_2$ compound

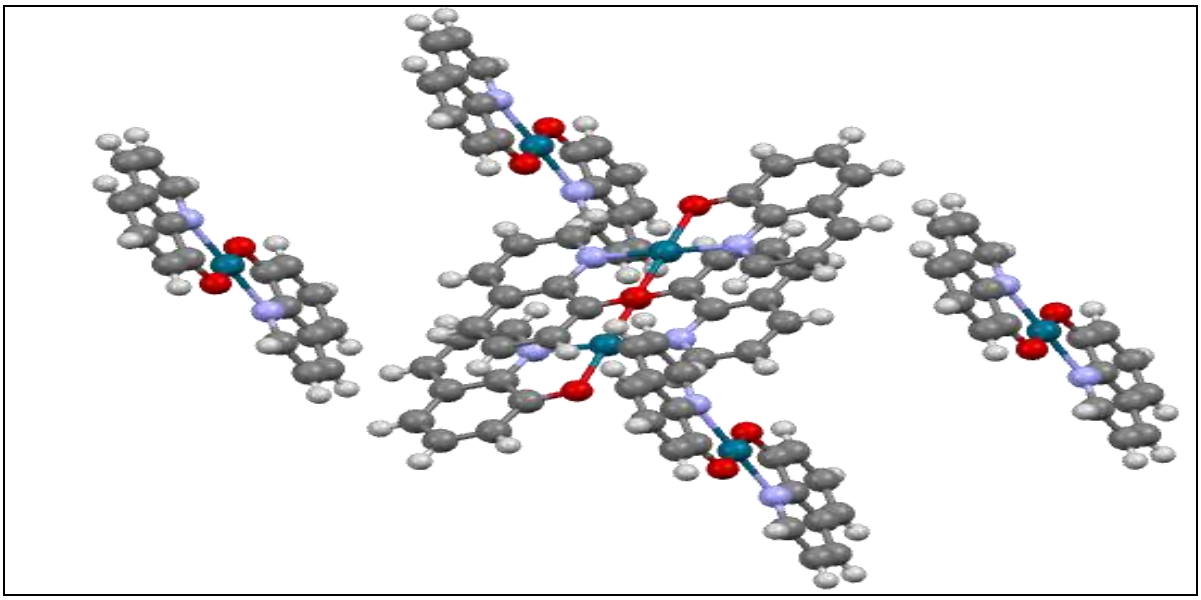

Figure 5.21: Packed unit cell of $C_{18}H_{12}N_2O_2Pd$ along the b axis

Previously, Bailey et al.[161] synthesised $Pd(oxine)_2$ and recrystallised the resulting yellow solid in chloroform, which produced scarlet needles. These crystals were later characterised by Prout et al.[162], and the crystal data showed that this $Pd(oxine)_2$ crystallised in a monoclinic prismatic, space group $P2_1/b$, with a = 11.49(3), b = 15.31(3), c = 4.77(2) Å , γ = 121.90(3)°, V = 713.6 $Å^3$ and Z = 2 .

[161] Bailey, A.S., Williams, R.J.P. & Wright, J.D. (1965). π-Complexes of 8-hydroxyquinoline and its metal complexes. *J.Chem.Soc.*, pp. 2579-2587.

[162] Prout, C.K. & Wheeler, A.G. (1966). Molecular complexes. Part VI. The crystal and molecular structure of 8-hydroxyquinolinatopalladium(II)., *J.Chem.Soc.*, A, pp. 1286-1289.

Table 5.13: Crystal data and crystal refinement for $Pd(oxine)_2$

Identification code	19Dpa1_0m
Empirical formula	$C_{18}H_{12}N_2O_2Pd$
Formula weight/gmol^{-1}	394.70
Temperature/K	100.01
Crystal system	monoclinic
Space group	$P2_1/n$
a/Å	11.204(4)
b/Å	4.7803(17)
c/Å	13.545(5)
α/°	90
β/°	105.580(13)
γ/°	90
Volume/Å^3	698.8(4)
Z	2
ρ_{calc}g/cm^3	1.876
μ/mm^{-1}	1.339
F(000)	392.0
Crystal size/mm^3	0.194 × 0.114 × 0.057
Radiation	MoKα (λ = 0.71073)
2Θ range for data collection/°	8.41 to 56
Index ranges	14 ≤ h ≤ 14, -6 ≤ k ≤ 6, -17 ≤ l ≤ 17
Reflections collected	9289
Independent reflections	672 [R_{int} = 0.0521, R_{sigma} = 0.0364]
Data/restraints/parameters	1672/0/106
Goodness-of-fit on F^2	1.125
Final R indexes [I>=2σ (I)]	R_1 = 0.0319, wR_2 = 0.0988
Final R indexes [all data]	R_1 = 0.0418, wR_2 = 0.1088
Largest diff. peak/hole / e Å^{-3}	0.47/-0.98

Table 5.14: The selected bond lengths and angles for $Pd(oxine)_2$

Selected bond lengths/Å			
Pd-O2	2.000(2)	C4-C6	1.413(6)
Pd-N2	2.000(3)	C5-C7	1.416(5)
O2-CB	1.317(4)	C7-C9	1.404(5)
Selected bond angles/°			
O2-Pd-O2	180.0	C9-C7-C5	125.0(3)
O2-Pd-N3	96.97(10)	C9-C7-CC	118.3(3)
O2-Pd-N3	83.03(10)	O2-CB-CC	119.3(3)
CB-O2-Pd	111.25(19)	N3-CC-C7	122.0(3)

5.6 SEPARATION AND PURIFICATION OF PGE FROM NON-PRECIOUS ELEMENTS USING SOLVENT EXTRACTION METHODS

In this part of the study, the possible separation of the PGE from the non-precious elements was investigated using TOPO (trioctylphosphine oxide) and NaPT (mercaptopyridine *N*-oxide sodium salt) as reactants.

5.6.1 Solvent Extraction with TOPO (Trioctylphosphine Oxide)

5.6.1.1 Experimental

Effect of ligand concentration

A solution containing 100 ppm of each PGE (Pt, Ru, Ir, Rh and Pd) was prepared using the previously indicated standard solutions. From this mixture, 1 ml was transferred into a 100 ml beaker and evaporated to dryness. The resulting residue was dissolved in HCl (10 ml, 0.5 M), transferred into a separation funnel containing TOPO dissolved in toluene. The extraction was performed at various TOPO concentrations (0.05, 0.1, 0.2 and 0.3 M). The two immiscible layers were mixed by shaking, and a waiting time of 15 minutes was allowed before separating the two layers. The raffinate was evaporated to almost dryness and dissolved in HCl (10 ml, 10 M). The resulting solution was then transferred into a volumetric flask (100.0 ml),

filled to the mark with ultra-pure water and taken for ICP-OES analysis. The results of TOPO concentration on the extraction of PGE are illustrated in **Figure 5.22**. The estimated percentage recoveries of PGE extracted into the organic layer before being stripped selectively were calculated using the elemental quantities obtained for the raffinate, since the ICP-OES does not tolerate the presence of organic solvents.

Effect of HCl concentration

From the previously prepared 100 ppm PGE solution, 1 ml was pipetted into a 100 ml beaker, evaporated to dryness and dissolved in the desired HCl (10 ml) concentration. The solution was extracted with TOPO (10 ml, 0.3 M) in toluene, while the concentration of HCl was varied from 0.5 M to 10 M. The two immiscible layers were mixed and allowed to stand for a period of 15 minutes before being separated. The raffinate was separated from the organic phase and evaporated to dryness. To this residue HCl (10 ml, 10 M) was added, transferred to a volumetric flask (100.0 ml) and filled to the mark with ultra-pure water. The sample was then analysed using ICP-OES. The estimated percentage recoveries of PGE extracted into the organic layer at various HCl concentrations were again calculated using the results obtained in the raffinate, as shown in **Figure 5.23**.

Effect of diluent

A solution (1 ml) was pipetted from the previously prepared PGE solution (100 ppm), and transferred into a beaker (100 ml). This solution was then evaporated to dryness and dissolved in HCl (10 ml, 4 M).The sample solution was then extracted with TOPO (10 ml, 0.3 M) dissolved in various diluents, including toluene, hexane, kerosene and chloroform. The effect of diluent on the extraction of PGE with TOPO was investigated, the results of which are shown in **Figure 5.24**.

Effect of various stripping reagents on PGE selectivity in the presence of non-precious metals

Synthetic mixtures containing non-precious metals (30 ppm) and PGE (5 ppm) were prepared. These were then evaporated to dryness, dissolved in HCl (10 ml, 4 M) and extracted with TOPO (10 ml, 0.3 M) dissolved in kerosene. The organic layer was stripped twice using 10 ml portions of various stripping reagents, such as HNO_3, water, HCl, *N'N*-dimethylthiourea and NH_4SCN. The resulting stripped solutions were also evaporated to dryness, dissolved in HCl (10 ml, 10 M), transferred into a volumetric flask (100.0 ml) and filled to the mark with ultra-pure water. The solutions were then analysed using the ICP-OES. The effect of stripping agents on the recovery of PGE in the presence of non-precious metals was determined, the results of which are shown in **Table 5.16**.

5.6.1.2 Results and discussion

Effect of ligand concentration

The results in **Figure 5.22** show that all the investigated PGE can be extracted to different degrees by TOPO in toluene. These results indicate that Pt is preferably extracted with a percentage recovery of 85.3(7) %, followed by Ir with 55.7(5) % and Pd with 49.9(9) % at 0.3 M TOPO and 0.5 M HCl. These results also indicate that increasing the ligand concentration improves the extraction of PGE from the aqueous layer.

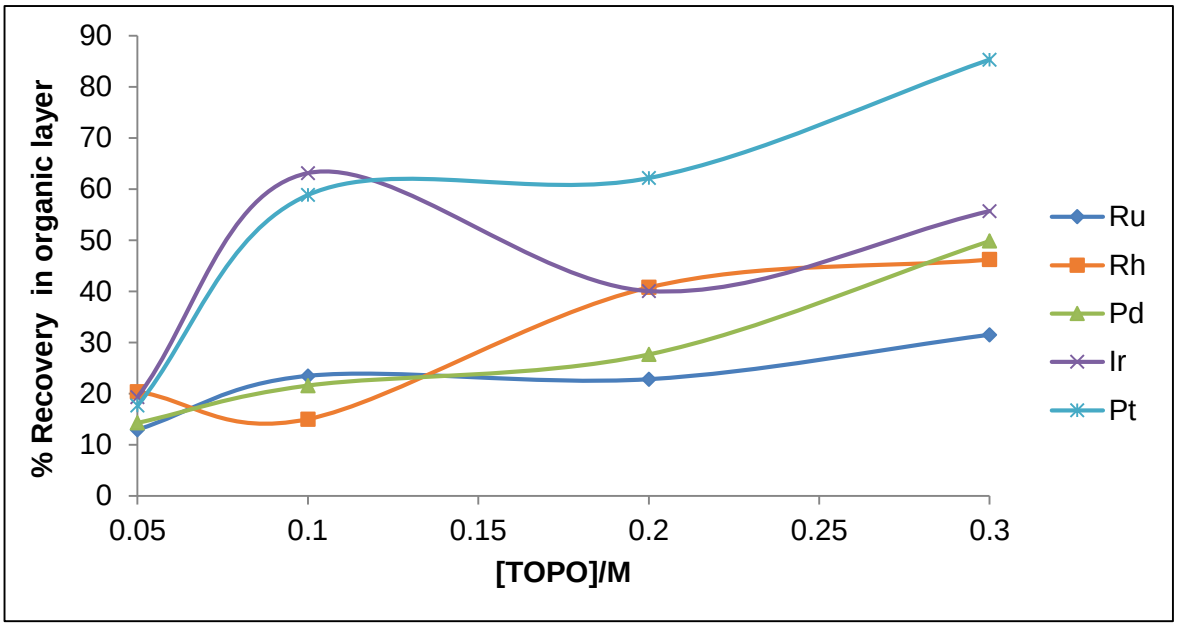

Figure 5.22: Effect of ligand concentration on the extraction of PGE at [HCl] = 0.5 M

Effect of HCl concentration

The results in **Figure 5.23** indicate that the maximum of all PGE extraction takes place around 4 M HCl. Pt and Pd are completely extracted at this acid concentration and are completely absent in the raffinate, while Ru, Rh and Ir are extracted with elemental recoveries of 62(1), 72(1) and 82.2(8) % respectively. The extraction of the PGE increased steadily with an increase in HCl concentration and then started to decrease at highly acidic solutions (6 M and 10 M), except for Pt. Pt is totally extracted from the aqueous layer in the [HCl] range of 1 to 10 M HCl. The dramatic effect on the extraction of the PGE in the presence of TOPO at the different HCl concentrations may be attributed to the variety of PGE chloride species formed in the presence of Cl^- which affect their reactivity with TOPO and, subsequently, their extraction into the organic layer (**Chapter 2, Section 2.5.1**).

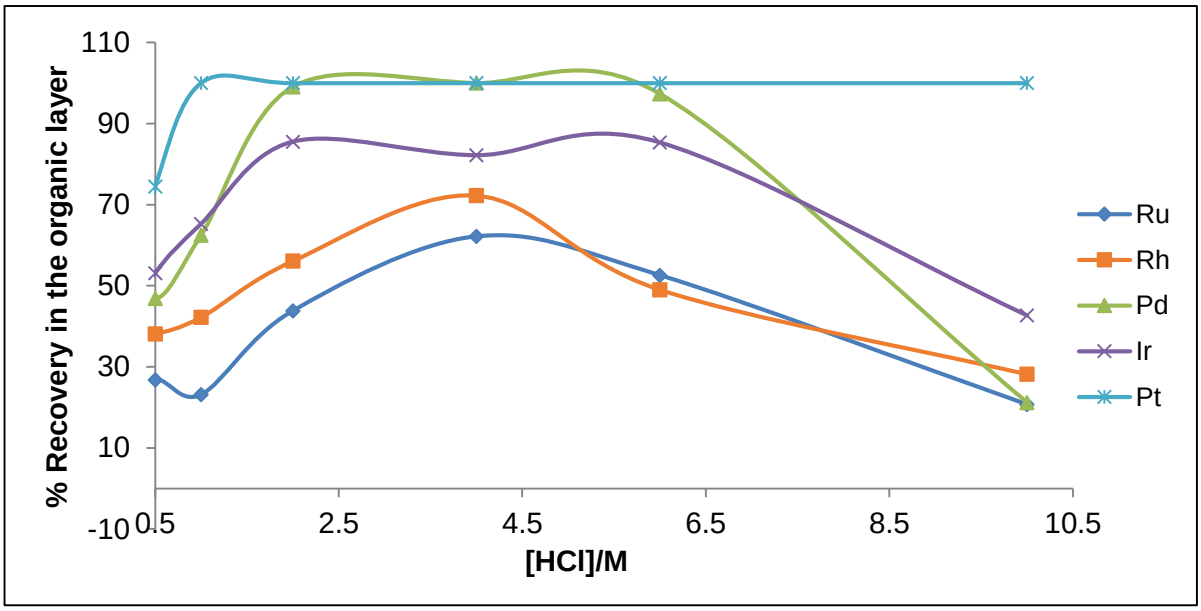

Figure 5.23: Effect of HCl concentration on the extraction of PGE, [TOPO] = 0.3 M in toluene

Effect of diluent

The results obtained from the variation of diluents indicate that kerosene and hexane were superior to toluene and chloroform in their extraction of PGE in the presence of TOPO. The quantification of the PGE indicated that they afforded the complete extraction of PGE while chloroform's extraction was the worst and only extracted 11.9(1) and 34.7(6) % of Ru and Pt respectively (**Figure 5.24**). The difference in the extraction between these organic solvents can be attributed to their dielectric constants. A comparison of the dielectric constants reported in **Table 5.16** indicates that kerosene and hexane have low dielectric constants (1.88 and 1.80) compared to toluene and chloroform (2.38 and 4.8). From these results it can be concluded that the lower the dielectric constant of the solvent, the higher the extraction percentage of PGE with TOPO. This predicts that the newly-formed PGE complexes in the presence of TOPO have substantial organic properties which dissolve more readily in the solvents with low dielectric constants.

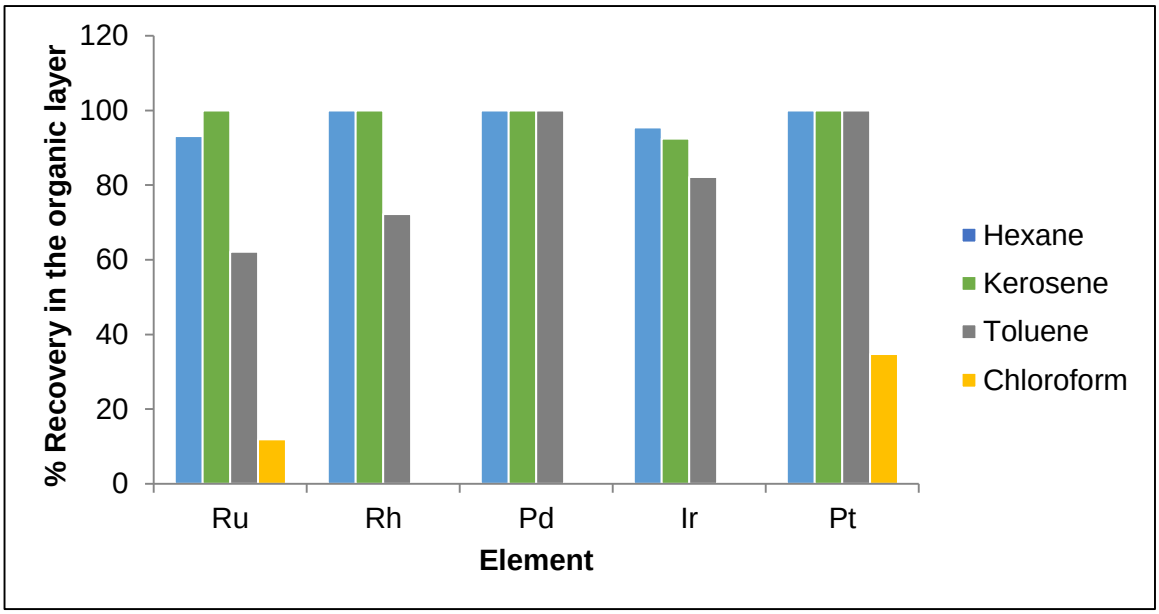

Figure 5.24: The effect of diluent on the extraction of PGE, [TOPO] = 0.3 M, [HCl] = 4 M

Table 5.15: Dielectric constants of solvents used in the extraction of PGE with TOPO

Solvent	Dielectric constant
Kerosene	1.80
Hexane	1.88
Toluene	2.38
Chloroform	4.81

Effect of various stripping reagents on PGE selectivity in the presence of non-precious metals

Once the optimum conditions with regard to the extraction of PGE with TOPO had been determined, the experiments were repeated in the presence of non-precious metals. Various reagents were used to try and strip the metals from the organic layer in order to selectively recover the PGE from the non-precious metals and from one another. The results shown in **Table 5.16** indicate that the back-extraction of metals using water, *N'N*-dimethylthiourea and 14 M HNO_3 is not that selective and almost all the elements are stripped by means of these reagents. Pd recovery after two

successive extractions with 10 M HCl, *N'N*-dimethylthiourea and 14 M HNO_3 were 80.0(9), 97(4) and 100(1) % respectively. Although Pd seemed to be successfully stripped using all the investigated solvents, water and 2 M HCl yielded the lowest Pd recoveries of 26.7(5) and 9.6(3) % respectively, while no stripping was observed with NH_4SCN. However, high Pt recoveries of 107(5) and 84.2(3) % were obtained when *N'N*-dimethylthiourea and NH_4SCN were used as stripping reagents while no stripping was observed with 2 and 10 M HCl. These results are extremely promising, suggesting the possible selective separation of Pt from the rest of the PGE, especially Pd and Rh, which are present in the automotive catalyst waste.

The results in **Table 5.16** also indicate that substantial amounts of Rh are back-extracted with 2 M HCl and 14 M HNO_3 and percentage recoveries of 45.5(9) and 45.55(7) % were obtained. Ir is the only PGE that was not stripped using most of the reagents investigated. However, NH_4SCN allowed for the recovery of 86.4(3) % of the added Ir. The results obtained with NH_4SCN as a stripping reagent are very promising in terms of the extraction of Pt, Ir and Ru as a group. Pt and Ir were the most favoured PGE back-extracted with NH_4SCN, followed by Ru with a recovery of 68.9(8) %.

The non-precious elements, including Cu, Fe and Zn co-back-excreted with the stripping of PGE for most of the stripping reagents used. Mg, Ce and Al are the only metals that did not interfere with the extraction of PGE and were not observed after stripping by means of all the investigated reagents (**Table 5.16**).

Table 5.16: The percentage recoveries of elements after solvent extraction with TOPO and stripping twice with various reagents

	% Recovery					
Element	**Water**	**2 M HCl**	**10 M HCl**	***N'N*-dimethylthiourea**	**14 M HNO_3**	**NH_4SCN**
Ru	51.9(3)	5.5(2)	48.3(1)	58(1)	35.6(2)	68.9(8)
Rh	34.1(9)	45.5(9)	37(1)	35.1(9)	45.55(7)	0
Ir	0	0	0	0	0	86.4(3)
Pt	66.3(8)	0	0	107(5)	66.5(4)	84.2(3)
Pd	26.7(5)	9.6(3)	80.0(9)	97(4)	100(1)	0
Mg	0	0	0	0	0	0
Fe	83(2)	0	0	71(1)	40.6(1)	0
Zn	67(1)	0	5.3(1)	102.3(1)	102.9(8)	0
Cu	50(1)	57.2(6)	22.9(2)	55.7(5)	47.02(3)	0
Al	0	0	0	0	0	0
Ce	0	0	0	0	0	0

5.6.2 Solvent Extraction with NaPT (Mercaptopyridine *N*-Oxide Sodium Salt)

5.6.2.1 Experimental

Effect of HCl concentration

A synthetic solution containing 100 ppm of each of the five PGE was prepared using separate PGE standard solutions containing 1 000 ppm of each PGE (Pt, Ru, Ir, Rh and Pd). From the prepared 100 ppm PGE mixture, 1 ml solution was transferred into a beaker (100 ml), evaporated to dryness, dissolved in a desired HCl (5 ml) concentration and transferred into a separating funnel containing NaPT (5 ml, 0.1 M) and toluene (10 ml). The solution was mixed by shaking, and the two immiscible layers were allowed to stand for a period of 15 minutes before being separated. The

resulting raffinate was separated from the pink-coloured organic layer, evaporated to almost dryness and dissolved in concentrated HCl (10 ml). The resulting solution was then transferred into a volumetric flask (100.0 ml), filled to the mark with ultra-pure water and analysed using ICP-OES. The percentage recoveries of the PGE in the organic layer were calculated using the quantification results of the raffinate. The effect of the HCl concentration on the extraction of PGE with NaPT in toluene was investigated, the results of which are shown in **Figure 5.26**.

Effect of NaPT concentration

From the previously prepared synthetic solution containing 100 ppm of each of the PGE, 1 ml was pipetted and evaporated to almost dryness in HCl (5 ml, 4 M), and extracted with desired concentrations of NaPT (5 ml) and toluene (10 ml). The raffinate was separated from the organic layer, evaporated to almost dryness, dissolved in concentrated HCl (10 ml, 10 M), transferred into a volumetric flask (100.0 ml), filled to the mark with ultra-pure water and analysed using ICP-OES. The experiment was repeated for each NaPT concentration, the results of which are shown in **Figure 5.28**.

Removal of Pd from the organic layer by recrystallisation

A highly concentrated synthetic PGE mixture (Pd, Pt, Rh, Ir, and Ru) was prepared by mixing 5 ml of the different PGE standard solutions (1 000 ppm) into a beaker (100 ml). This solution was evaporated to dryness, dissolved in HCl (10 ml, 4 M) and reacted with NaPT (10 ml, 0.1 M) and toluene (20 ml). The pink organic toluene layer (**Figure 5.25**) was separated from the raffinate, transferred into a 100 ml beaker and slowly evaporated on a hot plate. Bright pink crystals slowly formed during the evaporation process. The isolated product was re-dissolved in DMF and good quality crystals suitable for single X-ray crystallography were obtained. These crystals quickly turn opaque when exposed to air for extended periods. This is most probably due to the loss of solvated DMF molecules present in the crystals. The melting point of these crystals was determined to be between 254 and 256 °C. They were further characterised and discussed in **Section 5.6.2.3**.

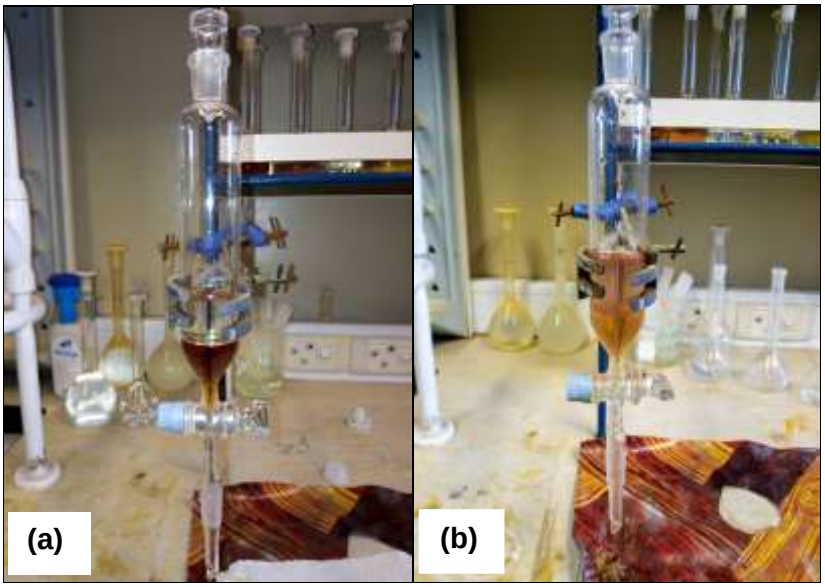

Figure 5.25: The extraction of PGE with NaPT in toluene, (a) before and (b) after the extraction process, showing the extracted pink $Pd(PT)_2$ compound in the organic layer

Effect of various stripping reagents on Pd selectivity in the presence of non-precious metals

A solution containing Pd (5 ppm) and non-precious elements (30 ppm) was evaporated to dryness, dissolved in HCl (10 ml, 4 M) and extracted with NaPT (5 ml, 0.02 M) and toluene (15 ml). The two immiscible layers were allowed to stand for a period of 15 minutes before being separated. The raffinate was isolated while the organic layer was stripped twice using the desired stripping agents, such as *N'N*-dimethylthiourea (10 ml, 0.2 M), water (10 ml) and HCl (10 ml, 2 and 10 M) in order to investigate the effect of stripping agents on the selective isolation of Pd from the non-precious metals. The resulting stripped solutions were evaporated to dryness and dissolved in HCl (10 ml, 10 M). The dissolved solutions were then transferred into volumetric flasks (100.0 ml), filled to the mark with distilled water, and the stripped elements were quantified using ICP-OES (**Table 5.17**).

Effect of Pd concentration on extraction with NaPT and on Pd stripping using N'N-dimethylthiourea

From the 1 000 ppm Pd standard solution, aliquots containing 5, 10, 20 and 40 ppm of Pd were transferred into beakers (100 ml), evaporated to dryness and dissolved in HCl (10 ml, 4 M). The dissolved solutions were then extracted with NaPT (5 ml, 0.02 M) and toluene (15 ml). The organic layer was stripped twice with *N'N*-dimethylthiourea (10 ml, 0.2 M). The resulting stripped solutions were evaporated to dryness, dissolved in HCl (10 ml, 10 M) and transferred into volumetric flasks (100.0 ml), filled to the mark with ultra-pure water and analysed using ICP-OES to determine the percentage recovery of Pd after stripping the organic layer with *N'N*-dimethylthiourea (**Table 5.18**).

5.6.2.2 Results and discussion

Effect of HCl concentration

The results in **Figure 5.26** show excellent selectivity for Pd, especially from Pt in the presence of other PGE. These results are crucial to the beneficiation of Pd. The results imply that the extraction of Pd with NaPT is independent on the Pd chloride species formed in solution. The extraction of Pt at low HCl concentration (0.5 and 1 M) is observed. This shows that at lower HCl concentrations, the tetrachloride complexes of Pt ($PtCl_4^{2-}$) are slightly extracted by this ligand. However, these further decrease at high HCl concentrations, and no Pt extraction is observed at [HCl] ≥ 2 M HCl, predicting complete isolation and separation of Pd from Pt and the other PGE. The pink appearance of the toluene after the PGE separation is attributed to the presence of Pd-mercaptopyridine type complex in the organic layer.

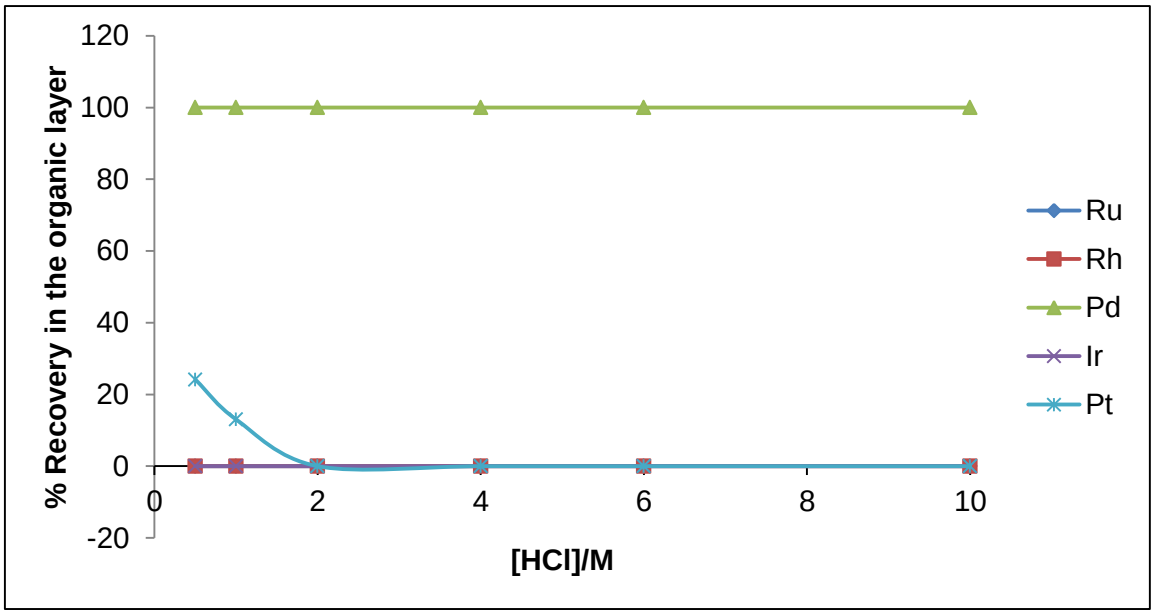

Figure 5.26: Effect of HCl concentration on the extraction of PGE at [NaPT] = 0.1 M

Effect of NaPT concentration

The concentration of NaPT was varied in order to determine the effectiveness of the ligand on the extraction of Pd. The results in **Figure 5.27** show that the extraction of Pd (1 ppm) was not affected by a decrease in ligand concentration, indicating that this method is highly effective in the isolation and purification of Pd from the other PGE.

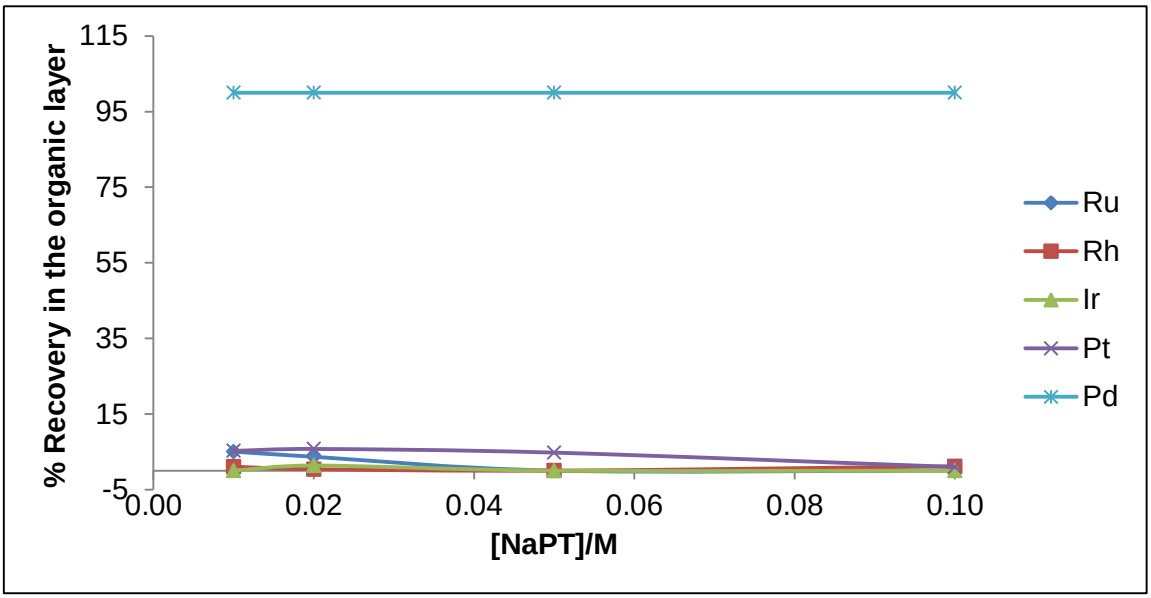

Figure 5.27: Effect of NaPT concentration on the extraction of PGE at [HCl] = 4 M

The extraction of Pd with NaPT can occur via a chelating reaction, and can be explained by means of **Equation 5.1**.

$$Pd^{2+} + 2PT^{-} \longrightarrow Pd(PT)_2(org) \qquad \textbf{(5.1)}$$

During the extraction of Pd with NaPT in the presence of non-precious metals, the organic layer was no longer pink, indicating that some of the non-precious metals also might have been extracted. Thus, various stripping reagents were investigated in order to find the one that would selectively recover Pd from the rest of the elements.

Effect of various stripping reagents on Pd selectivity in the presence of non-precious metals

The results in **Table 5.17** show that *N'N*-dimethylthiourea and 10 M HCl yielded the best results for the stripping of Pd, and percentage recoveries of 99(6) and 83(1) % were obtained respectively. The results also indicate that the non-precious metals do not interfere with the stripping of Pd when *N'N*-dimethylthiourea was employed as a stripping agent. However, Cu was back-extracted with Pd when 10 M HCl was used as a stripping agent. Water and 2 M HCl did not offer any stripping for Pd.

Table 5.17: The back-extraction of Pd using various stripping reagents after extraction with NaPT in the presence of non-precious metals

	% Recovery			
Element	***N'N*-dimethylthiourea**	**10 M HCl**	**Water**	**2 M HCl**
Pd	99(6)	83(1)	0	0
Cu	0	23.1(1)	0	0
Fe	0	0	0	0
Zn	0	0	0	0
Ce	0	0	0	0
Al	0	0	0	0
Mg	0	0	0	0

Effect of Pd concentration on extraction with NaPT and on Pd stripping using N'N-dimethylthiourea

An increase in Pd concentration from 5 to 40 ppm while keeping the concentration of NaPT at 0.02 M did not influence the percentage recovery of Pd. Furthermore, the element was completely recovered after extraction with NaPT and a two-step back-extraction process with *N'N*-dimethylthiourea as a reagent (**Table 5.18**).

Table 5.18: The percentage recovery of Pd after the extraction with NaPT and stripping using *N'N*-dimethylthiourea at various Pd concentrations

[Pd]/ppm	% Recovery after stripping
5	97(5)
10	96(3)
20	95.1(3)
40	99(1)

From these results it can be concluded that NaPT can be successfully used to selectively recover Pd in the presence of other PGE and non-precious metals investigated in this study. The results from both the TOPO and NaPT extraction methods indicate that these methods may be suitable for the selective separation of PGE from the ERM®-EBS504 catalyst sample. These methods showed excellent selectivity towards PGE isolation and recovery compared to the precipitation methods investigated in this study. Moreover, these methods may be appropriate for the beneficiation of PGE in low concentration PGE samples.

The proposed method for the separation and isolation of PGE from the automotive catalyst waste sample

The results obtained in this study are used to propose a method for the separation of PGE from the autocatalyst material. The separation should start with the isolation of Pd by solvent extraction using NaPT, followed by the stripping from the organic layer using *N'N*-dimethylthiourea. Next, Pt and Rh can be recovered by solvent extraction using TOPO and selectively recovered from the organic layer by stripping the Pt

using NH_4SCN. The Rh (contaminated with Cu) can be stripped using 2 M HCl (**Table 5.16**) and finally separated from Cu by precipitation using NH_4OH or oxine. The entire process is illustrated in **Figure 5.28**:

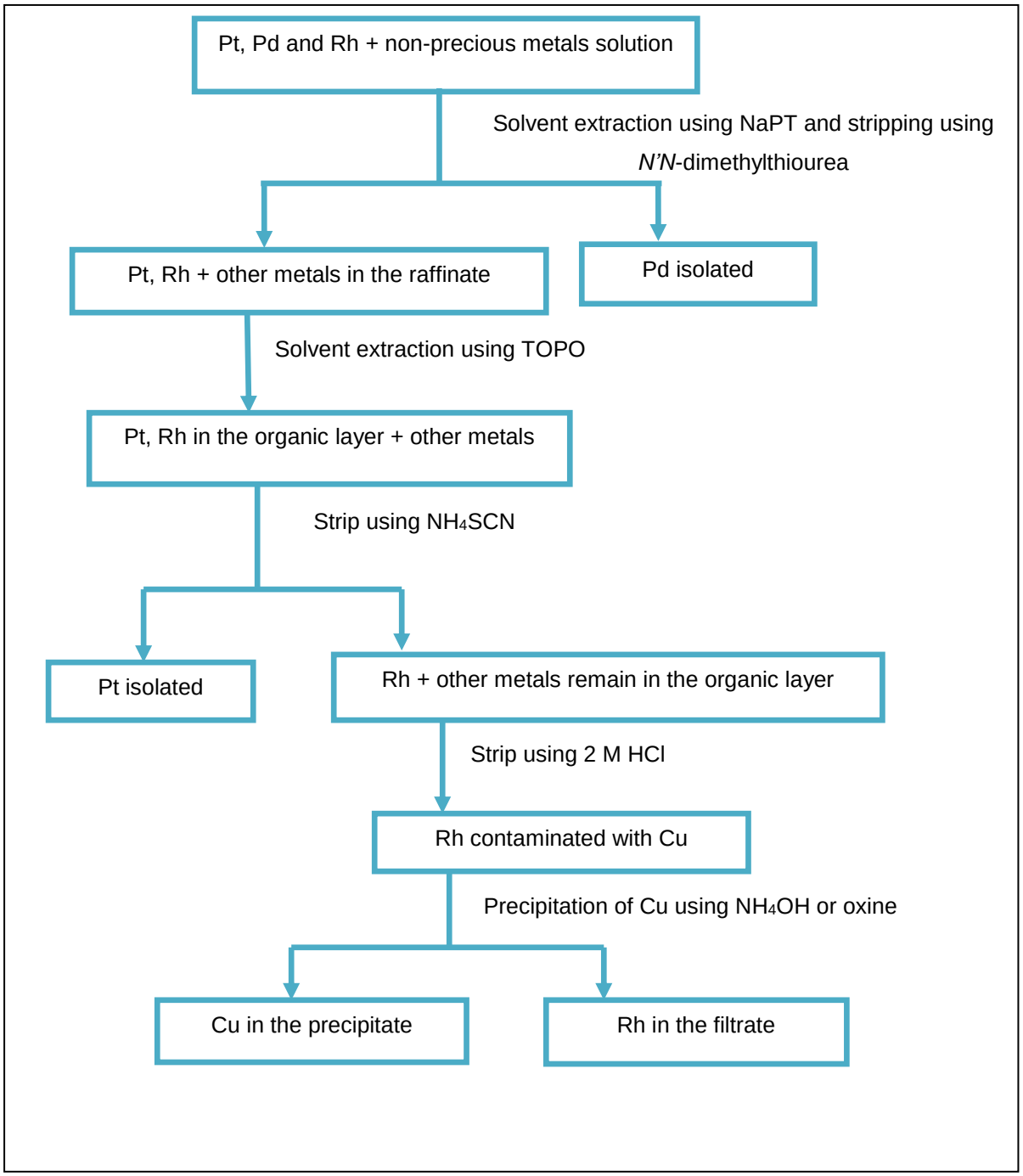

Figure 5.28: The proposed scheme for the isolation of Pt, Pd and Rh from the ERM®-EBS504 catalyst sample

5.6.2.3 Characterisation of the isolated $Pd(PT)_2$ crystals after extraction with NaPT

Characterisation of the isolated product using LECO and ICP-OES

Approximately 2 mg of the dried pink crystals were accurately weighed in a tin crucible. The percentage weights of N, C and H were determined using the LECO instrument. The weight percentage of Pd was determined using ICP-OES by dissolving ~7 mg of the $Pd(PT)_2$ with HNO_3 (20 ml, 14 M) in a beaker (100 ml) and slightly heating the solution. The cooled solution was transferred into a volumetric flask (50.0 ml), filled to the mark with ultra-pure water and analysed with ICP-OES. The oxygen was not analysed but is expected to be present in the product. The results show that this compound contains Pd, N, C, H and S in percentage weights of 26.1(1), 6.9(2), 33.3(6), 2.26(3) and 17(2) % respectively. The experimental percentage weights of the elements found in the product agree with the predicted chemical formula for $Pd(PT)_2$ (**Figure 5.29** and **Table 5.19**).

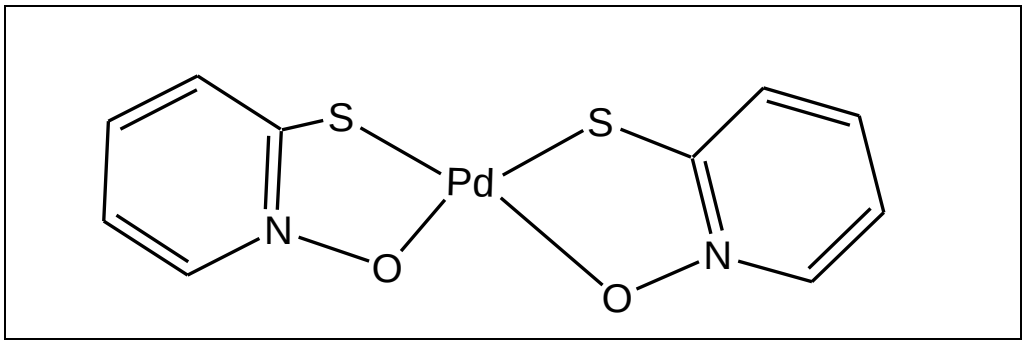

Figure 5.29: The predicted structure of the extracted Pd-mercaptopyridine complex

Table 5.19: The percentage weights of the elements in the $Pd(PT)_2$ as determined by LECO and ICP-OES

Element	Pd	N	C	H	S	O
Experimental %	26.1(6)	6.9(2)	33.3(6)	2.26(3)	17(2)	--
Theoretical %	28.14	7.99	34.22	2.22	18.25	9.12

--Not analysed

FT-IR analysis of the isolated $Pd(PT)_2$

The FT-IR spectrum of $Pd(PT)_2$ in **Figure 5.30** shows the peak at 1 547 cm^{-1}, which is indicative of the C=C aromatic stretching. The peak at 3 090 cm^{-1} is attributed to the C-H aromatic stretching. The stretching frequency at 1 458 cm^{-1} is attributed to C=N stretching peak while the peak at 1 251 cm^{-1} is attributed to aromatic N-O vibration and the peak at 702 cm^{-1} to C-S stretching. The spectrum also shows characteristic peaks of an aromatic ring at 817 and 743 cm^{-1} which are attributed to the pyridine ring in the PT^- ligand. The stretching frequencies in **Table 5.20** compared well to those obtained by Machado et al.[163] and Vietes et al.[164] for $Ga(PT)_3$ and $Pt(PT)_2$ complexes respectively, which also lie in the same region.

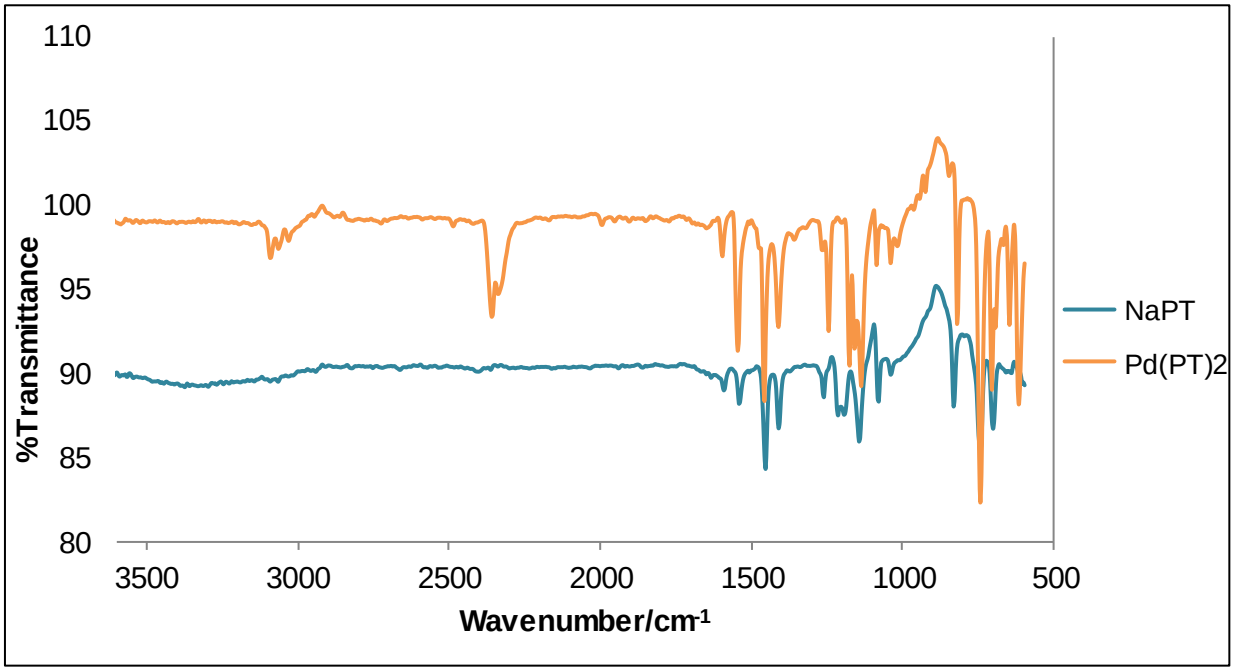

Figure 5.30: The FT-IR spectra of NaPT and the isolated $Pd(PT)_2$ after solvent extraction

[163] Machado, I., Marino, L.B., Demoro, B. & Echeverria, G.A. (2014). Bioactivity of pyridine-2-thiolato-1-oxide metal complexes: Bi(III), Fe(III) and Ga(III) complexes as potent anti-Mycobacterium tuberculosis prospective agents. *European journal of medicinal chemistry*, 87, pp.267–273.

[164] Vieites, M., Smircich, P., Parajon-Costa, B. & Rodriguez, J. (2008). Potent in vitro anti-trypanosoma cruzi activity of pyridine-2-thiol N-oxide metal complexes having an inhibitory effect on parasite-specific fumarate reductase. *Journal of Biological Inorganic Chemistry*: *JBIC: a publication of the Society of Biological Inorganic Chemistry*, 13(5), pp. 723-735.

Table 5.20: The stretching frequencies of mercaptopyridine (PT) complexes

	Stretching frequency/cm^{-1}				
	ν(C-H)	**ν(C=C)**	**ν(N-O)**	**δ(N-O)**	**ν(C-S)**
NaPT	3 068	1 542	1 262	831	702
$Pd(PT)_2$	3 090	1 547	1 260	814	702
$Ga(PT)_3$	3 103	1 545	1 226	829	712
$Pt(PT)_2$	3 098	1 551	1 250	814	711

NMR of $Pd(PT)_2$ crystals

The dry $Pd(PT)_2$ crystals were dissolved in deuterated chloroform ($CDCl_3$) and analysed using NMR. The proton NMR was recorded at 25 °C on a Bruker 300 MHz Fourier spectrometer and the ^{13}C on a Bruker 75 MHz. Full ^{1}H NMR is shown in **Figure 5.31**, while the ^{13}C and HQSC NMR spectra are illustrated in **Figures 5.32** and **5.33** respectively. The proton NMR shows four different proton environments as observed in the predicted structure, while the carbon NMR also confirms the predicted structure. This suggests that the compound has five different carbon environments in an aromatic ring since five lines are observed at δ = 117.90 to 158.97 ppm. The peak at $\delta \approx 77$ in the ^{13}C NMR is due to the carbon from the $CDCl_3$. The HSQC NMR spectrum in **Figure 5.33** shows the correlation between the carbon and its attached protons in the $Pd(PT)_2$ compound.

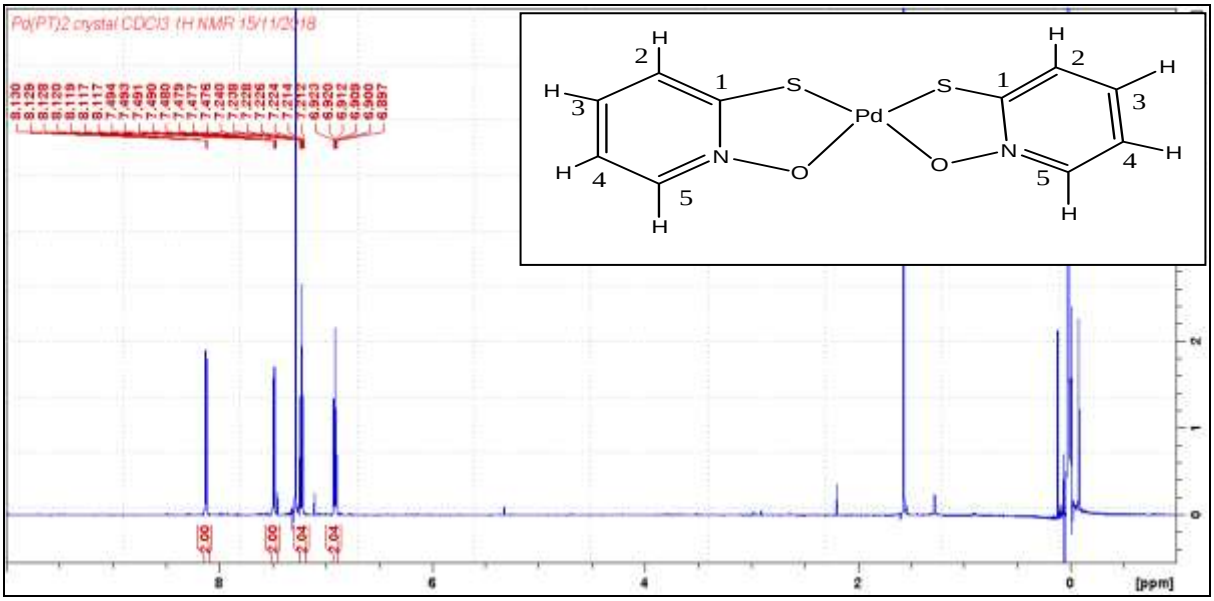

Figure 5.31: The ^{1}H NMR spectrum of $Pd(PT)_2$ crystals

According to the NMR spectra in **Figures 5.31** to **5.33**, the peaks can be assigned as follows: ^{1}H NMR (300 MHz, $CDCl_3$): δ = 8.12 (2H, ddd, J = 6.8, 1.3, 0.5 Hz, H5), 7.46 (2H, ddd, J = 8.4, 1.6, 0.5 Hz, H2), 7.23 (2H, ddd, J = 8.4, 6.9, 1.3 Hz, H3), 6.91 (2H, ddd, J = 6.9, 6.8, 1.6 Hz, H4). ^{13}C NMR (75 MHz, $CDCl_3$): δ = 158.97 (C1), 137.19 (C5), 129.30 (C3), 128.18 (C2), 117.90 (C4).

The chemical shift for H5 at 8.12 ppm is higher than those of other protons present in the structure of $Pd(PT)_2$. This is because it is attached closer to the nitrogen atom which is electron-withdrawing. This decreases the electron density around H5, resulting in the de-shielding of H5. Therefore, there is a high chemical shift since the proton needs a higher frequency to achieve resonance.

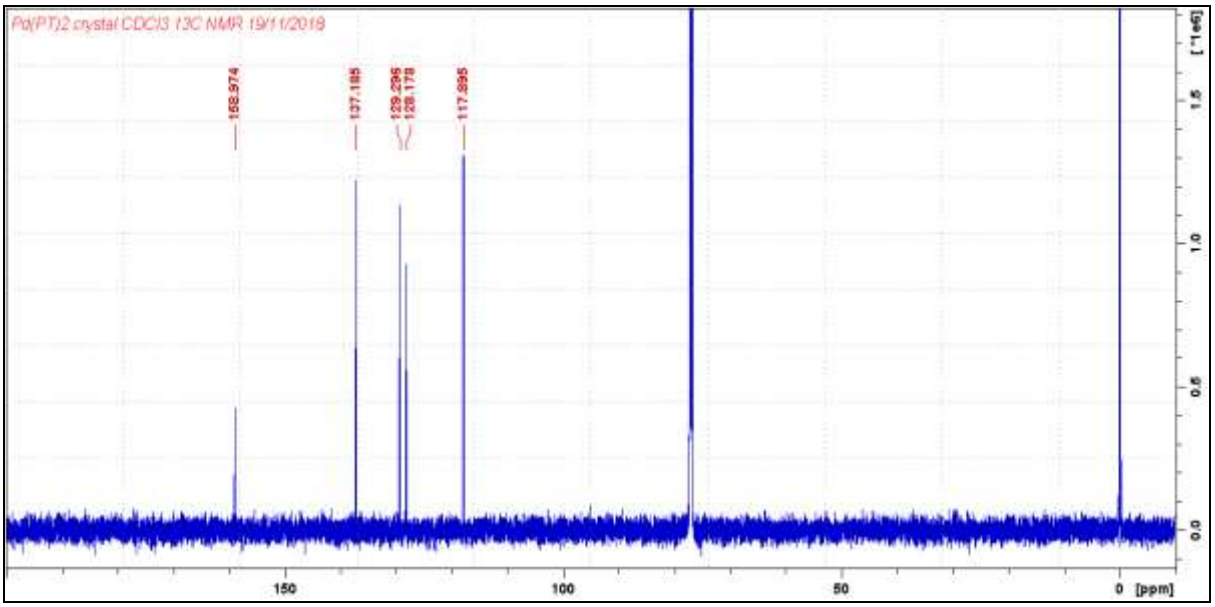

Figure 5.32: The ^{13}C NMR spectrum of $Pd(PT)_2$ crystals

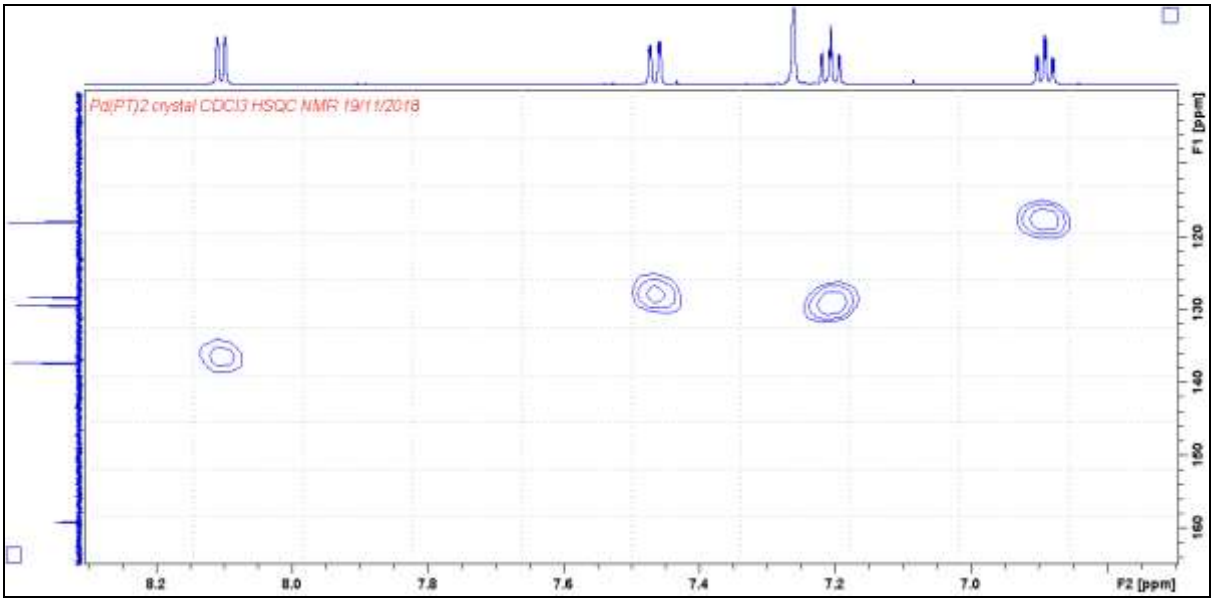

Figure 5.33: The ^{1}H -^{13}C HSQC NMR spectrum of $Pd(PT)_2$

X-Ray Crystallography: Crystal structure of $Pd(PT)_2$.DMF

An ORTEP view of the crystal structure of $Pd(PT)_2$.DMF is shown in **Figure 5.34** while its packed unit cell appears in **Figure 5.35**. The structure shows that Pd metal is coordinated to the mercaptopyridine in a square planer, with S and O in *cis* positions.

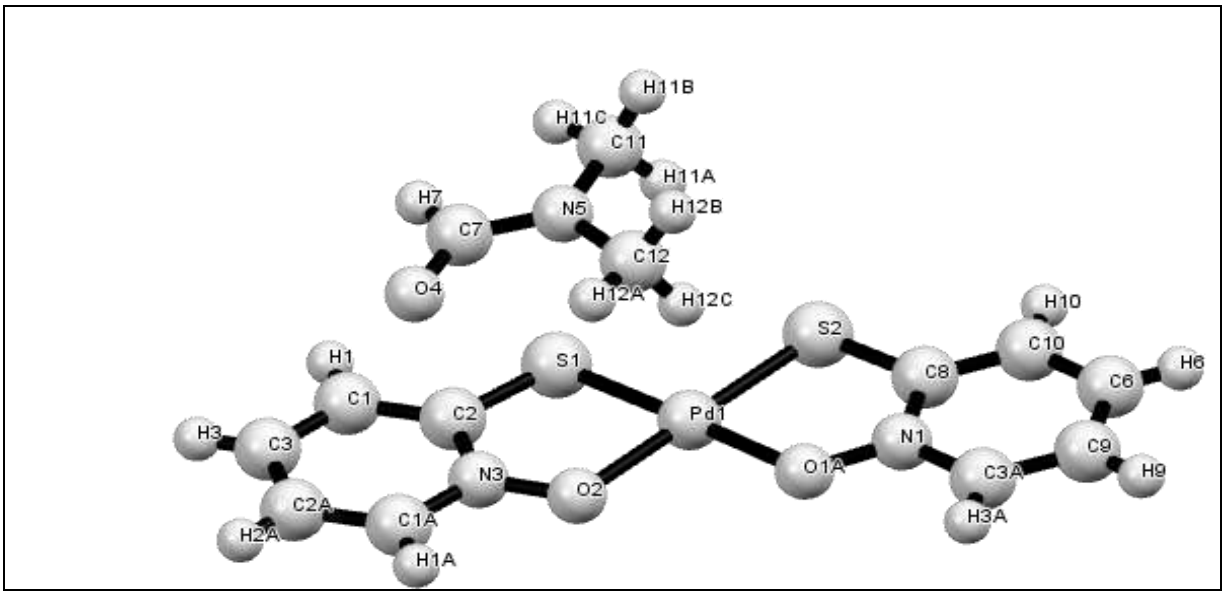

Figure 5.34: ORTEP view of the structure of $C_{10}HN_2O_2S_2Pd.C_3H_7NO$ with the atom numbering scheme

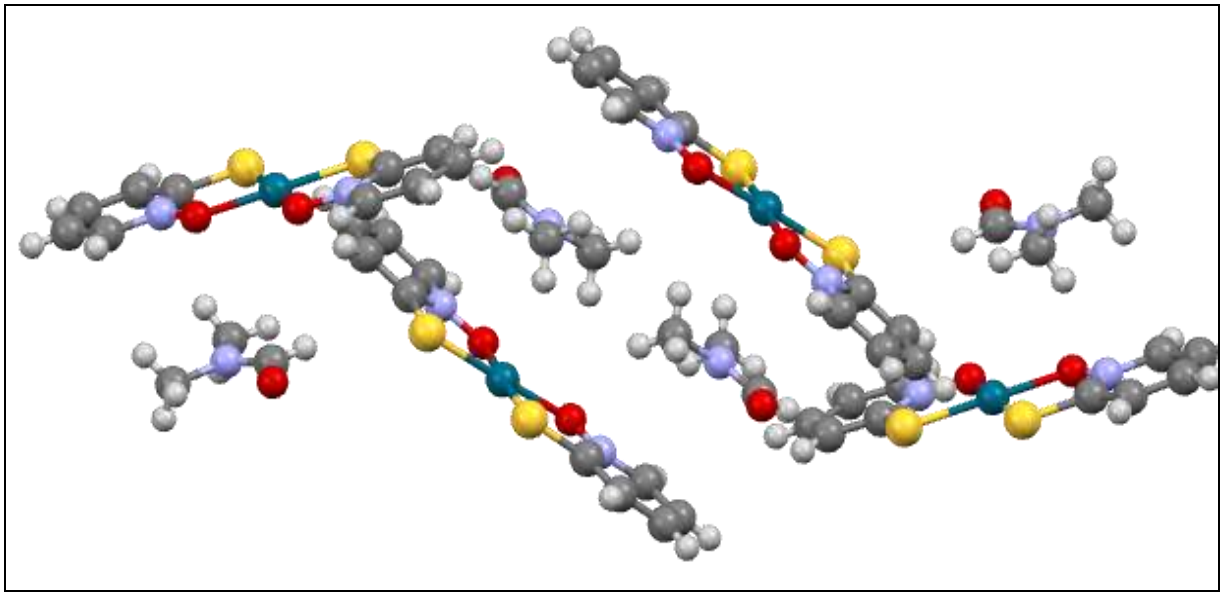

Figure 5.35: Packed unit cell of $C_{10}HN_2O_2S_2Pd.C_3H_7NO$ along the b axis

A similar $Pd(PT)_2$ compound was synthesised by Anacona et al.[165] This compound was crystallised using $CHCl_3$ to form a crystal that recrystallised in an orthorhombic crystal system, in space group $Pna2_1$, while the one obtained in this study crystallised

[165] Anacona, J.R., Leon, E. & Diaz-Delgado, G. (2008). Complexes of 1-hydroxypyridine-2-thione (LH) with Rh(III), Pd(II), Cd(III) and Hg(II): Crystal structure of $Pd(L)_2.CHCl_3$. *J.Coord.Chem*, 61(13), pp. 2142-2149.

in a monoclinic crystal system, in space group $P2_1/n$ and contains DMF as a recrystallisation solvent, with *a* = 9.326(5), *b* = 7.768(5) and *c* = 21.932(5). **Table 5.21** shows the selected bond lengths and distances obtained in this study, as well as those obtained by Anacona et al.[165] The crystal parameters for $C_{10}HN_2O_2S_2Pd.C_3H_7NO$ obtained in this study are shown in **Table 5.22**.

Table 5.21: Comparison of the selected bond lengths and distances obtained in this study, as well as those obtained by Anacona et al.

Crystal	Pd[a]	Pd[b]
Selected bond lengths		
Pd-O2	2.032(4)	2.040(3)
Pd-S1	2.2443(13)	2.2336(12)
Pd-S2	2.2416(15)	2.2361(13)
Pd-O1	2.030(3)	2.036(3)
Selected bond angles		
O1-Pd-O2	91.08(14)	91.92(12)
Pd-S1-C1	97.87(11)	97.65(15)
Pd-O1-N1	115.8(2)	114.8(2)

Pd[a] A crystal obtained in this study

Pd[b] A crystal obtained by Anacona et al.

Table 5.21 shows that the bond distance of Pd-O2 is 2.032(4) and is shorter than that of Pd-S2 which is 2.2443(13). This implies a stronger bond in the Pd-O than in Pd-S. This is attributed to the high electronegativity of O which is 3.44 while that of S is 2.58.

Table 5.22: Crystal data and crystal refinement for $Pd(PT)_2.DMF$

Identification code	17daan_0ma
Empirical formula	$C_{10}HN_2O_2S_2Pd.C_3H_7NO$
Formula weight	431.80
Temperature/K	293(2)
Colour	Bright pink
Crystal system	Monoclinic
Space group	$P2_1/n$
a/Å	9.326(5)
b/Å	7.768(5)
c/Å	21.932(5)
α/°	90.000(5)
β/°	101.750(5)
γ/°	90.000(5)
Volume/Å^3	1555.6(14)
Z	4
ρ_{calc}mg/mm^3	1.497
m/mm^{-1}	1.451
F(000)	672.0
Crystal size/mm^3	0.528 × 0.198 × 0.161
Radiation	Mo (λ = 0.71069)
2θ range for data collection(°)	3.794 to 55.99
Index ranges	$12 \leq h \leq 10$, $-10 \leq k \leq 10$, $-28 \leq l \leq 26$
Reflections collected	26210
Independent reflections	3738[R(int) = 0.0472]
Data/restraints/parameters	3738/72/177
Goodness-of-fit on F^2	1.250
Final R indexes [I>=2σ (I)]	R_1 = 0.0435, wR_2 = 0.1129
Final R indexes [all data]	R_1 = 0.0454, wR_2 = 0.1160
Largest diff. peak/hole / e Å^{-3}	1.33/-1.13

5.7 SEPARATION OF PGE FROM REAL SAMPLES, USING OPTIMAL CONDITIONS FROM DEVELOPED METHODS IN SECTIONS 5.5 AND 5.6

The final step in this study involved the evaluation of the proposed separation scheme (**Figure 5.28**) on the automotive catalyst sample and on a rhodium solution which had been accumulated as waste from synthesis, kinetics and crystal structure studies performed on rhodium organometallic studies in the department.

5.7.1 The ERM®-EBS504 Automotive Catalyst Sample

5.7.1.1 Experimental

Pre-concentration of the catalyst sample

The extremely low PGE concentrations (**Table 5.6**) in the catalyst sample necessitates the pre-concentration of the sample before the separation process is evaluated. A concentrated solution of the catalyst sample was prepared by dissolving approximately 7 g of the catalyst sample, using the peroxide fusion method in **Section 5.4.1**. As a result of the high flux content that was required to dissolve large quantities of the sample, a jelly-like, dense, yellow solution was obtained after the addition of *aqua-regia* to the milky solution. The solution was most probably due to its supersaturation with the formation of large amounts of NaCl, which is the result of the Na^+ introduced by the flux and Cl^- from the HCl in *aqua-regia.* In order to remove excess NaCl, this solution was evaporated to almost dryness and excess HCl (10 M) added. Large amounts of white NaCl crystals formed immediately and started to settle at the bottom of the beaker. This was left to stand for a period of over 24 hours to ensure complete sedimentation. The liquid sample at the top of the NaCl was separated by means of filtration while the isolated NaCl was washed in additional HCl until no further NaCl precipitated from the solution and the isolated NaCl clearly appeared to be white. All washed solutions were combined with the previously isolated sample solution, transferred into a beaker (600 ml), and evaporated to a desired volume (~100 ml) to obtain a concentrated solution containing substantial amounts of PGE which were suitable for separation purposes.

Separation and purification of Pt, Pd and Rh from the catalyst sample

Of the previously pre-concentrated catalyst solution, 20 ml was transferred into a volumetric flask (100.0 ml) and Sc (0.2 ml) was added as an internal standard. The solution was then filled to the mark with ultra-pure water and analysed for Pt, Pd and Rh, using the ICP-OES technique. The quantitative results showed that this solution contained 25(1) ppm of Pt, 3.63(3) ppm of Pd and 2.9(2) ppm of Rh. Another 20 ml solution from the original pre-concentrated sample was transferred into a beaker (250 ml) and evaporated to dryness. This residue was then re-dissolved in HCl (20 ml, 4 M) and extracted using NaPT (5 ml, 0.02 M) and toluene (20 ml). The raffinate was isolated and transferred into a beaker (250 ml). The organic layer was back-extracted three times using *N'N*-dimethylthiourea (20 ml, 0.2 M) to recover Pd. The isolated raffinate in a beaker (250 ml) was then evaporated to dryness, re-dissolved in HCl (20 ml, 4 M) and extracted using TOPO (20 ml, 0.3 M) in kerosene. The final raffinate was isolated while the remaining organic layer was stripped three times using NH_4SCN (20 ml, 0.5 M) to isolate Pt selectively. Finally, it was stripped three times using HCl (20 ml, 2 M) to isolate Rh which was expected to be contaminated with Cu. The final raffinate and the stripped solutions were then evaporated to dryness, dissolved in HCl (10 ml, 10 M), transferred into volumetric flasks (100.0 ml), filled to the mark with ultra-pure water and analysed using ICP-OES. The results are reported in **Table 5.23**.

5.7.1.2 Results and discussion

The results reported in **Table 5.23** are extremely promising and indicate that the majority of Pd and Pt were successfully isolated from the catalyst solution with percentage recoveries of 99(3) and 87(4) % respectively. However, it required at least three extractions using TOPO (0.3 M) to remove most of the Pt due to high concentrations thereof in the pre-concentrated catalyst sample as compared to the synthetic mixtures which were studied. It was interesting to observe that the extraction of Rh using TOPO was unsuccessful. An analysis of the final raffinate solution indicated that Rh had never been extracted into the organic layer. This might be due the introduction of NaCl salt during the dissolution process, which increased

the chloride concentration in the sample and might have prevented the extraction of Rh due to the formation of very stable $[RhCl_6]^{3-}$. These results agree somewhat with those obtained in **Figure 5.23**, where it was observed that an increase in chloride concentrations resulted in a decrease in the extraction of PGE using TOPO, except for Pt which had not been affected at high chloride concentrations.

Solvent extraction of Pt using TOPO was also investigated by Naj et al.[166] in the presence of alkaline metals, salts including NaCl, KCl and LiCl, and their results indicated improved Pt extraction at high salt concentrations in the presence of TOPO.

Table 5.23: The percentage recoveries of PGE after their isolation in the catalyst sample using the methods proposed in **Figure 5.28**

Metal	Initial concentration/ppm	% Recovered
Pt	25(1)	87(4)
Pd	3.63(3)	99(3)
Rh	2.9(2)	0

5.7.2 The Rhodium Waste Solution

5.7.2.1 Experimental

A rhodium waste solution, containing mostly rhodium and non-precious metals, was studied for possible isolation of Rh. This sample also proved to have very high salt content, and the solvent extraction of Rh using TOPO was also unsuccessful. Thus, the purity of Rh from this solution was improved by co-precipitation of the non-precious metals, using oxine. Due to the high Rh concentrations in this sample, precipitation methods were found to be suitable.

[166] Naj, H.H., Kazemeini, M. & Fattahi, M. (2012). Platinum extractions from spent catalyst by TOPO in presence of alkaline metals, pp.61-64.

From the rhodium waste solution, 5 ml was transferred into a volumetric flask (100.0 ml) and Sc (0.2 ml) was added. This solution was then filled to the mark with ultra-pure water and taken for ICP-OES analysis. The quantitative results indicated that this solution contained high concentrations of rhodium (28.44 ppm) and some non-precious metals; Al (40.54 ppm), Ti (0.62 ppm), Fe (4.52 ppm) and Ce (7.63 ppm). The Rh from this solution was separated from the non-precious metals by precipitation using oxine as follows: a concentrated solution from the original recycled solution (5 ml) was transferred into a beaker (250 ml) and water (10 ml) was added. The resulting solution was stirred slowly at room temperature while oxine (1 ml, 0.5 M) was added. The pH of this solution was then raised to about 10, and dark green precipitate formed. The precipitate was separated from the supernate by centrifugation. The supernate was transferred into a beaker (250 ml) and HCl (10 ml, 10 M) added, transferred into a volumetric flask (100.0 ml) and filled to the mark with ultra-pure water. The precipitate was dissolved in HCl (10 ml, 10 M), transferred into a volumetric flask (100.0 ml) and filled to the mark with ultra-pure water. Both solutions were analysed using ICP-OES, the results of which are shown in **Figure 5.36**.

5.7.2.2 Results and discussion

The results in **Figure 5.36** indicate that the non-precious metals, including Ti were mostly recovered in the precipitate while most of the rhodium was left in the filtrate, with a percentage recovery of 80(4) %. The percentage recoveries for Al, Fe, Ti and Ce in the precipitate were 91(3), 94(3), 92(2) and 104(2) % respectively.

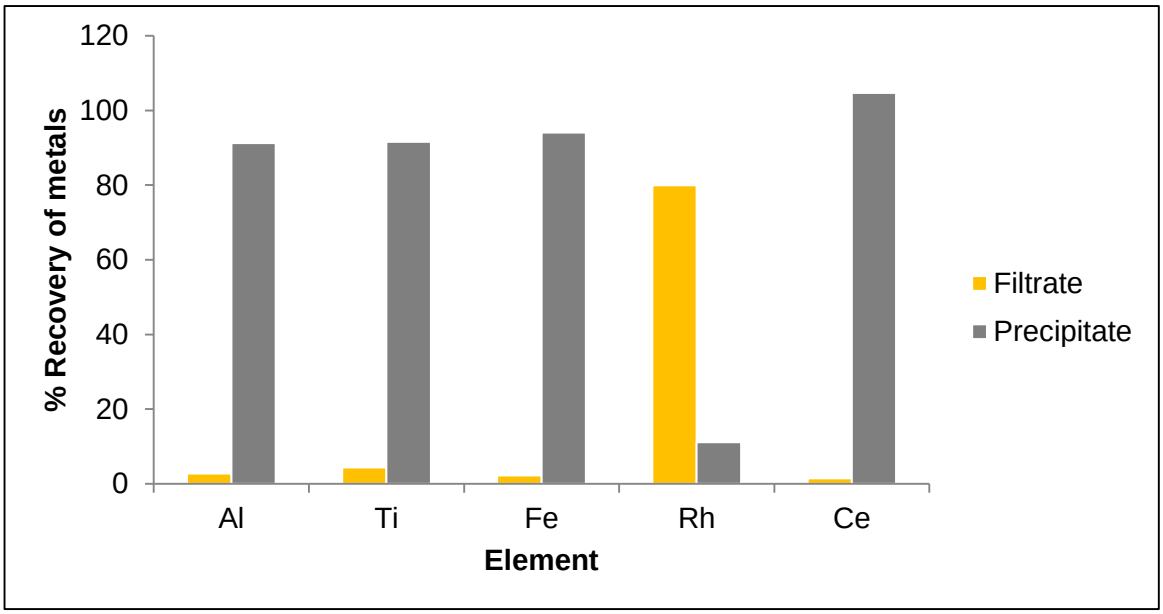

Figure 5.36: The percentage recoveries of metals in the filtrate and precipitate after precipitation with oxine

5.8 METHOD VALIDATION

One of the most important steps in analytical chemistry is method validation as it determines the quality of the results obtained. In this study, it was crucial to determine the reliability of the experimental methods and, most importantly, the suitability of the ICP-OES technique to accurately quantify the PGE. In all the experiments performed in this study, including both dissolution and separation methods, the reproducibility and reliability of the experimental methods were determined by repeating each experiment at least three times while that of ICP-OES was judged by calculating the errors in the calibration curves and assessing its ability to obtain consistent quantification results for replicate measurements. The acceptance and rejection of results was dependent on various statistical parameters, including recovery, precision, and accuracy.

The results for Pt, Pd and Rh in the automotive catalyst after dissolution at optimal conditions using *aqua-regia* and after a complete dissolution with Na_2O_2 fusion method were validated in this section (**Tables 5.24** to **5.27**). This was done in order to determine the most suitable method for the dissolution of the catalyst sample and to identify the most satisfactory conditions in which the PGE can be accurately

quantified using the ICP-OES technique at different separation stages. The acceptance and rejection of these results was mainly dependent on the calculated *t*-value (**Chapter 4**, **Equation 4.13**). This is one of the most important parameters as it indicates whether there is any statistical difference between the experimental and accepted values which, in this case, are the certified weight percentages in the catalyst sample for Pt, Pd and Rh, which are 0.1777, 0.0279 and 0.0338 % respectively. All *t*-tests were calculated at a 95 % confidence interval for two degrees of freedom (*N*-1) where *t*-critical is 4.30. All *t*-values which were less than -4.30 and those which were greater than 4.30 resulted in the rejection of results.

The results after a complete dissolution of the catalyst sample with Na_2O_2 and quantification with Sc were accepted since percentage recoveries for Pt, Pd and Rh were 100(1), 100(3) and 103(2) % respectively (**Table 5.25**), while the *t*-values were 0.35, 0.27 and 2.22 respectively. The results after the dissolution of the catalyst with *aqua-regia* at optimal conditions were rejected due to the low percentage recoveries obtained. In addition, the results obtained after complete dissolution of the catalyst with Na_2O_2 and quantified using external calibration and Cd internal standard were also rejected. This was mainly due to the inaccurate PGE recoveries which were either higher or lower than the certified values. Overall, excellent linearity in all the ICP-OES calibration curves was obtained with R^2 values which were greater than 0.997. Precisions (% RSD) in all the experimental results were less than 10 %, indicating consistency or precision in the experimental methods and the analytical instrument.

Table 5.24: Validation of Pd, Pt and Rh results after dissolution with *aqua-regia* at optimal conditions and quantification using ICP-OES

Validation Criteria	Parameter	Pd	Pt	Rh
Recovery	Mean %	63.9(4)	66.9(8)	41(1)
Precision	RSD %	1.27	0.57	3.50
Working range	Calibration curve	0.25 - 5 ppm	0.25 - 5 ppm	0.25 - 5 ppm
Linearity	R^2	1.000	1.000	1.000
Sensitivity	Slope	0.000004830	0.00066300	0.00012400
Error of the slope	Y-intercept	-0.05830	-0.2700	-0.0313
t-value		77.03	149.44	72.11
Decision		Reject	Reject	Reject

Table 5.25: Validation of Pd, Pt and Rh results after dissolution with Na_2O_2 and quantification by means of ICP-OES using external calibration

Validation Criteria	Parameter	Pd	Pt	Rh
Recovery	Mean %	219(7)	115(1)	105(1)
Precision	RSD %	3.22	0.99	1.30
Working range	Calibration curve	0.25 - 5 ppm	0.25 - 5 ppm	0.25 - 5 ppm
Linearity	R^2	0.9970	0.9980	1.0000
Sensitivity	Slope	0.02680	0.00006450	0.00009420
Error of the slope	Y-intercept	1.7200	-0.3370	0.6710
t-value		29.23	23.65	6.97
Decision		Reject	Reject	Reject

Table 5.26: Validation of Pd, Pt and Rh results after dissolution with Na_2O_2 and quantification by means of ICP-OES using Cd as an internal standard

Validation Criteria	Parameter	Pd	Pt	Rh
Recovery	Mean %	126.1(3)	76.8(6)	130.0(4)
Precision	RSD %	0.21	0.82	0.34
Working range	Calibration curve	0.25 - 5 ppm	0.25 - 5 ppm	0.25 - 5 ppm
Linearity	R^2	0.9990	1.0000	0.9990
Sensitivity	Slope	68.00	28.7	47.9
Error of the slope	Y-intercept	0.3610	-0.2920	0.9940
t-value		824.43	-63.82	507.68
Decision		Reject	Reject	Reject

Table 5.27: Validation of Pd, Pt and Rh results after dissolution with Na_2O_2 and quantification by means of ICP-OES using Sc as an internal standard

Validation Criteria	Parameter	Pd	Pt	Rh
Recovery	Mean %	100(3)	100(1)	103(2)
Precision	RSD %	2.98	1.02	2.25
Working range	Calibration curve	0.25 - 5 ppm	0.25 - 5 ppm	0.25 - 5 ppm
Linearity	R^2	0.9990	1.0000	0.9980
Sensitivity	Slope	1120	533	806
Error of the slope	Y-intercept	0.35	-0.318	0.817
t-value		0.27	0.35	2.22
Decision		Accept	Accept	Accept

5.9 CONCLUSIONS

Complete dissolution of the ERM®-EBS504 automotive catalyst sample was achieved by means of the sodium peroxide fusion method. Although the sample was completely dissolved, problems were encountered with the quantification of PGE using ICP-OES due to spectral interferences from Na ions which were introduced from the Na_2O_2 flux. Analysing the PGE using the external calibration curve yielded the worst results even after stringent matrix matching. This indicates an unacceptably high degree of spectral interferences on the PGE lines as a result of the presence of Na ions. It was also disappointing to obtain unsatisfactory results after Cd was employed as an internal standard. Nevertheless, Sc was able to correct for the Na ion spectral interferences, and excellent percentage recoveries of 100(1), 100(3) and 103(2) % were obtained for Pt, Pd and Rh respectively. These results were successfully validated for their suitability and were accepted as determined by the *t*-test and other statistical parameters. *Aqua-regia* also provided hope in the dissolution of PGE, and maximum percentage recoveries of 66.9(8), 63.9(4) and 41(1) % were obtained for Pt, Pd and Rh respectively.

Both precipitation and solvent extraction methods for the separation of PGE from the non-precious elements and from one another were investigated. Precipitation of the non-precious elements in the presence of PGE using NH_4OH was found tedious and unsatisfactory since many steps were required to precipitate the non-precious metals, thus reducing the PGE concentration in the solution and complicating deductions which could be made from the results. The results for the precipitation of non-precious metals using 8-hydroxyquinoline were very interesting. The method proved to be selective for the precipitation of Pd as a highly stable complex in the presence of non-precious elements and other PGE in highly acidic conditions. However, the difficulties involved in working with this compound in acidic mediums prohibited further analytical investigations in aqueous solutions. Crystals of this $Pd(oxine)_2$ complex were isolated and characterised using XRD, FT-IR, LECO micro-elemental analysis and NMR in order to gain a better understanding of the type of complex formed between Pd and oxine and to determine the geometry and crystal detail after the reaction between oxine and the Pd metal centre.

An investigation into the isolation of PGE using solvent extraction methods was also conducted. TOPO was able to extract all the PGE in the synthetic mixtures, especially when the extraction was performed in kerosene and hexane as diluents. Once optimal conditions had been determined, the experiments were also performed in the presence of non-precious metals. Various stripping reagents were employed to selectively isolate the PGE from one another and from the non-precious elements. Although selectivity was not an easy task when TOPO was used, conditions that were selective for the isolation of PGE from one another were obtained. However, poor Rh recoveries were obtained with maximum percentage recoveries of about 45 %.

Solvent extraction using NaPT showed excellent selectivity towards Pd, especially in the presence of Pt. During this investigation, only Pd was extracted in the presence of only the PGE, which allowed for the isolation and recrystallisation of Pd organometallic compound from the organic layer which was characterised with the XRD, LECO micro-elemental analysis, FT-IR and NMR techniques. The formation of crystals also proved to be that of only Pd as pure compound. The results also indicated that non-precious elements are co-extracted with Pd. However, when various stripping reagents were investigated, *N'N*-dimethylthiourea was found to be highly selective towards the stripping of only Pd. The extraction of Pd using NaPT was found to be unique since this method had never been reported before. Thus, it contributes extensively to the separation chemistry of Pd in the presence of all other PGE and non-precious elements.

A newly-proposed method, using optimal conditions developed in this study was successfully applied to the ERM®-EBS504 catalyst sample and a waste rhodium solution. Although satisfactory recoveries of 99(3) and 87(4) % were obtained for Pd and Pt after the isolation of these metals from the catalyst sample, the introduction of salt during the peroxide fusion method might have prevented the extraction process of Rh using TOPO. The chemistry of Rh in high chloride-containing solutions proved to be a possible reason why Rh isolation was ineffective. The best way to recover Rh was by isolating the rest of the PGE by means of the newly-established method while leaving the Rh in the raffinate. The purity of Rh in the rhodium waste solution was

successfully improved with the precipitation of large quantities of contaminants using oxine as a precipitant. The difficulties encountered and the inconclusive isolation of Rh in both these waste or recycled samples leave room for improvement in future studies.

6 Evaluation of This Study

6.1 INTRODUCTION

This chapter includes the evaluation of the achievements compared to the objectives discussed in **Chapter 1**, **Section 1.4**. Moreover, this chapter also aims to identify possible future projects that may complement this study.

6.2 DEGREE OF SUCCESS WITH RESPECT TO STATED OBJECTIVES

The main objectives of this study as mentioned in **Chapter 1**, **Section 1.4** were:

- To chemically characterise the supplied PGE-containing waste material, using ICP-OES and SEM-EDS in order to identify the chemical constituents of the material and their relative concentrations;
- To develop an effective method for the dissolution of the provided PGE waste material that does not require the use of dangerous chemicals;
- To accurately and precisely quantify the PGE from waste material by ICP-OES;
- To develop methods that can isolate the platinum group elements from the non-precious elements in solution;
- To separate and purify the individual PGE from one another to ensure a state of high purity and a high percentage of recovery; and
- To validate the methods in accordance with the criteria of the Internal Standards Organisation (ISO 17025).

This study has been successful in achieving most the above-mentioned objectives as reflected by the results obtained in **Chapter 5**. The supplied PGE automotive catalyst sample which proved to contain three of the PGE; Pt, Pd and Rh was successfully

characterised using the SEM-EDS and ICP-OES. However, the determination of PGE with the SEM-EDS was unsuccessful since the concentrations of these elements were below the detection limits of the SEM-EDS. Nevertheless, the successful determination of the main elements, their relative concentrations and the homogeneity of the sample were achieved.

Aqua-regia open-vessel dissolution and sodium peroxide fusion methods were investigated for the possible dissolution of the automotive catalyst sample. The former dissolution method offered partial digestion of the catalyst sample and promising results were obtained after optimising the experimental conditions. The peroxide fusion method on the other hand, was found very efficient for the complete dissolution of the catalyst sample which allowed for the total characterisation of the sample using the ICP-OES technique. However, severe spectral interferences from sodium ions were encountered during the quantification of PGE with the ICP-OES when external calibration curve was used, and this resulted in unsatisfactory PGE recoveries. Internal standards were employed to counteract this effect, and Sc was found very suitable for the accurate and precise quantification of PGE with the ICP-OES which resulted excellent PGE recoveries. The low detection limits offered by the ICP-OES and its ability to identify trace elements were found outstanding for the quantification of PGE in the automotive catalyst sample. Validation of the methods also qualified the ICP-OES as an exceptional technique for the precise and accurate quantification of PGE, and this was crucial for the determination of PGE at various separation stages.

The successful dissolution of PGE with peroxide fusion method permitted the separation and isolation studies of PGE in various aqueous solutions. The separation chemistry of PGE was successfully investigated in these solutions and interesting results were obtained, especially for palladium as it proved to be the most reactive element. Various parameters were optimised in order to obtain high percentage recoveries and high purity of PGE. Excellent selectivity and percentage recoveries of PGE were obtained when solvent extraction methods were employed, although those of rhodium remained relatively poor. Precipitation methods, on the one hand, proved to be less selective and not suitable for the isolation of PGE in low-concentrated PGE

samples. A new solvent extraction technique which is highly effective for the selective isolation of palladium was also discovered during this study.

6.3 FUTURE RESEARCH STUDIES

The results obtained in this study revealed numerous potential projects which could be further investigated succeeding current study. The following projects may be pursued to gain a better understanding of the chemistry of PGE:

- The dissolution of Pt, Pd and Rh in the automotive catalyst sample using microwave-assisted acid digestion with *aqua-regia*, since promising results were obtained when open-vessel digestion was used. This will also avoid the introduction of EIEs which complicated the quantification and separation of PGE;

- The use of hydrogen peroxide (H_2O_2) as an oxidising agent, thus replacing the sodium peroxide (Na_2O_2);

- Possible recovery of cerium (Ce) from the automotive catalyst sample as it is present in very high concentrations and is one of the more crucial rare-earth elements used for industrial purposes;

- Optimisation of Pt recovery with TOPO in such a way that at least a one-step extraction process can recover 100 % of Pt (25 ppm in pre-concentrated process) from the catalyst sample;

- Investigate the possible separation of Pd by solvent extraction with oxine which will be extremely relevant for Pd isolation in low-concentrated PGE samples;

- Possible conversion of the isolated Pd and Pt solutions to pure metals;

- Redesign the separation scheme in **Chapter 5**, **Figure 5.28**, as the results indicated that various reaction pathways can be followed to achieve the separation of PGE;

- Research on the use of other types of ligands in the solvent extraction of PGE, which may include ligands with large molecular weight and include amines such as trioctylamine and triisooctylamine;

- The most important research project would be to investigate the chemistry and possible separation of Rh to obtain high purity and high percentage recoveries of this element since poor recoveries and inconclusive results were obtained in this study. Furthermore, the literature review in **Chapter 3** also indicated that Rh is the least investigated element as compared to Pt and Pd with regard to separation studies;

- Studies on the possible separation and isolation of PGE using ion exchange resins will also contribute remarkably to the separation chemistry of PGE.